LOW PRESSURE EXPERIMENTS WITH BASANITE, HAWAIITE, AND PHONOLITE FROM MT. EREBUS, ANTARCTICA

A dissertation submitted to the

Division of Graduate Studies and Research
of the University of Cincinnati

in partial fulfillment of the
requirements for the degree of

DOCTOR OF PHILOSOPHY

in the Department of Geology
of the College of Arts and Sciences

1995

by

Tammie L. Gerke

M.S., University of Cincinnati, 1990

B.S., Indiana University, 1988

UNIVERSITY OF CINCINNATI

22 September, 19 95

I, Tammie L. Gerke,

hereby submit this as part of the requirements for the degree of:

Doctor of Philosophy

in Geology, Arts & Sciences

It is entitled Low Pressure Experiments with Basanite, Hawaiite, and Phonolite from Mt. Erebus, Antarctica.

Approved by:

James L. Brophy

Richard M. Saltz

C. Dietsch

Warren D. Huff

Robert J. Kelly

ABSTRACT

I conducted melting experiments with a basanite, two hawaiites (DVDP2 and 83415), and a phonolite from Mt. Erebus, Antarctic. All experiments were carried out a 1 atmosphere from 1224^{o} to 1049 ^{o}C at oxygen fugacity near QFM buffer. I have tested two hypothesis: (1) can a basanite parent magma differentiate at low pressures to produce hawaiite and phonolite magmas, and (2) do the Mt. Erebus rocks represent low pressure differentiation of a parental basanitic magma. Microprobe analyses of glasses and coexisting crystals were used to test these hypotheses.

Crystal-melt equilibria in basanite experiments are represented by olivine+melt (1224 ^{o}C), olivine+ clinopyroxene+melt (1138 ^{o}C), and olivine+clinopyroxene+ plagioclase+melt (1104 ^{o}C). In experiments with DVDP2 hawaiite from 1104^{o} to 1049 ^{o}C, olivine+clinopyroxene+ plagioclase+melt coexists. Data from 83415 hawaiite experiments show that at 1160 ^{o}C melt coexists with plagioclase; below 1104 ^{o}C with olivine+plagioclase.

Liquid lines of descent established using the compositions of melts on a T-Mg# plot show that basanite melt merges into hawaiite composition at about 1104 ^{o}C and melt of hawaiite composition merges into phonolite composition at 1049 ^{o}C. These data confirm the hypothesis

that low pressure differentiation of a basanitic melt can produce melts of hawaiite and phonolite composition.

Mt. Erebus rock compositions produce a continuous data array on K_2O-SiO_2, TiO_2-SiO_2, MgO-SiO_2, Al_2O_3-SiO_2, Na_2O-SiO_2, and P_2O_5-SiO_2 plots. Liquid lines of descent established from the experiments define a vector. I interpret the coincidence of this vector with the Mt. Erebus rock data array as the results of low-pressure fractionation of the basanitic parental magma.

DEDICATION

This dissertation is dedicated to

Virginia Ann Gerke

1943-1993

May AIDS never touch your life in the way it has mine

ACKNOWLEDGEMENTS

I would especially like to acknowledge the support and guidance of Professor Attila I. Kilinc. I would also like to thank my committee members Professor James Brophy, Professor Craig Dietsch, Professor John E. Grover, Professor Warren Huff, and Professor Richard O. Sack.

Dr. Sack I owe a special thanks to for the continuous thought provoking conversations about pyroxenes and science in general.

I would like to thank several people; Kenon Cetin, Charron Kirkland, and Richard Terry for their help with the technical aspects of this work.

I would like to thank Wayne A. Pryor for believing all along that I was able to do this and encouraging me when I needed it.

I would like to thank my best friend and biggest fan who also was my mother for never giving up on me, even when I had. I would not be here if it was not for her.

Finally, I would like to thank Galadriel for bringing life back into mine and Orin for making me feel special when I needed it most during the last stages of this study.

TABLE OF CONTENTS

LIST OF TABLES

APPENDIX D

APPENDIX E

LIST OF FIGURES

INTRODUCTION

Alkaline rocks are volumetrically insignificant compared to tholeiitic rocks, however they represent the greater diversity in chemical composition. This diversity stems, in part, from the different environments in which alkaline rocks form, including 1) subduction zones, 2) continental and oceanic intraplate anorogenic zones with minimal to no tectonic activity, and 3) continental rift zones. Another factor in the chemical diversity of alkaline rocks' is the depth of magma generation. (Fitton and Upton, 1987) Alkaline magmas are believed to originate at depths of 50 to 90 Km below the surface of the earth, where pressure is of the order of 1.5-2.5 GPa; by contrast, tholeiitic magmas are believed to originate at a depth of 30 Km (1.0 GPa); Ghiorso and Carmichael, 1980. Because alkaline magmas are generated at great depths in the mantle, their compositions are likely to be modified by magma mixing, assimilation of country rock, and by both high- and low-pressure crystal fractionation.

The study of alkaline rocks can provide insights into deep mantle composition and the role of magma mixing and/or assimilation in modifying primary magma composition. One way of evaluating how these processes affect differentiation of an alkaline magma is to conduct experiments using samples from an alkaline volcano. Experimental studies can define

mineral and melt stability fields as a function of bulk composition and can help assess the contributions of intensive thermodynamic variables such as pressure (P), temperature (T), and oxygen fugacity (f_{O2}) in the differentiation of alkaline magmas. Experiments on alkaline rocks also reveal the sequence and composition of mineral phases crystallizing from alkaline melts at various temperatures and pressures. The data generated from experiments can be used in a number of other ways as well. For example, 1) Comparison of the sequence of mineral crystallization and compositions, as obtained from experiments, with those of natural rocks can constrain petrological and geochemical models used in the interpretation of rocks; and 2) Experimental data can be used to construct empirical (Grove et al., 1992) or thermodynamic models (Ghiorso and Sack, 1995) to predict the behavior of magmas.

This dissertation is an experimental study of alkaline volcanic rocks from Mt. Erebus, Antarctica. A basanite, two hawaiites, and a phonolite from Mt. Erebus were used in the experiments for two reasons. First, previous interpretations of field and analytical data have produced only loosely constrained petrologic models for the rock series of Mt. Erebus. Confirmation of these interpretations requires experimental data. Second, there has been no systematic low-pressure experimental study of a series of

alkaline rocks from a well studied volcano. This is the first such study. The effects of high pressure fractionation, magma mixing, and/or assimilation, on alkaline magmas can be better evaluated after the low-pressure crystal fractionation processes for a basanite-hawaiite-phonolite series are understood. With these objectives in mind, experiments with Mt. Erebus rocks were conducted at one atmosphere in the temperature range 1224^{o} to 1049 ^{o}C at f_{O2} near QFM conditions.

PREVIOUS WORK

Mt. Erebus, an active alkaline volcano discovered in 1841, is located on the southern extension of the Terror Rift (Kyle, 1990) on Ross Island, Antarctica (Figures 1 and 2). Earlier studies of this volcano focused on the field geology, petrology, mineralogy, and geochemistry of the lavas (Smith, 1954; Kyle and Moore 1990). More recent studies concentrated on volcanic activity, seismicity, gravity, deformation of the summit, and magmatic gases (Kyle and Moore, 1990).

Mt. Erebus is the most active volcano in Antarctica and the southernmost volcano in the world. Presently there is an active lava lake located in its crater whose

Figure 1: Modified map of Ross Island from Moore 1986. Iset from Volcanoes of the Antarctica Plate and Southern Oceans, LeMasuier, W.E., and Thompson, J.W. (eds) 1990.

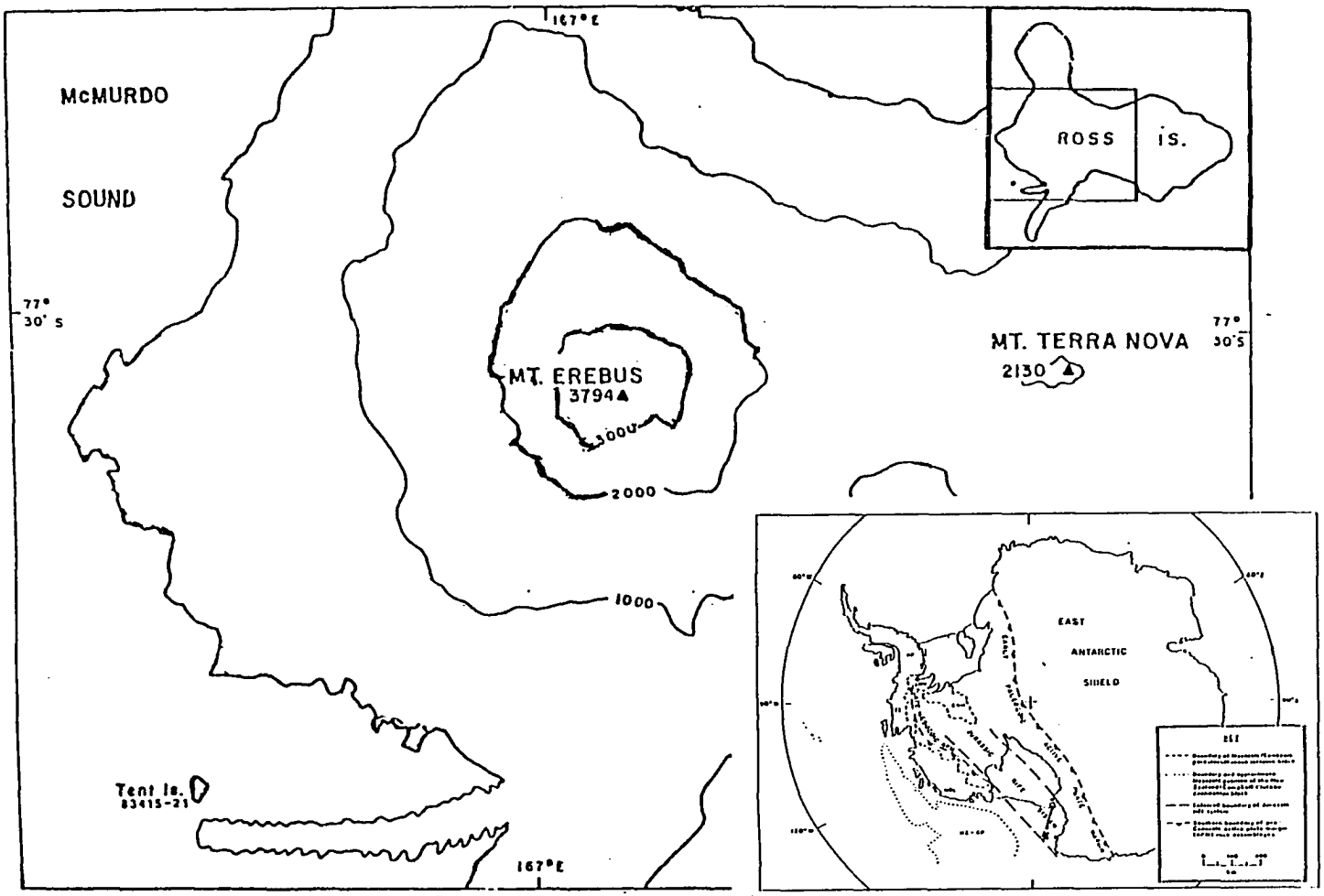

Figure 2: Generalized tectonic map of Ross Island, Antarctica, from Volcanoes of the Antarctica Plate and Southern Oceans, LeMasuier, W.E., and Thompson, J.W. (eds) 1990.

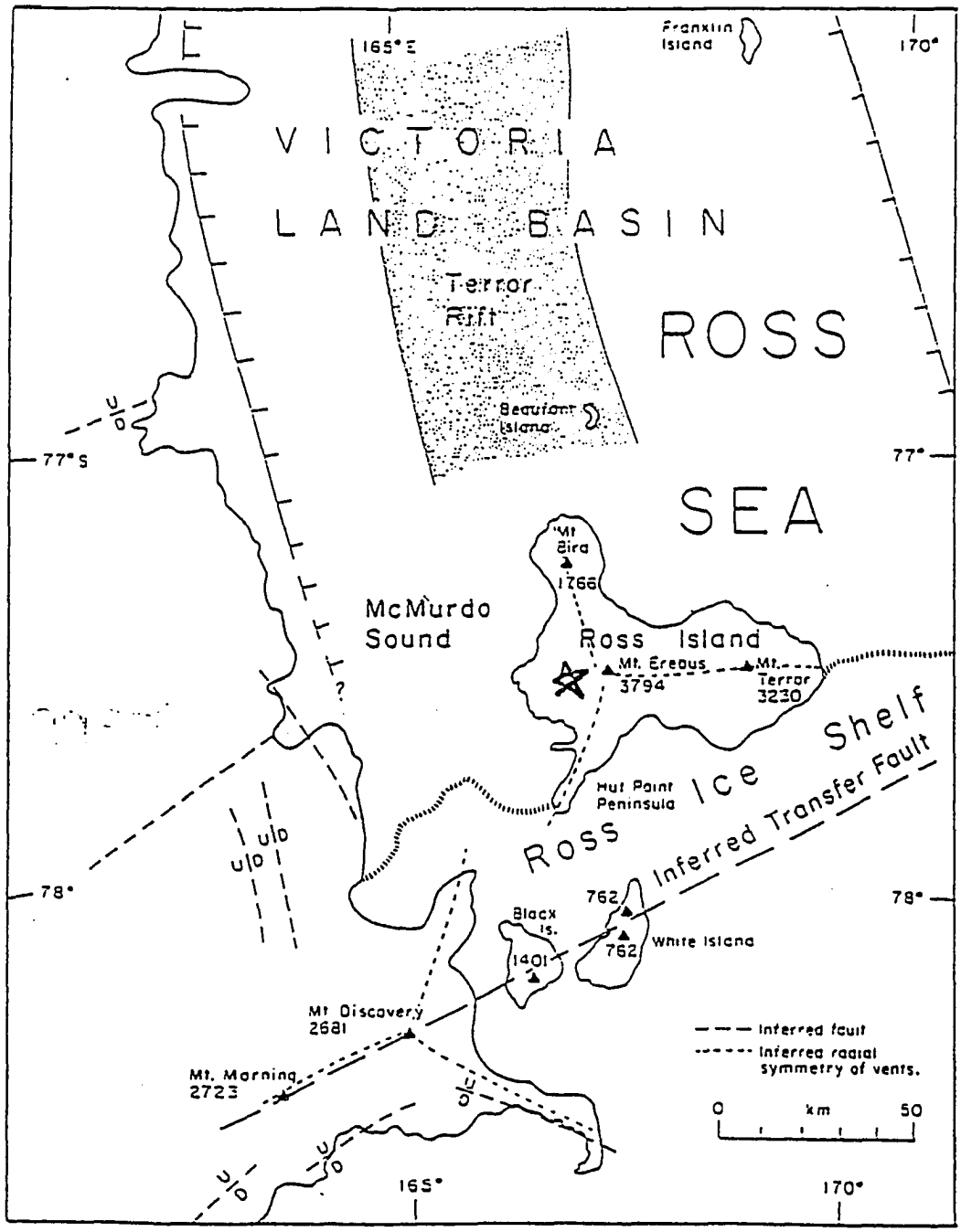

composition is anorthoclase phonolite. The anorthoclase crystals have been reported to grow to a length of 8 to approximately 20 cm. Because of their large size, these crystals have attracted the interest of researchers since the early 1960s for example, Carmichael, 1962, 1963, 1964, 1967; Carmichael and Mackenzie, 1964; Boudette and Ford, 1966; Berlin and Henderson, 1969; Mason et al., 1982; Jones et al., 1983; Irving and Frey, 1984.

Least-square mass balance calculations for major elements (Bryan et al., 1969) have been used by numerous researchers (Goldich et al., 1975; Moore, 1986; Kyle, 1990; Kyle and Moore, 1990; Kyle et al., 1992) to determine if the basanite can be parental to the hawaiite and phonolite at Mt. Erebus. Goldich et al., (1975) determined using major, minor, and trace elements that differentiation of the Mt. Erebus magma was controlled by fractional crystallization. They concluded that the early stages of magma differentiation were controlled by olivine, clinopyroxene, apatite, and opaque mineral crystallization followed by plagioclase and anorthoclase crystallization.

Moore (1986) evaluated both open and closed system processes to determine if the basanite magma could be parental to both the hawaiite and phonolite. He investigated the effects of assimilation and magma mixing for open systems and liquid immiscibility, volatile

transfer, Soret diffusion, boundary layer fractionation and crystal fractionation processes for closed systems. Moore concluded on the basis of field relations and geochemical trends (see Appendix A) the only model that fit both the field relations and geochemical trends was fractional crystallization. Moore, also used microprobe analysis of minerals and mass balance calculations to test the conditions under which basanite could differentiate to Ne-hawaiite. He then evaluated the conditions to generate Ne-benmoreite from Ne-hawaiite, and finally phonolite from Ne-benmoreite. Three different variations, based on major element chemistry, were tested for each step. Finally, trace element modeling was used to determine which of the tested models best fit the geochemical trends exhibited by these rocks. Moore (1986) concluded that it is possible for the basanite to be parental to the Ne-hawaiite, Ne-benmoreite, and phonolite.

According to Moore's (1986) model, the sequence of crystallization in the generation of Ne-hawaiite from basanite, was olivine, clinopyroxene, spinel and ilmenite, followed by apatite. Moore (1986) also estimated that the Ne-hawaiite represents 45% residual liquid of basanite. In order to form Ne-benmoreite from Ne-hawaiite the sequence of crystallization was olivine, clinopyroxene, magnetite, plagioclase (An_{64}), and apatite. The Ne-benmoreite represents 78% the residual liquid of the Ne-hawaiite.

Finally, for the anorthoclase phonolite to form from the Ne-benmoreite sequence of crystallization was olivine, clinopyroxene, magnetite, plagioclase (An_{44}), nepheline, and apatite. The anorthoclase phonolite represents 66% residual liquid of the Ne-benmoreite. Moore (1986) was able to calculate that the anorthoclase phonolite represents 23.5% residual liquid of the basanite.

Kyle (1990) concluded, on the basis of Moore's study, that phonolite may be derived from basanite by fractional crystallization. The mineral phases involved are olivine, clinopyroxene, feldspar, nepheline, apatite, and spinel.

In 1992 Kyle et al., (1992) restated Moore's (1986) findings, and provided a more detailed evaluation of the importance of feldspar during fractional crystallization. They determined that feldspar fractionation plays an increasingly important role as the magmas differentiate. Although all of the above models are only slightly different in their predictions, none of them can be confirmed without experimental work.

Phase diagrams have traditionally been used by petrologists to gain insights into equilibrium petrologic processes. In recent years, petrologists have developed algorithms to reduce multi-component magma systems to three or four components and have presented melt and mineral compositions using pseudo-ternary or pseudo-liquidus ternary

diagrams (Walker, 1979; Gerke and Kilinc, 1993; Sack et al., 1987; Figure 3). Pseudo-invariant points and cotectics on these diagrams are really regions in multi-component space (Langmuir et al., 1992). These diagrams attempt to represent invariant mantle melting with a large number of components and a limited number of mineral phases, which is not possible. Also, most pseudo-liquidus diagrams are developed at fixed pressures but mantle melting is a polybaric process. Although there are limitations to pseudo-liquidus diagrams, as long as these limitations are kept in mind these types of diagrams can still be useful.

Sack et al. (1987) established the first experimentally determined pseudo-liquidus diagram for alkaline rocks (Figure 3). To constrain the position of the ol+cpx+plag±sp cotectic in their diagrams, these authors used a wide range of natural starting materials from various alkaline volcanos throughout the world. This allowed them to generate a pseudo-ternary liquidus diagram for "alkaline magmas" from which general behavior of alkaline magmas can be predicted. Although clustering of data points enabled them to locate the position of the ol+cpx+plag±sp cotectic reasonably well, it remains to be seen if the position of this cotectic is affected by composition. Data generated by Kennedy et al. (1990) give a somewhat different cotectic when plotted on Sack et al.'s (1987) diagram using Sack et al.'s 1987 algorithm. If this is true for other

Figure 3: Pseudo-liquidus phase diagram from Sack et al. (1987, Figure 12). See text for discussion.

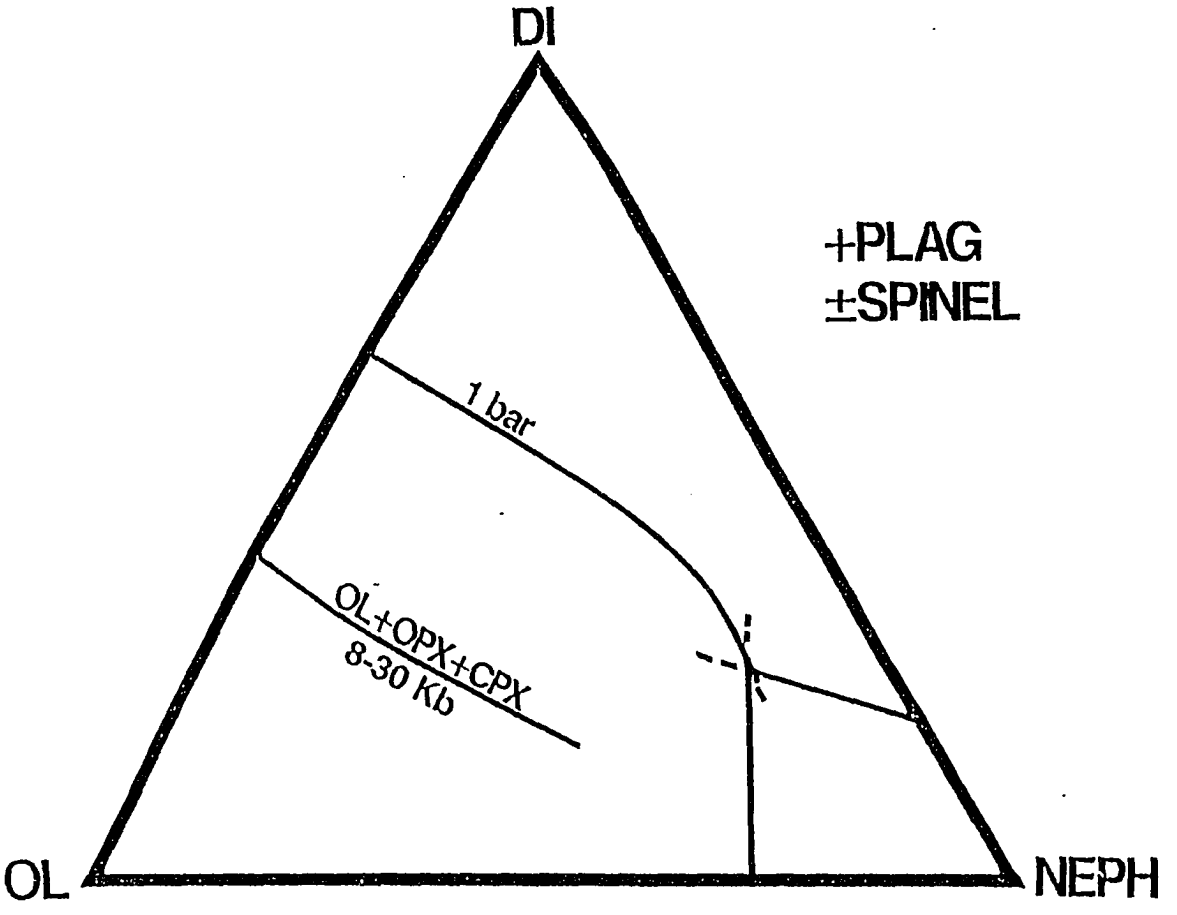

compositions, then Sack et al.'s (1987) diagram (Figure 3) cannot be used to predict the behavior of an alkaline magma of a given volcano. A corollary of this is that prediction of the behavior of magma of a given alkaline volcano requires experiments with rocks from that volcano.

STATEMENT OF PROBLEM AND ITS SIGNIFICANCE

Study of the petrologic and geochemical characteristics of alkaline rocks provides insight into the mineralogical and chemical characteristics of alkaline magma source regions, differentiation of alkaline magmas, and the extent of crustal assimilation in their petrogenesis. Volcanism within continental rift zones, such as the East African Rift Valley and the Terror Rift Zone in Antarctica, is typically alkaline in character. Alkaline rocks from Mt. Erebus, which range from silica poor basanites (SiO_2 44.23 wt%) to silica rich phonolites (SiO_2 55.53 wt%; Figures 4 and 5) provide an ideal rock association for investigating the evolution of alkaline magmas. The purpose of this study is to determine what role, if any, low pressure crystal fractionation plays in producing the observed compositional diversity in the alkaline rocks of Mt. Erebus.

Figure 4: CAMS system projection using procedure in Chapter 3 of BVSP (1981). Open squares = basanite, filled diamonds = Ne-hawaiite, arrows = Ne-mugearite, open circles = Ne-benmoreite, and filled stars = anothoclase phonolite.

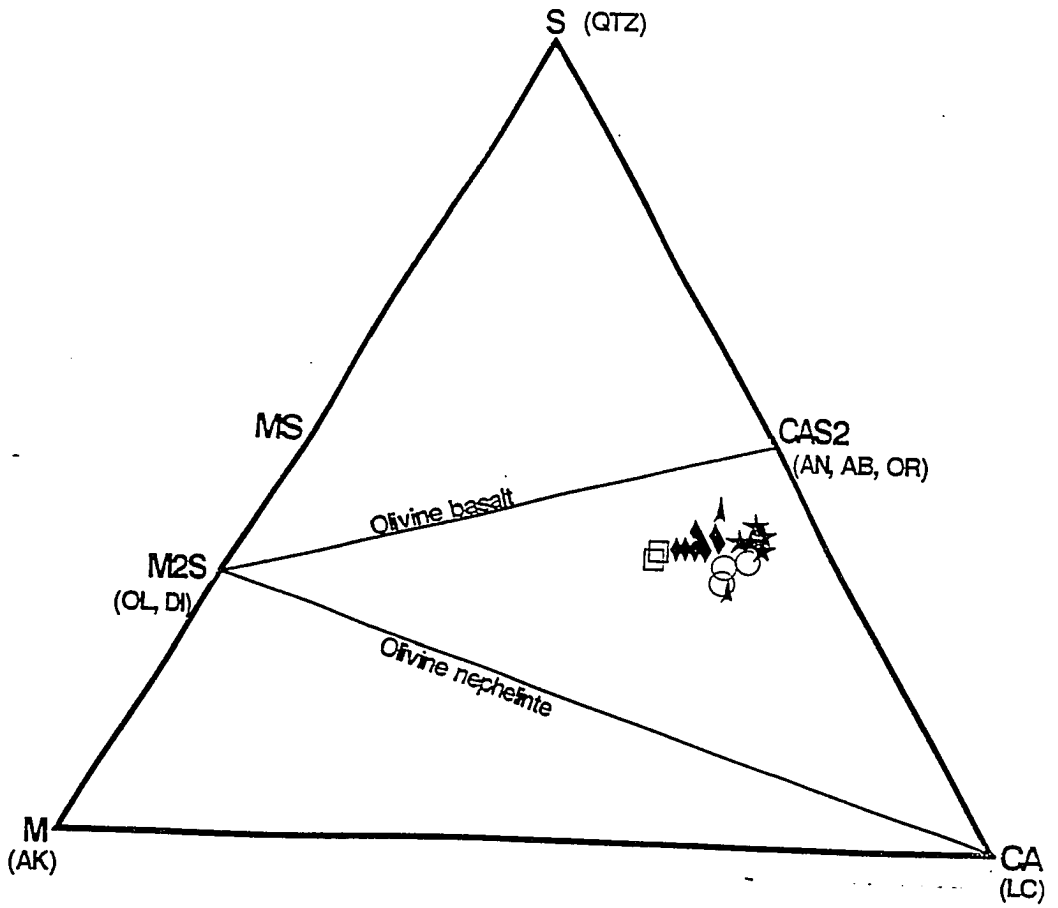

Figure 5: Plot of Na_2O+K_2O (wt%) versus SiO_2 (wt%) showing that Mt. Erebus volcanic rocks are alkaline. Open squares = basanite, open triangles = Ne-hawaiite, filled circles = Ne-mugearite, asterisks = Ne-benmoreite, and open circles = anothoclase phonolite.

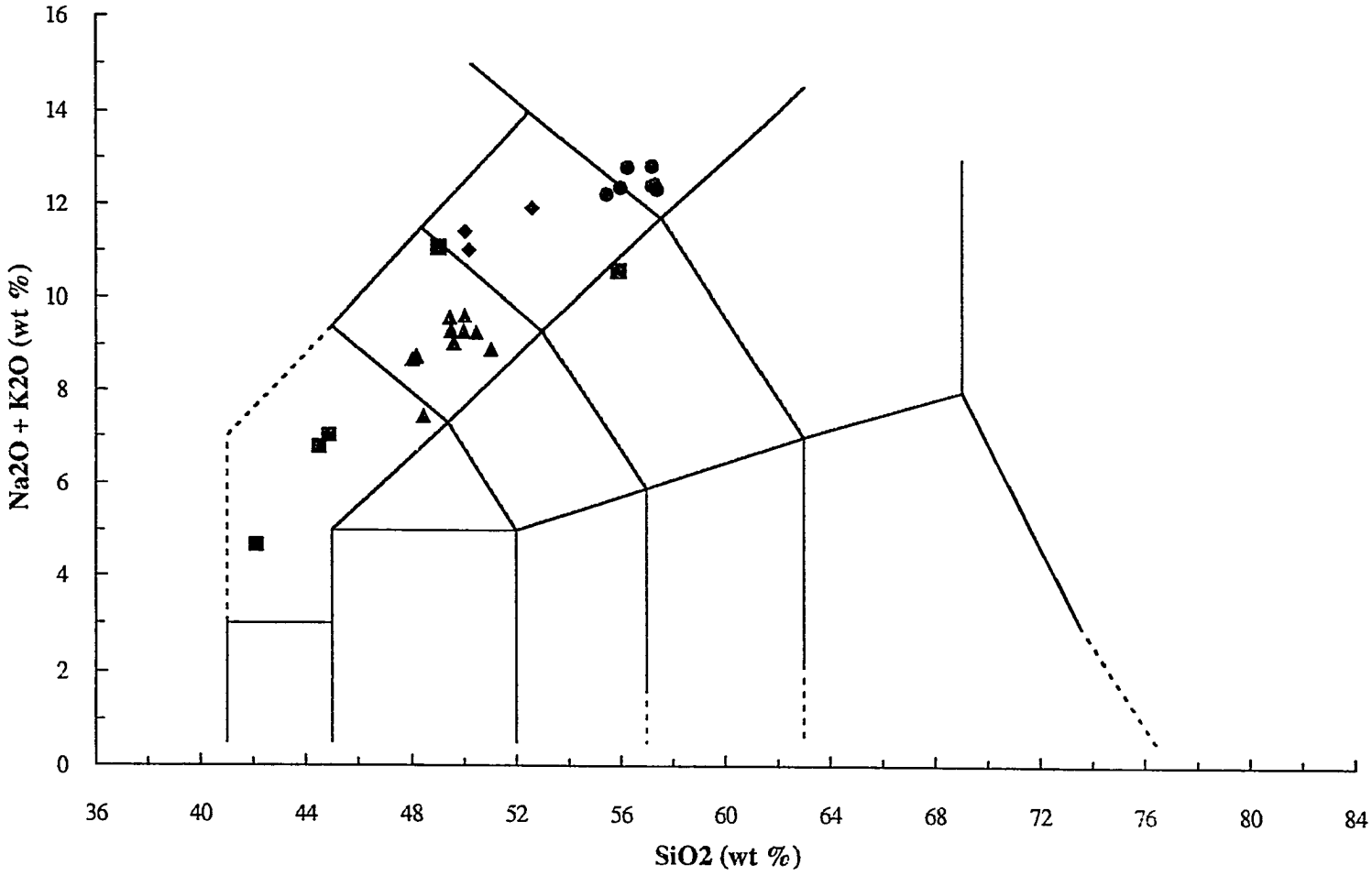

My objectives are: (1) to provide the first set of low pressure experimental data on melts and coexisting minerals in alkaline rocks from Mt. Erebus; (2) to test the hypothesis that the Ne-hawaiite and anorthoclase phonolite can be generated from the basanite at low pressures; and (3) to provide further constraints for geochemical-petrologic models on the origin of alkaline rocks.

In order to achieve the first objective of this study, a series of experiments at one atmosphere pressure were conducted at temperatures from 1224^{o} to 1049 ^{o}C using basanite, DVDP2 hawaiite, Ne-hawaiite, and anorthoclase phonolite from the Mt. Erebus volcano. In these experiments f_{O2} was controlled at about the QFM level. The second objective of this study i.e., testing the hypothesis that the Mt. Erebus basanite magma can differentiate at low pressures to produce Ne-hawaiite which, in turn, can differentiate to produce anorthoclase phonolite, can be achieved in a number of ways. A very common testing method used by some petrologists is mass balance calculations. This requires, as input to the calculations, the bulk composition of the parent magma, the bulk composition of the daughter magma, and the compositions of minerals assumed to be crystallizing from the parent magma. The drawback of this method is that one is forced to assume 1) the bulk compositions of parent and daughter magmas are identical to bulk compositions of rocks, 2) minerals used in the mass

balance calculations crystallize from the parent magma at or near liquidus conditions so that they are effectively removed from the melt, and 3) the compositions of the minerals used in the calculations are assumed to be the same compositions at the time of their fractionation. These assumptions are quite difficult to justify in many circumstances, and because the results depend upon these assumptions, I chose not to use this method.

A different method to test my hypothesis is to use thermodynamic melt-mineral equilibrium models such as that of Ghiorso and Sack (1995). Although this is a very powerful method, the model is very complicated and was only recently developed. It must be tested extensively before it can be applied to a specific case such as the Mt. Erebus.

The third and most direct method of testing my hypothesis is to conduct experiments with Mt. Erebus rocks themselves to determine the compositions of glasses at different temperatures. A comparison of the compositions of experimental melts with those of actual rock series can either verify the hypothesis or nullify it. For example, if the composition of melts in basanite experiments changes with decreasing temperature and ultimately become identical to the bulk composition of anorthoclase phonolite, it supports the model that anorthoclase phonolite can be a low pressure differentiation product of the basanite magma.

Because this is the most direct way to test my hypothesis, I chose the experimental method.

EXPERIMENTAL PROCEDURE

Starting Materials

Samples of basanite, DVDP2 hawaiite, Ne-hawaiite, and anorthoclase phonolite were provided by Dr. P. Kyle of the New Mexico Institute of Mining and Technology, Soccoro. The basanite and DVDP2 hawaiite samples are from the Dry Valley Drilling Project Two (DVDP2), and were collected from Hut Point Peninsula, Ross Island, Antarctica (Figure 2). 83415 Ne-hawaiite is from Tent Island (Figure 2) and the anorthoclase phonolite was collected from Mt. Erebus (Figure 2). Although the basanite and hawaiite (from DVDP2) came from a hydrous magmatic system at Hut Point Peninsula their use can be justified because (1) the basanite sample used for this study contained no observable hydrous phases such as kaersutite; (2) although the DVDP2 hawaiite does contain kaersutite, it comprises only about 2% of the rock, as determined optically, and (3) the compositions plot on the general compositional trends, indicating that they are genetically related (see Appendix A Figure 1 a-h).

Sample Preparation

Each sample was ground to a particle size of 5-10 microns. Five to six grams of this rock flour were mixed with polyvinyl alcohol and pressed into pellets. Each pellet, approximately 10 mm in diameter and 2 mm thick, was broken into 3 or 4 pieces and each smaller piece was than drilled with a 1/64" bit. Finally, each piece was hung on an Fe-electroplated platinum (Pt) wire.

Electroplating Process

To minimize the loss of iron from the samples to the Pt-wire, each 0.127 mm O.D. Pt-wire was electroplated in a Ferrous Ammonium Sulfate - Ferrous Sulfate solution, then annealed in a 95.25% CO_2 and 4.75% CO gas mixture in a Deltech one atmosphere gas mixing furnace for 72 hrs at 1200 ^{o}C.

Furnace Design

A vertical Deltech DT31VT one atmosphere gas mixing furnace at the University of Cincinnati was used for all experiments. Temperature was controlled by a Mode C controller (Deltech Inc.) and sample temperatures were measured using a Pt-Pt-10% Rh (rhodium) thermocouple. In

all temperature readings, a cold junction was used to eliminate external (room) temperature fluctuations. Temperature readings are believed accurate to $\pm$ 2 ^{o}C.

Oxygen Fugacity Control and Quenching Procedure

Kyle et al. (1977) and Moore (1986) examined magnetite-ilmenite pairs from Ne-hawaiites from the Erebus lava lineage to determine f_{O2} conditions. The f_{O2} values they calculated correspond to the Quartz-Fayalite-Magnetite (QFM) oxygen buffer, as is typical of most basaltic magmas (Haggerty, 1976).

Oxygen fugacity in my experiments was controlled using a 95.25% CO_2 and 4.75% CO gas mixture, corresponding to the QFM buffer. The flow rates of CO and CO_2 were controlled using a Matheson Inc. flow meter.

Samples were hung from a Pt basket positioned in the hot spot inside the furnace. They were quenched by dropping the basket into cold distilled-deionized water by melting the hang wire with an electric current.

Equilibrium in Experiments

Verification of equilibrium in experiments with rocks is difficult because 1) reversal experiments can not be performed and 2) some minerals may reach equilibrium with the melt while others may not. For example, clinopyroxene and plagioclase take a longer time to reach equilibrium with the melt but olivine typically does not. Since olivine usually reaches equilibrium with the melt in a short period of time it is possible to test equilibrium of Fe-Mg exchange between olivine and melt as follows. The Fo number of olivine crystallizing from a melt of known composition can be calculated from the glass data by using the following equation:

$$Fo = 100/1+[(K_D)(100-Mg_{\#}/Mg_{\#})]$$

where $Mg_{\#} = (100)(n_{Mg\#}/n_{Mg\#}+n_{Fe\#}) = (100)(X_{Mg}/X_{Mg}+X_{Fe})$ and K_D is equal to 3.0 ± 0.03. If the calculated olivine composition and the composition of olivines formed in an experiment are the same, equilibrium between olivine and melt is confirmed.

Figure 6 is a plot of the calculated Fo number (Fo#) of olivine that would be in equilibrium with melt in basanite, DVDP2 hawaiite, and 83415 Ne-hawaiite experiments versus Fo# of olivines in experiments with these rocks (filled squares = basanite; filled triangles = DVDP2 hawaiite; and the filled circles = 83415 Ne-hawaiite). The

Figure 6: Fo# calculated versus Fo# actual. Solid line has a slope of one. Filled squares represent basanite, filled triangles represent DVDP2 hawaiite, and the filled circles represent 83415 Ne-hawaiite.

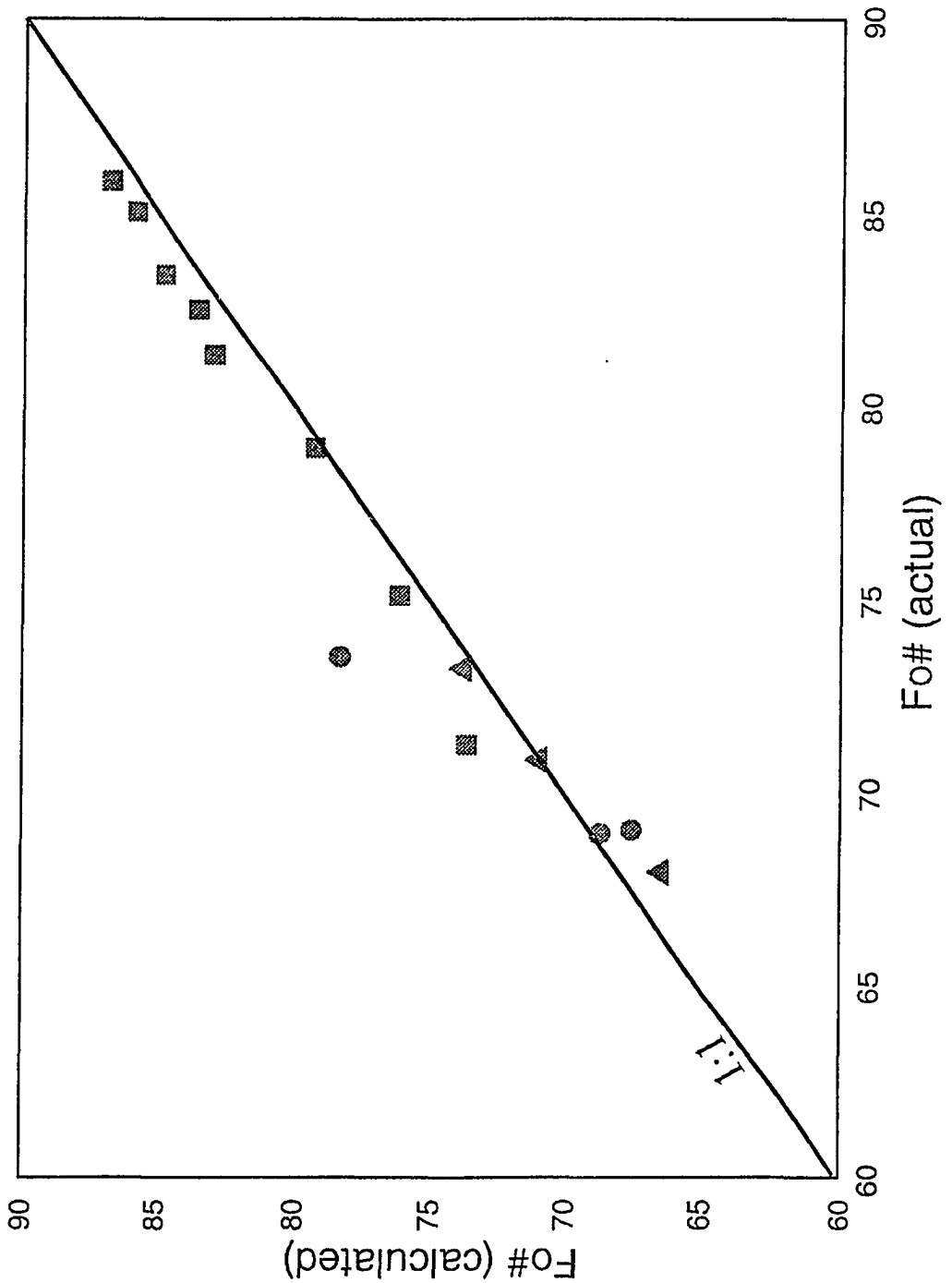

basanite data range from 1224° to 1089 °C; the DVDP2 hawaiite data ranges from 1104° to 1049 °C; and the 83415 Ne-hawaiite data ranges from 1104° to 1049 °C (see Table 1). The slope of the line plotted through the data set is one. For all three rock types calculated and actual Fo# are the same verifying that equilibrium between olivine and melt was achieved in my experiments.

Loss of Volatiles

Volatile components of a sample such as Na_2O and P_2O_5 can be lost in melting experiments above 1000 °C. They may also be lost when samples are analyzed by the electron microprobe. Little can be done to reduce volatile loss in the furnace, but when collecting data with the electron microprobe a larger beam size and two to three second analysis minimize volatization. Alternatively, a smaller beam size can be used if the beam is moved rapidly and continuously during analysis. Volatile loss in microprobe analysis is most pronounced with the glasses. The magnitude of volatile loss can be estimated by comparing the concentrations of volatile elements in glasses from experiments where the entire sample melted with their concentrations in the starting material

Figure 7 is a plot of weight percent (wt%) Na_2O content in anorthoclase phonolite glasses as a function of

Table 1: Fo# calculated and actual for basanite, DVDP2 hawaiite, and 83415 Ne-hawaiite

Sample	Temp (°C)	Cal. Fo#	Act. Fo#
Basanite	1224	85.80	86.82
	1197	85.00	85.83
	1177	83.38	84.73
	1160	82.47	83.47
	1138	81.30	82.90
	1120	78.90	79.26
	1104	75.10	76.14
	1089	71.20	73.67
DVDP2	1104	73.20	73.79
	1089	70.80	70.93
	1049	67.90	66.40
83415	1104	73.50	78.29
	1089	68.90	68.72
	1049	69.00	67.57

cal=calculated and act=actual

Figure 7: Na_2O (wt%) of glass compositions from the anorthoclase phonolite versus Temperature (^{o}C). Solid line represents the starting concentration of Na_2O (wt% = 7.77) from the anorthoclase phonolite (Moore, 1986). Filled triangles represent average measured Na_2O concentrations from single experimental temperatures.

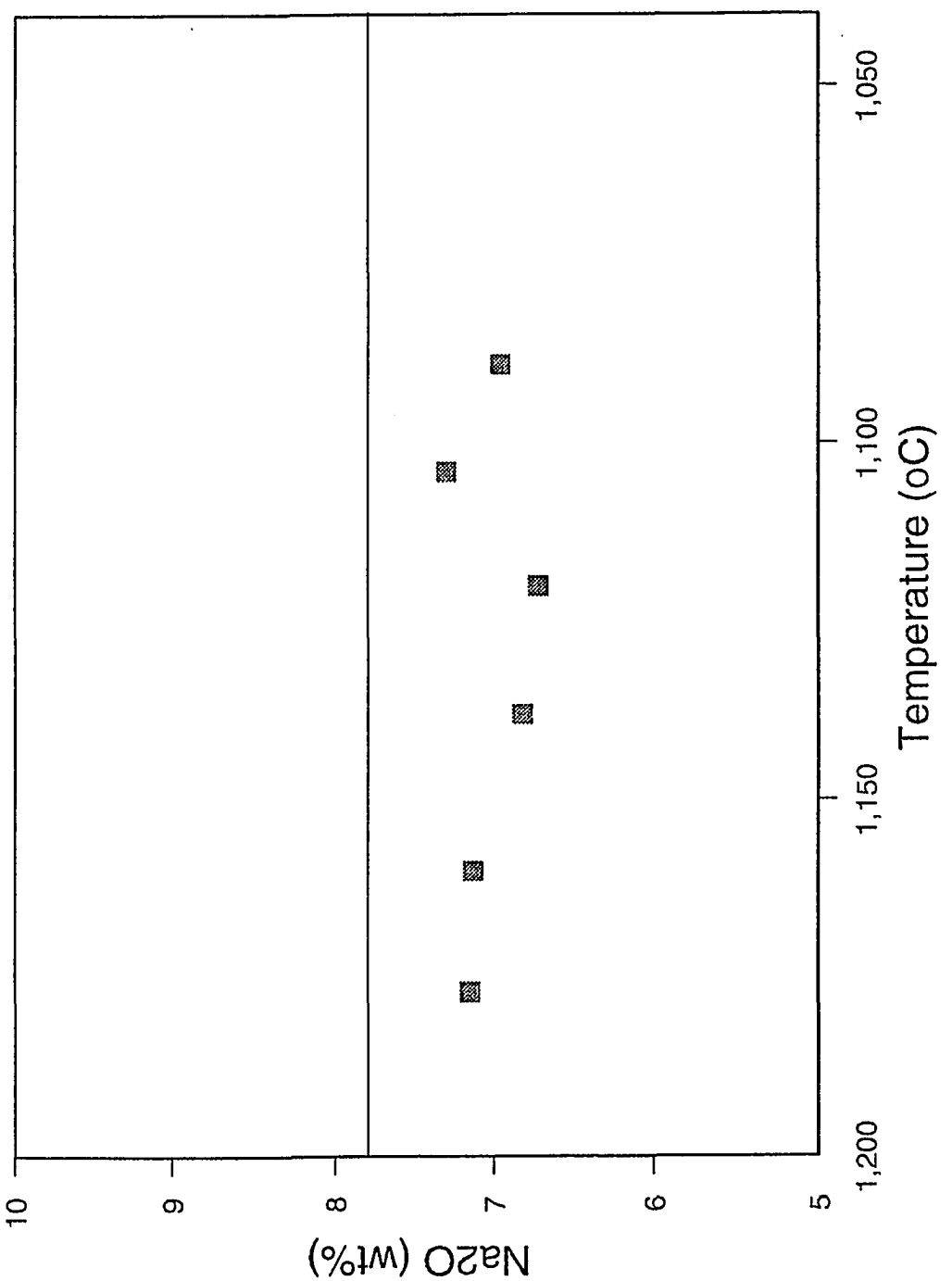

temperature (^{o}C). The solid line at 7.77 wt% is the "weight percent" of Na_2O in the anorthoclase phonolite whole-rock analysis from Moore (1986). This figure is based on data given in Table 2, where temperature, wt% of Na_2O in the glass, wt% of Na_2O in the starting material, and the loss of Na_2O for each experiment are given. Loss on Na_2O occurs in most experiments, probably both during the experiment and during data collection. The total amount of Na_2O lost is less than 10% of the amount present (9.74%).

Figure 8 is a plot of weight percent (wt%) P_2O_5 versus Temperature (^{o}C) for the anorthoclase phonolite. The solid line at 0.56 wt% is the "weight percent" of P_2O_5 in the anorthoclase phonolite whole-rock analysis from Moore (1986). This figure is based on data given in Table 3, where temperature, content of P_2O_5 in glass, wt% of P_2O_5 in the starting material, and the loss of P_2O_5 for each experiment is given. Loss of P_2O_5 occurs in most experiments, primarily during the experiment (Kilinc et al., 1983). The amount lost is more than 40% of the amount present (43.15%).

Table 2. Na_2O loss in anorthoclase phonolite experiments

Temp (^oC)	Na_2O^{gl}	Na_2O^{in}	wt loss*
1177	7.15	7.77	-0.62
1160	7.13	7.77	-0.64
1138	6.82	7.77	-0.95
1120	6.72	7.77	-1.05
1104	7.30	7.77	-0.47
1089	6.96	7.77	-0.81

Average wt loss = -0.76%

Total loss of Na_2O in terms of percent of the amount present 9.74%

* = where wt loss = wt% Na_2O^{gl} - wt% Na_2O^{in}

Figure 8: P_2O_5 (wt%) of glass compositions from the anorthoclase phonolite versus Temperature (^{o}C). Solid line represents the starting concentration of P_2O_5 (wt% = 0.56) from the anorthoclase phonolite (Moore, 1986). Filled triangles represent average measured P_2O_5 concentrations from single experimental temperatures.

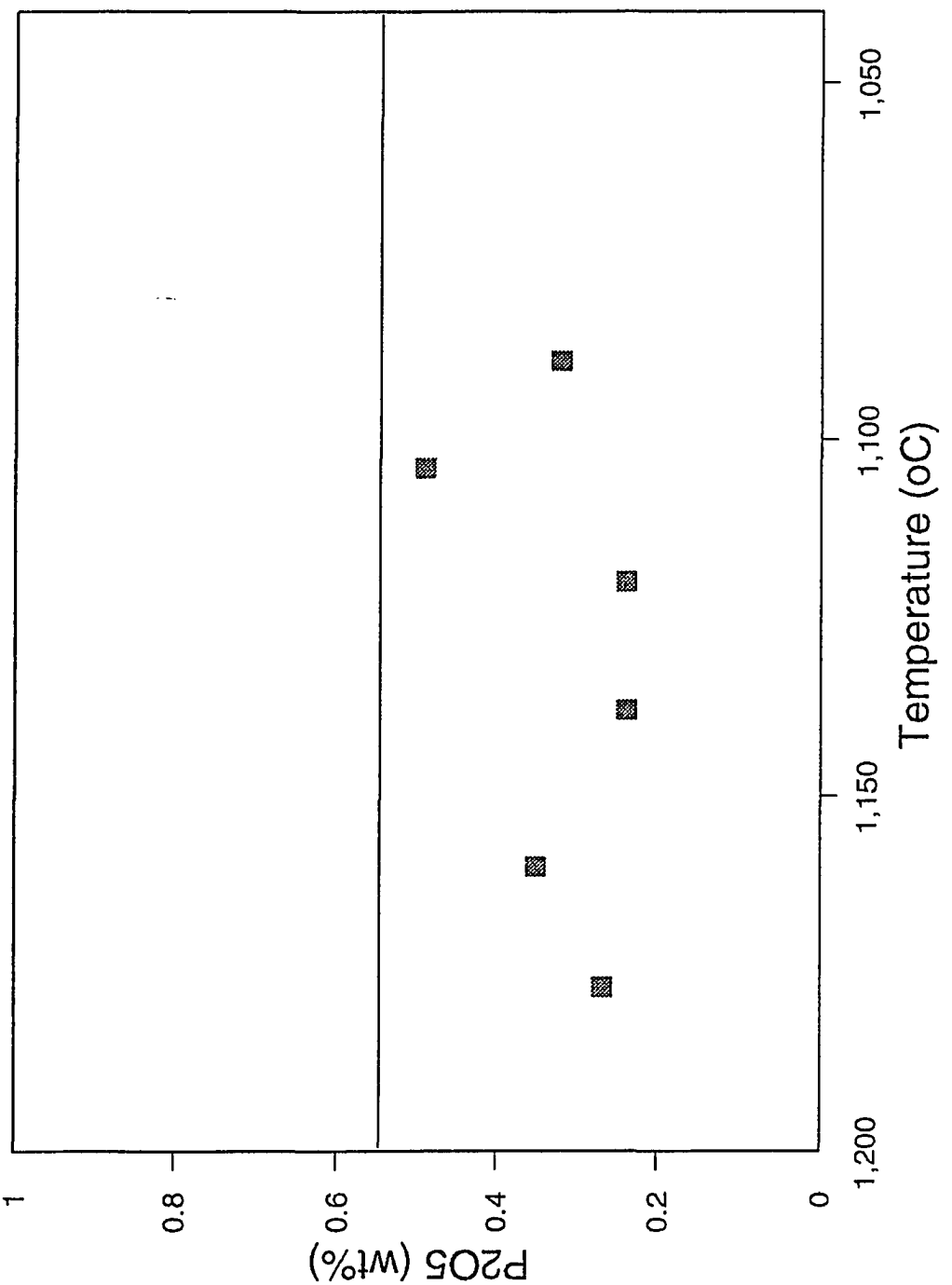

Table 3: P_2O_5 loss in anorthoclase phonolite experiments

Temp (^oC)	$P_2O_5^{gl}$	$P_2O_5^{in}$	wt loss*
1177	0.27	0.56	-0.29
1160	0.35	0.56	-0.21
1138	0.24	0.56	-0.32
1120	0.24	0.56	-0.32
1104	0.49	0.56	-0.07
1089	0.32	0.56	-0.24

Average wt loss = -0.24%

Total loss of P_2O_5 in terms of percent of the amount present 43.15%

* = where wt loss = wt% $P_2O_5^{gl}$ - wt% $P_2O_5^{in}$

ANALYTICAL PROCEDURE

Electron Microprobe

The four-channel Cameca SX-50 Electron Microprobe at Purdue University was used to determine chemical compositions of minerals and glasses. Methods for preparing microprobe thin sections are given in Appendix B. The parameters for the analyses were accelerating voltage of 15 kV and beam current of 0.20×10^{-7} amps. A one micron diameter beam was used over a twenty second (integrated) counting time for all elements except Na_2O; a 10-second integration time was used for Na_2O to minimize its volatilization under the beam. The sequence of analysis was Na_2O, FeO, K_2O, SiO_2; MgO, MnO, P_2O_5, Al_2O_3; TiO_2, CaO, NiO, and Cr_2O_3. The concentrations of each oxide was determined using the correction procedures outlined by Bence and Albee (1968) and Albee and Ray (1970).

Microprobe standards were provided by Dr. R. Sack and Dr. D. Ebel of Purdue University and by Cameca. Table 4 lists the standards and their compositions. Total iron is reported as FeO. Table 5 lists the standard deviation values for each oxide.

Table 4: Microprobe standards and compositions

	SiO_2	TiO_2	Al_2O_3	Cr_2O_3	FeO	MnO	MgO	NiO_2	CaO	Na_2O	K_2O	P_2O_5
Amelia Albite (Na)	68.73		19.43							11.75	0.09	
USP05 (Ti)		40.92			42.87		15.58					
Orthoclase (K)	64.39		18.58							1.14	14.92	
Shallow Water Enstatite (Mg, Si)	59.98		0.26				39.96					
Hort (Mn)	7.31				26.73	3.07	6.91		0.10			
Fayalite (Fe)	6.44				42.60							
Anorthite (Ca, Al)	43.20		36.64						20.16			
Mirot apatite (P)									27.59			7.77
NIOL (Ni)	28.30							71.15				
52NL11 (Cr)	0.10	0.49	19.40	44.48	21.49	0.18	11.60					

Table 5: Precision of Microprobe analysis in terms of 1 standard deviation.

Oxides	1	# of analyses
SiO_2	0.28	14
TiO_2	0.21	5
Al_2O_3	0.14	14
Cr_2O_3	0.00	2
FeO*	0.48	8
MnO	0.05	6
MgO	0.16	14
NiO	0.08	3
CaO	0.20	14
Na_2O	0.12	12
K_2O	0.06	5
P_2O_5	0.02	3

X-Ray Fluorescence

The bulk compositions of the DVDP2 basanite, DVDP2 hawaiite, Tent Island Ne-hawaiite, and Mt. Erebus anorthoclase phonolite used in this study came from published XRF analyses. DVDP2 basanite and DVDP2 hawaiite are from Kyle (1981) and the Ne-hawaiite and the anorthoclase phonolite are from Moore (1986). Table 6 lists the compositions of these rocks.

DATA PRESENTATION

Mineralogy and Chemistry of the Rocks

Basanite

The basanite from DVDP2 is an alkaline basalt composed of olivine, Fo_{74} to Fo_{87}; clinopyroxene, En_{34} to En_{42}; plagioclase, An_{38} to An_{71}; and apatite. Representative mineral analyses of olivine, clinopyroxene, plagioclase, alkali feldspar, and apatite are given in Tables 7-10. For the full data set see Appendix C, Tables 1-4. The bulk composition of the basanite is given in Table 6.

Table 6: XRF whole rock data for all for rock types

	DVDP2+ basanite	DVDP2+ hawaiite	83415* Ne-hawaiite	83452* Phonolite
SiO_2	41.68	47.27	49.53	55.00
TiO_2	4.06	2.95	2.12	1.36
Al_2O_3	12.96	17.61	19.87	18.29
Fe_2O_3	3.06	3.35	0.00	0.00
Cr_2O_3	0.00	0.00	0.00	0.00
FeO	8.48	6.06	7.41	6.59
MnO	0.18	0.21	0.17	0.27
MgO	12.13	3.72	3.00	1.64
NiO	0.00	0.00	0.00	0.00
CoO	0.00	0.00	0.00	0.00
CaO	11.32	7.76	6.93	3.34
Na_2O	3.16	6.07	6.22	7.77
K_2O	1.48	3.11	3.00	4.39
P_2O_5	0.84	0.81	0.85	0.56
SrO	0.00	0.00	0.00	0.00
BaO	0.00	0.00	0.00	0.00
Total	99.35	98.92	99.10	99.21

+ = data from Kyle (1981)
* = data from Moore (1986)

Table 7: Representative analysis of olivine from basanite

	4r	2c	c	r
SiO_2	38.77	38.14	39.42	39.21
TiO_2	0.01	0.04	0.00	0.03
Al_2O_3	0.09	0.08	0.06	0.03
Fe_2O_3	0.00	0.00	0.00	0.00
Cr_2O_3	0.00	0.00	0.00	0.00
FeO*	16.41	18.74	11.63	15.63
MnO	0.24	0.26	0.08	0.19
MgO	42.49	40.41	46.52	43.37
NiO	0.11	0.14	0.28	0.16
CoO	0.00	0.00	0.00	0.00
CaO	0.28	0.21	0.23	0.18
Na_2O	0.03	0.00	0.02	0.03
K_2O	0.00	0.01	0.00	0.00
P_2O_5	0.02	0.01	0.07	0.07
SrO	0.00	0.00	0.00	0.00
BaO	0.00	0.00	0.00	0.00
TOTAL	98.45	98.04	98.30	98.90
Fo	82.32	79.04	87.50	83.33
Fa	17.68	20.60	12.50	16.67

FeO* = total iron
c = core analysis, r = rim analysis
Fo=forsterite, Fa=fayalite

Table 8: Representative analysis of clinopyroxene from basanite

	c	r	c	r
SiO_2	44.72	44.51	44.77	40.12
TiO_2	3.22	3.19	3.25	6.37
Al_2O_3	8.74	9.05	9.56	11.53
Fe_2O_3	0.00	0.00	0.00	0.00
Cr_2O_3	0.00	0.00	0.00	0.00
FeO^*	5.34	5.42	6.42	6.77
MnO	0.09	0.01	0.04	0.00
MgO	12.80	12.49	11.51	10.48
NiO	0.09	0.06	0.02	0.03
CoO	0.00	0.00	0.00	0.00
CaO	22.55	22.56	21.97	22.90
Na_2O	0.59	0.54	1.10	0.46
K_2O	0.02	0.01	0.00	0.00
P_2O_5	0.02	0.01	0.00	0.02
SrO	0.00	0.00	0.00	0.00
BaO	0.00	0.00	0.00	0.00
TOTAL	98.17	97.86	98.62	98.69
En	39.78	39.44	37.36	34.09
Fs	9.39	9.44	11.49	12.50
Wo	50.83	51.11	51.15	53.41
En^+	43.37	43.03	40.88	39.26
Fs^+	10.24	10.30	12.58	14.38
Wo^+	46.39	46.67	46.54	46.41

FeO^* = total iron
c = core analysis, r = rim analysis
En=enstatite, Fs=ferrosilite, Wo=wollastonite
En^+, Fs^+, Wo^+ = Ca Tschermak ($CaAl_2SiO_6$) corrected

Table 9: Representative analysis of plagioclase from the basanite

Hole#	1	1	2	2	2	3	3	3	5	5	6
An#	27	29	7	15	20	3	13	23	4	9	3
SiO_2	50.35	49.60	49.18	50.23	50.29	50.71	50.58	56.62	50.68	51.28	50.91
TiO_2	0.11	0.30	0.26	0.22	0.19	0.29	0.17	0.17	0.19	0.13	0.27
Al_2O_3	30.92	31.60	31.54	30.78	30.69	30.61	30.52	27.19	30.90	30.56	30.70
Fe_2O_3	0.00	0.00	0.00	0.00	0.00	0.00	0.00	0.00	0.00	0.00	0.00
Cr_2O_3	0.00	0.00	0.00	0.00	0.00	0.00	0.00	0.00	0.00	0.00	0.00
FeO^*	0.33	0.47	0.53	0.39	0.48	0.44	0.59	0.27	0.38	0.38	0.30
MnO	0.00	0.02	0.00	0.00	0.00	0.04	0.01	0.00	0.00	0.04	0.01
MgO	0.04	0.03	0.02	0.04	0.05	0.03	0.05	0.02	0.05	0.04	0.00
NiO	0.00	0.00	0.05	0.02	0.00	0.00	0.00	0.05	0.01	0.00	0.00
CoO	0.00	0.00	0.00	0.00	0.00	0.00	0.00	0.00	0.00	0.00	0.00
CaO	13.11	14.16	14.42	13.15	12.84	13.02	12.98	7.95	13.07	12.63	13.09
Na_2O	3.79	3.34	2.97	3.80	4.03	3.85	3.88	6.76	3.99	4.06	3.78
K_2O	0.27	0.18	0.16	0.20	0.31	0.27	0.26	0.57	0.32	0.28	0.20
P_2O_5	0.06	0.06	0.04	0.02	0.03	0.08	0.07	0.01	0.05	0.04	0.06
SrO	0.00	0.00	0.00	0.00	0.00	0.00	0.00	0.00	0.00	0.00	0.00
BaO	0.00	0.00	0.00	0.00	0.00	0.00	0.00	0.00	0.00	0.00	0.00
TOTAL	98.97	99.75	99.15	98.82	98.91	99.35	99.09	99.61	99.63	99.41	99.31
An	64.36	69.31	71.72	65.00	62.38	64.00	63.37	38.00	63.37	62.00	64.65
Ab	33.66	29.70	27.27	34.00	35.64	34.00	34.65	59.00	34.65	36.00	34.34
Or	1.98	0.99	1.01	1.00	1.98	2.00	1.98	3.00	1.98	2.00	1.01

FeO^* = total iron
An = anorthite, Ab = albite, Or = orthoclase

Table 10: Representative analysis of apatite from the basanite

Hole#	2
An#	12
SiO_2	0.34
TiO_2	0.06
Al_2O_3	0.03
Fe_2O_3	0.00
Cr_2O_3	0.00
FeO^*	0.26
MnO	0.04
MgO	0.32
NiO	0.00
CoO	0.00
CaO	54.37
Na_2O	0.00
K_2O	0.01
P_2O_5	40.97
SrO	0.00
BaO	0.00
TOTAL	96.38

FeO^* = total iron

Some olivine grains display weak reverse zoning and others have normal zoning. The clinopyroxenes are predominantly homogeneous but one analyzed grain did display weak zoning. All the feldspar grains are laths in the groundmass and were too small to probe to determine if there is any zonation in composition.

DVDP2 Hawaiite

The DVDP2 hawaiite is a vesicular alkaline basalt composed of olivine, Fo_{85}; clinopyroxene, En_{30} to En_{41}; kaersutite; plagioclase; An_{27} to An_{57}; apatite; and opaques. The bulk composition of the hawaiite is given in Table 6. Representative analyses of olivine, clinopyroxene, kaersutite, plagioclase, and apatite are given in Tables 11-15. For the full data set see Appendix C, Tables 5-9.

Olivine displayed normal zoning. Clinopyroxene displays weak reverse zoning. All the feldspar grains are laths in the groundmass and too small to analyze for compositional zonation. The amphibole phase, kaersutite, is uniform in composition throughout the thin section.

Table 11: Representative olivine compositions from the DVDP2 hawaiite

Hole#	4	4
An#	13	14
SiO_2	39.67	39.41
TiO_2	0.00	0.00
Al_2O_3	0.04	0.06
Fe_2O_3	0.00	0.00
Cr_2O_3	0.00	0.00
FeO*	13.47	13.41
MnO	0.17	0.27
MgO	45.00	44.89
NiO	0.31	0.22
CoO	0.00	0.00
CaO	0.14	0.18
Na_2O	0.03	0.00
K_2O	0.01	0.00
P_2O_5	0.00	0.07
SrO	0.00	0.00
BaO	0.00	0.00
TOTAL	98.83	98.51
Fo	85.79	85.86
Fa	14.21	14.14

FeO* = total iron
Fo = forsterite, Fa = fayalite

Table 12: Representative analysis of clinopyroxene from DVDP2 hawaiite

	r	c	r	i/c
SiO_2	43.27	44.17	43.62	44.37
TiO_2	3.73	3.06	3.60	2.88
Al_2O_3	9.16	9.32	8.43	8.86
Fe_2O_3	0.00	0.00	0.00	0.00
Cr_2O_3	0.00	0.00	0.00	0.00
FeO*	7.88	8.44	8.24	10.04
MnO	0.14	0.24	0.25	0.27
MgO	10.89	10.33	11.00	9.34
NiO	0.03	0.00	0.02	0.02
CoO	0.00	0.00	0.00	0.00
CaO	22.10	21.63	22.31	21.24
Na_2O	0.72	0.88	0.61	1.10
K_2O	0.00	0.00	0.01	0.00
P_2O_5	0.03	0.04	0.08	0.03
SrO	0.00	0.00	0.00	0.00
BaO	0.00	0.00	0.00	0.00
TOTAL	97.94	98.10	98.15	98.15
En	35.20	33.71	34.62	31.03
Fs	13.97	15.43	14.84	18.39
Wo	50.84	50.86	50.55	50.57
En^+	38.65	36.88	37.95	33.75
Fs^+	15.34	16.88	16.27	20.00
Wo^+	46.01	46.25	45.78	46.25

FeO* = total iron
c = core analysis, i/c = intermediate/core analysis
r = rim analysis
En^+, Fs^+, Wo^+ = Ca Tschermak ($CaAl_2SiO_6$) corrected

Table 13: Representative kaersutite compcsitions from the DVDP2 hawaiite

Hole#	1	1	5	5	5	5	5	6	6	6	7	7
An#	1	2	6	7	8	9	10	2	3	4	1	2
	r	r/i	c	r/i	r	i/r	i/c	r	r	r	r	r
SiO_2	37.63	37.64	37.82	37.73	37.51	36.89	38.13	37.96	37.52	37.56	37.31	37.14
TiO_2	5.63	5.94	6.19	5.96	5.93	5.62	5.83	6.11	6.01	5.89	5.51	5.59
Al_2O_3	14.36	14.40	14.05	14.51	14.41	14.95	14.08	13.98	14.11	14.80	14.43	14.71
Fe_2O_3	0.00	0.00	0.00	0.00	0.00	0.00	0.00	0.00	0.00	0.00	0.00	0.00
Cr_2O_3	0.00	0.00	0.00	0.00	0.00	0.00	0.00	0.00	0.00	0.00	0.00	0.00
FeO*	13.10	13.20	10.94	12.54	13.33	12.71	10.99	10.45	10.49	10.27	11.12	11.61
MnO	0.25	0.17	0.17	0.17	0.17	0.18	0.15	0.08	0.17	0.12	0.15	0.22
MgO	10.05	10.14	11.57	10.66	9.99	10.27	11.66	12.08	12.11	11.81	11.10	10.85
NiO	0.00	0.00	0.01	0.01	0.00	0.01	0.02	0.05	0.00	0.05	0.01	0.00
CoO	0.00	0.00	0.00	0.00	0.00	0.00	0.00	0.00	0.00	0.00	0.00	0.00
CaO	11.58	11.70	11.98	11.66	11.50	11.65	11.79	11.83	11.74	12.01	11.51	11.39
Na_2O	2.58	2.52	2.47	2.56	2.48	2.33	2.53	2.36	2.42	2.20	2.47	2.42
K_2O	1.28	1.26	1.25	1.20	1.22	1.16	1.22	1.40	1.38	1.53	1.35	1.19
P_2O_5	0.06	0.06	0.06	0.12	0.03	0.00	0.07	0.06	0.09	0.08	0.04	0.06
SrO	0.00	0.00	0.00	0.00	0.00	0.00	0.00	0.00	0.00	0.00	0.00	0.00
BaO	0.00	0.00	0.00	0.00	0.00	0.00	0.00	0.00	0.00	0.00	0.00	0.00
TOTAL	96.51	97.03	96.51	97.13	96.57	95.75	96.47	96.36	96.04	96.32	95.00	95.18

FeO* = total iron
c = core analysis, i/c = intermediate/core analysis
i/r = intermediate/rim analysis, r = rim analysis

Table 14: Representative analysis of feldspar from the DVDP2 hawaiite

Hole#	3	4	4	4	4	5	7	7	8
An#	6	5	6	7	16	3	11	12	3
SiO_2	56.38	61.45	52.92	53.43	58.18	52.38	55.55	59.24	55.23
TiO_2	0.18	0.12	0.16	0.18	0.12	0.17	0.18	0.14	0.30
Al_2O_3	27.68	25.23	29.68	29.16	26.67	29.74	27.73	26.64	27.30
Fe_2O_3	0.00	0.00	0.00	0.00	0.00	0.00	0.00	0.00	0.00
Cr_2O_3	0.00	0.00	0.00	0.00	0.00	0.00	0.00	0.00	0.00
FeO*	0.54	0.31	0.62	0.61	0.43	0.55	0.65	0.72	0.58
MnO	0.00	0.00	0.03	0.07	0.00	0.05	0.00	0.09	0.02
MgO	0.08	0.03	0.08	0.09	0.06	0.07	0.10	0.21	0.09
NiO	0.00	0.00	0.00	0.00	0.07	0.00	0.08	0.06	0.04
CoO	0.00	0.00	0.00	0.00	0.00	0.00	0.00	0.00	0.00
CaO	8.84	5.42	11.59	10.98	7.85	11.66	9.13	7.52	8.73
Na_2O	6.16	7.30	4.85	5.09	6.80	4.60	5.95	6.46	5.87
K_2O	0.52	1.38	0.40	0.32	0.86	0.30	0.47	0.68	0.55
P_2O_5	0.06	0.03	0.02	0.03	0.20	0.51	0.01	0.10	0.09
SrO	0.00	0.00	0.00	0.00	0.00	0.00	0.00	0.00	0.00
BaO	0.00	0.00	0.00	0.00	0.00	0.00	0.00	0.00	0.00
TOTAL	100.43	101.26	100.34	99.95	101.24	99.53	99.85	101.85	98.78
An	42.42	27.08	42.57	53.00	38.14	57.00	44.44	37.23	43.88
Ab	54.55	64.58	55.45	45.00	60.82	41.00	52.53	58.51	53.06
Or	3.03	8.33	1.98	2.00	1.03	2.00	3.03	4.26	3.06

FeO* = total iron
An = anorthite, Ab = albite, Or = orthoclase

Table 15: Representative apatite composition the DVDP2 hawaiite

Hole#	7	3
An#	10	1
SiO_2	0.39	0.36
TiO_2	0.00	0.10
Al_2O_3	0.02	0.06
Fe_2O_3	0.00	0.00
Cr_2O_3	0.00	0.00
FeO*	0.30	0.30
MnO	0.06	0.11
MgO	0.35	0.32
NiO	0.02	0.00
CoO	0.00	0.00
CaO	55.29	55.90
Na_2O	0.00	0.00
K_2O	0.04	0.01
P_2O_5	40.87	41.25
SrO	0.00	0.00
BaO	0.00	0.00
TOTAL	97.34	98.41

FeO* = total iron

Ne-hawaiite (83415)

The Ne-hawaiite is a porphyritic alkaline basalt composed of olivine, Fo_{65} to Fo_{84}; clinopyroxene, En_{36} to En_{38}; plagioclase, An_{40} to An_{58}; apatite; and opaques. Representative analyses of olivine, clinopyroxene, plagioclase, and apatite are given in Tables 16-19. For the full data set see Appendix C, Tables 10-13. The bulk composition of the Ne-hawaiite is given in Table 6.

The olivine grains display both normal and reverse zoning. The clinopyroxenes are homogeneous. Plagioclase grains have normal zoning in general, but some have weak reverse zoning.

Anorthoclase Phonolite

The anorthoclase phonolite is a vesicular, porphyritic alkaline basalt composed of olivine, Fo_{46} to Fo_{57}; clinopyroxene, En_{34} to En_{41}; anorthoclase Or_{16} to Or_{30}; apatite; and opaques.

The olivine grains display minimal to no zonation. The clinopyroxenes are homogeneous. The bulk composition of the anorthoclase phonolite is given in Table 6. Representative analyses of olivine, clinopyroxene, anorthoclase, and apatite are given in Tables 20-23. For the full data set see Appendix C Tables 14-17.

Table 16: Representative analysis of olivine from the 83415 Ne-hawaiite

	r	c	c	r
SiO_2	37.41	37.03	36.92	37.39
TiO_2	0.09	0.04	0.07	0.08
Al_2O_3	0.04	0.05	0.05	0.08
Fe_2O_3	0.00	0.00	0.00	0.00
Cr_2O_3	0.00	0.00	0.00	0.00
FeO*	25.15	27.80	27.99	25.39
MnO	0.75	0.91	0.68	0.63
MgO	34.90	32.78	32.35	34.66
NiO	0.00	0.00	0.00	0.02
CoO	0.00	0.00	0.00	0.00
CaO	0.43	0.37	0.37	0.41
Na_2O	0.04	0.05	0.04	0.05
K_2O	0.03	0.00	0.01	0.00
P_2O_5	0.06	0.10	0.11	0.12
SrO	0.00	0.00	0.00	0.00
BaO	0.00	0.00	0.00	0.00
TOTAL	98.90	99.13	98.58	98.81
Fo	71.21	67.77	67.32	70.87
Fa	28.79	32.23	32.68	29.13

FeO* = total iron
c = core analysis, r = rim analysis
Fo = forsterite, Fa = fayalite

Table 17: Representative analysis of clinopyroxene from the 83415 Ne-hawaiite

	r	c	r	c
SiO_2	46.16	46.70	47.44	47.99
TiO_2	3.42	2.65	2.56	2.43
Al_2O_3	6.72	6.10	5.88	5.13
Fe_2O_3	0.00	0.00	0.00	0.00
Cr_2O_3	0.00	0.00	0.00	0.00
FeO*	7.68	7.52	7.66	7.60
MnO	0.28	0.23	0.29	0.25
MgO	11.38	11.66	11.87	12.37
NiO	0.00	0.11	0.02	0.05
CoO	0.00	0.00	0.00	0.00
CaO	21.47	21.85	21.34	21.69
Na_2O	0.98	0.87	1.00	0.89
K_2O	0.00	0.00	0.01	0.00
P_2O_5	0.00	0.03	0.03	0.06
SrO	0.00	0.00	0.00	0.00
BaO	0.00	0.00	0.00	0.00
TOTAL	98.08	97.72	98.11	98.47
En	36.57	36.93	37.64	38.39
Fs	13.84	13.36	13.48	13.23
Wo	49.59	49.71	48.88	48.38
En^+	39.16	39.18	39.64	40.46
Fs^+	15.06	14.04	14.20	13.87
Wo^+	45.78	46.78	46.15	45.66

FeO* = total iron
c = core analysis, r = rim analysis
En = enstatite, Fs = ferrosilite, Wo = wollastonite
En^+, Fs^+, Wo^+ = Ca Tschermak ($CaAl_2SiO_6$) corrected

Table 18: Representative analysis of plagioclase from the 83415 Ne-hawaiite

	r	c	r	i	c	r	c
SiO_2	56.36	55.76	55.20	55.98	58.22	55.00	55.38
TiO_2	0.23	0.13	0.17	0.13	0.14	0.07	0.18
Al_2O_3	27.11	27.28	28.12	27.94	26.89	28.62	28.48
Fe_2O_3	0.00	0.00	0.00	0.00	0.00	0.00	0.00
Cr_2O_3	0.00	0.00	0.00	0.00	0.00	0.00	0.00
FeO^*	0.31	0.26	0.29	0.28	0.44	0.25	0.19
MnO	0.01	0.04	0.00	0.04	0.07	0.00	0.00
MgO	0.08	0.05	0.06	0.05	0.06	0.07	0.03
NiO	0.05	0.03	0.00	0.00	0.00	0.00	0.02
CoO	0.00	0.00	0.00	0.00	0.00	0.00	0.00
CaO	8.61	8.87	9.95	9.33	8.13	10.27	10.04
Na_2O	5.92	5.69	5.30	5.64	6.04	5.09	5.25
K_2O	0.68	0.83	0.69	0.77	1.04	0.66	0.69
P_2O_5	0.05	0.01	0.01	0.02	0.02	0.01	0.06
SrO	0.00	0.00	0.00	0.00	0.00	0.00	0.00
BaO	0.00	0.00	0.00	0.00	0.00	0.00	0.00
TOTAL	99.40	98.95	99.78	100.18	101.02	100.05	100.31
An	42.6	43.88	48.98	47.37	40.05	50.65	49.30
Ab	53.06	51.02	46.94	48.42	53.84	45.46	46.69
Or	4.08	5.10	4.08	4.21	6.11	3.90	4.01

FeO^* = total iron
c = core analysis, r = rim analysis
An = anorthite, Ab = albite, Or = orthoclase

Table 19: Representative analysis of apatite from 83415 Ne-hawaiite

SiO_2	0.25
TiO_2	0.03
Al_2O_3	0.03
Fe_2O_3	0.00
Cr_2O_3	0.00
FeO*	0.28
MnO	0.05
MgO	0.24
NiO	0.03
CoO	0.00
CaO	55.54
Na_2O	0.00
K_2O	0.01
P_2O_5	41.47
SrO	0.00
BaO	0.00
TOTAL	97.94

FeO* = total iron

Table 20: Representative analysis of olivine from the anorthoclase phonolite

Hole#	3	5	5	5	5	5	6	6	6	6	6	6
An#	8	6	28	29	30	31	3	19	20	21	22	23
	c	c	c	c	c	c	c	r	i/r	r	r	c
SiO_2	33.66	33.62	33.55	33.58	33.46	33.61	35.36	33.77	33.74	33.75	33.57	33.57
TiO_2	0.00	0.00	0.02	0.02	0.06	0.04	0.00	0.04	0.04	0.11	0.01	0.00
Al_2O_3	0.04	0.01	0.03	0.02	0.05	0.04	0.04	0.02	0.05	0.00	0.05	0.02
Fe_2O_3	0.00	0.00	0.00	0.00	0.00	0.00	0.00	0.00	0.00	0.00	0.00	0.00
Cr_2O_3	0.00	0.00	0.00	0.00	0.00	0.00	0.00	0.00	0.00	0.00	0.00	0.00
FeO*	41.69	41.05	41.47	40.70	41.15	41.03	34.95	41.50	41.53	41.92	41.44	40.93
MnO	2.50	2.68	2.66	2.86	2.52	2.60	2.06	2.68	2.71	2.62	2.55	2.56
MgO	20.85	20.64	20.30	20.71	20.60	20.80	26.69	20.48	20.65	20.53	20.52	20.50
NiO	0.00	0.04	0.03	0.01	0.00	0.05	0.00	0.01	0.10	0.01	0.02	0.00
CoO	0.00	0.00	0.00	0.00	0.00	0.00	0.00	0.00	0.00	0.00	0.00	0.00
CaO	0.54	0.52	0.54	0.52	0.52	0.51	0.48	0.48	0.49	0.52	0.51	0.69
Na_2O	0.04	0.04	0.04	0.03	0.04	0.03	0.02	0.04	0.00	0.02	0.06	0.05
K_2O	0.00	0.00	0.01	0.00	0.00	0.00	0.01	0.00	0.00	0.00	0.00	0.00
P_2O_5	0.06	0.02	0.04	0.02	0.06	0.04	0.06	0.02	0.06	0.08	0.09	0.08
SrO	0.00	0.00	0.00	0.00	0.00	0.00	0.00	0.00	0.00	0.00	0.00	0.00
BaO	0.00	0.00	0.00	0.00	0.00	0.00	0.00	0.00	0.00	0.00	0.00	0.00
TOTAL	99.38	98.63	98.68	98.46	98.46	98.74	99.65	99.04	99.36	99.56	98.83	98.39
Fo	47.14	47.26	46.60	47.564	47.16	47.47	57.65	46.80	46.98	46.62	46.89	47.17
Fa	52.86	52.74	53.40	52.436	52.84	52.53	42.35	53.20	53.02	53.38	53.11	52.84

FeO* = total iron
c = core analysis, i/r = intermediate/rim analysis, r = rim analysis
Fo = forsterite, Fa = fayalite

Table 21: Representative analysis of clinopyroxene from anorthoclase phonolite

	r	i/r	c	c	c	c
SiO_2	50.24	50.39	50.62	48.66	45.80	48.92
TiO_2	1.20	1.08	1.14	1.95	3.33	1.85
Al_2O_3	2.49	2.46	2.48	4.09	7.04	3.98
Fe_2O_3	0.00	0.00	0.00	0.00	0.00	0.00
Cr_2O_3	0.00	0.00	0.00	0.00	0.00	0.00
FeO^*	10.96	10.86	10.82	8.79	9.00	8.39
MnO	0.77	0.80	0.69	0.41	0.41	0.39
MgO	11.46	11.45	11.36	12.88	11.44	13.09
NiO	0.05	0.01	0.01	0.00	0.05	0.00
CoO	0.00	0.00	0.00	0.00	0.00	0.00
CaO	20.51	20.59	20.67	21.17	20.48	21.06
Na_2O	1.09	1.11	1.13	0.71	0.99	0.74
K_2O	0.01	0.00	0.01	0.00	0.00	0.01
P_2O_5	0.03	0.00	0.04	0.12	0.00	0.06
SrO	0.00	0.00	0.00	0.00	0.00	0.00
BaO	0.00	0.00	0.00	0.00	0.00	0.00
TOTAL	98.81	98.75	98.96	98.78	98.54	98.46
En	35.33	35.41	35.19	39.00	36.66	39.75
Fs	19.02	18.84	18.80	14.94	16.19	14.29
Wo	45.65	45.75	46.01	46.07	47.16	45.96
En^+	36.11	35.91	35.71	40.56	39.16	41.11
Fs^+	19.44	19.34	19.23	15.56	17.47	15.00
Wo^+	44.44	44.75	45.05	43.89	43.37	43.89

FeO^* = total iron
c = core analysis, i = intermediate/rim analysis, and r = rim analysis
En = enstatite, Fs = ferrosilite, Wo = wollastonite
En^+, Fs^+, Wo^+ = Ca Tschermak ($CaAl_2SiO_6$) corrected

Table 22: Representative analysis of anorthoclase from the anorthoclase phonolite

	i/c	c	r	i/r	r	i/r	i/c	c
SiO_2	64.50	63.53	63.48	63.04	63.51	62.64	56.16	63.11
TiO_2	0.10	0.12	0.10	0.06	0.07	0.10	1.26	0.10
Al_2O_3	23.28	22.11	21.27	21.53	21.38	21.42	19.84	21.41
Fe_2O_3	0.00	0.00	0.00	0.00	0.00	0.00	0.00	0.00
Cr_2O_3	0.00	0.00	0.02	0.00	0.00	0.00	0.04	0.00
FeO*	0.22	0.17	0.25	0.18	0.22	0.15	5.92	0.15
MnO	0.00	0.02	0.03	0.03	0.00	0.00	0.33	0.00
MgO	0.05	0.00	0.06	0.02	0.02	0.02	0.87	0.00
NiO	0.00	0.03	0.02	0.07	0.00	0.05	0.00	0.02
CoO	0.00	0.00	0.00	0.00	0.00	0.00	0.00	0.00
CaO	3.50	2.92	2.36	2.78	2.53	2.82	1.47	2.64
Na_2O	3.82	6.31	7.28	7.49	7.55	7.62	8.27	7.46
K_2O	2.68	3.49	3.71	3.37	3.81	3.45	5.22	3.61
P_2O_5	0.02	0.03	0.01	0.03	0.01	0.01	0.36	0.04
SrO	0.00	0.00	0.00	0.00	0.00	0.00	0.00	0.00
BaO	0.00	0.00	0.00	0.00	0.00	0.00	0.00	0.00
TOTAL	98.17	98.73	98.59	98.61	99.12	98.27	99.74	98.55
An	26.15	15.73	11.46	13.27	12.00	13.86	6.14	13.13
Ab	50.77	61.80	66.67	67.35	66.00	66.34	66.67	65.66
Or	23.08	22.47	21.88	19.39	22.00	19.80	27.19	21.21

FeO* = total iron
c = core analysis, i/c = intermediate/core analysis
i/r = intermediate/rim analysis, r = rim analysis
An = anorthite, Ab = albite, Or = orthoclase

Table 23: Representative analysis of apatite from the anorthoclase phonolite

SiO_2	0.48	0.48	0.49	0.47	0.45	0.48
TiO_2	0.07	0.04	0.00	0.02	0.06	0.03
Al_2O_3	0.02	0.03	0.03	0.03	0.04	0.02
Fe_2O_3	0.00	0.00	0.00	0.00	0.00	0.00
Cr_2O_3	0.00	0.00	0.00	0.00	0.00	0.00
FeO^*	0.43	0.31	0.24	0.27	0.50	0.26
MnO	0.11	0.20	0.13	0.19	0.21	0.08
MgO	0.11	0.12	0.16	0.16	0.20	0.14
NiO	0.05	0.01	0.00	0.00	0.00	0.00
CoO	0.00	0.00	0.00	0.00	0.00	0.00
CaO	54.58	54.21	55.02	54.31	54.50	54.72
Na_2O	0.00	0.00	0.00	0.00	0.00	0.00
K_2O	0.02	0.02	0.02	0.00	0.01	0.00
P_2O_5	40.78	40.81	41.15	40.34	41.41	39.97
SrO	0.00	0.00	0.00	0.00	0.00	0.00
BaO	0.00	0.00	0.00	0.00	0.00	0.00
TOTAL	96.63	96.23	97.24	95.78	97.37	95.69

FeO^* = total iron

Figures 9-11 are plots of the compositional variations in olivine, clinopyroxene, and feldspars from all four rock types. They were generated using data from Tables 1-3, 5, 6, 8, 10-12, and 15-17 in Appendix C.

EXPERIMENTAL RESULTS

The objective of the experiments reported here is to provide the first set of low pressure (one atmosphere) experimental data on the melts and coexisting minerals of a series of cogenetic alkaline rocks from Mt. Erebus. Table 24 lists the results of these experiments for the basanite, DVDP2 hawaiite, 83415 Ne-hawaiite, and the anorthoclase phonolite. I used multiple regression analysis to calculate the weight percent of each phase (minerals and melt), and to determine the amount of Na_2O and FeO loss. For each temperature a representatie analysis of the melt, the mineral phase(s) if present, and total Na_2O and FeO were regressed against the bulk composition of the sample. The results are reported in Table 24.

Figure 9 a-d: Variation of MgO and FeO in olivines from a) basanite; b) DVDP2 hawaiite; c) 83415 Ne-hawaiite; and d) Anorthoclase phonolite

Natural Olivines

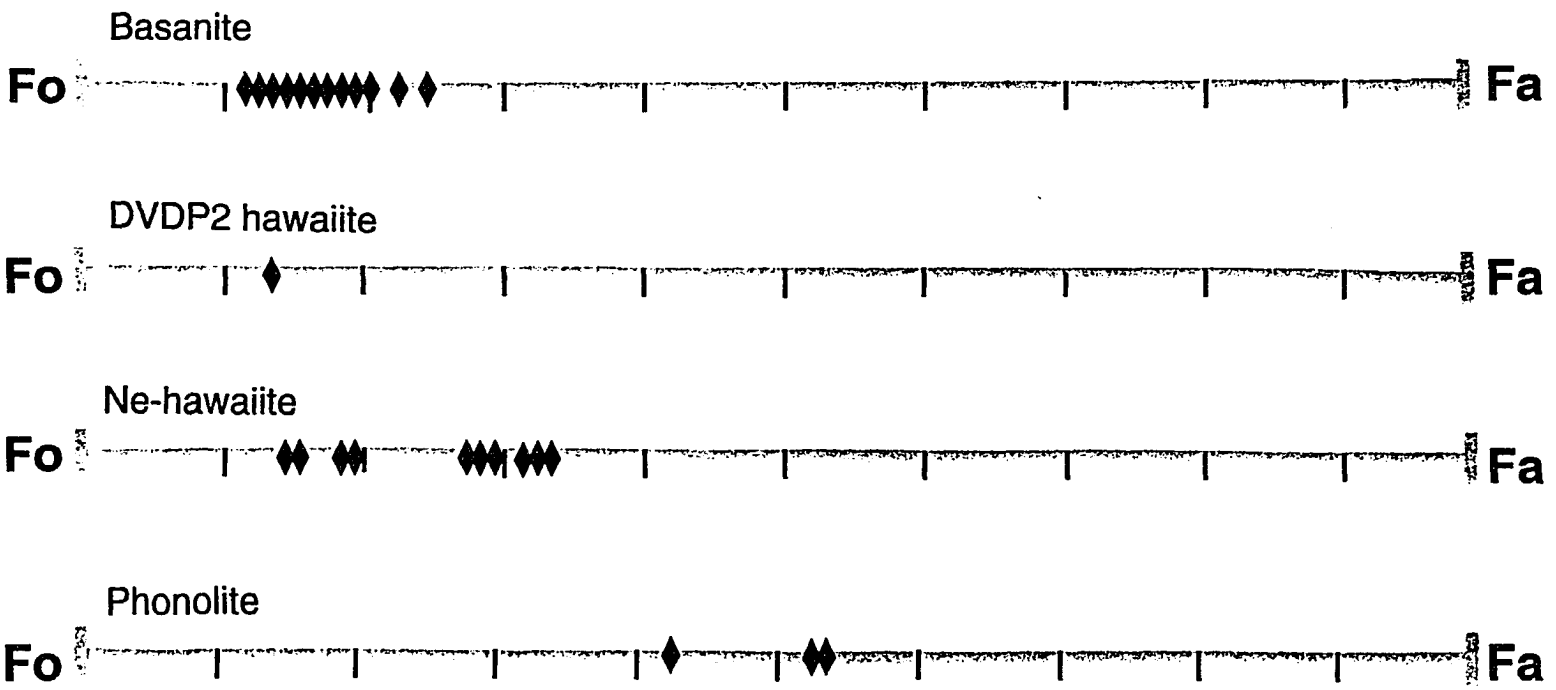

Figure 10 a-d: Pyroxene quadralateral from a) basanite; b) DVDP2 hawaiite; c) 83415 Ne-hawaiite; and d) Anorthoclase phonolite

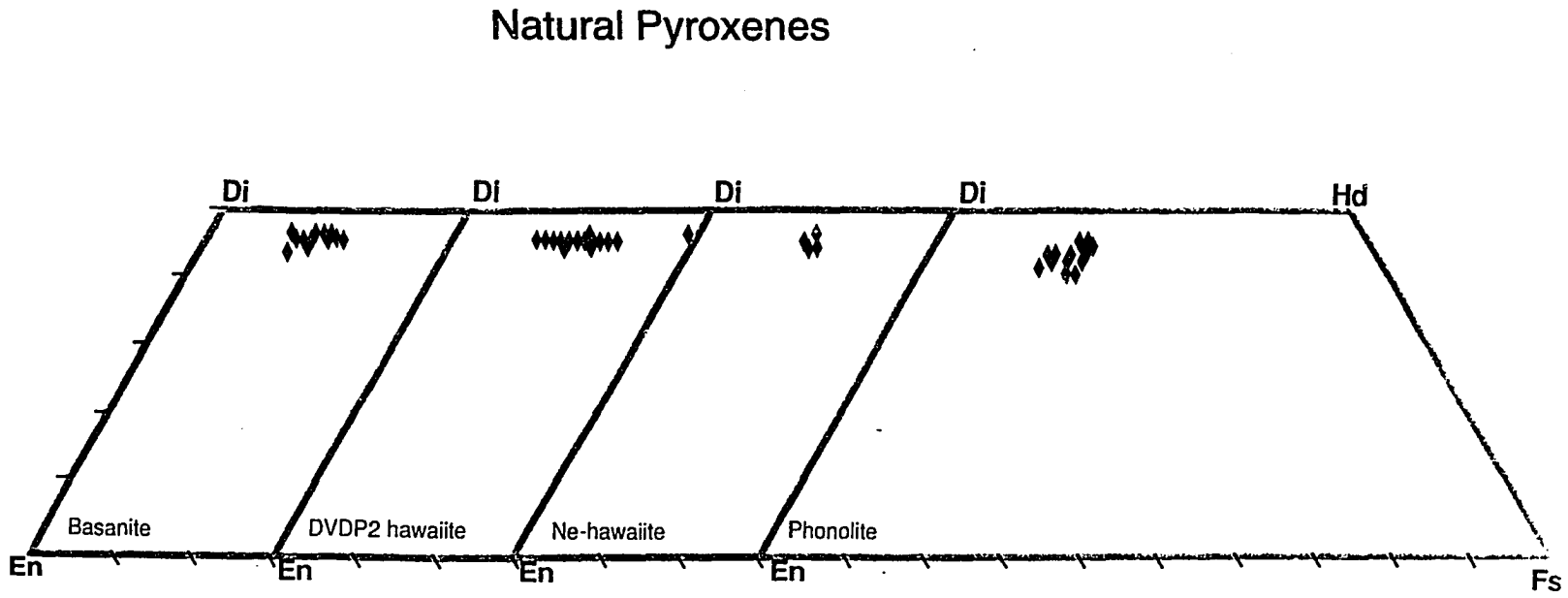

Figure 11 a-d: Ternary feldspar diagram a) basanite; b) DVDP2 hawaiite; c) 83415 Ne-hawaiite; and d) Anorthoclase phonolite

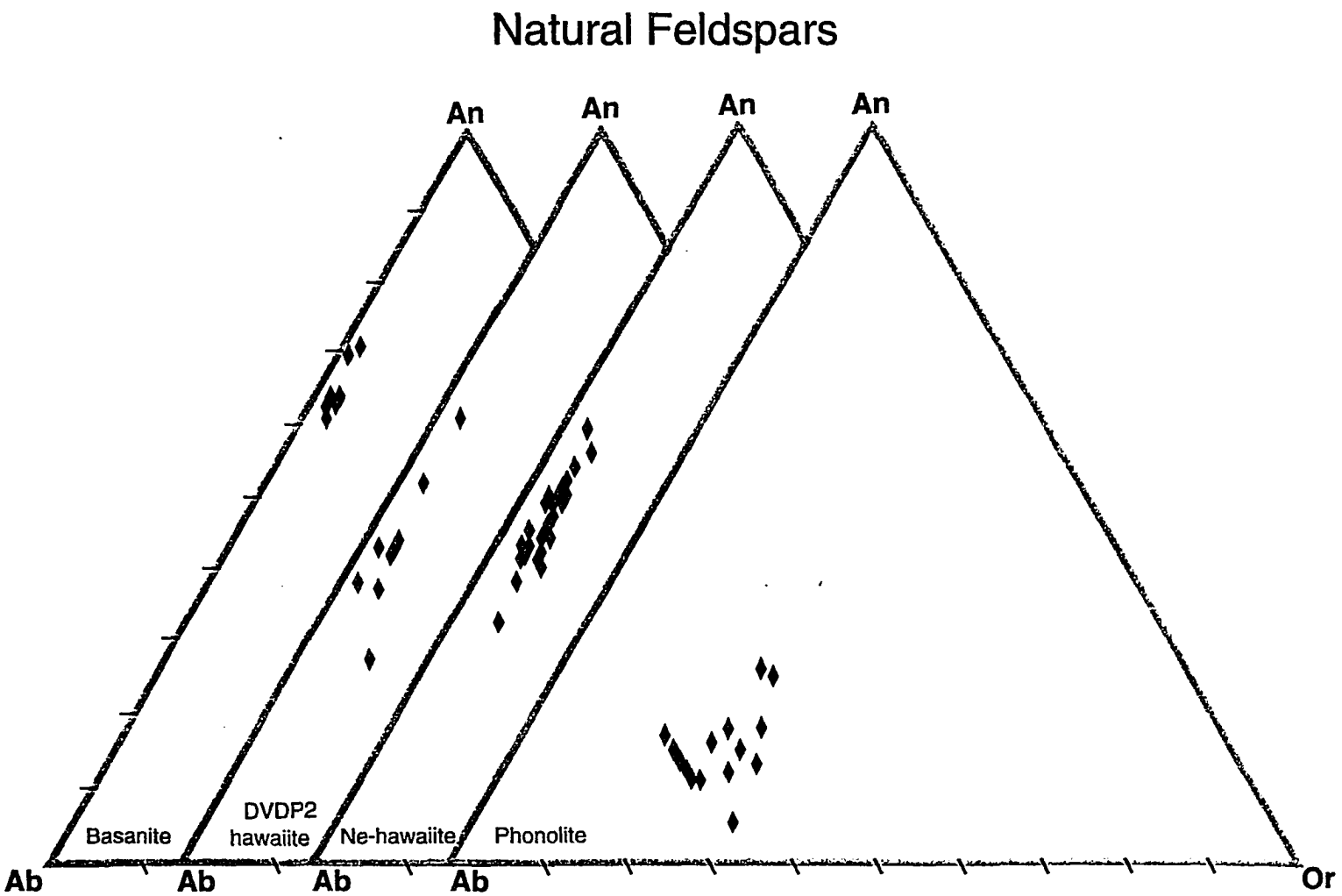

Table 24: Phase assemblages of the one atmosphere experiments for all four rock types

Sample Run #	T (°C)	log f_{O2}	Hours	Run Products	Phase proportions (wt%) gl	ol	cpx	pl	Loss (wt%) Na_2O	FeO
Basanite										
11	1224	-8.12	96	gl, ol	90.70	8.30			0.93	
8	1197	-8.38	120	gl, ol	89.70	10.00			0.84	
9	1177	-8.66	120	gl, ol	86.60	13.40			0.50	
10	1160	-8.94	168	gl, ol	85.10	15.10			0.51	
12	1138	-9.23	360	gl, ol, cpx	78.20	15.30	5.50		0.82	
13	1120	-9.53	360	gl, ol, cpx, op	69.80	15.20	13.70		1.17	
15	1104	-9.83	264	gl, ol, cpx, pl, op	42.20	18.60	23.90	13.10	0.60	
Hawaiite DVDP2										
11	1224	-8.12	96	gl	97.90				1.30	
8	1197	-8.38	120	gl	99.60				0.68	
9	1177	-8.66	120	gl	99.80				0.56	
10	1160	-8.94	168	gl	99.60				0.68	
12	1138	-9.23	360	gl	98.62				0.90	
13	1120	-9.53	360	gl	97.70				1.47	
15	1104	-9.83	264	gl, pl, ol, cpx	93.60	1.14	5.39	0.58	0.42	
17	1089	-9.93	840	gl, pl, ol	82.50	2.61	12.86	0.79	0.90	
16	1049	-10.64	1000	gl, pl, ol, cpx, op	61.40	2.97	22.81	8.21	1.08	

Table 24. continued

Sample Run #	T (°C)	log f_{O2}	Hours	Run Products	Phase proportions (wt%) gl	ol	cpx	pl	Loss (wt%) Na_2O	FeO
Ne-hawaiite										
83415										
11	1224	-8.12	96	gl	98.20				0.73	0.94
8	1197	-8.38	120	gl	99.20				0.64	1.05
9	1177	-8.66	120	gl	100.00				0.40	0.50
10	1160	-8.94	168	gl, pl	97.50			1.33	0.87	0.36
12	1138	-9.23	360	gl, pl	91.10			8.07	0.47	0.31
13	1120	-9.53	360	gl	96.20				1.41	0.88
15	1104	-9.83	264	gl, pl, ol	75.30	1.85		21.40	0.98	1.34
17	1089	-9.93	840	gl, pl, ol, op	69.80	2.58		27.02	0.99	0.06
16	1049	-10.64	1000	gl, pl, ol, op	60.20	3.89		34.34	0.78	1.27
Anorthoclase										
phonolite										
9	1177	-8.66	120	gl	97.81				0.78	1.13
10	1160	-8.94	168	gl	97.67				0.81	1.03
12	1138	-9.23	360	gl	96.87				1.16	1.21
13	1120	-9.53	360	gl	97.58				1.21	0.93
15	1104	-9.83	264	gl	98.71				0.56	1.14
17	1089	-9.93	840	gl	98.60				0.91	0.86
16	1049	-10.64	1000	gl, pl	93.05			5.64	0.91	0.49

gl=glass, ol=olivine, cpx=clinopyroxene
pl=plagioclase, op=opaques

Compositional Variation of Melts

Temperature (^{o}C) versus Magnesium number ($Mg_{\#}$)

Because Mg tends to be partitioned into solid phases relative to Fe, which is enriched in residual liquids, the $Mg_{\#}$ decreases as minerals containing MgO and FeO crystallize in a differentiating magma. Therefore, variation of the $Mg_{\#}$ with temperature reflects the effects of decreasing temperature on the differentiation of magmas. The $Mg_{\#}$ was calculated using the following equation:

$$Mg_{\#} = (100)(X_{Mg}/X_{Mg}+X_{Fe})^{melt} \text{ where } Fe = Fe^{+2}$$

Basanite

Experiments with the basanite starting material range in temperature from 1224^{o} to 1104 ^{o}C. Temperature (^{o}C) versus $Mg_{\#}$ is plotted in Figure 12a using the data from Table 25. $Mg_{\#}$ decreases approximately linearly from 68 to 54 and from 54 to 48 over the temperature range of 1224^{o} to 1138 ^{o}C and 1138^{o} to 1104 ^{o}C respectively. The "rate of change" of $Mg_{\#}$ is given by the slope of a tangent to the best fit line in Figure 12a. The slope of the best fit line through the data for 1224^{o} to 1138 ^{o}C is 10.70, and that for data from 1138^{o} to 1104 ^{o}C is 3.33. Varying rates at which

Figure 12a: Plot of Temperature ($_{o}$C) versus Mg$_{\#}$ for the experiments on basanite at one atmosphere.

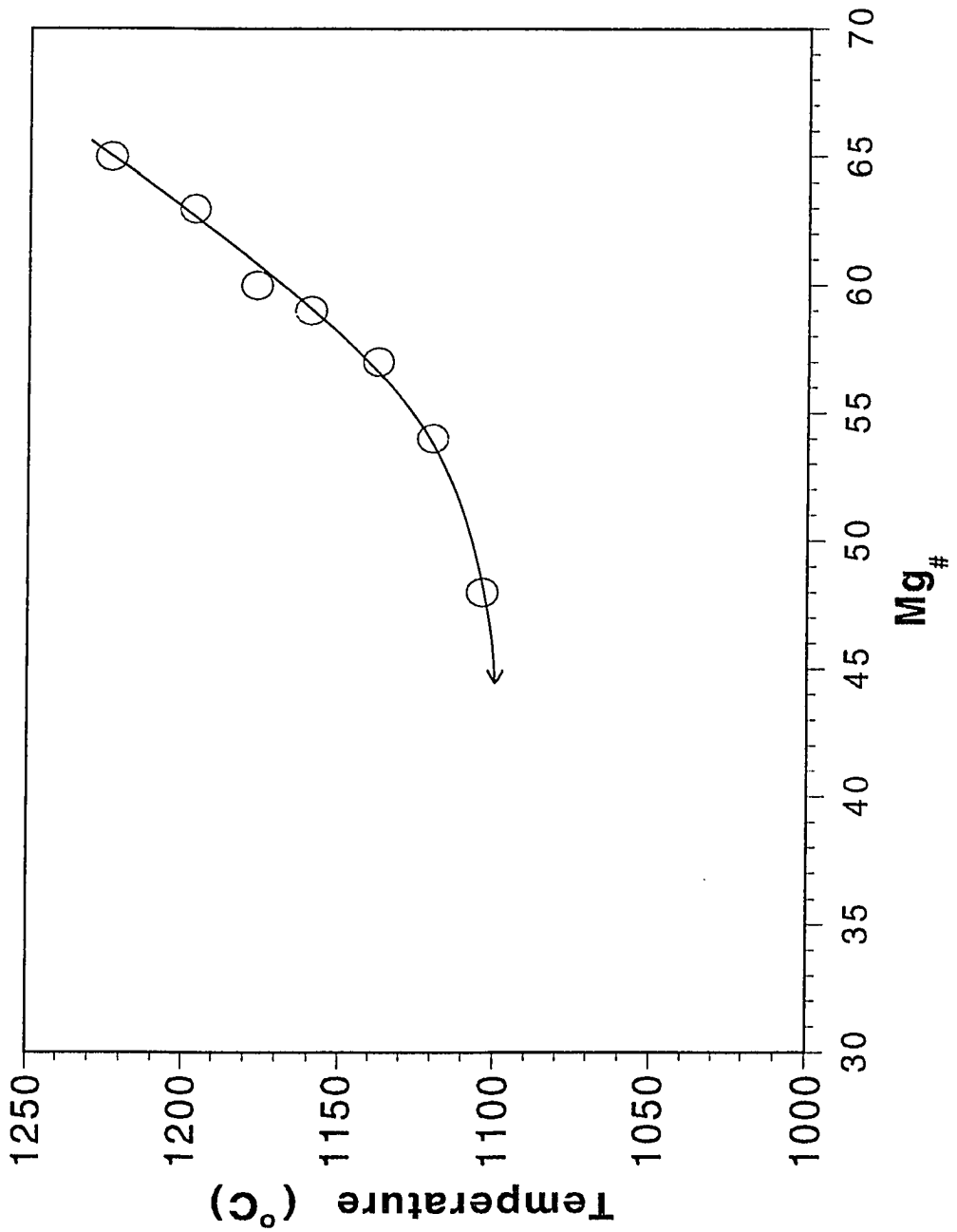

Table 25: Average melt compositions of the basanite (one atmosphere)

Temp (^{o}C)	1224	1197	1177	1160	1138	1120	1104
SiO_2	42.49	42.16	42.05	42.12	42.62	43.04	42.64
TiO_2	4.75	4.72	5.03	5.07	5.18	5.31	5.39
Al_2O_3	13.94	14.06	14.79	15.07	15.82	16.40	15.92
Fe_2O_3*	1.60	1.68	1.65	1.58	1.54	1.46	1.67
Cr_2O_3	0.08	0.06	0.05	0.04	0.02	0.02	0.01
FeO*	8.84	8.79	8.42	8.21	8.38	8.75	8.32
MnO	0.18	0.13	0.16	0.22	0.16	0.18	0.19
MgO	9.02	8.36	7.09	6.49	6.12	5.67	4.23
NiO	0.05	0.04	0.03	0.02	0.02	0.03	0.04
CoO	0.00	0.00	0.00	0.00	0.00	0.00	0.00
CaO	12.26	12.60	12.88	13.15	12.68	11.67	9.48
Na_2O	2.46	2.59	3.07	3.11	2.96	2.76	4.82
K_2O	1.26	1.34	1.50	1.51	1.52	1.33	2.76
P_2O_5	0.74	0.79	0.91	0.92	0.99	0.59	1.87
SrO	0.00	0.00	0.00	0.00	0.00	0.00	0.00
BaO	0.00	0.00	0.00	0.00	0.00	0.00	0.00
TOTAL	97.66	97.31	97.62	97.49	98.00	97.20	97.30
# of analysis	3	4	4	3	2	3	3
$Mg_{\#}$	65	63	60	59	57	54	48

* = FeO and Fe_2O_3 determined using method given by Kilinc et al., 1983.
Each column represents the average of the number of analysis listed at the bottom of the table. Also included is the calculated $Mg_{\#}$. The full data base is given in Appendix E, Table 1.

$Mg_{\#}$ changes with temperature reflects the rate of changing proportions and compositions of crystallizing minerals i.e. steeper the slope, greater the amounts of minerals crystallizing from the in smaller proportions. The higher temperature range (1224^{o} to 1138 ^{o}C) is dominated by the rapid crystallization of olivine. At lower temperatures (1138^{o} to 1104 ^{o}C) clinopyroxene, plagioclase, and olivine are crystallizing from the melt concurrently at a much lower rate.

DVDP2 hawaiite

The temperatures of experiments of the DVDP2 hawaiite range from 1224^{o} to 1049 ^{o}C. Figure 12b which displays Temperature (^{o}C) versus $Mg_{\#}$, was generated using data from Table 26. The $Mg_{\#}$ between 1224^{o} and 1120 ^{o}C does not change and between 1120^{o} to 1049 ^{o}C it decreases from 49 to 39. For this composition no magnesium-rich mineral phase(s) were forming from 1224^{o} to 1120 ^{o}C, but at 1104 ^{o}C olivine, plagioclase, and clinopyroxene begin to simultaneously crystallize from the melt.

Ne-hawaiite (83415)

Experiments with the 83415 Ne-hawaiite were carried out at temperatures from 1224^{o} to 1049 ^{o}C. Figure 12c, generated from Table 27, is a plot of Temperature (^{o}C)

Figure 12b: Plot of Temperature ($_{o}C$) versus $Mg_{\#}$ for the experiments on DVDP2 hawaiite at one atmosphere.

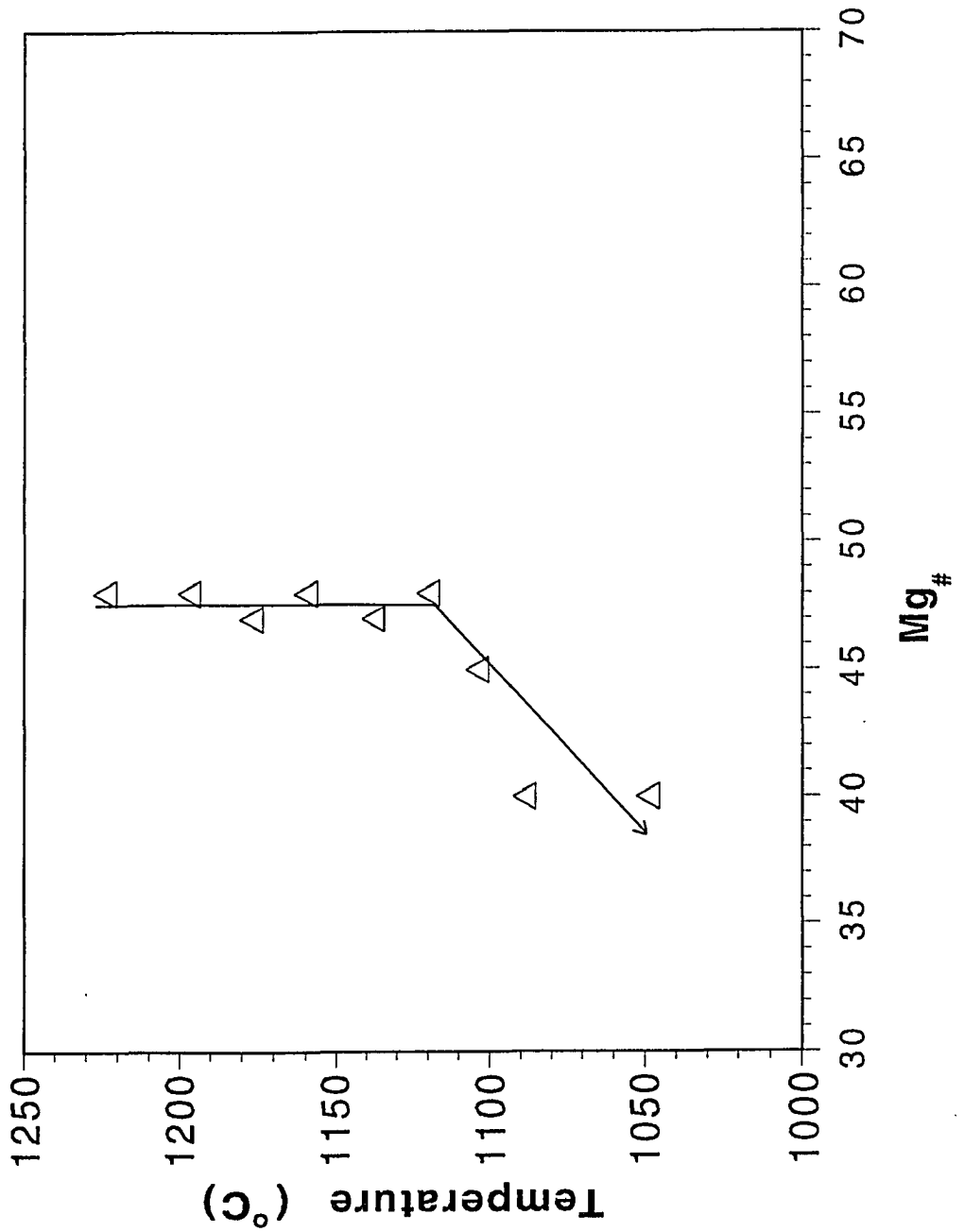

Table 26: Average melt compositions of the DVDP2 hawaiite (one atmosphere)

Temp (^{o}C)	1224	1197	1177	1160	1138	1120	1104	1089	1049
SiO_2	48.31	47.44	47.33	47.41	47.81	48.33	46.80	47.63	49.39
TiO_2	3.15	3.27	3.17	3.11	3.34	3.10	3.36	3.83	3.29
Al_2O_3	18.04	17.80	17.73	17.85	18.16	18.15	17.14	16.67	17.36
Fe_2O_3*	1.45	1.60	1.57	1.47	1.45	1.27	1.52	1.70	1.35
Cr_2O_3	0.03	0.00	0.01	0.02	0.01	0.00	0.01	0.01	0.01
FeO*	7.23	7.31	7.24	7.17	7.26	6.99	7.52	8.07	6.76
MnO	0.22	0.18	0.20	0.19	0.23	0.25	0.21	0.19	0.23
MgO	3.83	3.76	3.82	3.78	3.83	3.88	3.45	3.29	2.41
NiO	0.01	0.00	0.03	0.07	0.03	0.06	0.00	0.01	0.02
CoO	0.00	0.00	0.00	0.00	0.00	0.00	0.00	0.00	0.00
CaO	7.92	7.82	7.77	7.67	7.84	8.01	7.44	7.19	5.78
Na_2O	4.86	5.41	5.52	5.41	5.24	4.71	5.80	5.62	6.16
K_2O	2.62	2.72	2.81	2.82	2.86	2.54	3.07	3.23	3.91
P_2O_5	0.35	0.55	0.68	0.65	0.65	0.20	0.79	0.67	1.22
SrO	0.00	0.00	0.00	0.00	0.00	0.00	0.00	0.00	0.00
BaO	0.00	0.00	0.00	0.00	0.00	0.00	0.00	0.00	0.00
TOTAL	97.85	97.83	97.84	97.62	98.71	97.49	97.09	97.94	97.86
# of analysis	4	2	2	4	3	3	4	3	4
$Mg_{\#}$	49	48	49	48	48	50	45	42	39

* = FeO and Fe_2O_3 determined using method given by Kilinc et al., 1983.
Each column represents the average of the number of analysis listed at the bottom of the table. Also included is the calculated $Mg_{\#}$. The full glass data base is given in Appendix E, Table 2.

Figure 12c: Plot of Temperature ($_{o}C$) versus $Mg_{\#}$ for the experiments on 83415 Ne-hawaiite at one atmosphere.

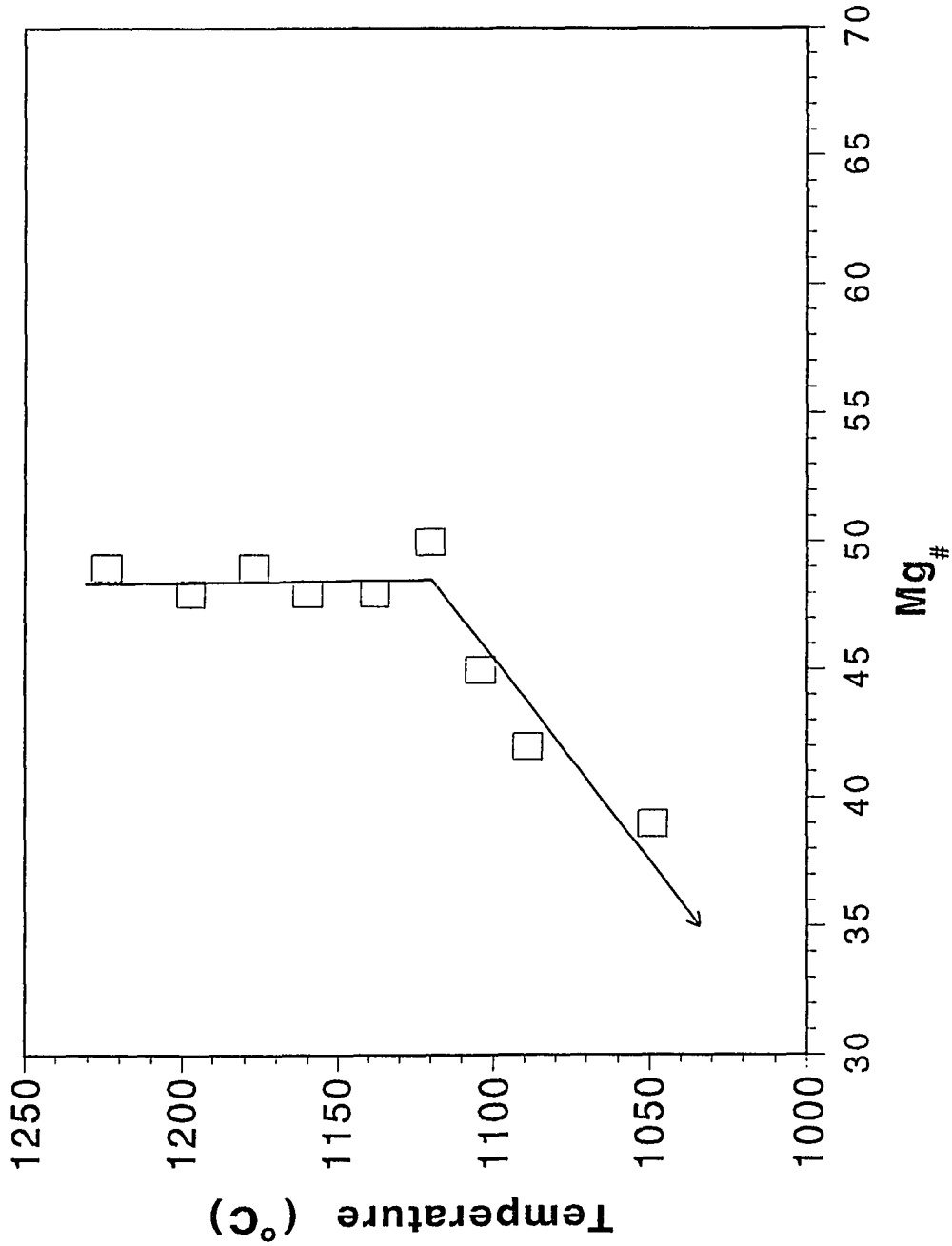

Table 27: Average melt compositions for 83415 Ne-hawaiite (one atmosphere)

Temp(°C)	1224	1197	1177	1160	1138	1120	1104	1089	1049
SiO_2	50.19	49.76	49.35	50.00	49.72	51.43	49.61	48.72	48.70
TiO_2	2.33	2.37	2.37	2.63	2.83	2.29	2.88	3.10	3.25
Al_2O_3*	20.78	20.41	20.21	20.14	19.35	21.02	18.52	17.57	16.97
Fe_2O_3*	1.12	1.10	1.19	1.17	1.32	1.00	1.19	1.60	1.37
Cr_2O_3	0.03	0.00	0.00	0.01	0.01	0.01	0.02	0.01	0.02
FeO*	5.58	5.42	5.84	6.17	6.58	5.89	6.42	7.96	6.90
MnO	0.11	0.16	0.18	0.18	0.20	0.15	0.22	0.21	0.29
MgO	2.93	2.84	2.88	3.16	3.30	3.03	2.99	2.97	2.59
NiO	0.03	0.04	0.03	0.00	0.01	0.01	0.05	0.02	0.00
CoO	0.00	0.00	0.00	0.00	0.00	0.00	0.00	0.00	0.00
CaO	7.16	7.06	6.95	6.80	6.33	6.96	5.77	5.71	5.67
Na_2O	5.59	5.62	5.82	5.43	5.95	5.00	5.59	5.53	6.04
K_2O	2.79	2.69	2.79	2.93	3.18	2.67	3.62	3.60	3.71
P_2O_5	0.55	0.46	0.64	0.79	0.71	0.28	0.97	1.20	1.52
SrO	0.00	0.00	0.00	0.00	0.00	0.00	0.00	0.00	0.00
BaO	0.00	0.00	0.00	0.00	0.00	0.00	0.00	0.00	0.00
TOTAL	99.19	97.94	98.25	99.41	99.51	99.69	97.84	98.00	97.01
# of analysis	1	3	3	4	3	2	3	4	2
$Mg_{\#}$	48	48	47	48	47	48	45	40	40

* = FeO and Fe_2O_3 determined using method given by Kilinc et al., 1983.
Each column represents the average of the number of analysis listed at the bottom of the table. Also included is the calculated $Mg_{\#}$. The full glass data base is given in Appendix E, Table 3.

versus $Mg_{\#}$. $Mg_{\#}$ remains constant at 48 from 1224° to 1120 °C, then decreases rapidly from 48 to 40 from 1120° to 1049 °C. The slope of the best fit line for the temperature range of 1120° to 1049 °C is 4.41. The decrease in the $Mg_{\#}$ of the melt is produced by the crystallization of olivine from 1104° to 1049 °C. Although plagioclase begins to crystallize at 1160 °C it does not consume MgO or FeO from the melt.

Anorthoclase Phonolite

Experiments on the anorthoclase phonolite range in temperature from 1177° to 1049 °C. Figure 12d which shows Temperature (°C) versus $Mg_{\#}$ was generated using data in Table 28. There is no change in the $Mg_{\#}$ between 1177° and 1049 °C, indicating that no mineral phase(s) containing magnesium or iron were crystallizing in this temperature range.

Weight percent Melt (wt%) versus Temperature (°C)

It is possible to estimate the rate of crystallization for a mineral or a group of minerals as a function of temperature. One approach is to calculate the amount a mineral phase(s) crystallize over a range of decreasing temperature. Another way which provides a more general

Figure 12d: Plot of Temperature ($_{o}C$) versus $Mg_{\#}$ for the experiments on anorthoclase phonolite glass at one atmosphere.

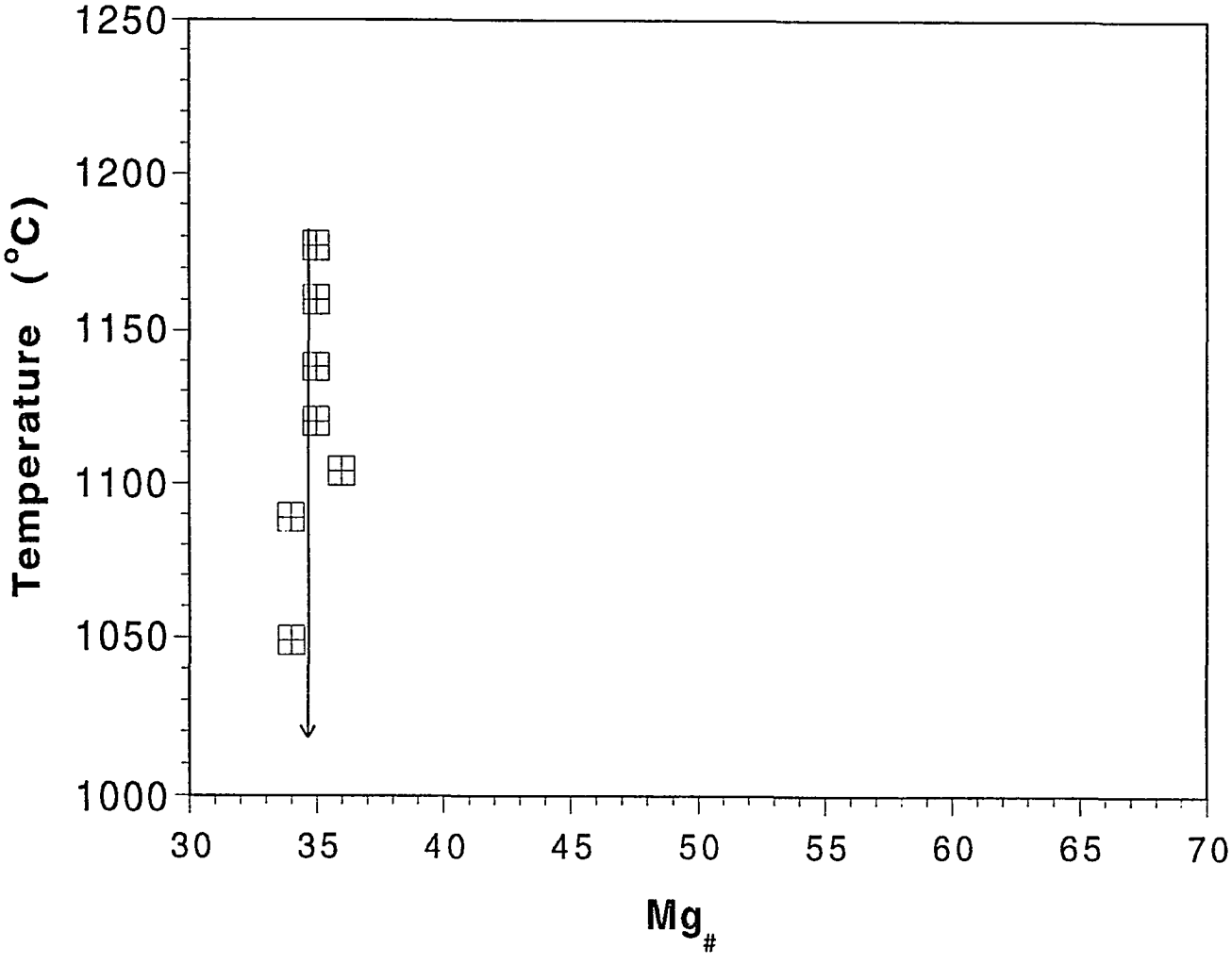

Table 28: Average melt compositions for anorthoclase phonolite (one atmosphere)

Temp (°C)	1177	1160	1138	1120	1104	1089	1049
SiO_2	55.96	56.07	56.55	56.09	55.44	55.58	55.56
TiO_2	1.53	1.48	1.55	1.44	1.48	1.42	1.61
Al_2O_3	19.56	19.52	19.65	19.65	19.40	19.24	18.19
Fe_2O_3*	1.02	1.01	0.95	0.96	0.93	0.99	1.05
Cr_2O_3	0.00	0.00	0.00	0.02	0.01	0.00	0.01
FeO*	4.66	4.78	4.70	4.94	4.68	4.92	5.58
MnO	0.29	0.28	0.27	0.26	0.27	0.28	0.36
MgO	1.42	1.41	1.42	1.45	1.45	1.41	1.64
NiO	0.02	0.02	0.01	0.01	0.03	0.01	0.00
CoO	0.00	0.00	0.00	0.00	0.00	0.00	0.00
CaO	3.34	3.38	3.33	3.43	3.25	3.29	2.87
Na_2O	7.15	7.13	6.82	6.72	7.30	6.96	6.97
K_2O	4.17	4.19	4.14	3.96	4.24	4.11	4.40
P_2O_5	0.27	0.35	0.24	0.24	0.49	0.32	0.45
SrO	0.00	0.00	0.00	0.00	0.00	0.00	0.00
BaO	0.00	0.00	0.00	0.00	0.00	0.00	0.00
TOTAL	99.40	99.63	99.64	99.14	98.97	98.42	98.69
# of analysis	3	8	6	2	4	5	3
$Mg_{\#}$	35	35	35	35	36	34	34

* = FeO and Fe_2O_3 determined using method given by Kilinc et al., 1983.
Each column represents the average of the number of analysis listed at the bottom of the table. Also included is the calculated $Mg_{\#}$. The full glass data base is given in Appendix E, Table 4.

impression of the crystallization of a mineral phase(s) is to examine how the melt fraction of a magma decreases with decreasing temperature. Examples of both of these approaches will be presented in the following figures. For all the Melt (wt%) versus Temperature (^{o}C) plots (Figure 13 a-c) the data are taken from Table 24.

Basanite

Figure 13a shows the wt% of melt versus Temperature (^{o}C) in basanite experiments. Olivine is the only phase crystallizing between 1224^{o} and 1160 ^{o}C. The weight percent of olivine crystallizing from the melt increases from 8.3 wt% to 15.1 wt% respectively (Table 24). The average change in the weight fraction of olivine with crystallization in this temperature interval is 0.11 wt% olivine/^{o}C. When clinopyroxene begins to crystallize with olivine at 1138 ^{o}C the average change in weight percent with crystallization for olivine decreases significantly, from 0.11 to 0.0025 wt% olivine/^{o}C over the temperature range of 1138^{o} to 1120 ^{o}C. Finally when olivine, clinopyroxene, and plagioclase are crystallizing from the melt, olivine reaches a maximum rate of crystallization of 0.21 wt% olivine/^{o}C between 1120^{o} and 1104 ^{o}C.

Figure 13a: Plot of melt (wt%) versus temperature (^{o}C) of the temperature range 1224^{o} to 1104 ^{o}C for basanite one atmosphere experiments.

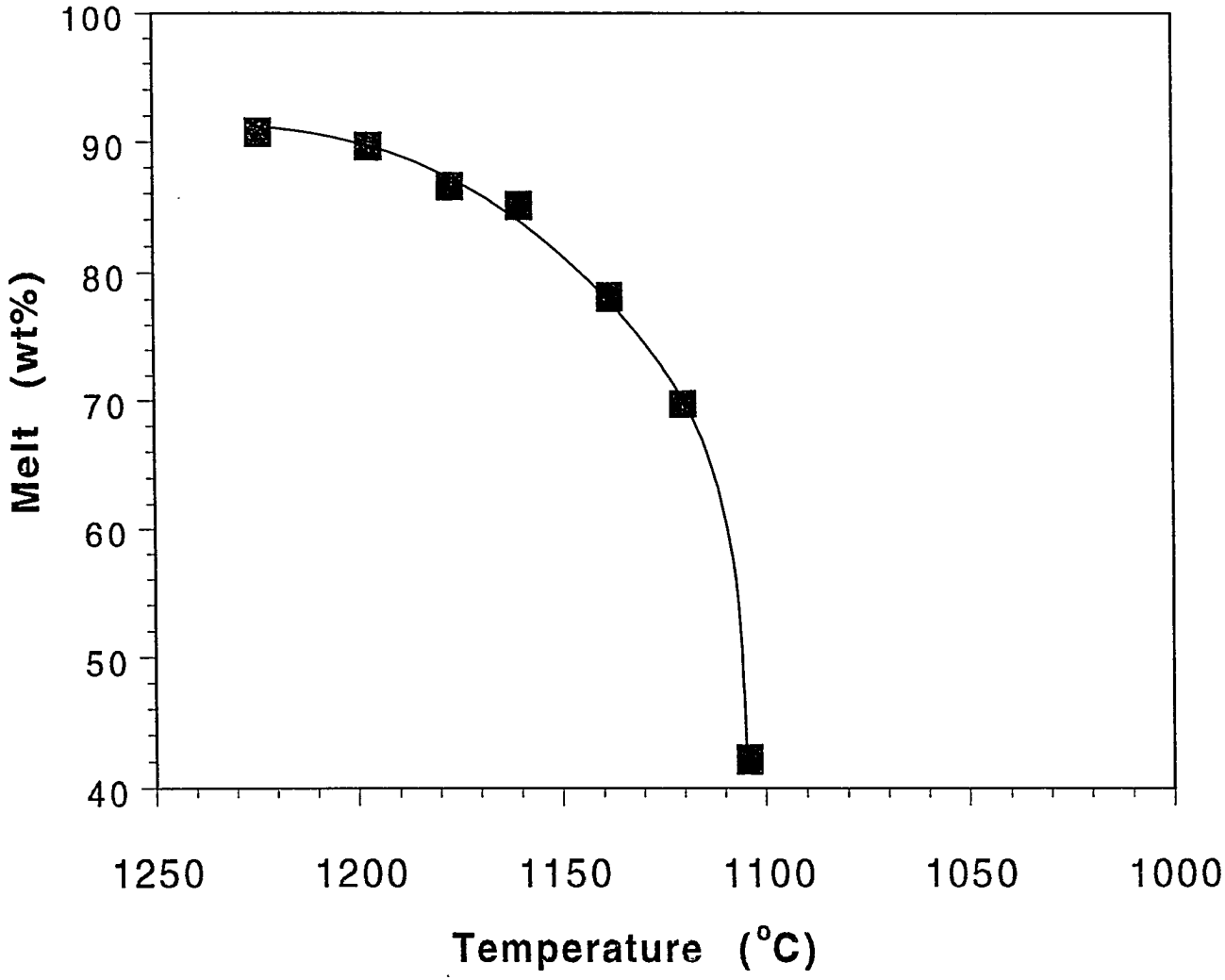

DVDP2 hawaiite

Figure 13b is a plot of wt% of melt versus Temperature (^{o}C). The percentage of melt between 1224^{o} and 1120 ^{o}C changes insignificantly, but from about 1120^{o} to 1049 ^{o}C the percentage of melt decreases dramatically from 96 wt% to 62 wt%. The slope of the best fit line is approximately equal to zero between 1224^{o} and 1120 ^{o}C. The lower temperature ranges, from 1120^{o} to 1049 ^{o}C, has a steeper gradient, indicating that mineral phase(s) are crystallizing from the melt. These phases are plagioclase, olivine, and clinopyroxene (Table 24).

Ne-hawaiite (83415)

Figure 13c represents wt% of melt plotted against Temperature (^{o}C). From 1224^{o} to 1177 ^{o}C the weight percent of melt displays minimal change. However, between 1177^{o} to 1049 ^{o}C the percentage of melt decreases from 98 wt% to 60 wt%. At 1160 ^{o}C plagioclase begins to crystallize and by the time the temperature reaches 1104 ^{o}C, olivine is also crystallizing (Table 24). The amount of melt decreases rapidly because at 1104 ^{o}C 21 wt% plagioclase is crystallizing from the melt whereas at 1049 ^{o}C 34 wt% of plagioclase is crystallizing.

Figure 13b: Plot of melt (wt%) versus temperature (^{o}C) of the temperature range 1224^{o} to 1049 ^{o}C for the DVDP2 hawaiite one atmosphere experiments.

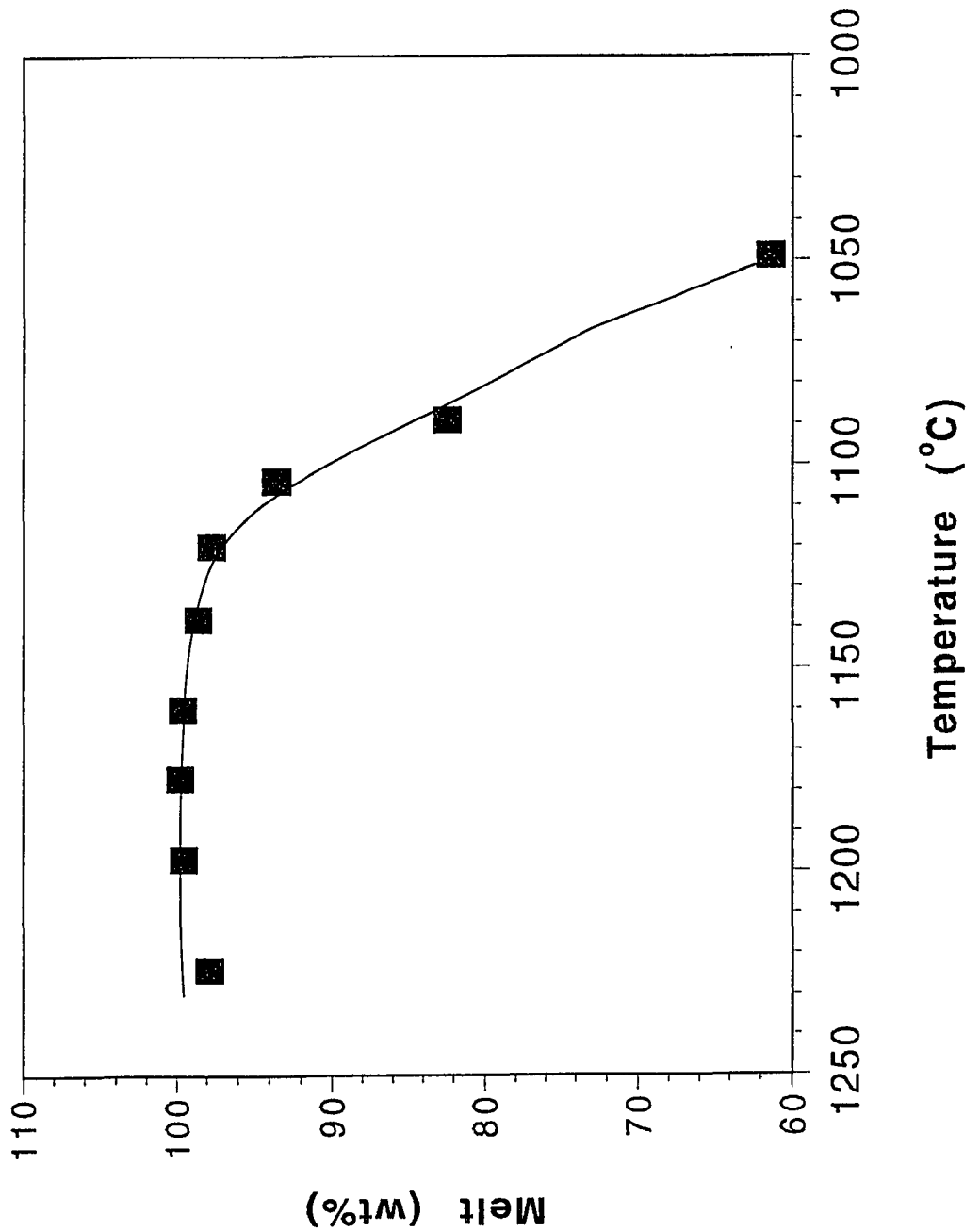

Figure 13c: Plot of melt (wt%) versus temperature (^{o}C) of the temperature range 1224^{o} to 1049 ^{o}C for 83415 Ne-hawaiite one atmosphere experiments.

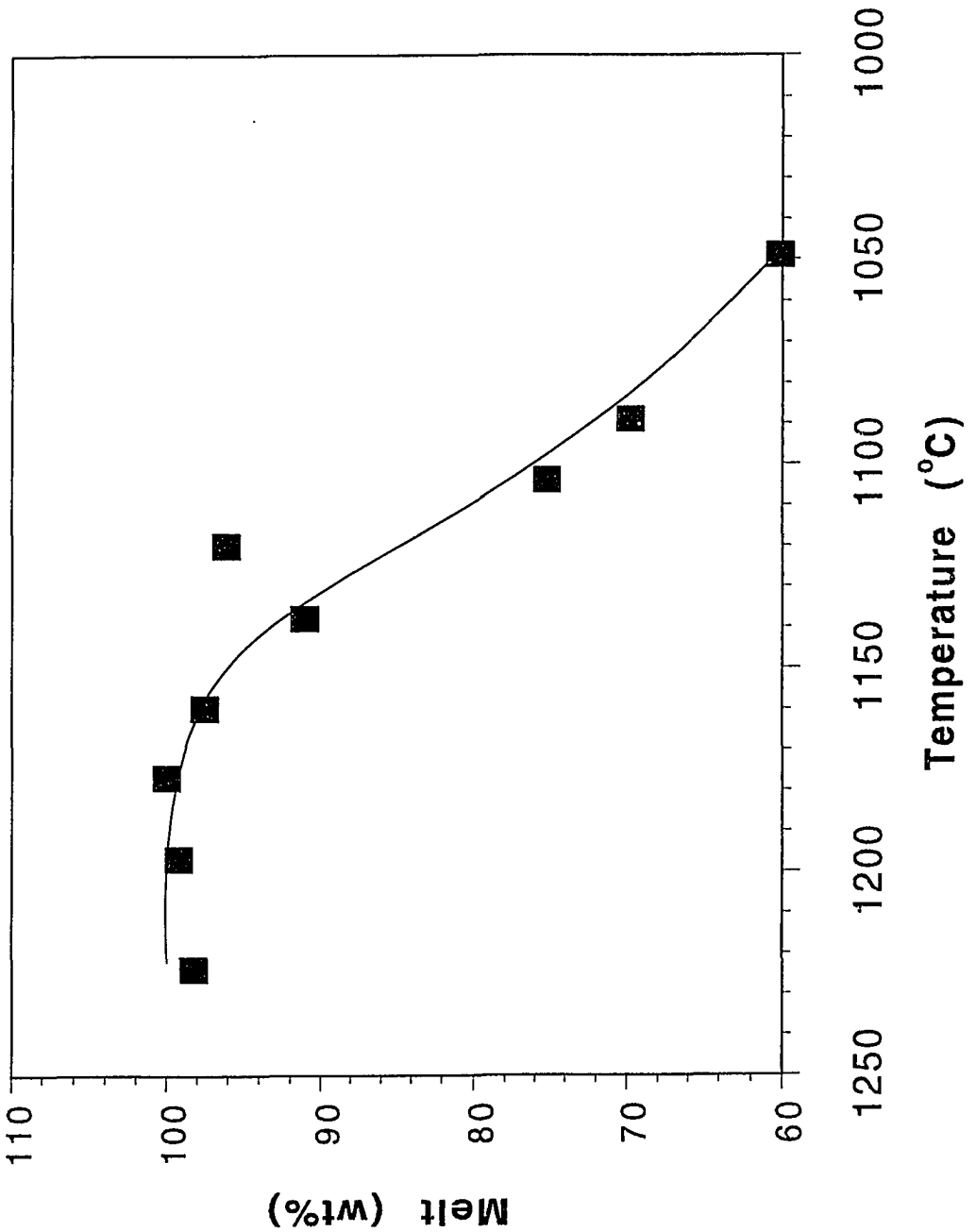

One datum plots above the curve for the weight percent of melt calculated at 1120 ^{o}C. Table 24 shows that glass plus plagioclase are present in the 83415 Ne-hawaiite at 1138^{o} and at 1104 ^{o}C, but in the 1120 ^{o}C experiment only glass was observed. Because plagioclase is present in the experiments above and below the 1120 ^{o}C experiment I will assume that plagioclase also crystallized in the 1120 ^{o}C experiment. Despite the small sizes of charges in the experiments, minerals sometimes float or sink. As a result, the experimental charge that is used in preparing the polished sections for microprobe analysis may contain only glass and no mineral phase(s). If the 1120 ^{o}C experimental data point is projected onto a smooth curve, the wt% of the melt would be approximately equal to 82 wt% (Figure 14).

Anorthoclase Phonolite

Figure 15 represents the wt% of melt versus Temperature (^{o}C) and was generated using data from Table 24. The percentage of melt is fairly constant until 1049 ^{o}C, at which point there is a slight decrease. This decrease is the result of plagioclase crystallizing from the melt.

Figure 14: Modified plot of melt (wt%) versus temperature (^{o}C) of the temperature range 1224^{o} to 1049 ^{o}C for 83415 Nehawaiite one atmosphere experiments.

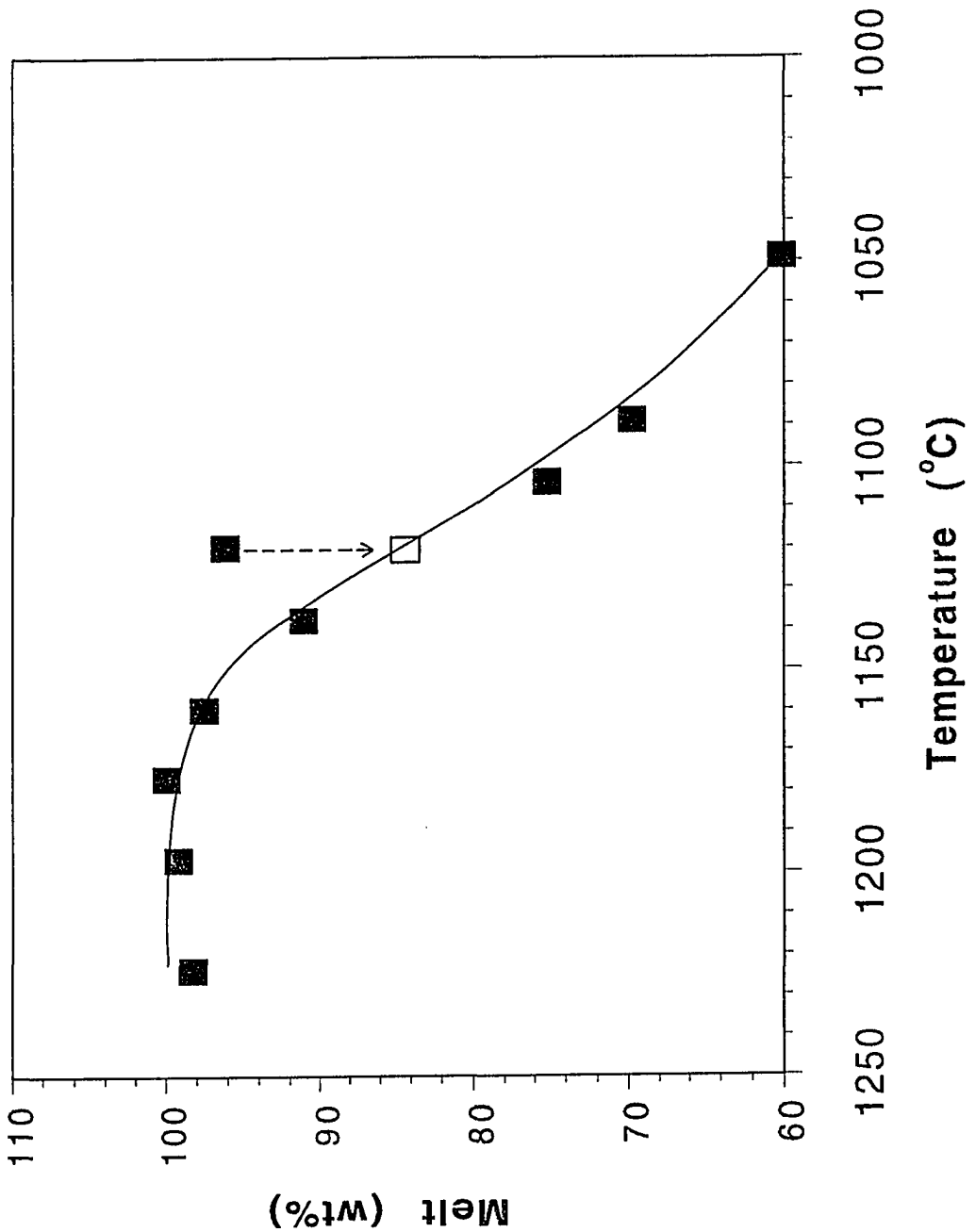

Figure 15: Plot of melt (wt%) versus temperature (^{o}C) of the temperature range 1177^{o} to 1049 ^{o}C for the anorthoclase phonolite one atmosphere experiments.

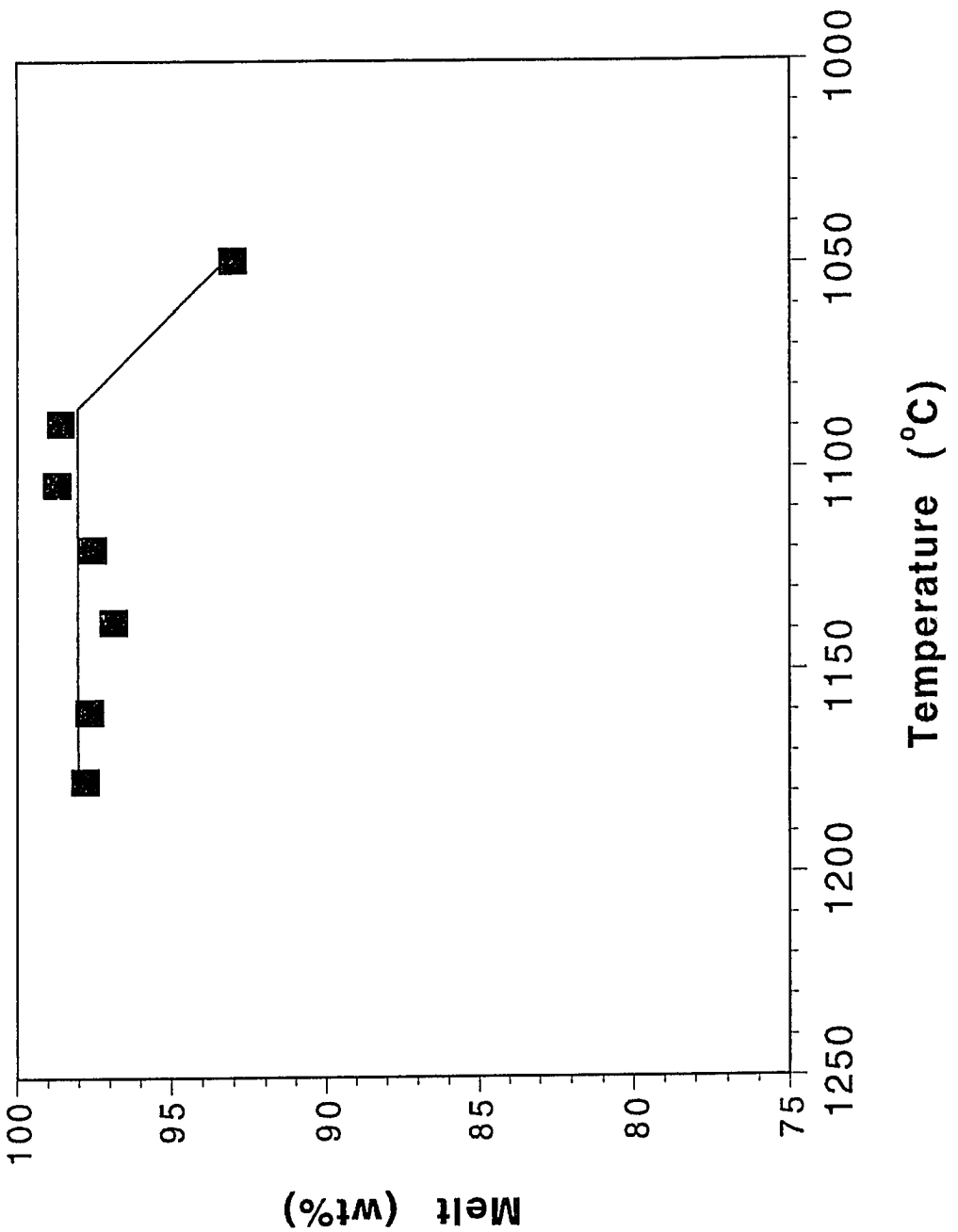

Mineral Chemistry

Olivine

Figure 16 a-c was developed using representative analysis of olivine from the one atmosphere experiments of basanite, DVDP2 hawaiite, and the 83415 Ne-hawaiite (Tables 29, 30, and 31 respectively). The full data base is given in Appendix E, Tables 1, 2, and 3.

The $Mg/(Mg+Fe^{+2})$ ratios for olivines in basanite, DVDP2 hawaiite and the Ne-hawaiite range from 66-87. It should be noted that the $Mg/(Mg+Fe^{+2})$ ratio decreases with decreasing temperature in all three rock types. For example, in the basanite sample at 1224 ^{o}C, the $Mg/(Mg+Fe^{+2})$ ratio is 87 and at 1049 ^{o}C it is 66. For the 83415 Ne-hawaiite, at 1104 ^{o}C the $Mg/(Mg+Fe^{+2})$ ratio is 78 and at 1049 ^{o}C it is 68. Similar variations in the $Mg/(Mg+Fe^{+2})$ ratio of olivine with temperature have been reported by Camur (1989), Sack et al. (1987), Kennedy et al. (1990), and Thy (1991).

Iron-Magnesium Exchange Between Melt and Olivine

Iron-magnesium exchange between a silicate melt and the coexisting olivine has been investigated experimentally, by Roedder and Emslie (1970). For tholeiitic compositions, the Fe-Mg distribution coefficient for olivine-melt, K_D, has

Figure 16 a-c: Variation of MgO and FeO in olivines from a) basanite, b) DVDP2 hawaiite, and c) 83415 Ne-hawaiite. Range of olivine compositions from Mt. Erebus basanite and 83415 Ne-hawaiite are shown by double headed arrows for comparison with the compositions of olivines in the experiments.

Experimental Olivines

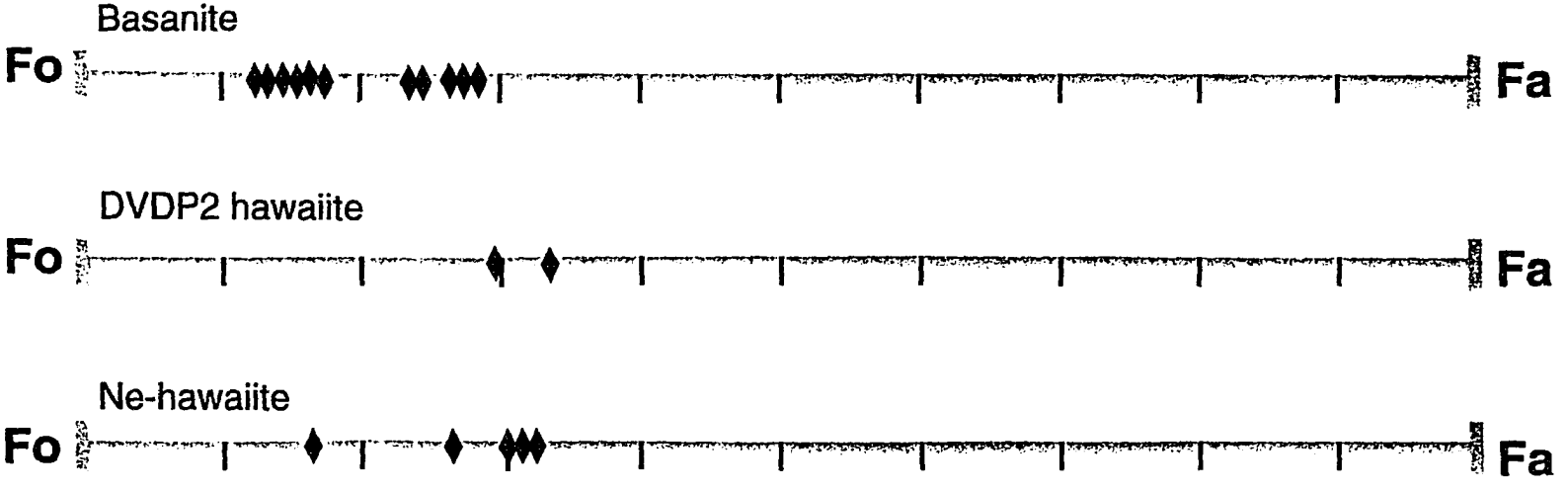

Table 29: Representative analysis of olivine from basanite (one atmopshere)

Temp (^{o}C)	1224	1197	1177	1160	1138	1120	1104
SiO_2	39.44	39.90	39.79	39.12	39.14	38.16	37.95
TiO_2	0.06	0.05	0.07	0.04	0.07	0.12	0.09
Al_2O_3	0.11	0.08	0.08	0.08	0.07	0.08	0.07
Fe_2O_3	0.00	0.00	0.00	0.00	0.00	0.00	0.00
Cr_2O_3	0.00	0.00	0.01	0.01	0.00	0.03	0.00
FeO*	12.54	13.45	14.27	15.26	16.00	18.11	21.34
MnO	0.18	0.20	0.22	0.22	0.26	0.27	0.33
MgO	45.86	45.41	44.38	43.26	43.32	41.36	38.19
NiO	0.16	0.00	0.13	0.10	0.11	0.14	0.15
CoO	0.00	0.00	0.00	0.00	0.00	0.00	0.00
CaO	0.49	0.53	0.57	0.54	0.58	0.46	0.56
Na_2O	0.02	0.02	0.02	0.02	0.02	0.01	0.01
K_2O	0.01	0.02	0.01	0.01	0.00	0.00	0.01
P_2O_5	0.05	0.04	0.03	0.03	0.03	0.05	0.02
SrO	0.00	0.00	0.00	0.00	0.00	0.00	0.00
BaO	0.00	0.00	0.00	0.00	0.00	0.00	0.00
TOTAL	98.92	99.76	99.57	98.69	99.60	98.79	98.70
Fo	86.87	85.86	84.77	83.33	82.83	80.28	76.14
Fa	13.13	14.14	15.23	16.67	17.17	19.65	23.87

FeO* = total iron
Fo = forsterite, Fa = fayalite

Table 30: Representative analysis of olivine from DVDP2 hawaiite (one atmosphere)

Temp (^{o}C)	1104	1089	1049
SiO_2	36.97	38.23	37.47
TiO_2	0.10	0.16	0.41
Al_2O_3	0.07	1.17	1.35
Fe_2O_3	0.00	0.00	0.00
Cr_2O_3	0.01	0.00	0.01
FeO*	23.20	24.18	26.94
MnO	0.57	0.57	0.79
MgO	36.65	33.09	29.92
NiO	0.00	0.00	0.02
CoO	0.00	0.00	0.00
CaO	0.52	0.85	0.93
Na_2O	0.04	0.23	0.43
K_2O	0.02	0.05	0.28
P_2O_5	0.19	0.06	0.14
SrO	0.00	0.00	0.00
BaO	0.00	0.00	0.00
TOTAL	98.31	98.58	98.68
Fo	73.79	70.93	66.40
Fa	26.21	29.07	33.60

FeO* = total iron
Fo = forsterite, Fa = fayalite

Table 31: Representative analysis of olivine from 83415 Ne-hawaiite (one atmosphere)

Temp (^{o}C)	1104	1089	1049
SiO_2	38.12	36.16	36.41
TiO_2	0.11	0.03	0.07
Al_2O_3	0.14	0.08	0.06
Fe_2O_3	0.00	0.00	0.00
Cr_2O_3	0.03	0.00	0.01
FeO*	19.41	26.91	27.56
MnO	0.40	0.61	0.77
MgO	39.50	33.16	32.22
NiO	0.09	0.04	0.02
CoO	0.00	0.00	0.00
CaO	0.41	0.39	0.45
Na_2O	0.03	0.05	0.04
K_2O	0.00	0.00	0.00
P_2O_5	0.08	0.06	0.05
SrO	0.00	0.00	0.00
BaO	0.00	0.00	0.00
TOTAL	98.31	97.48	97.66
Fo	78.29	68.72	67.57
Fa	21.71	31.28	32.43

FeO* = total iron
Fo = forsterite, Fa = fayalite

a value of 0.3±0.03; this value for K_D has been extensively used in basalt petrology (Ringwood, 1975; BVSP, 1981). Although K_D is often assumed to be independent of composition, recent experimental data indicate otherwise. Gee and Sack (1988) reported that K_D is a monotonically increasing function of silica activity in the composition range from melilitite-nephelinite to alkali basalt to tholeiite. K_D values reported by Gee and Sack (1988) for the Fe-Mg exchange reaction between olivine and melt (melilitites and nephelinites) are considerably lower (0.17-0.24) than those for tholeiites (0.30). Camur (1989) determined that K_D ranges from 0.22 to 0.26 in potassium-rich alkali basalts. Thy (1991) determined that an average K_D for high-temperature olivine-melt pairs in mildly alkalic lavas is 0.25, and for low temperature olivine-melt pairs the K_D ranges from 0.23 to 0.25. Gerke (1990) and Smith (1992) have determined olivine-melt K_D for certain high silica melts. Gerke (1990) determined a K_D value of 0.40±0.02 for the Grassy Mountain Ignimbrite, and Smith (1992) reported K_D values from the Magdelena rhyolitic obsidian as 0.43±0.02. These studies confirm the compositional- and T-dependence of Fe-Mg exchange between olivine and coexisting melt.

This research has generated additional K_D data. The K_D values in this study ranged from 0.24 to 0.32 (see Table 32).

Table 32: K_D values for olivine-melt pairs from the one atmosphere experiments with basanite and 83415 Ne-hawaiite

	Temp (°C)	ol Fe^{+2}/Mg	gl Fe^{+2}/Mg	K_D ol/gl
Basanite	1224	0.15	0.64	0.24
	1197	0.17	0.59	0.28
	1177	0.18	0.67	0.27
	1160	0.20	0.71	0.28
Ne-hawaiite 83415	1104	0.28	1.20	0.23
	1089	0.46	1.78	0.26
	1049	0.48	1.50	0.32

ol=olivine, gl=glass

Clinopyroxene

Representative analyses of clinopyroxenes from basanite and DVDP2 hawaiite experiments are given in Table 33 and 34. Calculation of clinopyroxene analyses, without any correction, as enstatite (En = Mg_2SiO_6), ferrosilite (Fs = Fe_2SiO_6), and wollastonite (Wo = Ca_2SiO_6) components in Tables 33 and 34 show that some compositions would plot above diopside-hedenbergite join on the pyroxene quadrilateral. This suggests that the clinopyroxenes in these experiments have a certain amount of Ca-Tschermak ($CaAl_2SiO_6$) component (Yagi and Onuma, 1967). Indeed natural clinopyroxenes that contain the Ca-Tschermak component plot above the diopside-hedenbergite join (Brown and Carmichael, 1969). Figure 17 a and b show the composition of clinopyroxenes from the basanite and DVDP2 hawaiite experiments after the Ca-Tschermak component correction. Corrected enstatite, ferrosilite, and wollastonite components are listed as En^+, Fs^+, and Wo^+ in Tables 33 and 34. For the full data base see Appendix E, Tables 4 and 5.

Figure 17 a and b show that pyroxenes in the basanite and DVDP2 hawaiite experiments are high calcium pyroxenes plotting within the augite field in the quadrilateral. Figure 17 and b as well as data in Tables 33 and 35 also show an increase in the ferrosilite/enstatie ratio of the

Table 33: Representative analysis of clinopyroxene from the basanite (one atmosphere)

Temp (^{o}C)	1138	1120	1104
SiO_2	43.31	44.11	43.99
TiO_2	4.68	3.86	4.68
Al_2O_3	9.62	8.91	8.15
Fe_2O_3	0.00	0.00	0.00
Cr_2O_3	0.00	0.58	0.02
FeO*	4.90	5.74	6.66
MnO	0.04	0.08	0.14
MgO	12.21	12.56	12.03
NiO	0.07	0.04	0.06
CoO	0.00	0.00	0.00
CaO	22.84	21.32	22.11
Na_2O	0.35	0.42	0.53
K_2O	0.00	0.07	0.03
P_2O_5	0.01	0.05	0.10
SrO	0.00	0.00	0.00
BaO	0.00	0.00	0.00
TOTAL	98.01	97.73	98.48
En	38.76	40.57	37.99
Fs	8.99	10.29	11.73
Wo	52.25	49.71	50.28
En^+	42.86	44.38	41.72
Fs^+	9.945	11.25	12.88
Wo^+	47.20	44.38	45.40

FeO* = total iron
En = enstatite, Fs = ferrosilite, Wo = wollastonite
En^+, Fs^+, Wo^+ = Ca Tschermak ($CaAl_2SiO_6$) corrected

Table 34: Representative analysis of clinopyroxene from DVDP2 hawaiite (one atmosphere)

Temp (^{o}C)	1104	1049
SiO_2	46.56	46.75
TiO_2	2.83	3.15
Al_2O_3	5.44	5.83
Fe_2O_3	0.00	0.00
Cr_2O_3	0.02	0.01
FeO*	7.45	7.52
MnO	0.20	0.22
MgO	12.63	12.20
NiO	0.06	0.01
CoO	0.00	0.00
CaO	21.74	21.69
Na_2O	0.62	0.61
K_2O	0.03	0.06
P_2O_5	0.09	0.07
SrO	0.00	0.00
BaO	0.00	0.00
TOTAL	97.63	98.09
En	38.92	37.91
Fs	12.97	13.19
Wo	48.11	48.90
En+	41.14	40.35
Fs+	13.71	14.04
Wo+	45.14	45.61

FeO* = total iron
En = enstatite, Fs = ferrosilite, Wo = wollastonite
En^{+}, Fs^{+}, Wo^{+} = Ca Tschermak ($CaAl_2SiO_6$) corrected

Figure 17 a and b: Pyroxene quadralateral for the experimentally formed clinopyroxenes from a) basanite and b) DVDP2 hawaiite.

Experimental Pyroxenes

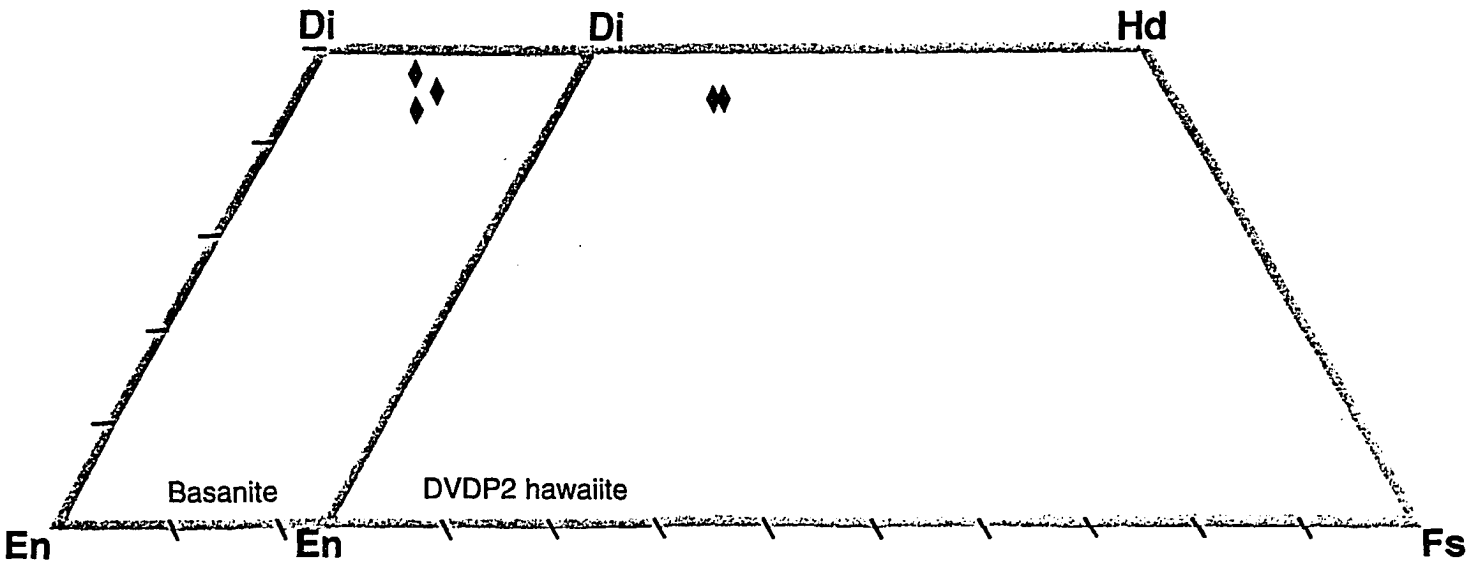

clinopyroxenes with decreasing temperature indicating that lower temperature clinopyroxenes are richer in iron compared to the higher temperature clinopyroxenes.

In addition to the Ca-Tschermak molecule, one atmosphere experimental clinopyroxenes also contain significant amounts of titanium (TiO_2) and aluminum (Al_2O_3). To determine if this feature was a result of disequilibrium in the experiments or if it is reflecting the equilibrium composition of pyroxenes one must first examine the clinopyroxenes from the rocks (Appendix C, Tables 2, 6, 11, and 15). These tables indeed show that natural clinopyroxenes also have higher TiO_2 and Al_2O_3, and interestingly within each rock type there are two different compositions of clinopyroxenes! One composition has TiO_2 up to 5 wt% and Al_2O_3 up to 11 wt% and the other composition has TiO_2 no more than 1 wt% and Al_2O_3 values no more than 4 wt%.

Since I verified the presence of two different clinopyroxenes in a given rock from Mt. Erebus, I decided to examine my microprobe data (Appendix E, Tables 4 and 5) to see if coexisting clinopyroxene compositions are also present in a given experiment as well. Examination of my probe data showed that there are two high calcium clinopyroxenes forming in some experiments. I decided to determine if the coexisting clinopyroxenes in the

experiments grew simultaneously from the melt or one represents a remnant crystal from the starting material. If the compositions of the two clinopyroxenes are found to be different from each other as well as from clinoproxenes in the starting material, one must conclude that they did grow from the melt and neither represents a remnant crystal.

Data are given in Tables 2 and 6 (Appendix C) and 4 and 5 (Appendix E) show that the coexisting clinopyroxenes in the experiments are different from the starting materials indicating that the clinopyroxenes in the experiments did grow from the melt and do not represent remnant crystals. This is the first experimental study documenting that two clinopyroxenes can simultaneously crystallize from melts and it confirms theoretical predictions of Sack and Ghiorso (1994, Part I). In addition, the presence of two different clinopyroxenes in the rocks and in the experiments imply that their compositions can not be described by the components of the pyroxene quadrilateral (En, Fs, Di, and Hd). New components based on crystal chemistry must be defined and Sack and Ghiorso (1994, Part I and III) have proposed some new components. I will use their components and in the Discussion section of this dissertation, a way to characterize these clinopyroxenes with additional components will be presented.

Plagioclase

Figure 18 a, b, c, and d represents the compositions of plagioclases from one atmosphere experiments for all rock types used in the experiments. Data for these figures are given in Tables 35, 36, 37, and 38, and the full data base is given in Appendix E, Tables 6, 7, 8, and 9.

As temperature decreases, compositions of experimental plagioclases shift from more calcium-rich to more sodium-rich types. In the basanite and the anorthoclase phonolite, plagioclase formed in only one or two experiments this limited sample does not provide enough data to document sodium-enrichment in plagioclases with decreasing temperature for those rock types. However, the number of experiments on the DVDP2 hawaiite and the 83415 Ne-hawaiite compositions in which plagioclase occurs is sufficient to define compositional trends with changing temperatures. For the DVDP2 hawaiite the first plagioclase composition produced at 1104 ^{o}C was An_{60} (labradorite) and that at 1049 ^{o}C was An_{48} (andesine). The 83415 Ne-hawaiite had plagioclase form from 1160^{o} to 1049 ^{o}C. At 1160 ^{o}C the plagioclase composition was An_{63} (labradorite) and An_{48} (andesine) at 1049 ^{o}C.

Figure 18 a-d: Ternary feldspar diagram for the experimentally formed plagioclases from a) basanite, b) DVDP2 hawaiite, c) 83415 Ne-hawaiite, and d) anorthoclase phonolite.

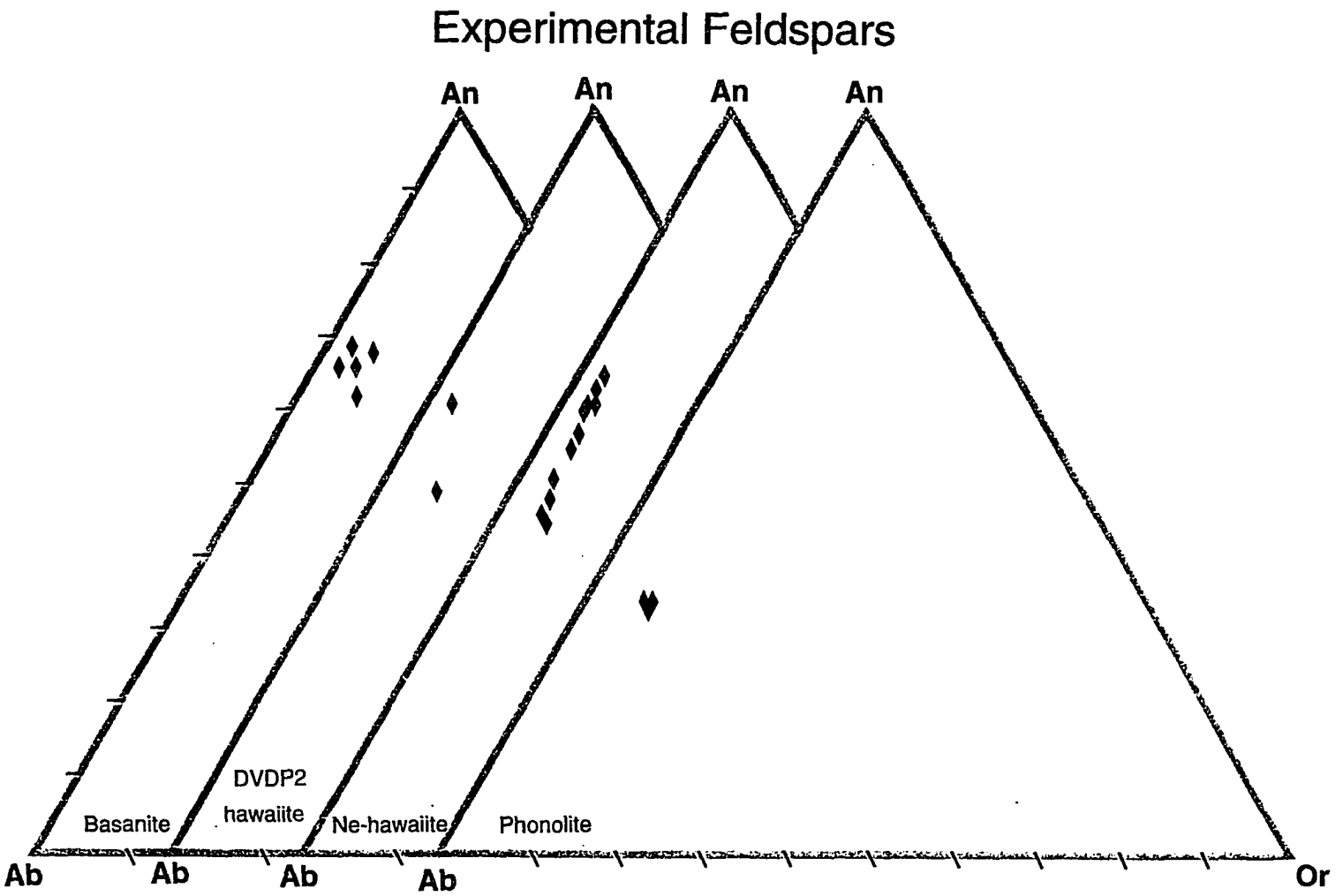

Table 35: Repesentative analysis of plagioclase from the basanite (one atmosphere)

Temp (oC)	1104
SiO_2	48.75
TiO_2	0.74
Al_2O_3	29.70
Fe_2O_3	0.00
Cr_2O_3	0.02
FeO*	1.27
MnO	0.03
MgO	0.44
NiO	0.04
CoO	0.00
CaO	13.39
Na_2O	3.37
K_2O	0.58
P_2O_5	0.16
SrO	0.00
BaO	0.00
TOTAL	98.45
An	66.34
Ab	30.69
Or	2.97

FeO* = total iron
An = anorthite, Ab = albite, Or = orthoclase

Table 36: Representative analysis of plagioclase from the DVDP2 hawaiite (one atmosphere)

Temp (oC)	1104	1089	1049
SiO_2	51.74	51.73	53.56
TiO_2	0.20	0.19	0.66
Al_2O_3	29.04	29.42	26.70
Fe_2O_3	0.00	0.00	0.00
Cr_2O_3	0.00	0.01	0.00
FeO*	0.57	0.66	1.82
MnO	0.00	0.02	0.05
MgO	0.13	0.14	0.46
NiO	0.01	0.00	0.00
CoO	0.00	0.00	0.00
CaO	11.91	12.23	9.79
Na_2O	4.12	4.05	5.02
K_2O	0.50	0.49	1.19
P_2O_5	0.06	0.06	0.21
SrO	0.00	0.00	0.00
BaO	0.00	0.00	0.00
TOTAL	98.27	98.99	99.46
An	59.60	60.61	48.00
Ab	37.37	36.36	45.00
Or	3.03	3.03	7.00

FeO* = total iron
An = anorthite, Ab = albite, Or = orthoclase

Table 37: Representative analysis of plagioclase from the 83415 hawaiite (one atmosphere)

Temp (oC)	1160	1138	1104	1089	1049
SiO_2	51.51	51.60	53.67	54.11	55.20
TiO_2	0.22	0.25	0.17	0.19	0.16
Al_2O_3	30.25	30.15	28.31	28.03	27.52
Fe_2O_3	0.00	0.00	0.00	0.00	0.00
Cr_2O_3	0.01	0.00	0.02	0.02	0.01
FeO*	0.54	0.31	0.36	0.33	0.52
MnO	0.01	0.01	0.00	0.00	0.00
MgO	0.15	0.02	0.11	0.08	0.06
NiO	0.01	0.09	0.02	0.01	0.00
CoO	0.00	0.00	0.00	0.00	0.00
CaO	12.61	12.40	10.50	10.21	9.51
Na_2O	3.78	4.08	4.82	5.07	5.26
K_2O	0.42	0.39	0.59	0.67	0.78
P_2O_5	0.06	0.04	0.01	0.03	0.04
SrO	0.00	0.00	0.00	0.00	0.00
BaO	0.00	0.00	0.00	0.00	0.00
TOTAL	99.57	99.30	98.55	98.75	99.04
An	63.27	61.62	53.06	50.51	47.42
Ab	34.69	36.36	43.88	45.45	47.42
Or	2.04	2.02	3.06	4.04	4.65

FeO* = total iron
An = anorthite, Ab = albite, Or = orthoclase

Table 38: Representative analysis of anorthoclase from the anorthoclase phonolite (one atmosphere)

Temp (oC)	1049
SiO_2	58.80
TiO_2	0.17
Al_2O_3	25.14
Fe_2O_3	0.00
Cr_2O_3	0.00
FeO*	0.54
MnO	0.04
MgO	0.09
NiO	0.02
CoO	0.00
CaO	6.72
Na_2O	6.56
K_2O	1.26
P_2O_5	0.03
SrO	0.00
BaO	0.00
TOTAL	99.36
An	33.33
Ab	59.38
Or	7.29

FeO* = total iron

An = anorthite, Ab = albite, Or = orthoclase

Calcium-Sodium Exchange Between Melt and Plagioclase

There is no equation describing the distribution coefficient, K_D, for plagioclase-melt equilibrium that is generally accepted. In developing a K_D equation for plagioclase, one must account for the coupled substitution between (CaSi) and (NaAl), which is required to maintain the charge balance. Any thermodynamic model for plagioclase-melt pairs must account for Ca and Na components (Brown and Parsons, 1981; Ghiorso, 1984; Price, 1985; Green and Udansky, 1986; Fuhrman and Lindsley, 1988; and Elkins and Grove, 1990) as well as the Si and Al in the tetrahedral site.

The K_D model I chose was proposed by Grove et al., 1992. Their model deals with the coupled substitutions of NaAl and CaSi. The components they chose to represent the plagioclase compositions are mole fraction of $NaAlSi_3O_8$ and $CaAl_2Si_2O_8$. Choosing the components for the melt is a more complicated problem. Grove et at., 1992 used Bottinga and Weill's (1972) liquid components and assumed that these components are best to deal with the coupled substitution problem. They recast liquid compositions in mole fractions of SiO_2, $KAlO_2$, $NaAlO_2$, $CaAl_2O_4$, CaO, MgO, FeO, TiO_2, and $PO_{2.5}$. The following equations represent the mineral reaction with the melt.

$$NaAlSi_3O_8^X + CaAl_2O_4^L = CaAl_2Si_2O_8^X + SiO_2^L + NaAlO_2^L$$

$$KD = \frac{[XAn][XSiO_2][XNaAlO_2]}{[XAb][XCaAl_2O_4]}$$

The K_Ds of plagioclase obtained from this study are presented in Table 39. The lack of a consistent pattern reflects the difficulty in plagioclase-melt equilibrium.

DATA INTERPRETATION

The main purpose of this study was to evaluate what role low pressure crystal fractionation played in producing the observed compositional diversity in the alkaline rocks of Mt. Erebus, Antarctica. The objectives in the study were to: 1) conduct one atmosphere experiments and generate an experimental data base; 2) determine the sequence of crystallization and the composition of the mineral and melt phases that formed; 3) determine if at one atmosphere pressure it is possible to generate hawaiite and phonolite magmas from a parental basanitic melt; and 4) test if the rock compositions from Mt. Erebus reflect a low pressure crystal fractionation system.

Table 39: K_D values for plagioclase-melt pairs from the one atmosphere experiments with 83415 Ne-hawaiite and the anorthoclase phonolite

	Temp (^oC)	K_D
Ne-hawaiite 83415	1160	2.28
	1138	3.02
	1104	2.33
	1089	2.46
	1049	3.69
Phonolite	1049	4.13

Mineral Data

Olivine

When examining Figure 16 a-c it is observed that the range of compositions for olivine from the one atmosphere experiments for the basanite and the 83415 Ne-hawaiite primarily overlap with the compositions obtained from the olivines in the corresponding rock types (see Figure 9 a-d). This implies that the temperature range in my experiments were similar to the temperatures at which the natural olivines formed. From the experimental data one can also observe that as expected, with decreasing temperature the $Fe^{+2}/(Mg+Fe^{+2})$ ratio increases.

The DVDP2 hawaiite rock sample only provided one composition and only two compositions were obtained from the experiments, thus there is not enough data to accurately compare the olivine compositions from the rock and experimental charges. Finally, the anorthoclase phonolite experiments did not produce any olivine, thus indicating that experiments were not performed at low enough temperatures. The olivine in the anorthoclase phonolite must have formed below 1049 ^{o}C.

Clinopyroxenes

Clinopyroxene formed only in the basanite and DVDP2 hawaiite one atmosphere experiments. The compositional ranges of clinopyroxenes of the rocks and those of the experiments were similar to temperatures at which the clinopyroxenes in the rocks formed. In the experimental charges there is a general increase in the $Fe^{+2}/(Mg+Fe^{+2})$ ratio as the temperature decreases. Again, as in the case of the olivines, this is the expected result. The clinopyroxenes from the DVDP2 hawaiite rock display weak reverse zonation indicating that more than just crystal fractionation probably effected that magma. Possibly minor amounts of magma mixing and/or assimilation effected this magmas' ascent to the surface. The clinopyroxenes in the experimental charges displayed no signs of zonation either normal or reverse.

For the 83415 Ne-hawaiite and the anorthoclase phonolite experiments no clinopyroxenes crystallized from the melts. This indicates that the clinopyroxenes in these two rock types crystallized from their respective magmas below 1049 ^{o}C.

Plagioclase

Plagioclase from the basanite and 83415 Ne-hawaiite rocks and the experimental charges cover the same compositional range. The DVDP2 hawaiite plagioclase compositions from the experiments display a smaller compositional range than observed in the rock. Finally, the anorthoclase phonolite compositions from the experiments are more calcium-rich than the plagioclases present in the rock. All but the anorthoclase phonolite experiments display a sodium enrichment trend as the temperature decreases. There was not enough data available from the anorthoclase phonolite one atmosphere experiments to determine if there was a sodium enrichment trend with decreasing temperature.

It is observed that as composition changes from the basanite to DVDP2 and 83415 hawaiites to the anorthoclase phonolite there is a gradual decrease in the calcium content of plagioclase. The phenocrysts present in the 83415 Ne-hawaiite display both normal and reverse zonation, thus indicating that crystal fractionation was not the only magmatic process involved in the formation of this rock.

In general all of the experimental mineral data for olivine, clinopyroxene, and plagioclase displays enrichment trends in Fe^{+2} and/or Na. These trends are expected, based on extensive experimental work on anhydrous one atmosphere mineral-melt systems (Camur, 1989; Gee and Sack, 1988;

Kennedy et al., 1990; Mayhood and Baker, 1986; Sack et al., 1987; Thy, 1991).

Aluminum-titanium-ferric iron rich clinopyroxenes

As stated in the Data Presentation section most of the clinopyroxene compositions plot in the pyroxinoid field unless the Ca-Tschermak correction is applied. Although this molecule does allow for adjustments in the calcium and aluminum components it does not deal with how titanium and ferric iron affect the clinopyroxenes. When pyroxene compositions are plotted onto the quadrilateral, presence of titanium (Ti^{+4}), ferric (Fe^{+3}) iron, and aluminum (Al^{+3}) are ignored. In order to develop a model which will account for these ions in pyroxenes, the thermodynamics of the pyroxene system must be reevaluated.

Sack and Ghiorso (1994, Part III) believe that pyroxenes are probably the most chemically diverse igneous rock forming mineral except for maybe spinels. These "non traditional" or non quadrilateral compositions probably play a more significant role in petrologic interpretations of igneous systems than previously believed (Sack and Ghiorso, 1994, Part III). Sack and Ghiorso (1994, Part I) envision pyroxenes to have the general structure of:

$$M_2M_1T_2O_6$$

$M_2 = Ca^{+2}, Fe^{+2}, Mg+2, Na^{+1}$ where $X_{Ca} >> X_{Na}$

$M_1 = Mg^{+2}, Fe^{+2}, Ti^{+4}, Fe^{+3}, Al^{+3}$

$T = Si^{+4}, Al^{+3}, Fe^{+3}$

The clinopyroxene subsystem $CaAl_2SiO_2$+$CaFeSiO_2$ - $CaMgSi_2O_6$ - $CaTiAl_2O_6$ (see Figure 19) can be used to better represent the clinopyroxenes in basic (silica undersaturated) igneous rocks. Al^{+3}, Ti^{+4}, Fe^{+3}-rich clinopyroxenes are common in the silica undersaturated igneous rocks there is not enough silica available to fill the tetrahedral site. When other elements fill this site the charge balance must still be maintained, thus Al^{+3}, Ti^{+4}, and Fe^{+3} are present in the clinopyroxene structure to achieve this. Theoretical studies of Sack and Ghiorso (1994, Part I) predict that two clinopyroxenes must coexist with melt, reflecting low and high silica activities in the melt. These two pyroxenes plot on opposite sides of a "miscibility gap" shown by the tie lines in Figure 19 and 20.

In this study the 1138 ^{o}C DVDP2 hawaiite experiment contained two coexisting clinopyroxenes (see Figure 20). Originally I interpreted this to be an error in data collection, or disequilibrium in my experiments. However, upon closer examination I determined that these two compositions are real and do not represent an analytical error or presence of remnant crystals. In addition, when I

Figure 19: $CaAl_2SiO_2$-$CaMgSi_2O_6$-$CaTiAl_2O_6$ from Sack and Ghiorso (1994, Part I, Figure 1). Open squares = Yagi an Onuma (1967), filled squares and open circles = Yang (1975), and filled circles Allende = Yagi and Onuma (1967) and Yang (1975). Shaded half of diagram represents space where there is greater than 50% titanium in the M1 site.

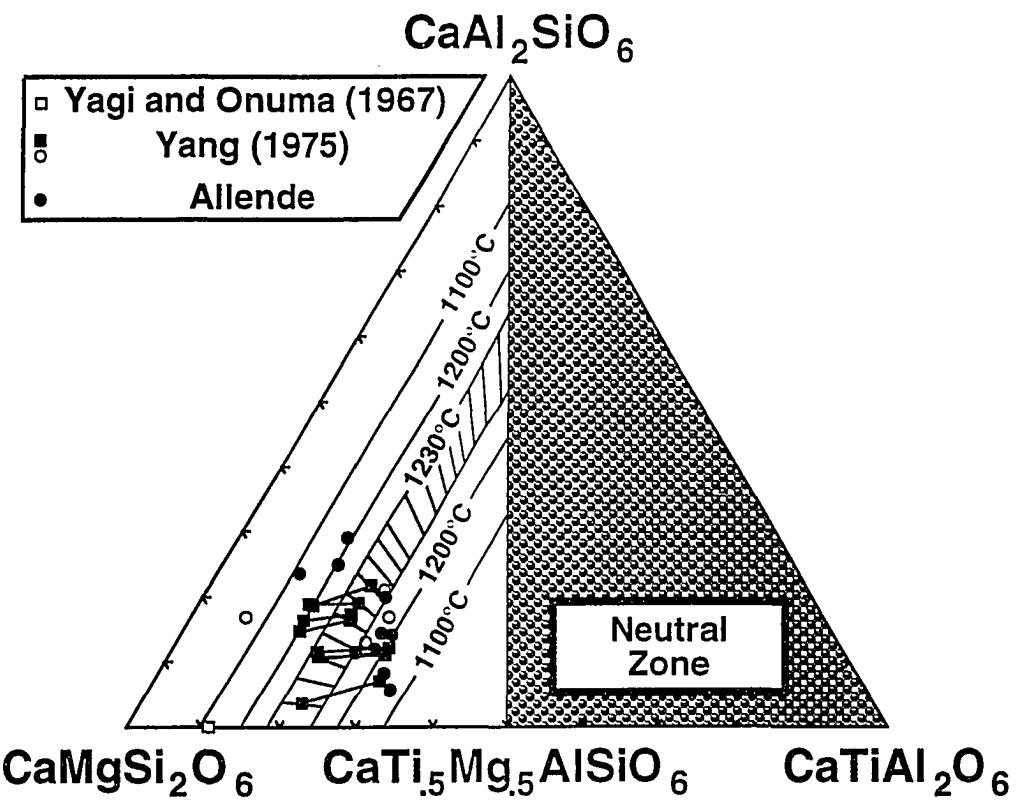

Figure 20: Modified $CaAl_2SiO_2$+$CaFeSiO_2$-$Ca(Mg, Fe^{+2})Si_2O_6$-$CaTiAl_2O_6$ from Sack and Ghiorso (1994, Part I, Figure 1). Filled diamonds represent DVDP2 hawaiite clinopyroxene compositions which formed in the 1138 ^{o}C experiment.

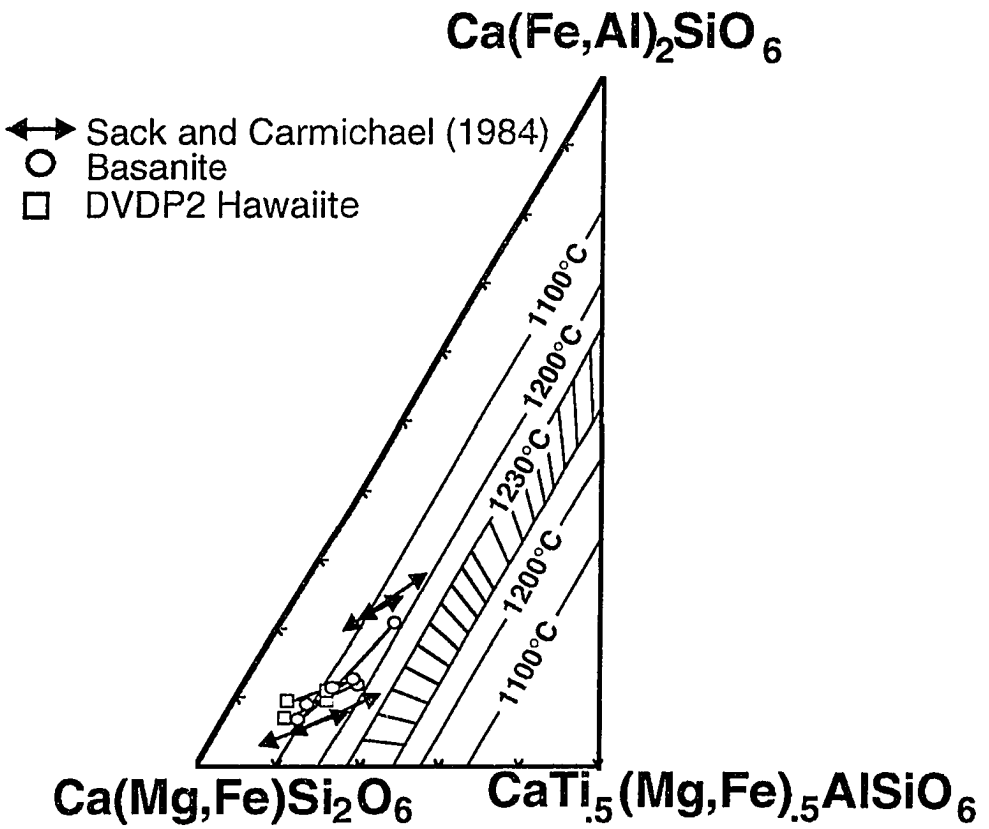

closely examined the rock data I confirmed that two clinopyroxenes were also present in the rocks. Following the procedure of Sack and Ghiorso (1994, Part I) and personal communication with Sack (1995), I calculated the compositions of two coexisting high calcium clinopyroxenes in my experiments and plotted them on Figure 20. It should be noted that this is the first experimental data set that verifies Sack and Ghiorso's (1994, Part I) predictions of two high-calcium clinopyroxenes forming at a given pressure and temperature.

As more data are collected Sack and Ghiorso's (1994, Part I) subsystem will be even better understood which will ultimately produce more accurate geothermometers and barometers. Moreover, as the scientific community becomes more aware of this feature it will enable scientists to develop models which will be able to accurately predict liquid lines of descent for magmatic systems. Also it will enable scientists to determine partitioning of rare earth elements (REE) between liquid and clinopyroxenes during partial melting of mantle source regions (Gallahan and Nielsen, 1992; Nielsen et al., 1992; and Sack and Ghiorso, 1994 Part I). This last point maybe the most important because alkaline rocks originate from the deepest part of the upper mantle relative to all other igneous rocks and if partitioning of REE can be understood during partial melting

it will provide needed insight into how magmatic processes work.

Glass Data

Double Y Graphs

In the Data Presentation section plots of Melt percent (wt%) versus Temperature (^{o}C) for basanite, DVDP2 and 83415 hawaiites, and the anorthoclase phonolite were presented. For all four compositions used in my experiments the melt percent decreased with temperature. The decrease in melt percent was caused by the crystallization of one or more mineral phases. Figures 13 a-c and 15, however, I did not indicate what mineral phase(s) were crystallizing from the melt or what the sequence of crystallization is for the basanite, hawaiites, or anorthoclase phonolite. Following is a discussion of the relationship between melt percent and percent of minerals crystallizing from the melt.

Figures 21 a-d are plots of Mineral phase(s) wt% and Melt percent (wt%) versus Temperature (^{o}C). This type of diagram enables one to see how the wt% of melt is decreasing as mineral phases crystallize from the melt. One can also determine at what temperature each mineral phase formed and what the sequence of crystallization for each magma system

(basanite, DVDP2 hawaiite, 83415 Ne-hawaiite, and anorthoclase phonolite) is. All of these figures were developed using data from Table 24.

Basanite

Figure 21a represents these changes in the one atmosphere basanitic magma. The liquidus temperature was not reached in these experiments. The highest temperature run was 1224 ^{o}C and at that temperature, the melt was in equilibrium with olivine. Clinopyroxene was the next phase to crystallize from the melt at 1138 ^{o}C, and at 1104 ^{o}C plagioclase began to crystallize. Thus the sequence of crystallization in the basanitic magma is olivine-> clinopyroxene->plagioclase.

The amount of olivine crystallizing from the melt displays minimal change from 1160^{o} to 1120 ^{o}C. At 1138 ^{o}C clinopyroxene begins to crystallize, which has an effect on the crystallization of olivine. Plagioclase begins crystallizing from the magma at 1104 ^{o}C. By this temperature clinopyroxene is crystallizing the greatest quantities (24 wt%) followed by olivine (19-20 wt%) and finally plagioclase (14 wt%). This trend indicates that even though olivine is the liquidus phase, by the time the magma has cooled to 1104 ^{o}C over half of the melt has solidified and clinopyroxene has become the controlling

Figure 21a: Mineral phases (wt%) and Melt (wt%) versus Temperature (^{O}C) for basanite. Melt fraction = filled sqares, olivine = filled triangles, filled diamonds = clinopyroxene, and filled circle = plagioclase.

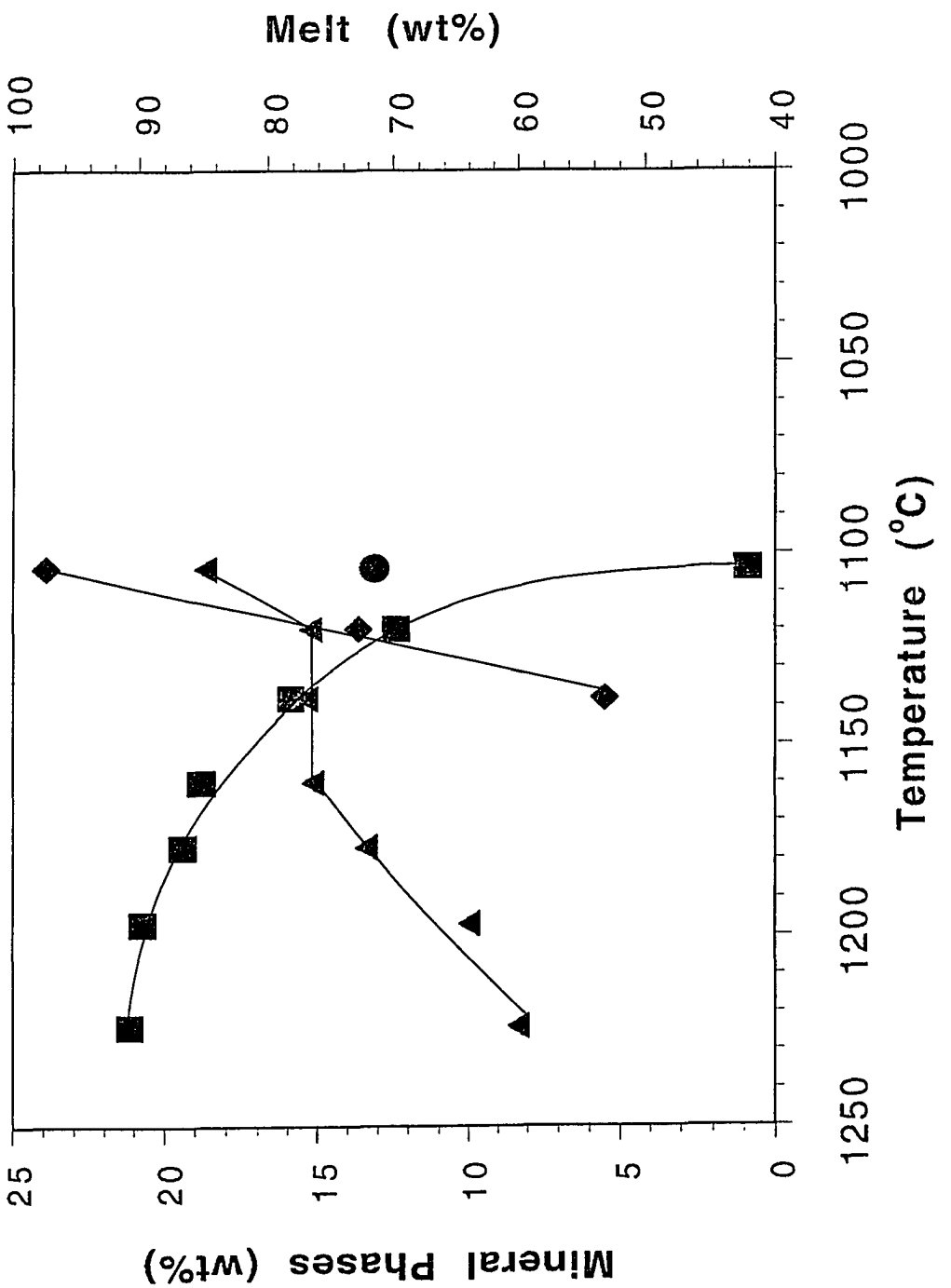

mineral phase. Clinopyroxene crystallizing from the magma effects not only composition but also the amount of the other mineral phases crystallizing.

DVDP2 hawaiite

Figure 21b shows that in the DVDP2 hawaiite at 1104 ^{o}C plagioclase, olivine, and clinopyroxene begin to crystallizing from the melt. The weight percent of plagioclase crystallizing increases rapidly between 1104^{o} and 1049 ^{o}C. Olivine shows an initial increase in crystallization from 1104^{o} to 1089 ^{o}C but there is minimal change after that. Finally, clinopyroxene crystallizing between 1104^{o} and 1089 ^{o}C displays minimal change but by 1049 ^{o}C the amount of clinopyroxene crystallizing from the magma has more than doubled. The liquidus for this composition appears to be multiply saturated with plagioclase, olivine, and clinopyroxene. However, if one evaluates how the amount (wt%) of melt changes with respect to the minerals it is observed that from 1224^{o} to 1138 ^{o}C there is minimal change, but from 1138^{o} to 1104 ^{o}C there is a decrease in melt fraction. If no minerals are present until 1104 ^{o}C but the amount of melt fraction is decreasing at higher temperatures what are the implications of this feature? One explanation is that microlites of one or more mineral phase(s) are forming in the 1138^{o} and 1120 ^{o}C

Figure 21b: Mineral phases (wt%) and Melt (wt%) versus Temperature (^{o}C) for DVDP2 hawaiite. Melt fraction = filled sqares, olivine = filled triangles, filled diamonds = clinopyroxene, and filled circle = plagioclase.

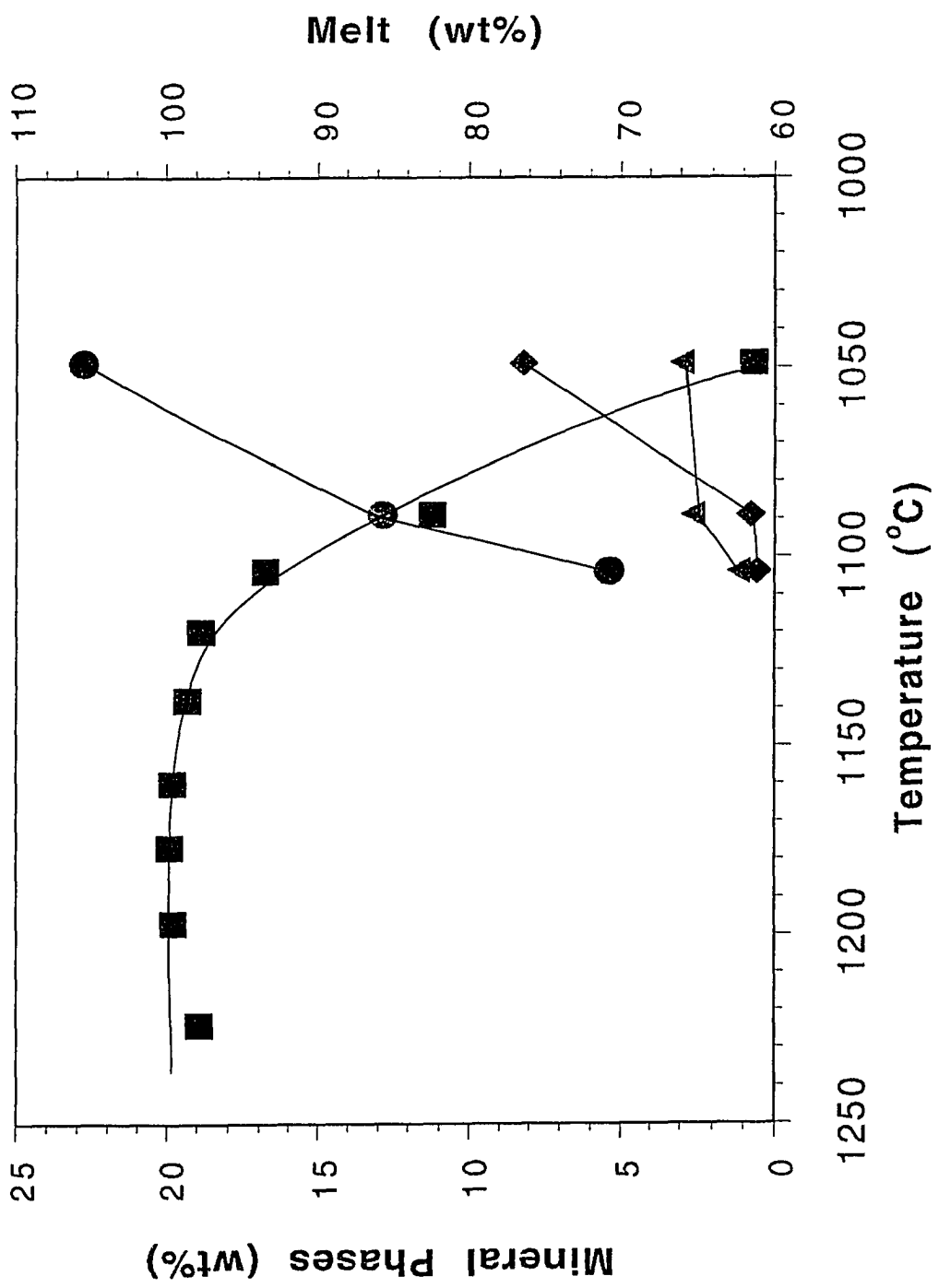

experiments. I would interpret the sequence of crystallization in DVDP2 hawaiite as follows. Probably plagioclase is the liquidus phase. The next phase to form is most likely to be olivine followed by clinopyroxene (plagioclase->olivine->clinopyroxene).

83415 Ne-hawaiite

Plagioclase is the liquidus phase for 83415 Ne-hawaiite (Figure 21c). The sequence of crystallization is plagioclase->olivine which is the same for the DVDP2 hawaiite. Contrary to the DVDP2 hawaiite crystallization, however, I did not see any clinopyroxene forming from 83415 Ne-hawaiite. The trend of crystallization in hawaiites id different from that of the basanite.

Anorthoclase Phonolite

In Figure 21d the only mineral phase present is plagioclase, at 1049 ^{o}C. No experiments were preformed below this temperature. Thus, the liquidus phase is plagioclase but the sequence of crystallization was not determined. By 1049 ^{o}C there is still over 90 wt% melt, but additional experiments would require that the duration of the experiments preformed below 1049 ^{o}C must be longer. This is because 1) the kinetics of these high viscosity

Figure 21c: Mineral phases (wt%) and Melt (wt%) versus Temperature (^{O}C) for 83415 Ne-hawaiite. Melt fraction = filled squares, olivine = filled triangles, and filled circle = plagioclase.

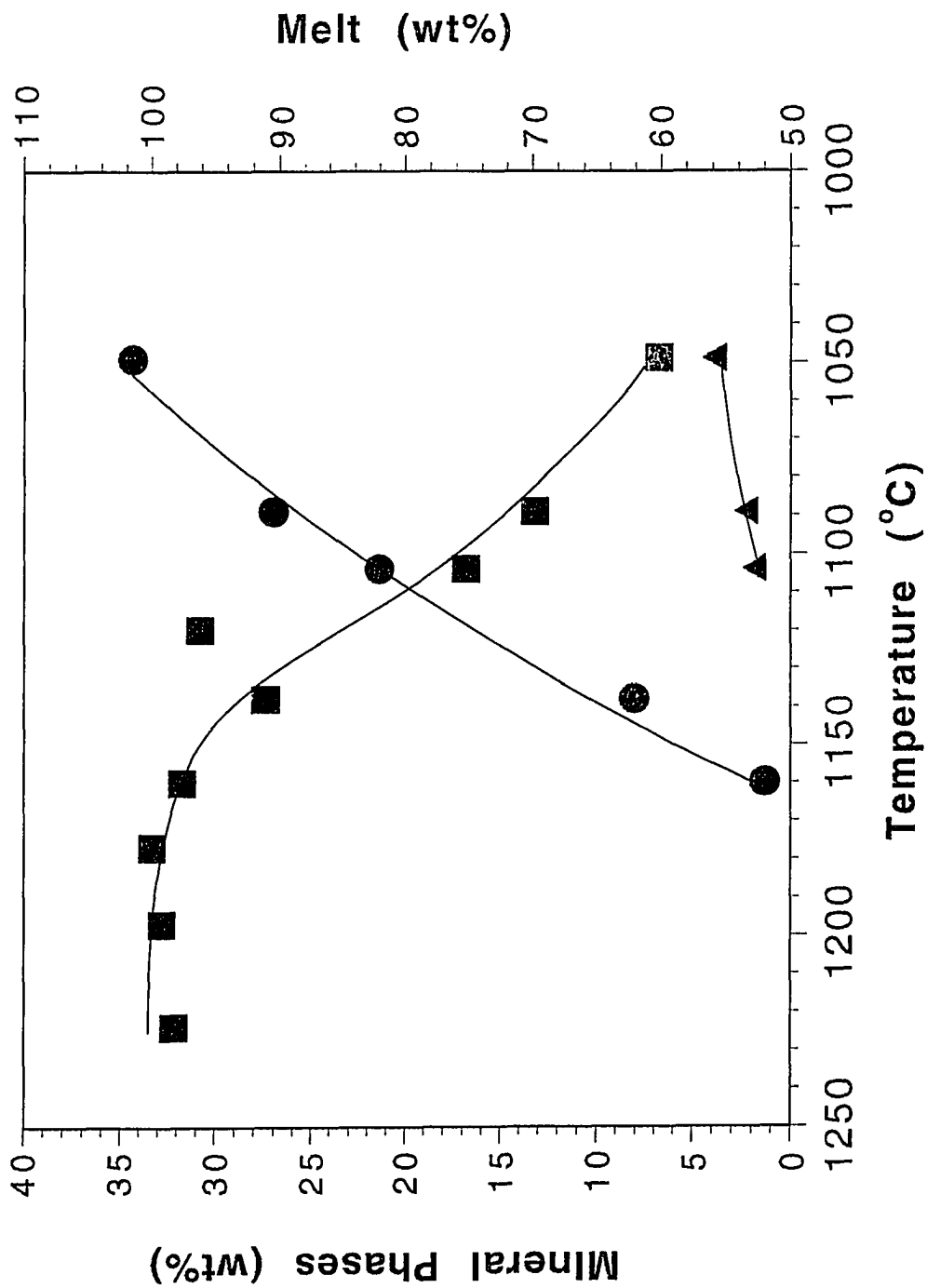

Figure 21d: Mineral phases (wt%) and Melt (wt%) versus Temperature (^{o}C) for anorthoclase phonolite. Melt fraction = filled sqares, and filled circle = plagioclase.

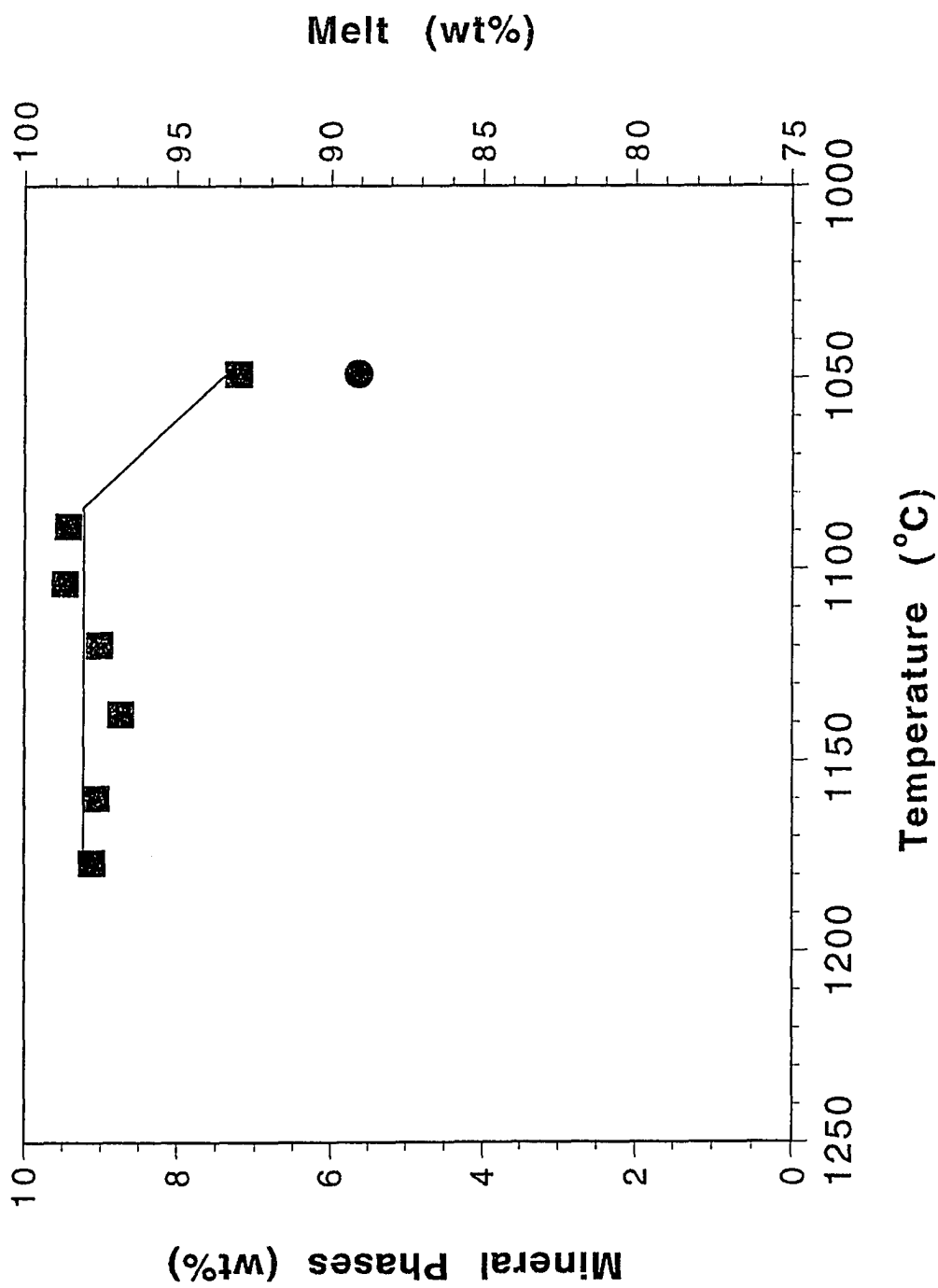

systems require such a long period of time, possibly up to one year (R. Sack, pers com), to reach equilibrium and 2) during that period of time excessive loss of volatiles such as Na_2O and P_2O_5, would occur making the experiments worthless. For these reasons, I did not experiment below 1049 ^oC.

In summary, the liquidus phase for basanite is olivine and for the DVDP2 and 83415 hawaiites and anorthoclase phonolite it is plagioclase. This reflects the differences in the bulk compositions. The liquid line of decent for the basanite is olivine->clinopyroxene->plagioclase, for the DVDP2 hawaiite it is plagioclase->olivine->clinopyroxene, and for 83415 Ne-hawaiite it is plagioclase->olivine. For the DVDP2 hawaiite, 83415 Ne-hawaiite, and the anorthoclase phonolite the solidus was not reached. Thus only partial liquid lines of descent were determined for these compositions. Figures 21 a-d provide a detailed quantitative picture of crystallization in each magma. The next question is weather or not a hawaiite and phonolite melt can be generated from a basanitic parental melt. To try to answer that question a Temperature versus $Mg_{\#}$ plot will be evaluated.

Temperature versus $Mg_{\#}$

The third objective of this study is to determine if at one atmosphere pressure a hawaiitic and phonolitic melt can be generated from a basanitic melt by crystal fractionation. In the Data Presentation section Temperature versus $Mg_{\#}$ plots were presented for the melts of the basanite, DVDP2 hawaiite, 83415 Ne-hawaiite, and anorthoclase phonolite (Figure 12 a-d). These figures provide insight as to how the $Mg/(Mg+Fe^{+2})$ ratio decreases with temperature.

Figure 22 is a plot of Temperature versus $Mg_{\#}$ which shows the differentiation of the basanitic, hawaiitic, and phonolitic melts. This figure was generated using data from Tables 25-28. What is observed is that the differentiation trend for the basanite crosses over the $Mg_{\#}$, 45, of the bulk composition for the hawaiites at 1104 ^{o}C. This data clearly show that a basanitic parental magma can differentiate at low pressures to produce a hawaiitic magma. The differentiation trend for the hawaiitic melts cross over the $Mg_{\#}$, 34, of the bulk composition for the phonolite at 1049 ^{o}C which confirms that a hawaiitic magma itself can differentiate at low pressures to produce a phonolitic magma. The implications of these liquid lines of descent is that at one atmosphere pressure it is indeed possible to generate melts of hawaiitic and phonolitic compositions from a parental basanitic melt.

Figure 22: Temperature (^{o}C) versus $Mg_{\#}$ for all four magma compositions. Basanite = open circles, DVDP2 hawaiite = open squares, 83415 Ne-hawaiite = open triangles, anorthoclase phonolite = open squares with plus signs.

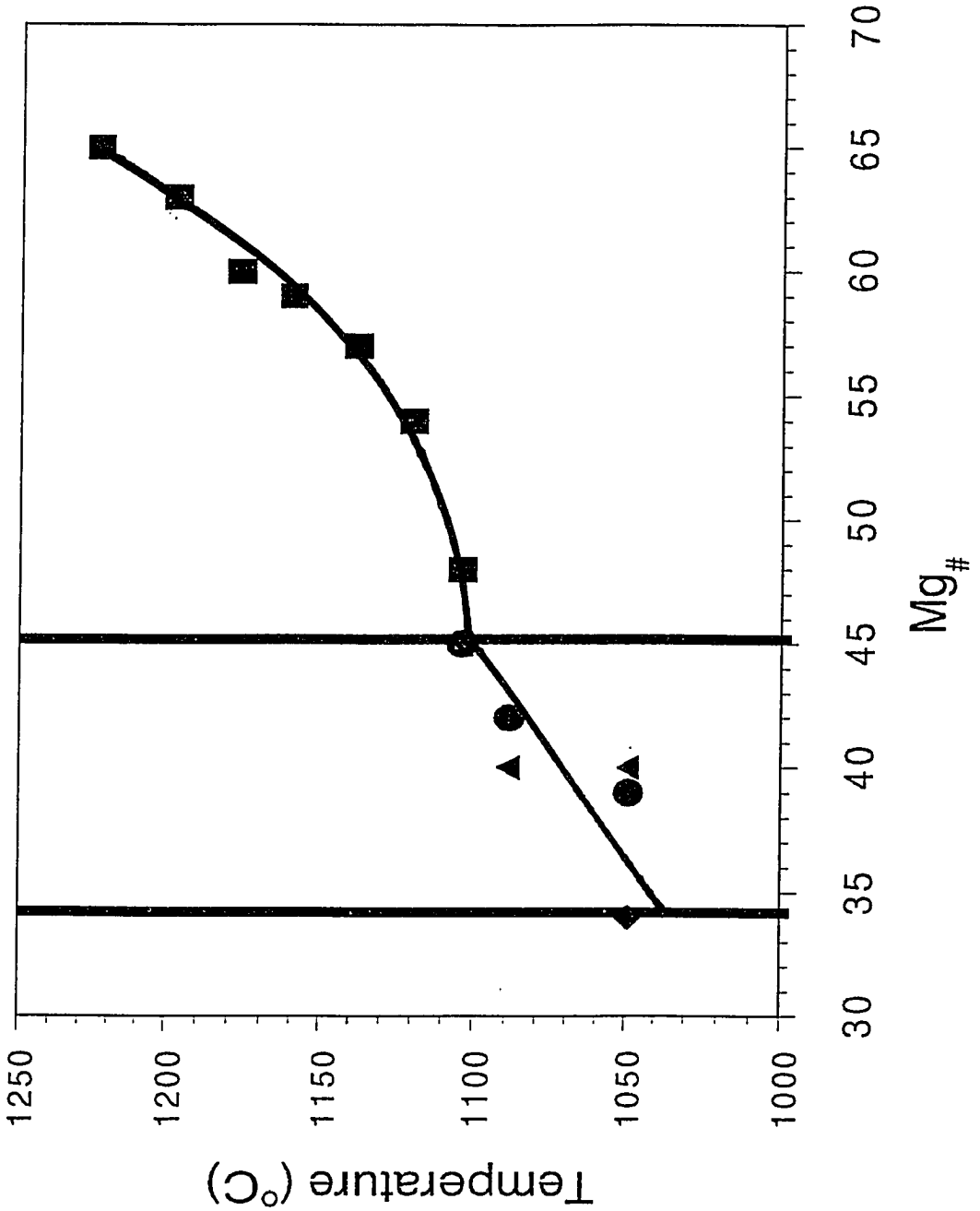

The final objective of this study is to determine if the alkaline rocks from Mt. Erebus were generated by low pressure crystal fractionation of the basanitic magma. One way to test this is to use a pseudo-liquidus diagram that has been developed by Sack et al. (1987) for alkaline rocks. If rock compositions from Mt. Erebus plot on or near the low pressure cotectic in Sack et al. (1987) olivine-high calcium pyroxene-nepheline diagram, then one can assume that they are low pressure differentiation products. Figure 23 is the pseudo-liquidus diagram of Sack et al. (1987) with basanite, hawaiite, benmoreite, mugearite, and phonolite bulk compositions, reported by Kyle (1977) and Moore (1986), of Mt. Erebus plotted on it. Error in the position of the one atmosphere cotectic is shown by two dashed lines running parallel to the cotectic. Figure 23 shows that the bulk compositions of the Mt. Erebus rocks display a general tend that is parallel to but just below the one atmosphere cotectic. This supports the conclusion that the Mt. Erebus rocks are the products of pressure differentiation of a basanitic parental magma. As discussed earlier pseudo-liquidus diagrams do not accurately portray how changing pressure conditions affects the position of the cotectics in these types of diagrams. Thus, one would want additional tests that the rocks of Mt. Erebus are indeed low pressure differentiation products of a parent magma.

Figure 23: Figure 3: Pseudo-liquidus phase diagram from Sack et al. (1987, Figure 12) with basanite through phonolite compositions from the Mt. Erebus rocks. See text for discussion.

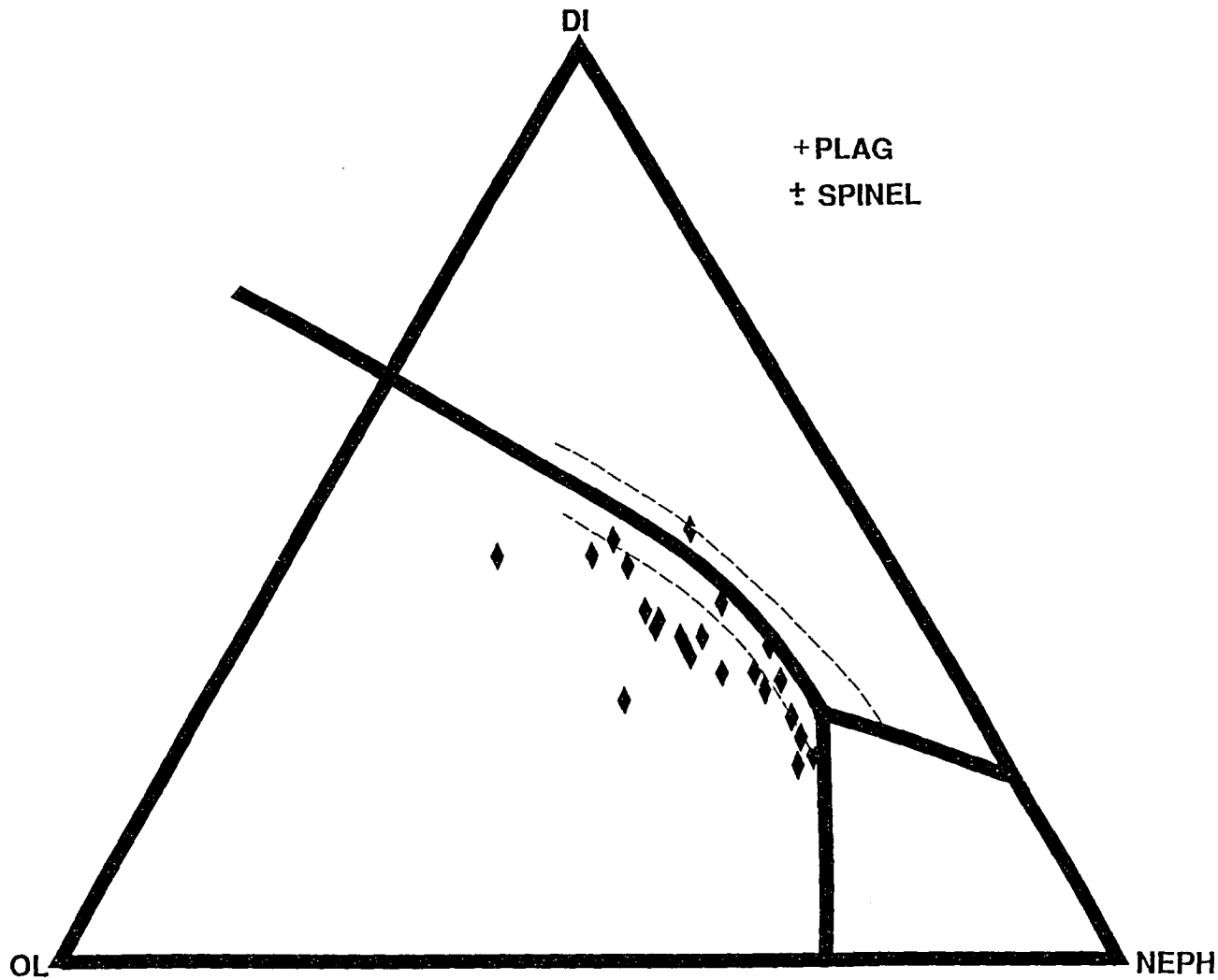

One such additional test would be to compare liquid lines of descent (LLD) defined by the experimental melts with the bulk compositional trends of rocks represented by variation diagrams. Rock data from Mt. Erebus can be summarized in terms of major element variation diagrams where TiO_2, Al_2O_3, FeO, MgO, CaO, Na_2O, K_2O, and P_2O_5 are plotted against SiO_2. Such plots result in curvilineon data arrays which suggest that the basanites, hawaiites mugerites, benmories, and phonolites are genetically related. Although such rocks series are likely the result of crystal fractionation, variation diagrams alone are not sufficient to judge if crystal fractionation took place at high or low pressures. Previous workers including Goldich (1975), Kyle and Moore (1990), Kyle et al. (1992), and Moore (1986) concluded that they formed by crystal fractionation at high pressures. One way to evaluate if the Mt. Erebus rocks are high pressure or low pressure crystal fractionation products is to superimpose the one atmosphere melt compositions from the present experiments onto Figure 1 a-h (Appendix A). If the data arrays from the XRF data of Moore (1986) and Kyle (1977) and the LLD defined by my glass compositions overlap then it is more likely that the rocks formed from low pressure fractionation of the basanitic magma. On the other hand, if the LLD trend is very different than the major element data array, the process is not low pressure crystal fractionation and may be the result

of high pressure crystallization (Gaetani and DeLong, 1995). In Figure 24 a-h TiO_2, Al_2O_3, FeO, MgO, CaO, Na_2O, K_2O, and P_2O_5 have been plotted against SiO_2. The open squares are the XRF data from Moore (1986) and Kyle (1977). The one atmosphere melt data from present experiments were corrected for Na_2O and/or FeO loss where applicable (see Table 24). What is observed in all these diagrams is that the LLD vector and major element data arrays overlap each other supporting the interpretation that the rocks of Mt. Erebus are the products of low pressure rather than high pressure crystal fractionation of a basanitic magma

CONCLUSIONS

Major conclusions reached in this study can be summarized as follows:

1) At one atmosphere pressure it is possible for a basanitc magma to differentiate to hawaiite and phonolite compositions.

2) Present experiments confirm that Mt. Erebus anorthoclase phonolite and hawaiite are the low pressure crystal fractionation products of a parental basanitic magma.

3) Presence of two high-calcium clinopyroxenes at a given temperature in the experiments is the first

Figure 24 a-h: Chemical variation diagrams. Open squares = Kyle (1977) and Moore (1986) XRF data. Filled triangles = basanite magma, filled circles = DVDP2 and 83415 hawaiite magmas, and the filled circles = anorthoclase phonolite magma.

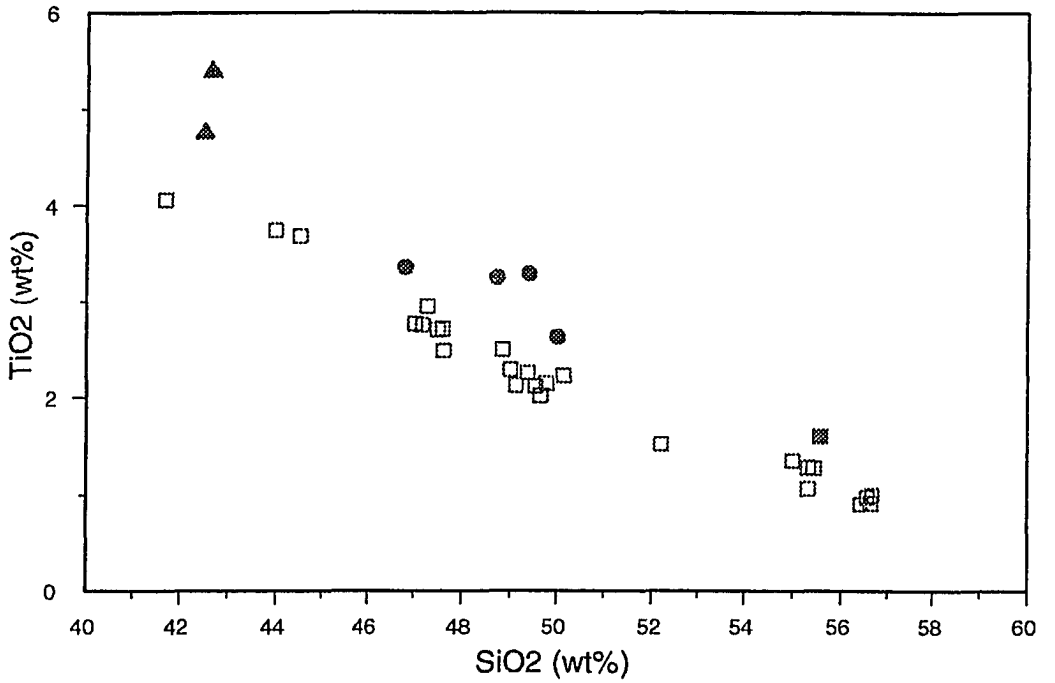

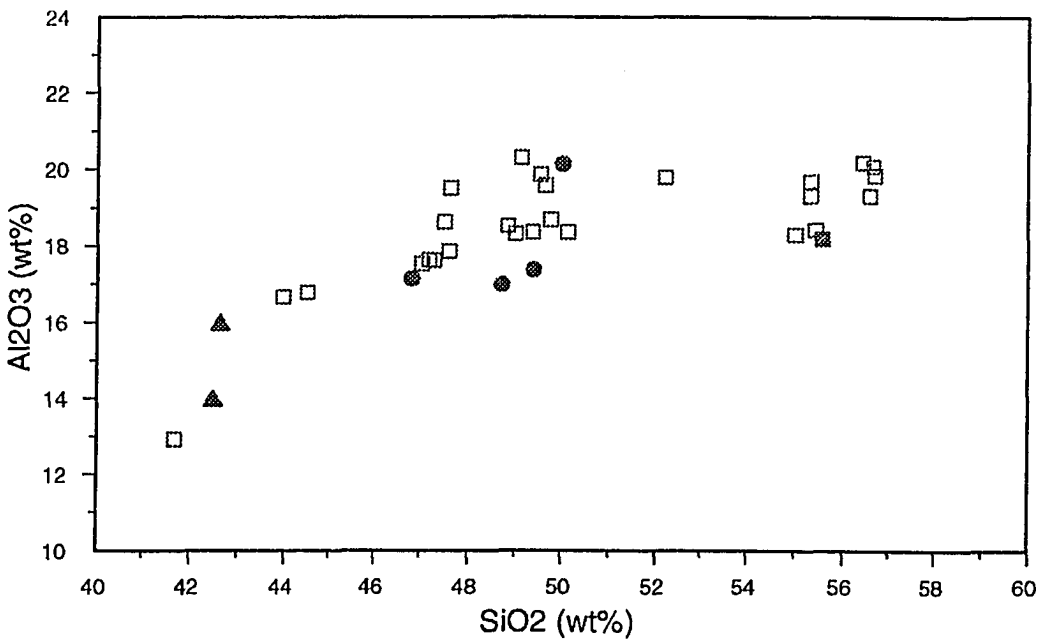

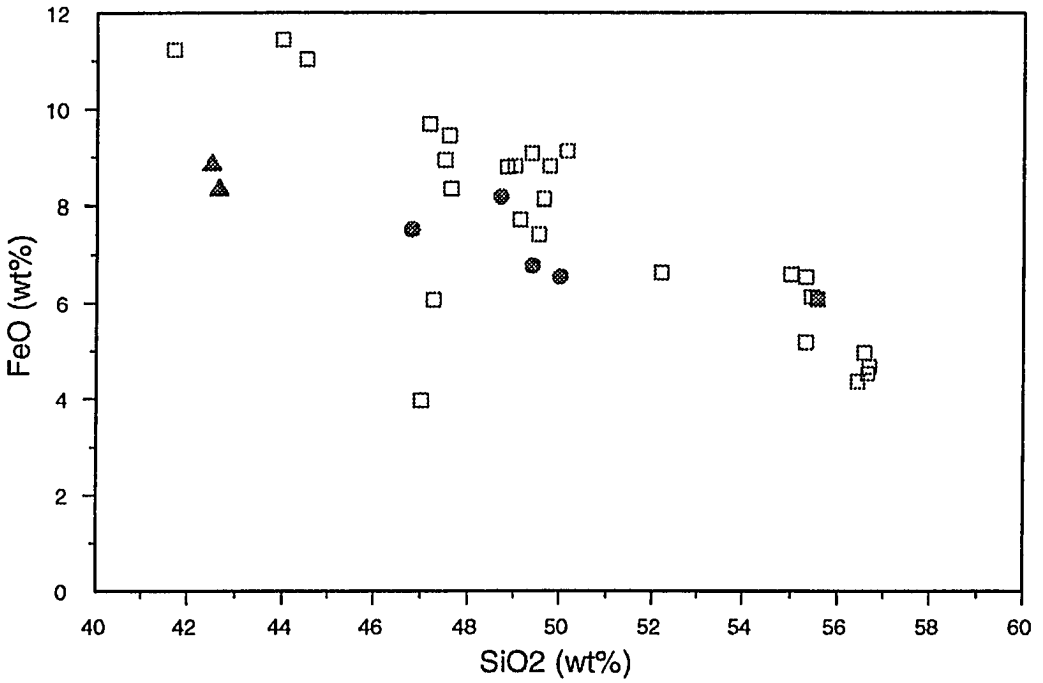

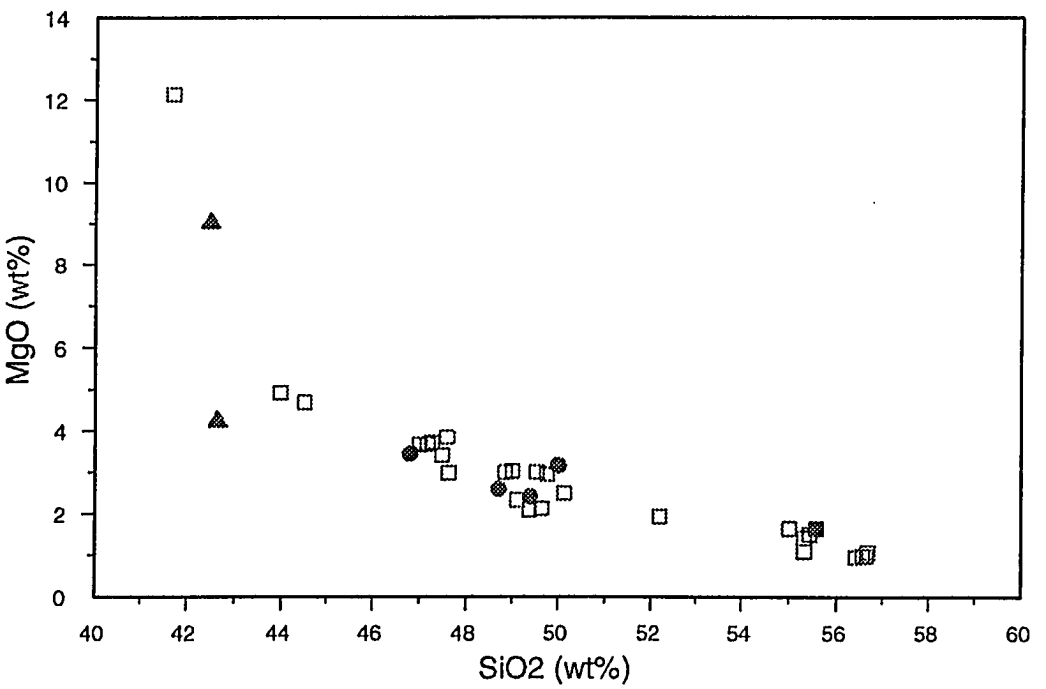

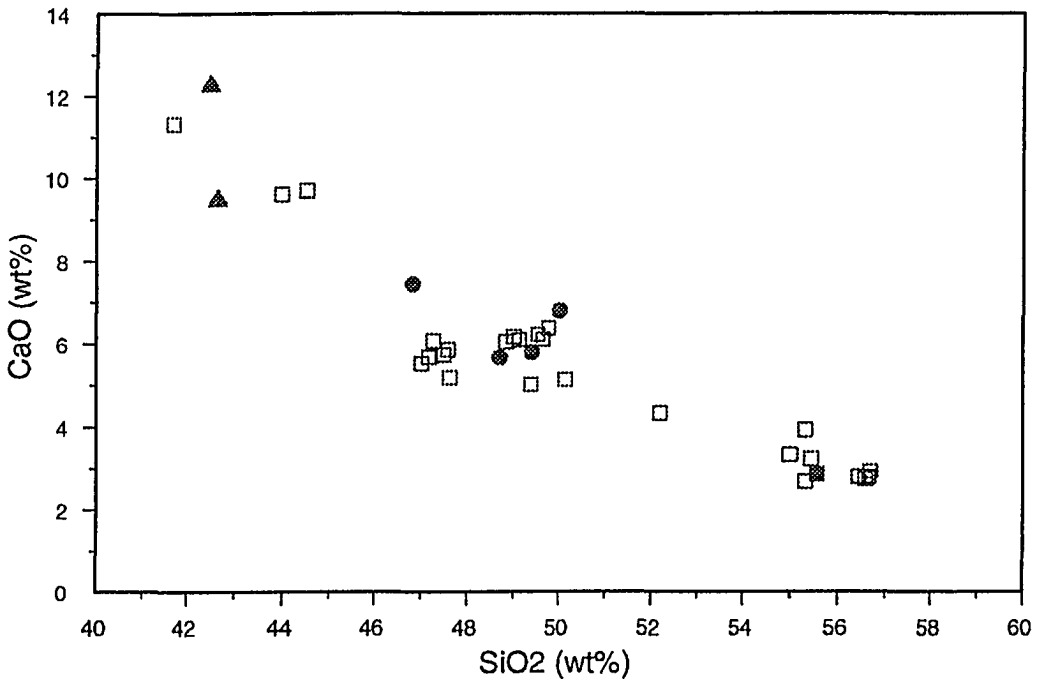

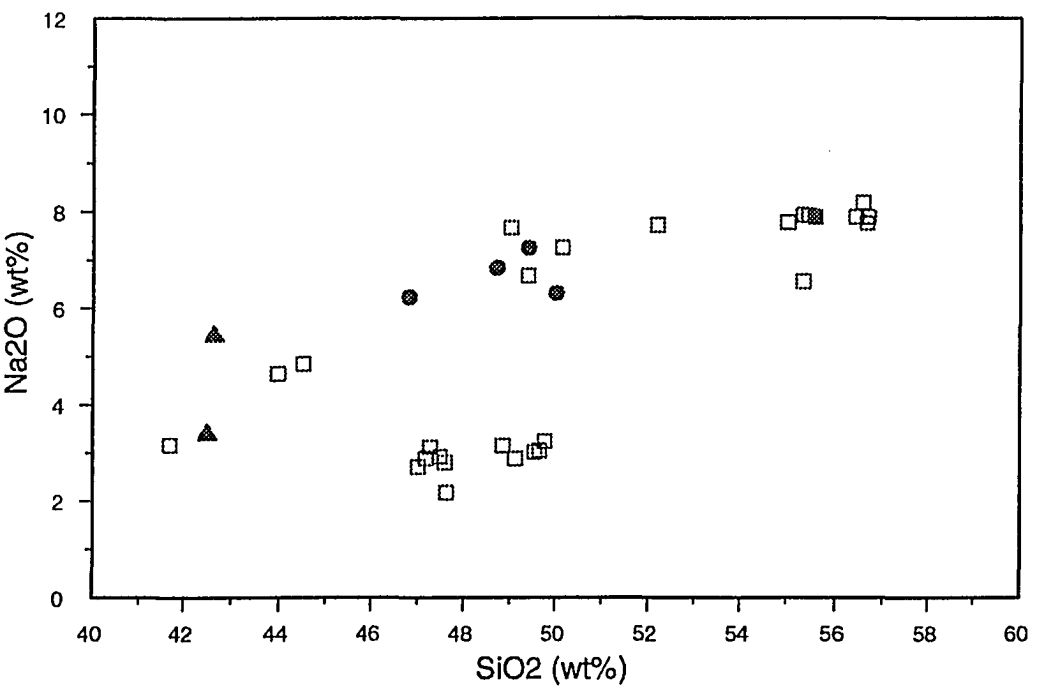

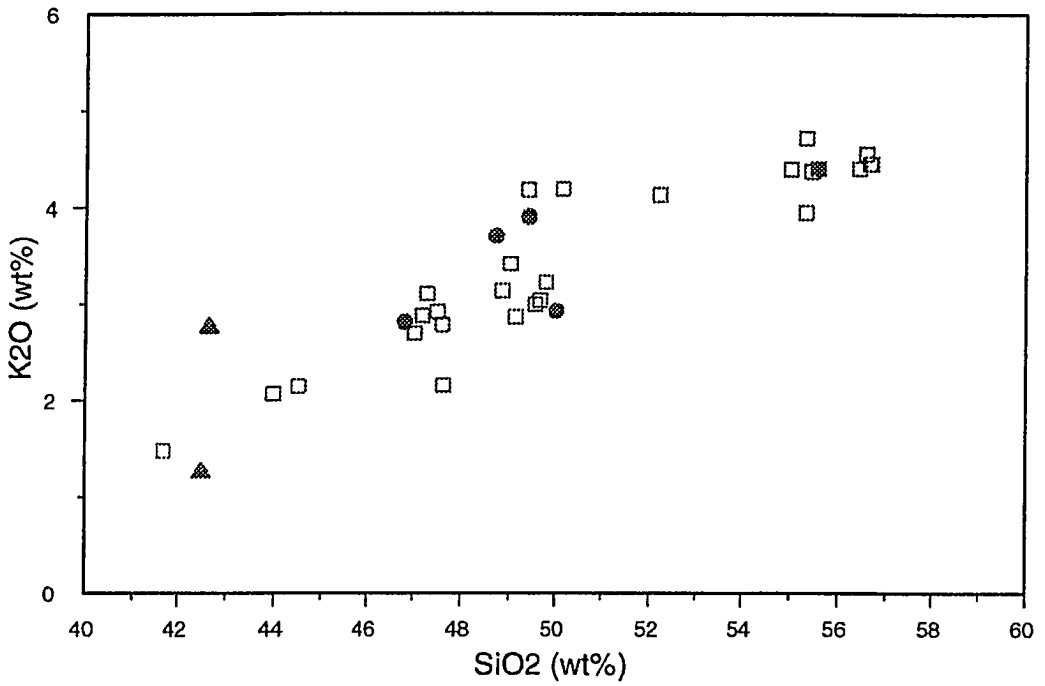

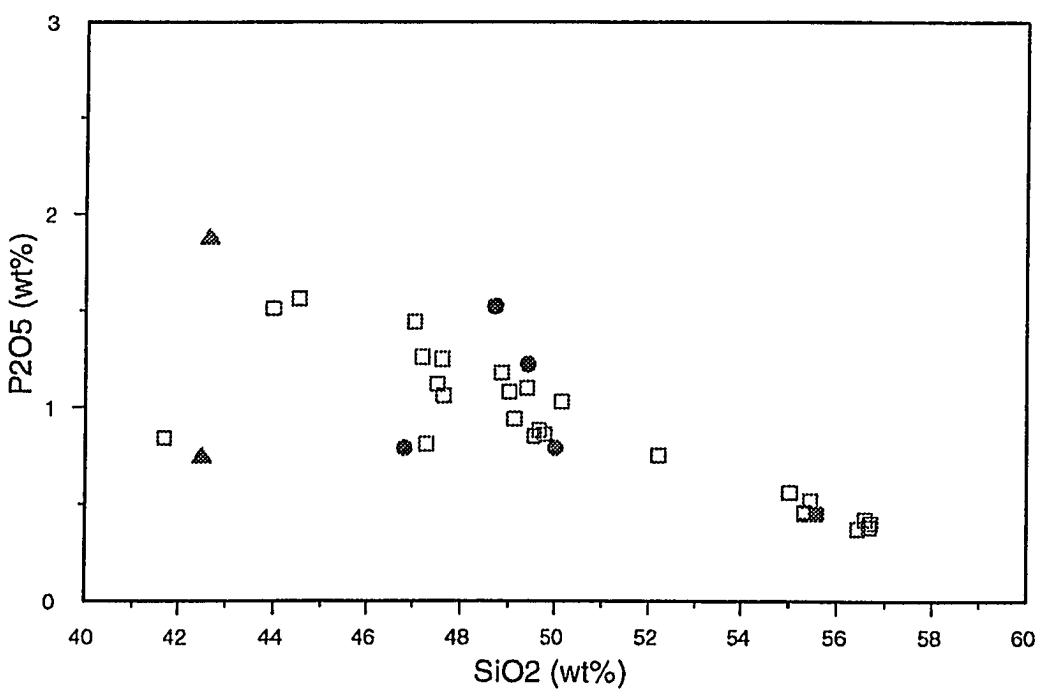

confirmation of the theoretically determined miscibility gap in clinopyroxenes as first suggested by Sack and Ghiorso (1994, Part I). Stability of two calcium-rich clinopyroxenes are further evidence that older representation of pyroxene compositions using the pyroxene quadrilateral is not sufficient. Both new pyroxene compositions must be defined and new graphical tools must be developed to accurately represent pyroxene compositions in natural and experimental systems.

4) Stability of two high-calcium clinopyroxenes at a given temperature casts considerable doubt on the validity of many crystal fractionation models where only one clinopyroxene composition is modelled.

BIBLIOGRAPHY

Albee, A.L. and Ray, L., 1970. Correction factors for election microprobe and microanalysis of silicates, oxides, carbonates, phosphates, and sulfates. Anal. Chem., 42: 1408-14.

Basaltic Volcanism Study Project, 1981. Basaltic volcanism on the Terrestrial Planets. New York, Pergamon Press, 1286 pp.

Bence, A.E.,and Albee, A.L., 1968. Experimental correction factors for the electron microanaylsis of silicates, and oxides. J Geol., 76: 382-403.

Berlin, R., and Henderson, C.M.B., 1969. The distribution of Sr and Ba between the alkalifeldspar, plagioclase, and groundmass phases of porphytitic trachytes, and phonolites. Geochim. Cosmochim. Acta., 33: 247-255.

Bottinga, Y., and Weill, 1972. The viscosity of magmatic silicate liquids: a model for calculation. Am. J. Sci., 272: 438-475.

Boudette, D.L., and Ford, A.B., 1966. Phyical properties of anorthoclase from Antarctic. Am. Miner., 51: 1374-1387.

Brown, F.H., and Carmichael, I.S.E., 1969. Quaternary volcanoes of the Lake Rudolf Region: 1. The basanite-tephrite series of the Korath Range. Lithos, 2: 239-260.

Brown, W.L., and Parsons, I., 1981. Towards a more practical two-feldspar geothermometer. Contr. Miner. Petrol., 76: 369-377.

Bryan, W.B., Finger, L.W., and Chayes, F., 1969. Estimating proportions in petrographic mixing equations by lease squares approximation. Science, 163: 926-927.

Camur, M.Z., 1989. Experimental and numerical study of low pressure equilibria in alkaline lavas., Ph.D. Dissertation, University of Cincinnati.

Carmichael, I.S.E., 1962. Pantelleritic liquids and their phenocrysts., Miner. Mag., 119: 95-131.

Carmichael, I.S.E., 1963. The crystallization of feldspar in vocanic acid liquids. Q.J. Geol. Soc. London, 119: 95-131.

Carmichael, I.S.E., 1964. Natural liquids and the phonolite minimum. Geol. J., 4: 55-60.

Carmichael, I.S.E., 1967. The iron-titanium oxides of salic volcanic rocks and their associated ferromagnesian silicates. Contr. Miner. Petrol., 14: 36-64.

Carmichael, I.S.E., and Mackenzie, W.S., 1964. The lattice parameters of high temperature triclinic sodic feldspar. Miner Mag., 33: 949-962.

Elkins, L.T., and Grove, T.L., 1990. Ternary feldspar experiments and thermodynamic models. Am. Miner., 75: 544-559.

Fitton, J.G., and Upton, B.G.J., 1987. Alkaline igneous rocks. Great Britian, Blackwell Scientific Publ., 568.

Fuhrman, M.L., and Lindsley, D.H., 1988. Ternary feldspar modeling and thermometry. Am. Miner., 73: 201-215.

Gaetani, G.A., DeLong, S.E., and Wark, D.A., 1995. Petrogenesis of basalts from the Blanco Trough, northeast Pacific: Inferences for off-axis melt generation. J. Geophys. Research, 100: 4197-4214.

Gallahan, W.L., and Wielsen, R.L., 1992. The partitioning of Sc, Y, and REE between high-Ca pyroxene and natural mafic to intermediate lavas at 1 atmosphere. Geochim. Cosmochim. Acta., 56: 2387-2404.

Gaskell, D.R., 1981. The thermodymanic properties and structures of slag. In: Tien, J.K., and Elliot, J.F.(eds) Metallurgical Treatises., Warrendale: Metallurgical Soc., AIME, 59-77.

Gee, L.L., and Sack, R.O., 1988. Experimental petrology of melilite and nephelinites. J. Petrology, 29: 1233-1255.

Gerke, T.L., 1990. Experimental Study of Granitic Rocks from the St. Francois Mountains, Missouri. M.S. thesis, University of Cincinnati, 119 pp.

Gerke, T.L., and Kilinc, A.I., 1993. Experimental Study of Granitic Rocks from the St. Francois Mountains, Missouri. Lithos, 29: 1-11.

Ghiorso, M.S., 1984. Activity/composition relations in the ternary feldspars. Contr. Miner. Petrol., 87: 282-296.

Ghiorso, M.S., and Carmichael, I.S.E., 1980. A regular solution model for met-aluminous silicate liquids: Applications to geothermometry, immiscibility, and the source regions of basic magma. Contr. Miner. Petrol., 71: 323-342

Ghiorso, M.S., and Sack, R.O., 1995. Chemical mass transfer in magmatic prodesses IV. A revised and intenally consistant thermodynamic model for the interpolation and extrapolation of liquid-solid equlibria in magmatic systems at elevated temperatures and pressures. Contr. Miner. Petrol., 119: 196-212.

Goldich, S.S., S.B., Suhr, N.H., and Stuckless, J.S.,1975. Geochemisrty of the cenozoic volcanic rocks of Ross Island and vicinity, Antarctica. J. Geol., 83: 415-435.

Green, N.L., and Udansky, S.I., 1986. Ternary-feldspar mixing relations and feldspar thermobarometry. Am. Miner., 71: 1100-1108.

Grove, T.L., Kinzler, R.J., and Bryan, W.B., 1992. Fractionation of Mid-Ocean Ridge Basalts (MORB). In Mantle Flow and Melt Generation at Mid-Ocean Ridges Morgan, J.P., Blackman, D.K., and Sinton, J.M. (eds), Geophysical Monograph, 71: 281-310

Haggerty, S.E., 1976. Opaque mineral oxides in terrestrial igneous rocks. In: Rumble, DIII (eds), Oxide Minerals, Miner, Soc. Am Shortcourse notes, 3, Hg101-Hg300.

Irving, A.J., and Frey, F.A., 1984. Trace element abundances in megacrysts and their host basalts: Constraints on partition coefficients and megacryst genesis. Geochim. Cosmochim. Acta., 48: 1201-1221.

Jones Faure, G., Taylor, K.S., and Corbato, E.E., 1983. The origin of salts on Mount Erebus and along the coast of Ross Island, Antarctica. Isotope Geoscience, 1: 57-64.

Kennedy, A.K., Grove, T.L., and Johnson, R.W., 1990. Experimental and major element constraints on the evolution of lavas from Lihir Island, Papua New Guinea. Contri. Miner. Petrol., 104: 722-734.

Kilinc, A.I., Carmicheal, I.S.E., Rivers, M.L.,and Sack, R.O., 1983. The Ferric-Ferrous ratio of nature silica liquids. Contr. Miner. Petrol., 83: 136-140.

Kyle, P.R., 1976. Geology, mineralogy, and geochemistry of late cenozoic McMurdo Volcanic Group, Victoria Land, Antarctica. Unpubl. Ph. D. thesis, Dept. of Geology, Victoria University of Wellington.

Kyle P.R., 1977. Mineralogy and glass chemistry of recent volcanic ejecta from Mt. Erebus, Ross Island, Antarctica. N.Z.J. Geol. Geophys., 20: 1123-1146.

Kyle, P.R., 1981b. Mineralogy and geochemistry of a basanite to phonolite sequence at Hut Point Peninsula, Antarctica, based on core from Dry Valley Drilling Project drillholes 1, 2, 3. J. Petrology, 22: 451-500.

Kyle, P.R., 1990. A.III. Erebus volcanic province. In: Volcanoes of the Antarctic Plate and Southern Oceans, Le Masurier, W.E., and Thomson, J.W. (eds), Antarctic Research Series, 48: 81-88.

Kyle, P.R., and Moore J.A., 1990. A.17. Mount Erebus. In:Volcanoes of the Antarctic Plate and Southern Oceans Le Masurier, W.E., and Thomson, J.W. (eds), Antarctic Research Series, 48: 103-108.

Kyle, P.R., Moore J.A., and Thirlwall, M.F., 1992. Petrologic evolution of anorthoclase phonolitic lavas at Mount Erebus, Ross Island, Antarctica. J. Petrology, 33: n.4, 849-876.

Langmuir, C.H., Klein, E.M., and Plank, T., 1992. Petrological Systematics of Mid-Ocean Ridge Basalts: Constraints on Melt Generation Beneath Ocean Ridges. In Mantle Flow and Melt Generation at Mid-Ocean Ridges Morgan, J.P., Blackman, D.K., and Sinton, J.M. (eds), Geophysical Monograph, 71: 183-280

Mason, R.A., Smith, J.V., Dawson, J.B., and Treves, S.B., 1982. A reconnaissance of trace elements in anorthoclase megacrysts. Miner. Mag., 46: 7-11.

Mayhood, G.A., and Baker, D.R. 1986. Experimental constraints on depths of fractionation of mildly alkalic basalts and associated felsic rocks: Pantelleria, Strait of Sicily. Contr. Miner. Petrol., 93: 251-264.

Moore, J.A., 1986. Mineralogy, geochemistry, and petrology of lavas of Mt. Erebus, Antarctica. M.S. thesis, New Mexico Institute of Mining and Technology, Socorro, New Mexico.

Nielsen, R.L., Gallahan W.L., and Newberger, F., 1992. Experimentally determined mineral-melt partition coefficients for Sc, Y, and REE for olivine, low-Ca pyroxene, magnetite, and natural silicate magmas. Contr. Miner. Petrol., 110: 488-499.

Price, J.G., 1985. Ideal site-mixing in solid solutions with applications to two-feldspar geothermometry. Am. Miner., 70: 696-701.

Richardson, F.D., 1956. Activities in ternary melts. Trans. Faraday Soc., 52: 1312-1324.

Ringwood, A.E., 1975. Composition and petrology of the earth's mantel. New York: McGraw-Hill, 618.

Roedder, P.L., and Emslie, R.F., 1970. Olivine-liquid equilibrium. Contr. Miner. Petrol., 29: 275-289.

Sack, R.O., Walker, D., and Carmichael, I.S.E., 1987. Experimental petrology of alkalic lavas: Constraints on cotectics of multiple saturation in natural basic liquids. Contri. Miner. Petrol., 96: 1-23.

Sack, R.O., and Ghiorso, M.S., 1994. Thermodynamics of multicomponent pyroxenes: I. Formulation of a general model. Contri. Miner. Petrol., 116: 277-286.

Sack, R.O., Ghiorso, M.S., 1994. Thermodynamica of multicomponent pyroxenes: III. Calibration of $Fe^{+2}(Mg)_{-1}$, $TiAl_2(MgSi_2)$-1, $Ti(Fe^{+3})_2(MgSi_2)_{-1}$, $AlFe^{+3}(MgSi)_{-1}$, $NaAl(CaMg)_{-1}$, and $Ca(Mg)_{-1}$ exchange reactions between pyroxenes and silicate melts. Contri. Miner. Petrol., 118: 271-296.

Schairer, J.F., and Yoder, H.S., 1961. Crystallization in the system Nepheline-Forsterite-Silica at one atmosphere. Carnegie Inst. Washington Yearb., 60: 141-144.

Schairer, J.F., and Yoder, H.S., 1960. The nature of residual liquids from crystallization with data on the system Nepheline-Diopside-Silica. Am. J. Sci., 258A: 273-283.

Smith, A.J., 1992. Experimental study of the Magdelena Obsidian: Iron-magnesium exchange between olivine and high silica melt. M.S. thesis, University of Cincinnati, 70.

Smith, W.C., 1954. The volcanic rocks of the Ross Archipalego. Brit. Antarctic Exped., 1910, Natural Hist. Rep., Geol., 2: 1-107.

Thompson, J.B. Jr., 1982. Composition space: an algebraic and geometric approach. In: Ferry, J.W. (eds) Characterization of metamorphism through mineral equilibria, Rev. Miner., 10: 1-32

Thy, P., 1991. High and low pressure phase equilibria of a mildly alkalic lava from the 1965 Surtsey eruption: Experimental results. Lithos, 26: 223-243.

Walker, D., Shibata, T., and DeLong, S.E., 1979. Abyssal tholeiites from the Oceanographer Fracture Zone II. Phase Equilibria and Mixing. Contri. Miner. Petrol., 70: 111-125.

Yagi, K., and Onuma, K., 1967. The join $CaMgSi_2O_6$-$CaTiAl_2O_6$ and its bearing on the titanaugites. J. Fac. Sci. Hokkaido Univ., Ser. IV, 8: 463-483.

Yang, H.L., 1975. Al- and Ti-rich clinopyroxene in the system $CaMgSi_2O_6$-$CaAl_2SiO_6$-$CaTiAl_2O_6$. Proc. Geol. Soc. China 18: 48-58.

Zoltai, T., and Stout, J.H., 1984. Mineralogy concepts and principles. STATE, Burgess Publishing Company, 505 pp.

APPENDIX A

Using variation diagrams Kyle et al. (1992) concluded that the Ne-hawaiite and anorthoclase phonolite are derivative magmas of the Mt. Erebus basanite magma. Figure 1 a-h, are harker diagrams I generated using data from Moore (1986) and Kyle (1976). TiO_2, FeO, MgO, CaO, and P_2O_5 show a general decrease as the SiO_2 content increases, whereas the Na_2O and K_2O content increase as the SiO_2 content increases. In all diagrams open squares = basanite, open triangles = Ne-hawaiite, filled circles = Ne-mugearite, asterisks = Ne-benmorite, and open circles = anorthoclase phonolite. Although these diagrams suggest a genetic relationship amoung basanite, Ne-hawaiite, Ne-mugearite, Ne-benmoreite, and anorthoclase phonolite, they cannot be used to discriminate among single out crystal fractionation, assimilation, or magma mixing as the mechanism producing differentiation.

Figure 1 a-h: Major element compositions of natural alkaline basalts from Ross Island and Tent Island. Data from Moore (1986) and Kyle (1976). In all diagrams the open squares=basanite, open triangles=Ne-hawaiite, flled circles=Ne-mugearite, astersks=Ne-benmoreite, and open circles=anorthoclase phonolite.

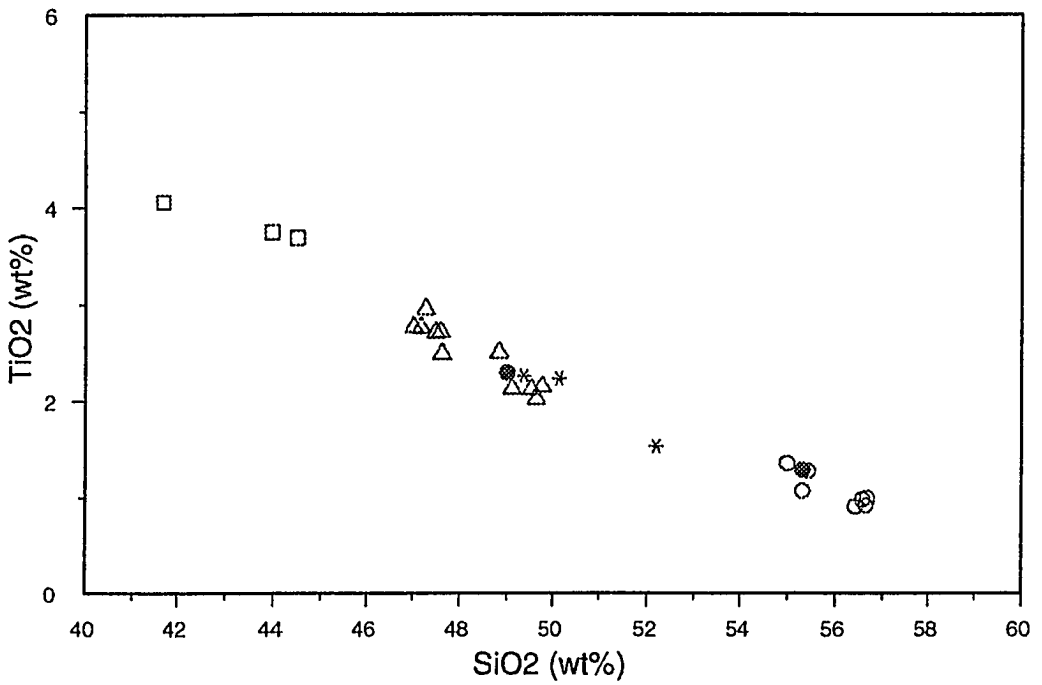

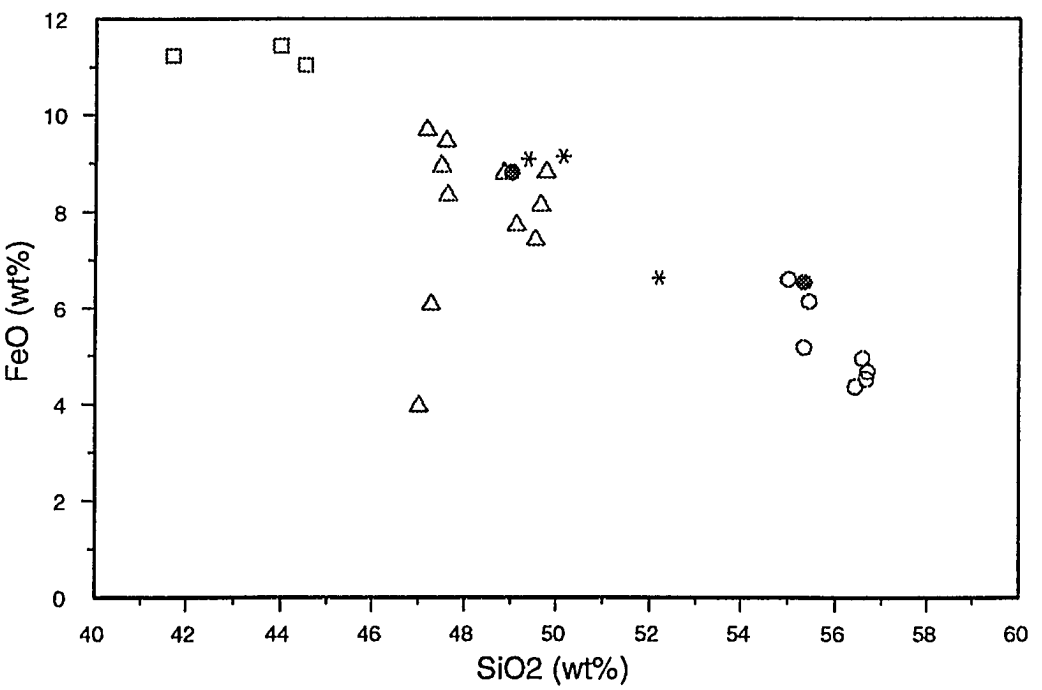

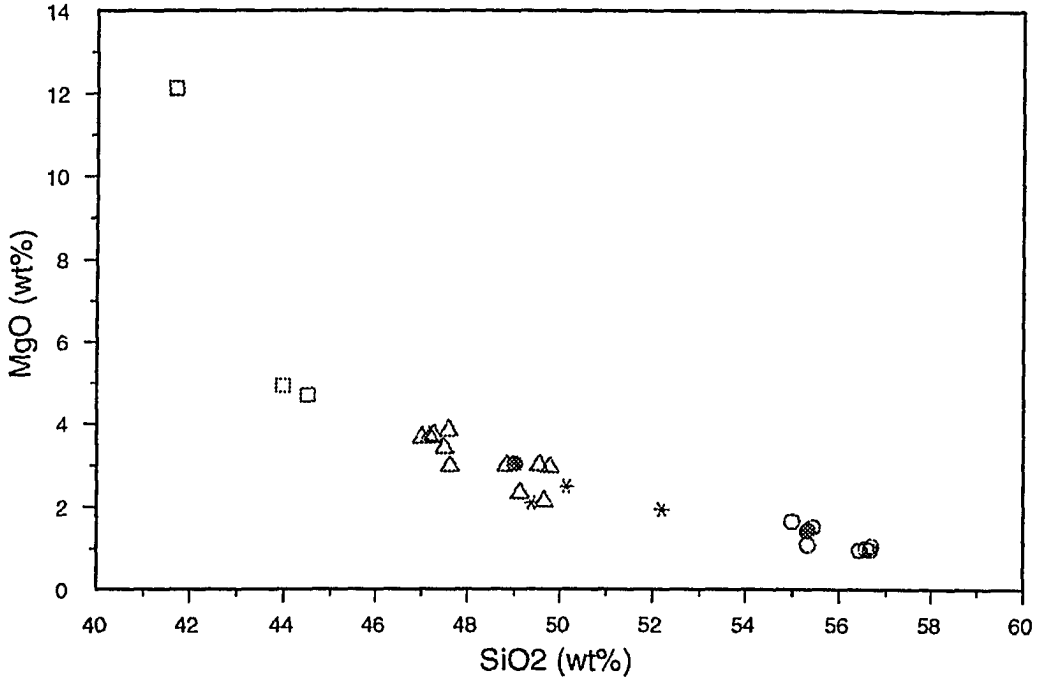

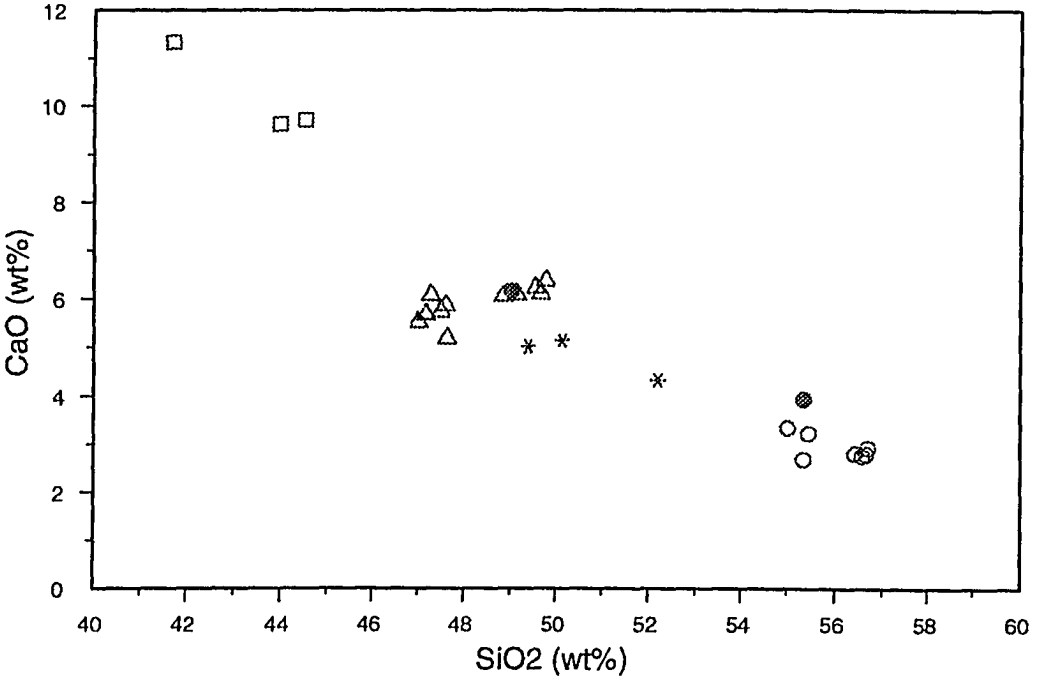

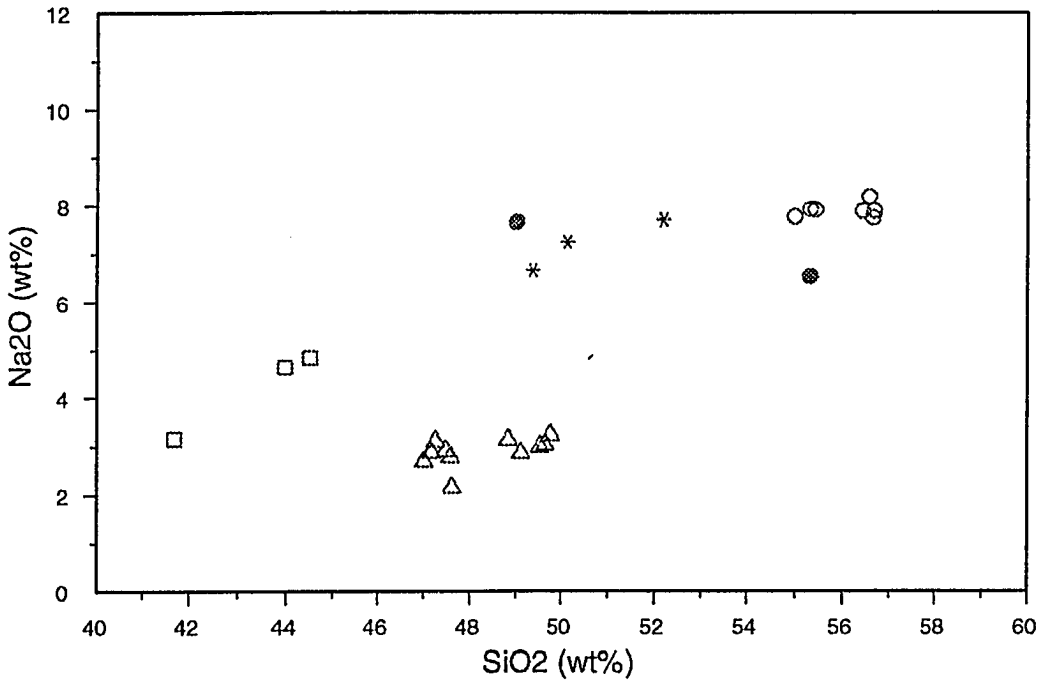

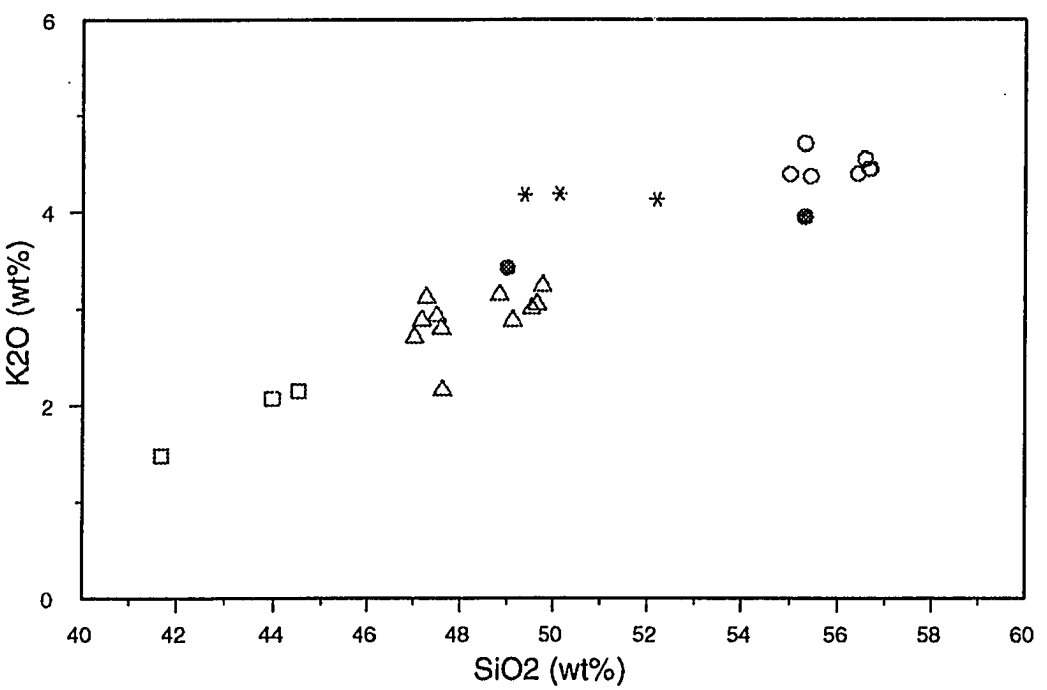

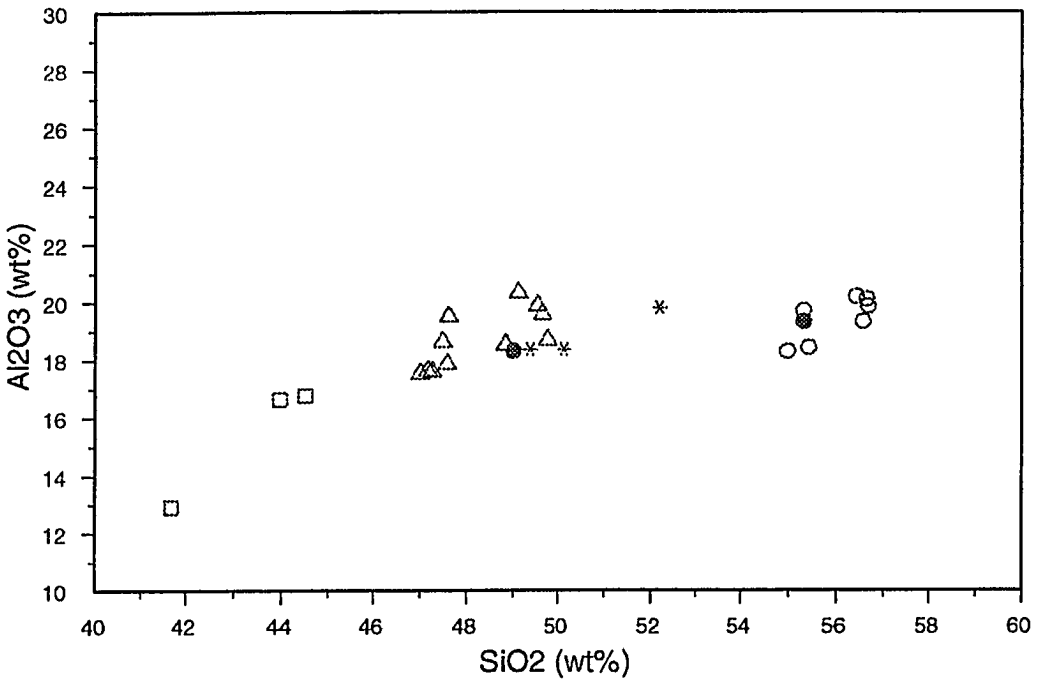

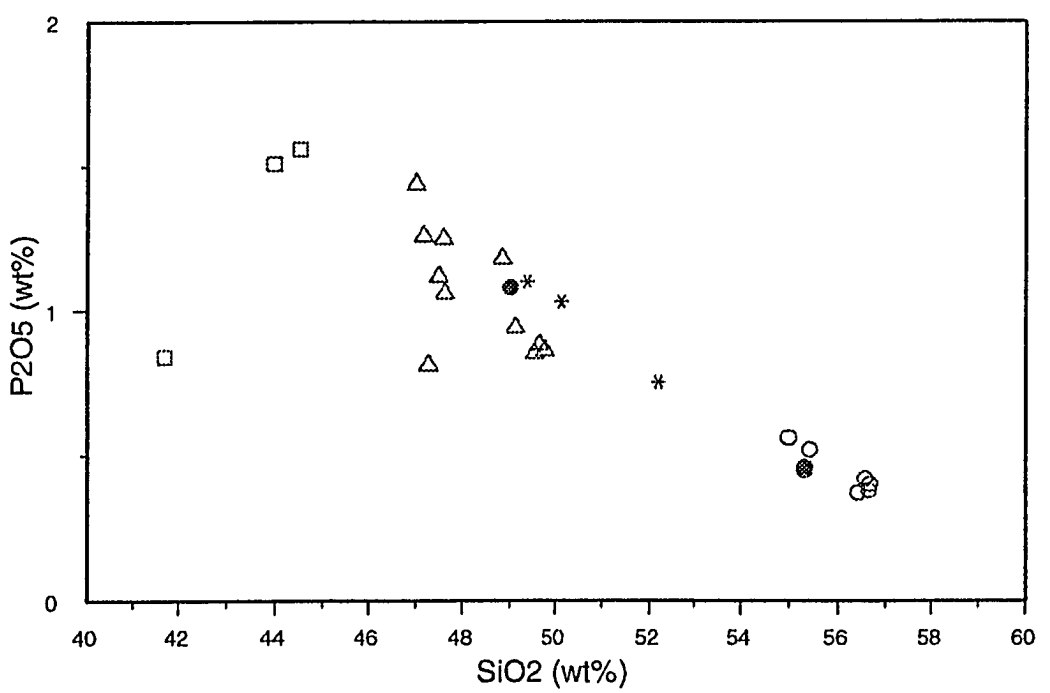

APPENDIX B

Microprobe Thin Section Preparation

AB epoxy was poured into 5 dram medicine vials and cured for 48 hours. The epoxy plugs were approximatley 2.2cm in diameter. The plugs were cut to a approximatley thickness of 1.27 cm. Six holes, 0.4 cm in diameter, were drilled in each section. A notch was made on the outer edge along one side as a reference point. Each disk was faced on an LP 30 Lappong machine and taped faced side down onto an index card. A drop of AB epoxy was placed in each hole and a small amount of each charge was pushed down into the epoxy. The holes were then completely filled with epoxy. The disks cured at room temperature for 24 to 48 hours. They were cut, ground, and faced with the LP 30 Lappong machine to thin sections approximately 35 microns thick. The sections were then hand polished using 1.0 and 0.05 micron alpha alumina. All sections were carbon coated at Purdue University.

APPENDIX C

Table 1: Olivine composition from the basanite

Hole#	1	1	1	1	1	1
An#	1	2	3	4	5	11
	r	r	i/c	i/c	i/r	r
SiO_2	38.77	38.95	38.11	38.16	38.46	38.93
TiO_2	0.01	0.00	0.04	0.03	0.00	0.02
Al_2O_3	0.06	0.12	0.10	0.07	0.09	0.10
Fe_2O_3	0.00	0.00	0.00	0.00	0.00	0.00
Cr_2O_3	0.00	0.00	0.00	0.00	0.00	0.00
FeO*	16.13	16.04	18.87	18.61	17.71	15.75
MnO	0.21	0.26	0.27	0.25	0.21	0.28
MgO	42.66	42.39	40.46	40.36	41.45	43.47
NiO	0.12	0.08	0.14	0.14	0.05	0.19
CoO	0.00	0.00	0.00	0.00	0.00	0.00
CaO	0.28	0.29	0.20	0.23	0.23	0.33
Na_2O	0.06	0.02	0.00	0.00	0.02	0.02
K_2O	0.00	0.00	0.01	0.01	0.01	0.00
P_2O_5	0.03	0.00	0.01	0.02	0.04	0.00
SrO	0.00	0.00	0.00	0.00	0.00	0.00
BaO	0.00	0.00	0.00	0.00	0.00	0.00
TOTAL	98.32	98.16	98.21	97.87	98.26	99.08
Fo	82.41	82.32	79.40	79.29	80.80	82.91
Fa	17.59	17.68	20.60	20.70	19.19	17.09

Hole#	1	1	1	1	1	1
An#	14	15	16	17	18	19
	c	i/r	r	r	r	r/c
SiO_2	38.31	39.11	38.42	38.83	37.97	38.75
TiO_2	0.02	0.01	0.00	0.09	0.12	0.12
Al_2O_3	0.06	0.05	0.05	0.08	0.05	0.06
Fe_2O_3	0.00	0.00	0.00	0.00	0.00	0.00
Cr_2O_3	0.00	0.00	0.00	0.00	0.00	0.00
FeO*	18.75	15.69	19.23	15.91	19.20	17.98
MnO	0.23	0.20	0.35	0.18	0.32	0.23
MgO	40.95	43.12	40.04	42.95	40.08	41.11
NiO	0.02	0.14	0.16	0.18	0.16	0.11
CoO	0.00	0.00	0.00	0.00	0.00	0.00
CaO	0.25	0.32	0.30	0.28	0.36	0.23
Na_2O	0.02	0.04	0.02	0.00	0.02	0.02
K_2O	0.01	0.01	0.00	0.01	0.00	0.01
P_2O_5	0.03	0.01	0.01	0.03	0.00	0.01
SrO	0.00	0.00	0.00	0.00	0.00	0.00
BaO	0.00	0.00	0.00	0.00	0.00	0.00
TOTAL	98.64	98.70	98.58	98.53	98.28	98.62
Fo	79.50	82.83	78.79	82.83	78.79	80.20
Fa	20.50	17.17	21.21	17.17	21.21	19.80

Hole#	1	1	1	2	2	2
An#	22	23	24	1	6	8
	c	c	c	c	c	c
SiO_2	39.48	38.51	39.42	39.53	38.51	39.76
TiO_2	0.09	0.00	0.06	0.00	0.03	0.09
Al_2O_3	0.09	0.06	0.05	0.07	0.09	0.05
Fe_2O_3	0.00	0.00	0.00	0.00	0.00	0.00
Cr_2O_3	0.00	0.00	0.00	0.00	0.00	0.00
FeO*	14.80	19.04	13.09	11.75	15.75	11.88
MnO	0.22	0.31	0.18	0.17	0.29	0.22
MgO	43.97	40.24	45.22	45.84	42.78	46.38
NiO	0.23	0.29	0.29	0.35	0.16	0.23
CoO	0.00	0.00	0.00	0.00	0.00	0.00
CaO	0.29	0.31	0.25	0.25	0.37	0.25
Na_2O	0.00	0.07	0.02	0.02	0.04	0.07
K_2O	0.01	0.00	0.02	0.00	0.00	0.02
P_2O_5	0.01	0.00	0.09	0.04	0.01	0.02
SrO	0.00	0.00	0.00	0.00	0.00	0.00
BaO	0.00	0.00	0.00	0.00	0.00	0.00
TOTAL	99.19	98.84	98.68	98.03	98.03	98.95
Fo	84.26	79.19	85.86	87.37	82.41	87.37
Fa	15.74	20.81	14.14	12.63	17.59	12.63

Hole#	2	2	2	2	3	3
An#	9	10	11	18	8	12
	i/r	i/c	i/r	i/c	i/r	c
SiO_2	39.20	39.42	39.21	38.73	39.40	38.60
TiO_2	0.04	0.00	0.03	0.06	0.00	0.00
Al_2O_3	0.08	0.06	0.03	0.07	0.06	0.08
Fe_2O_3	0.00	0.00	0.00	0.00	0.00	0.00
Cr_2O_3	0.00	0.00	0.00	0.00	0.00	0.00
FeO*	14.62	11.63	15.63	17.27	14.85	16.20
MnO	0.20	0.08	0.19	0.26	0.21	0.23
MgO	44.52	46.52	43.37	41.96	43.91	42.82
NiO	0.13	0.28	0.16	0.11	0.24	0.22
CoO	0.00	0.00	0.00	0.00	0.00	0.00
CaO	0.30	0.23	0.18	0.30	0.28	0.32
Na_2O	0.03	0.02	0.03	0.07	0.09	0.03
K_2O	0.00	0.00	0.00	0.00	0.03	0.07
P_2O_5	0.08	0.07	0.07	0.06	0.04	0.03
SrO	0.00	0.00	0.00	0.00	0.00	0.00
BaO	0.00	0.00	0.00	0.00	0.00	0.00
TOTAL	99.19	98.30	98.90	98.87	99.09	98.59
Fo	84.42	87.94	83.33	81.31	83.84	82.41
Fa	15.58	12.06	16.67	18.69	16.16	17.59

Hole#	3	3	3	3	3	3
An#	14	15	16	17	18	21
	i/c	i/r	c	r	r	i/c
SiO_2	38.29	38.45	39.74	39.71	39.59	38.23
TiO_2	0.05	0.00	0.04	0.00	0.02	0.00
Al_2O_3	0.09	0.08	0.08	0.07	0.08	0.02
Fe_2O_3	0.00	0.00	0.00	0.00	0.00	0.00
Cr_2O_3	0.00	0.00	0.00	0.00	0.00	0.00
FeO*	18.11	18.08	12.77	11.93	12.18	21.06
MnO	0.30	0.19	0.18	0.19	0.18	0.43
MgO	41.06	41.74	45.37	46.61	46.08	39.09
NiO	0.22	0.10	0.30	0.31	0.19	0.10
CoO	0.00	0.00	0.00	0.00	0.00	0.00
CaO	0.18	0.19	0.29	0.24	0.31	0.37
Na_2O	0.08	0.02	0.05	0.11	0.07	0.05
K_2O	0.00	0.00	0.00	0.03	0.04	0.03
P_2O_5	0.11	0.02	0.01	0.04	0.06	0.00
SrO	0.00	0.00	0.00	0.00	0.00	0.00
BaO	0.00	0.00	0.00	0.00	0.00	0.00
TOTAL	98.49	98.88	98.81	99.25	98.79	99.37
Fo	80.3	80.5	86.29	87.44	86.93	76.77
Fa	19.7	19.5	13.71	12.56	13.07	23.23

Hole#	3	5	5	5	5	5
An#	22	1	2	3	4	5
	c	c	r	r	r	i/r
SiO_2	39.30	38.13	39.34	39.61	38.68	37.44
TiO_2	0.04	0.09	0.00	0.00	0.06	0.04
Al_2O_3	0.06	0.07	0.10	0.04	0.06	0.07
Fe_2O_3	0.00	0.00	0.00	0.00	0.00	0.00
Cr_2O_3	0.00	0.00	0.00	0.00	0.00	0.00
FeO*	14.01	18.66	13.10	12.37	15.16	22.49
MnO	0.20	0.27	0.21	0.17	0.30	0.39
MgO	44.51	40.38	45.13	46.23	43.53	37.47
NiO	0.14	0.29	0.28	0.31	0.23	0.16
CoO	0.00	0.00	0.00	0.00	0.00	0.00
CaO	0.30	0.26	0.25	0.21	0.30	0.33
Na_2O	0.06	0.09	0.05	0.02	0.04	0.01
K_2O	0.01	0.03	0.00	0.01	0.01	0.00
P_2O_5	0.00	0.03	0.06	0.04	0.02	0.01
SrO	0.00	0.00	0.00	0.00	0.00	0.00
BaO	0.00	0.00	0.00	0.00	0.00	0.00
TOTAL	98.64	98.29	98.51	99.01	98.38	98.39
Fo	84.92	79.29	85.86	86.93	83.42	74.75
Fa	15.08	20.71	14.14	13.07	16.58	25.25

FeO* = total iron, Fo = forsterite, Fa = fayalite
c = core analysis, i/c = intermediate/core analysis,
i/r = intermediate/rim analysis, r = rim analysis

Table 2: Clinopyroxene composition from the basanite

Hole#	1	1	2	2	2	2
An#	25	26	3	4	13	15
	c	c	c	i/r	c	c
SiO_2	44.85	44.82	44.72	44.51	44.41	44.77
TiO_2	4.13	4.15	3.22	3.19	3.16	2.93
Al_2O_3	7.54	7.02	8.74	9.05	8.97	8.63
Fe_2O_3	0.00	0.00	0.00	0.00	0.00	0.00
Cr_2O_3	0.00	0.00	0.00	0.00	0.00	0.00
FeO*	6.62	6.49	5.34	5.42	8.49	7.98
MnO	0.05	0.15	0.09	0.01	0.16	0.21
MgO	12.43	12.59	12.80	12.49	10.77	11.08
NiO	0.01	0.03	0.09	0.06	0.05	0.06
CoO	0.00	0.00	0.00	0.00	0.00	0.00
CaO	22.51	22.48	22.55	22.56	21.54	21.54
Na_2O	0.41	0.41	0.59	0.54	0.97	0.94
K_2O	0.02	0.02	0.02	0.01	0.01	0.01
P_2O_5	0.06	0.06	0.02	0.01	0.03	0.06
SrO	0.00	0.00	0.00	0.00	0.00	0.00
BaO	0.00	0.00	0.00	0.00	0.00	0.00
TOTAL	98.63	98.22	98.17	97.86	98.55	98.20
En	38.25	38.92	39.78	39.44	34.66	35.59
Fs	11.48	11.35	9.39	9.44	15.34	14.69
Wo	50.27	49.73	50.83	51.11	50.00	49.72
En+	41.67	42.11	43.37	43.03	37.89	38.65
Fs+	12.50	12.28	10.24	10.30	16.77	15.95
Wo+	45.83	45.61	46.39	46.67	45.34	45.40

Hole#	2	3	3	3	3	3
An#	16	1	2	5	10	11
	c	c	r	c	c	c
SiO_2	44.61	44.77	40.12	44.79	39.48	42.92
TiO_2	2.87	3.25	6.37	3.78	5.87	4.19
Al_2O	8.82	9.56	11.53	7.23	12.12	10.31
Fe_2O	0.00	0.00	0.00	0.00	0.00	0.00
Cr_2O	0.00	0.00	0.00	0.00	0.00	0.00
FeO*	8.28	6.42	6.77	6.25	7.02	6.24
MnO	0.15	0.04	0.00	0.12	0.02	0.05
MgO	10.86	11.51	10.48	12.59	10.30	11.95
NiO	0.00	0.02	0.03	0.00	0.01	0.00
CoO	0.00	0.00	0.00	0.00	0.00	0.00
CaO	21.67	21.97	22.90	22.69	22.64	21.93
Na_2O	1.03	1.10	0.46	0.48	0.58	0.74
K_2O	0.01	0.00	0.00	0.06	0.02	0.04
P_2O_5	0.02	0.00	0.02	0.03	0.05	0.00
SrO	0.00	0.00	0.00	0.00	0.00	0.00
BaO	0.00	0.00	0.00	0.00	0.00	0.00
TOTAL	98.32	98.62	98.69	98.02	98.10	98.36

En	34.83	37.36	34.09	38.92	33.52	38.42
Fs	15.17	11.49	12.50	10.81	13.07	11.30
Wo	50.00	51.15	53.41	50.27	53.41	50.28
En+	37.80	40.88	39.22	42.11	38.82	42.77
Fs+	16.46	12.58	14.38	11.07	15.13	12.58
Wo+	45.73	46.54	46.41	46.20	46.05	44.65

Hole#	3	3	5	6
An#	19	20	6	2
	c	i/r	i/c	c
SiO_2	45.48	41.61	46.54	40.69
TiO_2	3.08	4.97	2.86	6.13
Al_2O	8.29	10.83	6.85	11.05
Fe_2O	0.00	0.00	0.00	0.00
Cr_2O	0.00	0.00	0.00	0.00
FeO*	5.14	6.57	6.31	6.72
MnO	0.01	0.07	0.11	0.10
MgO	12.88	10.90	13.89	10.55
NiO	0.05	0.00	0.07	0.02
CoO	0.00	0.00	0.00	0.00
CaO	22.60	22.66	21.50	22.84
Na_2O	0.57	0.49	0.49	0.48
K_2O	0.02	0.03	0.00	0.00
P_2O_5	0.02	0.04	0.10	0.03
SrO	0.00	0.00	0.00	0.00
BaO	0.00	0.00	0.00	0.00
TOTAL	98.13	98.16	98.71	98.61
En	40.33	35.23	42.16	34.09
Fs	19.34	11.93	10.81	12.50
Wo	50.83	52.84	53.41	47.03
En+	43.71	39.74	45.09	38.96
Fs+	9.58	13.46	11.56	14.29
Wo+	46.71	46.79	43.35	46.75

FeO* = total iron
c = core analysis, i/c = intermediate/core analysis
i/r = intermediate/rim analysis, r = rim analysis
En = enstitate, Fs = ferrosilite, Wo = wollastonite
En+, Fs+, Wo+ = Ca Tschermak ($CaAl_2SiO_6$) corrected

Table 3: Plagioclase compositions from the basanite

Hole#	1	1	2	2	2	3
An#	27	29	7	15	20	3
SiO_2	50.35	49.60	49.18	50.23	50.29	50.71
TiO_2	0.11	0.30	0.26	0.22	0.19	0.29
Al_2O_3	30.92	31.60	31.54	30.78	30.69	30.61
Fe_2O_3	0.00	0.00	0.00	0.00	0.00	0.00
Cr_2O_3	0.00	0.00	0.00	0.00	0.00	0.00
FeO*	0.33	0.47	0.53	0.39	0.48	0.44
MnO	0.00	0.02	0.00	0.00	0.00	0.04
MgO	0.04	0.03	0.02	0.04	0.05	0.03
NiO	0.00	0.00	0.05	0.02	0.00	0.00
CoO	0.00	0.00	0.00	0.00	0.00	0.00
CaO	13.11	14.16	14.42	13.15	12.84	13.02
Na_2O	3.79	3.34	2.97	3.80	4.03	3.85
K_2O	0.27	0.18	0.16	0.20	0.31	0.27
P_2O_5	0.06	0.06	0.04	0.02	0.03	0.08
SrO	0.00	0.00	0.00	0.00	0.00	0.00
BaO	0.00	0.00	0.00	0.00	0.00	0.00
TOTAL	98.97	99.75	99.15	98.82	98.91	99.35
An	64.36	69.31	71.72	65.00	62.38	64.00
Ab	33.66	29.70	27.27	34.00	35.64	34.00
Or	1.98	0.99	1.01	1.00	1.98	2.00

Hole#	3	3	5	5	6
An#	13	23	4	9	3
SiO_2	50.58	56.62	50.68	51.28	50.91
TiO_2	0.17	0.17	0.19	0.13	0.27
Al_2O_3	30.52	27.19	30.90	30.56	30.70
Fe_2O_3	0.00	0.00	0.00	0.00	0.00
Cr_2O_3	0.00	0.00	0.00	0.00	0.00
FeO*	0.59	0.27	0.38	0.38	0.30
MnO	0.01	0.00	0.00	0.04	0.01
MgO	0.05	0.02	0.05	0.04	0.00
NiO	0.00	0.05	0.01	0.00	0.00
CoO	0.00	0.00	0.00	0.00	0.00
CaO	12.98	7.95	13.07	12.63	13.09
Na_2O	3.88	6.76	3.99	4.06	3.78
K_2O	0.26	0.57	0.32	0.28	0.20
P_2O_5	0.07	0.01	0.05	0.04	0.06
SrO	0.00	0.00	0.00	0.00	0.00
BaO	0.00	0.00	0.00	0.00	0.00
TOTAL	99.09	99.61	99.63	99.41	99.31
An	63.37	38.00	63.37	62.00	64.65
Ab	34.65	59.00	34.65	36.00	34.34
Or	1.98	3.00	1.98	2.00	1.01

FeO* = total iron
An = anorthite, Ab = albite, Or = orthoclase

Table 4: Apatite compositions of the basanite

Hole#	2
An#	12
SiO_2	0.34
TiO_2	0.06
Al_2O_3	0.03
Fe_2O_3	0.00
Cr_2O_3	0.00
FeO*	0.26
MnO	0.04
MgO	0.32
NiO	0.00
CoO	0.00
CaO	54.37
Na_2O	0.00
K_2O	0.01
P_2O_5	40.97
SrO	0.00
BaO	0.00
TOTAL	96.38

FeO* = total iron

Table 5: Olivine compositions from the DVDP2 hawaiite

Hole#	4	4
An#	13	14
SiO_2	39.67	39.41
TiO_2	0.00	0.00
Al_2O_3	0.04	0.06
Fe_2O_3	0.00	0.00
Cr_2O_3	0.00	0.00
FeO*	13.47	13.41
MnO	0.17	0.27
MgO	45.00	44.89
NiO	0.31	0.22
CoO	0.00	0.00
CaO	0.14	0.18
Na_2O	0.03	0.00
K_2O	0.01	0.00
P_2O_5	0.00	0.07
SrO	0.00	0.00
BaO	0.00	0.00
TOTAL	98.83	98.51
Fo	85.79	85.86
Fa	14.21	14.14

FeO* = total iron
Fo = forsterite, Fa = fayalite

Table 6: Clinopyroxene compositions from the DVDP2 hawaiite

Hole#	3	3	3	3	4	4
An#	2	3	4	5	1	3
	r	i/r	i/r	r	r	c
SiO_2	44.48	44.55	44.19	42.76	44.31	44.17
TiO_2	3.07	2.94	2.83	4.13	3.34	3.06
Al_2O_3	7.82	8.69	9.03	9.03	8.54	9.32
Fe_2O_3	0.00	0.00	0.00	0.00	0.00	0.00
Cr_2O_3	0.00	0.00	0.00	0.00	0.00	0.00
FeO*	8.15	10.26	9.81	8.33	7.24	8.44
MnO	0.28	0.22	0.33	0.21	0.11	0.24
MgO	11.40	9.38	9.29	10.60	11.71	10.33
NiO	0.01	0.04	0.00	0.03	0.00	0.00
CoO	0.00	0.00	0.00	0.00	0.00	0.00
CaO	22.24	21.38	21.10	22.38	22.04	21.63
Na_2O	0.58	1.05	1.16	0.63	0.70	0.88
K_2O	0.01	0.01	0.00	0.00	0.00	0.00
P_2O_5	0.09	0.03	0.03	0.07	0.01	0.04
SrO	0.00	0.00	0.00	0.00	0.00	0.00
BaO	0.00	0.00	0.00	0.00	0.00	0.00
TOTAL	98.13	98.54	97.76	98.17	98.01	98.10
En	35.52	30.86	31.03	33.70	37.22	33.71
Fs	15.30	18.86	18.39	14.92	12.73	15.43
Wo	49.18	50.29	50.57	51.38	50.00	50.86
En+	38.46	33.54	33.75	37.20	40.16	36.88
Fs+	15.38	20.50	20.00	16.46	13.94	16.88
Wo+	46.15	45.96	46.25	46.34	45.45	46.25

Hole#	4	4	4	4	4	4
An#	4	9	10	11	12	15
	r	i/c	i/r	r	r	gm
SiO_2	43.78	44.55	43.25	44.22	44.62	46.02
TiO_2	3.32	2.48	3.03	3.18	3.41	2.44
Al_2O_3	9.28	8.55	10.10	8.08	7.63	6.59
Fe_2O_3	0.00	0.00	0.00	0.00	0.00	0.00
Cr_2O_3	0.00	0.00	0.00	0.00	0.00	0.00
FeO*	7.42	10.03	9.46	8.48	8.14	7.78
MnO	0.06	0.39	0.21	0.24	0.18	0.18
MgO	11.18	9.41	9.60	11.18	11.34	12.23
NiO	0.02	0.05	0.00	0.08	0.00	0.00
CoO	0.00	0.00	0.00	0.00	0.00	0.00
CaO	21.82	21.36	21.73	21.95	22.30	21.85
Na_2O	0.81	1.11	0.90	0.72	0.66	0.63
K_2O	0.00	0.01	0.00	0.01	0.00	0.00
P_2O_5	0.00	0.03	0.01	0.15	0.00	0.06
SrO	0.00	0.00	0.00	0.00	0.00	0.00
BaO	0.00	0.00	0.00	0.00	0.00	0.00
TOTAL	97.71	97.96	98.29	98.29	98.28	97.80
En	35.96	30.68	31.25	35.36	35.52	37.84
Fs	13.48	18.75	17.61	14.92	14.21	13.51
Wo	50.56	50.57	51.14	49.72	50.27	48.65
En+	39.51	33.13	34.38	33.55	38.46	40.23
Fs+	14.81	20.25	19.38	16.27	15.38	14.37
Wo+	45.68	46.63	46.25	45.18	46.15	45.40

Hole#	4	4	4	5	5	5
An#	17	18	19	1	2	11
	r	c	r	r	r	r
SiO_2	47.53	45.47	48.24	47.50	44.98	39.39
TiO_2	2.24	1.71	2.24	2.39	3.69	1.77
Al_2O_3	4.64	6.87	4.47	4.91	7.13	3.84
Fe_2O_3	0.00	0.00	0.00	0.00	0.00	0.00
Cr_2O_3	0.00	0.00	0.00	0.00	0.00	0.00
FeO*	7.21	14.34	7.15	7.44	7.40	5.70
MnO	0.21	0.49	0.19	0.17	0.21	0.14
MgO	12.98	6.51	13.11	12.88	11.93	10.80
NiO	0.03	0.00	0.06	0.05	0.08	0.01
CoO	0.00	0.00	0.00	0.00	0.00	0.00
CaO	22.44	20.35	22.39	22.34	22.20	28.19
Na_2O	0.52	1.85	0.55	0.56	0.59	0.40
K_2O	0.01	0.00	0.00	0.01	0.02	0.01
P_2O_5	0.06	0.02	0.05	0.00	0.03	7.56
SrO	0.00	0.00	0.00	0.00	0.00	0.00
BaO	0.00	0.00	0.00	0.00	0.00	0.00
TOTAL	97.87	97.60	98.45	98.24	98.27	97.82
En	39.15	27.91	39.36	38.83	37.16	31.63
Fs	12.17	22.09	12.23	12.77	13.11	9.18
Wo	48.68	50.00	48.40	48.40	49.73	59.18
En+	41.11	23.46	41.11	40.78	40.24	36.05
Fs+	12.78	29.63	12.78	13.41	14.20	10.47
Wo+	46.11	46.91	46.11	45.81	45.56	53.49

Hole#	5	5	5	5	5	5
An#	12	14	15	16	17	18
	i	i	i/r	r	gm	gm
SiO_2	42.33	42.20	42.21	42.32	47.60	42.51
TiO_2	3.87	3.51	3.50	3.77	2.53	4.27
Al_2O_3	11.22	11.24	11.53	11.61	4.89	8.89
Fe_2O_3	0.00	0.00	0.00	0.00	0.00	0.00
Cr_2O_3	0.00	0.00	0.00	0.00	0.00	0.00
FeO*	8.33	9.13	8.32	8.16	7.27	8.39
MnO	0.16	0.22	0.20	0.16	0.21	0.26
MgO	9.90	9.41	9.70	10.10	12.94	10.65
NiO	0.10	0.06	0.00	0.05	0.00	0.02
CoO	0.00	0.00	0.00	0.00	0.00	0.00
CaO	21.82	21.48	21.63	22.18	22.30	22.09
Na_2O	0.87	0.98	0.88	0.88	0.54	0.66
K_2O	0.01	0.00	0.01	0.01	0.01	0.01
P_2O_5	0.02	0.03	0.01	0.01	0.10	0.08
SrO	0.00	0.00	0.00	0.00	0.00	0.00
BaO	0.00	0.00	0.00	0.00	0.00	0.00
TOTAL	98.62	98.25	98.00	99.27	98.40	97.83
En	37.76	31.40	32.56	32.95	39.04	34.25
Fs	15.52	16.86	15.70	15.03	12.30	14.92
Wo	51.72	51.74	51.74	52.02	48.66	50.83
En+	36.77	35.06	36.66	37.01	41.01	37.80
Fs+	17.42	18.83	17.53	16.88	12.92	16.46
Wo+	45.81	46.10	46.10	46.10	46.07	45.73

Hole#	6	6	6	6	6	6
An#	5	6	8	9	10	14
	i/r	c	r	i	c	r
SiO_2	44.37	41.20	43.38	47.01	44.79	46.46
TiO_2	3.03	5.12	3.72	1.99	2.74	2.92
Al_2O_3	7.55	10.00	8.25	7.27	9.06	5.36
Fe_2O_3	0.00	0.00	0.00	0.00	0.00	0.00
Cr_2O_3	0.00	0.00	0.00	0.00	0.00	0.00
FeO*	7.92	8.27	8.43	5.68	5.98	7.75
MnO	0.23	0.22	0.24	0.08	0.08	0.34
MgO	11.41	10.26	11.02	13.37	12.36	12.54
NiO	0.02	0.03	0.00	0.08	0.03	0.12
CoO	0.00	0.00	0.00	0.00	0.00	0.00
CaO	22.17	22.09	22.40	21.95	21.99	22.44
Na_2O	0.69	0.66	0.68	0.57	0.67	0.51
K_2O	0.01	0.00	0.01	0.01	0.00	0.00
P_2O_5	0.04	0.06	0.05	0.04	0.00	0.06
SrO	0.00	0.00	0.00	0.00	0.00	0.00
BaO	0.00	0.00	0.00	0.00	0.00	0.00
TOTAL	97.89	101.45	98.19	98.05	97.70	98.50
En	35.87	33.15	34.43	41.21	39.11	37.77
Fs	14.13	15.17	14.75	9.89	10.61	13.30
Wo	50.00	51.69	50.82	48.90	50.28	51.06
En+	38.82	37.34	37.72	43.86	42.42	40.11
Fs+	15.29	17.09	16.17	10.53	11.52	14.12
Wo+	45.88	45.57	46.11	45.61	46.06	45.76

Hole#	7	7
An#	6	7a
	r	i/c
SiO_2	43.39	43.32
TiO_2	3.80	3.24
Al_2O_3	9.77	9.88
Fe_2O_3	0.00	0.00
Cr_2O_3	0.00	0.00
FeO^*	7.25	7.29
MnO	0.08	0.16
MgO	11.12	11.23
NiO	0.00	0.00
CoO	0.00	0.00
CaO	21.57	21.91
Na_2O	0.74	0.83
K_2O	0.00	0.00
P_2O_5	0.01	0.06
SrO	0.00	0.00
BaO	0.00	0.00
TOTAL	97.72	97.91
En	36.36	36.16
Fs	13.07	12.99
Wo	50.57	50.85
En+	40.00	40.00
Fs+	14.38	14.38
Wo+	45.63	45.63

FeO^* = total iron
c = core analysis, i/c = intermediate/core analysis
i/r = interdediate/rim analysis, r = rim analysis, gm = ground mass
En = enstatite, Fs = ferrosilite, Wo = wollastonite
En+, Fs+, Wo+ = Ca Tschermak ($CaAl_2SiO_6$) corrected

Table 7: Kaersutite compositions from the DVDP2 hawaiite

Hole#	1	1	5	5	5	5	5
An#	1	2	6	7	8	9	10
			r	r/i	c	r/i	r
SiO_2	37.63	37.64	37.82	37.73	37.51	36.89	38.13
TiO_2	5.63	5.94	6.19	5.96	5.93	5.62	5.83
Al_2O_3	14.36	14.40	14.05	14.51	14.41	14.95	14.08
Fe_2O_3	0.00	0.00	0.00	0.00	0.00	0.00	0.00
Cr_2O_3	0.00	0.00	0.00	0.00	0.00	0.00	0.00
FeO*	13.10	13.20	10.94	12.54	13.33	12.71	10.99
MnO	0.25	0.17	0.17	0.17	0.17	0.18	0.15
MgO	10.05	10.14	11.57	10.66	9.99	10.27	11.66
NiO	0.00	0.00	0.01	0.01	0.00	0.01	0.02
CoO	0.00	0.00	0.00	0.00	0.00	0.00	0.00
CaO	11.58	11.70	11.98	11.66	11.50	11.65	11.79
Na_2O	2.58	2.52	2.47	2.56	2.48	2.33	2.53
K_2O	1.28	1.26	1.25	1.20	1.22	1.16	1.22
P_2O_5	0.06	0.06	0.06	0.12	0.03	0.00	0.07
SrO	0.00	0.00	0.00	0.00	0.00	0.00	0.00
BaO	0.00	0.00	0.00	0.00	0.00	0.00	0.00
TOTAL	96.51	97.03	96.51	97.13	96.57	95.75	96.47

Hole#	6	6	6	7	7	8	8
An#	2	3	4	1	2	1	2
	i/r	i/c	r	r	r	r	r
SiO_2	37.96	37.52	37.56	37.31	37.14	37.32	37.59
TiO_2	6.11	6.01	5.89	5.51	5.59	5.49	6.10
Al_2O_3	13.98	14.11	14.80	14.43	14.71	13.74	14.18
Fe_2O_3	0.00	0.00	0.00	0.00	0.00	0.00	0.00
Cr_2O_3	0.00	0.00	0.00	0.00	0.00	0.00	0.00
FeO*	10.45	10.49	10.27	11.12	11.61	10.54	9.08
MnO	0.08	0.17	0.12	0.15	0.22	0.17	0.09
MgO	12.08	12.11	11.81	11.10	10.85	11.54	12.54
NiO	0.05	0.00	0.05	0.01	0.00	0.03	0.05
CoO	0.00	0.00	0.00	0.00	0.00	0.00	0.00
CaO	11.83	11.74	12.01	11.51	11.39	11.49	11.61
Na_2O	2.36	2.42	2.20	2.47	2.42	2.62	2.34
K_2O	1.40	1.38	1.53	1.35	1.19	1.27	1.39
P_2O_5	0.06	0.09	0.08	0.04	0.06	0.09	0.05
SrO	0.00	0.00	0.00	0.00	0.00	0.00	0.00
BaO	0.00	0.00	0.00	0.00	0.00	0.00	0.00
TOTAL	96.36	96.04	96.32	95.00	95.18	94.31	95.00

FeO* = total iron
c = core analysis, i/c = intermediate/core analysis
i/r = intermediate/rim analysis, r = rim analysis

Table 8: Analysis of feldspar from the DDP2 hawaiite

Hole#	3	4	4	4	4	5
An#	6	5	6	7	16	3
SiO_2	56.38	61.45	52.92	53.43	58.18	52.38
TiO_2	0.18	0.12	0.16	0.18	0.12	0.17
Al_2O_3	27.68	25.23	29.68	29.16	26.67	29.74
Fe_2O_3	0.00	0.00	0.00	0.00	0.00	0.00
Cr_2O_3	0.00	0.00	0.00	0.00	0.00	0.00
FeO*	0.54	0.31	0.62	0.61	0.43	0.55
MnO	0.00	0.00	0.03	0.07	0.00	0.05
MgO	0.08	0.03	0.08	0.09	0.06	0.07
NiO	0.00	0.00	0.00	0.00	0.07	0.00
CoO	0.00	0.00	0.00	0.00	0.00	0.00
CaO	8.84	5.42	11.59	10.98	7.85	11.66
Na_2O	6.16	7.30	4.85	5.09	6.80	4.60
K_2O	0.52	1.38	0.40	0.32	0.86	0.30
P_2O_5	0.06	0.03	0.02	0.03	0.20	0.00
SrO	0.00	0.00	0.00	0.00	0.00	0.00
BaO	0.00	0.00	0.00	0.00	0.00	0.00
TOTAL	100.43	101.26	100.34	99.95	101.24	99.53
An	42.42	27.08	42.57	53.00	38.14	57.00
Ab	54.55	64.58	55.45	45.00	60.82	41.00
Or	3.03	8.33	1.98	2.00	1.03	2.00

Hole#	5	7	7	8
An#	5	11	12	3
SiO_2	61.50	55.55	59.24	55.23
TiO_2	0.17	0.18	0.14	0.30
Al_2O_3	22.04	27.73	26.64	27.30
Fe_2O_3	0.00	0.00	0.00	0.00
Cr_2O_3	0.00	0.00	0.00	0.00
FeO*	0.55	0.65	0.72	0.58
MnO	0.02	0.00	0.09	0.02
MgO	0.04	0.10	0.21	0.09
NiO	0.06	0.08	0.06	0.04
CoO	0.00	0.00	0.00	0.00
CaO	0.81	9.13	7.52	8.73
Na_2O	5.82	5.95	6.46	5.87
K_2O	8.00	0.47	0.68	0.55
P_2O_5	0.51	0.01	0.10	0.09
SrO	0.00	0.00	0.00	0.00
BaO	0.00	0.00	0.00	0.00
TOTAL	99.52	99.85	101.85	98.78
An	3.92	44.44	37.23	43.88
Ab	50.00	52.53	58.51	53.06
Or	46.08	3.03	4.26	3.06

FeO* = total iron
An = anorthite, Ab = albite, Or = orthoclase

Table 9: Apatite composition
the DVDP2 hawaiite

Hole#	7	3
An#	10	1
SiO_2	0.39	0.36
TiO_2	0.00	0.10
Al_2O_3	0.02	0.06
Fe_2O_3	0.00	0.00
Cr_2O_3	0.00	0.00
FeO*	0.30	0.30
MnO	0.06	0.11
MgO	0.35	0.32
NiO	0.02	0.00
CoO	0.00	0.00
CaO	55.29	55.90
Na_2O	0.00	0.00
K_2O	0.04	0.01
P_2O_5	40.87	41.25
SrO	0.00	0.00
BaO	0.00	0.00
TOTAL	97.34	98.41

FeO* = total iron

Table 10: Olivine compositions from the 83415 Ne-hawaiite

Hole#	1	1	2	2	2	2
An#	5	8	2	3	4	9
	i/r	i/c	c	i	r	r
SiO_2	36.64	36.53	37.22	36.74	37.77	37.41
TiO_2	0.06	0.03	0.04	0.01	0.09	0.09
Al_2O_3	0.08	0.06	0.06	0.06	0.05	0.04
Fe_2O_3	0.00	0.00	0.00	0.00	0.00	0.00
Cr_2O_3	0.00	0.00	0.00	0.00	0.00	0.00
FeO*	28.53	28.28	26.23	28.57	25.28	25.15
MnO	0.82	0.80	0.85	0.85	0.65	0.75
MgO	32.38	32.08	34.05	32.83	34.92	34.90
NiO	0.00	0.00	0.06	0.03	0.00	0.00
CoO	0.00	0.00	0.00	0.00	0.00	0.00
CaO	0.32	0.36	0.44	0.42	0.50	0.43
Na_2O	0.03	0.05	0.03	0.06	0.03	0.04
K_2O	0.01	0.02	0.00	0.00	0.00	0.03
P_2O_5	0.03	0.06	0.00	0.07	0.21	0.06
SrO	0.00	0.00	0.00	0.00	0.00	0.00
BaO	0.00	0.00	0.00	0.00	0.00	0.00
TOTAL	98.88	98.26	98.95	99.63	99.49	98.90
Fo	66.92	66.91	69.83	67.20	71.12	71.21
Fa	33.08	33.09	30.17	32.80	28.88	28.79

Hole#	2	2	2	2	2	2
An#	10	10	10	12	15	16
	i/c	c	r	r	i	i
SiO_2	37.03	36.92	37.39	38.58	39.45	39.61
TiO_2	0.04	0.07	0.08	0.00	0.00	0.00
Al_2O_3	0.05	0.05	0.08	0.07	0.08	0.09
Fe_2O_3	0.00	0.00	0.00	0.00	0.00	0.00
Cr_2O_3	0.00	0.00	0.00	0.00	0.00	0.00
FeO*	27.80	27.99	25.39	17.97	14.51	14.39
MnO	0.91	0.68	0.63	0.32	0.17	0.24
MgO	32.78	32.35	34.66	40.98	43.72	44.24
NiO	0.00	0.00	0.02	0.15	0.20	0.19
CoO	0.00	0.00	0.00	0.00	0.00	0.00
CaO	0.37	0.37	0.41	0.32	0.35	0.40
Na_2O	0.05	0.04	0.05	0.02	0.00	0.00
K_2O	0.00	0.01	0.00	0.01	0.00	0.00
P_2O_5	0.10	0.11	0.12	0.00	0.03	0.02
SrO	0.00	0.00	0.00	0.00	0.00	0.00
BaO	0.00	0.00	0.00	0.00	0.00	0.00
TOTAL	99.13	98.58	98.81	98.43	98.51	99.19
Fo	67.77	67.32	70.87	80.26	84.31	84.57
Fa	32.23	32.68	29.13	19.75	15.69	15.43

Hole#	2	2	4	4	6	6
An#	17	18	1	15	8	16
	r	c	gm	gm	gm	r
SiO_2	38.48	39.46	36.41	35.74	37.24	36.95
TiO_2	0.04	0.05	0.06	0.05	0.13	0.10
Al_2O_3	0.09	0.05	0.06	0.05	0.03	0.03
Fe_2O_3	0.00	0.00	0.00	0.00	0.00	0.00
Cr_2O_3	0.00	0.00	0.00	0.00	0.00	0.00
FeO*	18.56	15.26	29.54	25.13	25.61	25.61
MnO	0.23	0.21	0.82	0.77	0.68	0.71
MgO	40.53	43.18	31.55	33.41	35.05	34.74
NiO	0.07	0.17	0.01	0.03	0.00	0.00
CoO	0.00	0.00	0.00	0.00	0.00	0.00
CaO	0.36	0.34	0.40	0.01	0.37	0.42
Na_2O	0.01	0.03	0.05	2.09	0.06	0.00
K_2O	0.01	0.00	0.01	0.00	0.01	0.00
P_2O_5	0.04	0.00	0.08	1.30	0.05	0.03
SrO	0.00	0.00	0.00	0.00	0.00	0.00
BaO	0.00	0.00	0.00	0.00	0.00	0.00
TOTAL	98.42	98.76	98.97	98.58	99.24	98.58
Fo	79.56	83.46	65.57	70.33	70.92	70.75
Fa	20.44	16.54	34.43	29.67	29.08	29.26

Hole#	6	6
An#	17	18
	i/c	c
SiO_2	37.40	36.93
TiO_2	0.01	0.01
Al_2O_3	0.06	0.06
Fe_2O_3	0.00	0.00
Cr_2O_3	0.00	0.00
FeO*	25.84	27.12
MnO	0.72	0.75
MgO	34.68	34.10
NiO	0.00	0.07
CoO	0.00	0.00
CaO	0.42	0.36
Na_2O	0.03	0.02
K_2O	0.01	0.00
P_2O_5	0.07	0.05
SrO	0.00	0.00
BaO	0.00	0.00
TOTAL	99.23	99.46
Fo	70.52	69.15
Fa	29.48	30.85

FeO* = total iron
c = core analysis, i/c = intermediate/core analysis
i/r = intermediate/rim analysis, r = rim analysis,
gm = groundmass Fo = forsterite, Fa = fayalite

Table 11: Clinopyroxene compositions from the 83415 Ne-hawaiite

Hole#	3	3	3	3	3	3
An#	1	3	9	10	11	13
	r	i/r	r	r	i/r	c
SiO_2	47.15	46.16	48.14	47.54	46.65	47.99
TiO_2	2.83	3.42	2.39	2.46	2.81	2.43
Al_2O_3	6.61	6.72	5.37	5.85	6.40	5.13
Fe_2O_3	0.00	0.00	0.00	0.00	0.00	0.00
Cr_2O_3	0.00	0.00	0.00	0.00	0.00	0.00
FeO*	7.77	7.68	7.71	7.67	7.62	7.60
MnO	0.23	0.28	0.29	0.31	0.28	0.25
MgO	11.53	11.38	12.14	11.89	11.60	12.37
NiO	0.00	0.00	0.04	0.02	0.00	0.05
CoO	0.00	0.00	0.00	0.00	0.00	0.00
CaO	20.92	21.47	21.47	21.09	21.47	21.69
Na_2O	1.11	0.98	0.99	1.02	0.99	0.89
K_2O	0.01	0.00	0.01	0.02	0.00	0.00
P_2O_5	0.00	0.00	0.02	0.05	0.02	0.06
SrO	0.00	0.00	0.00	0.00	0.00	0.00
BaO	0.00	0.00	0.00	0.00	0.00	0.00
TOTAL	98.16	98.08	98.58	97.91	97.84	98.47
En	37.29	36.57	38.07	37.92	37.05	38.39
Fs	14.09	13.84	13.55	13.73	13.66	13.23
Wo	48.63	49.59	48.38	48.35	49.30	48.38
En+	39.39	38.92	40.12	40.24	39.29	40.46
Fs+	15.15	14.97	13.95	14.20	14.29	13.87
Wo+	45.45	46.12	45.93	45.56	46.43	45.66

Hole#	4	4	4	4	4	6
An#	7	8	9	0	12	14
	r	c	i	i/r	r	gm
SiO_2	46.41	46.70	47.75	47.33	46.35	47.95
TiO_2	2.93	2.65	2.24	2.75	3.03	2.64
Al_2O_3	6.53	6.10	5.40	5.90	6.86	4.77
Fe_2O_3	0.00	0.00	0.00	0.00	0.00	0.00
Cr_2O_3	0.00	0.00	0.00	0.00	0.00	0.00
FeO*	7.63	7.52	7.84	7.53	7.64	7.88
MnO	0.30	0.23	0.26	0.29	0.22	0.33
MgO	11.61	11.66	11.70	11.99	11.46	12.69
NiO	0.00	0.11	0.01	0.00	0.06	0.07
CoO	0.00	0.00	0.00	0.00	0.00	0.00
CaO	21.66	21.85	21.70	21.53	21.48	0.58
Na_2O	0.94	0.87	0.87	0.82	0.93	22.11
K_2O	0.01	0.00	0.00	0.00	0.01	0.00
P_2O_5	0.00	0.03	0.01	0.00	0.01	0.11
SrO	0.00	0.00	0.00	0.00	0.00	0.00
BaO	0.00	0.00	0.00	0.00	0.00	0.00
TOTAL	98.01	97.72	97.80	98.15	98.04	99.12
En	36.90	36.93	36.91	37.84	36.75	38.45
Fs	13.60	13.36	13.88	13.34	13.75	13.40
Wo	49.50	49.71	49.20	48.83	49.50	48.15
En+	39.29	39.18	38.73	40.00	39.16	40.45
Fs+	14.29	14.04	14.45	14.12	14.46	14.04
Wo+	46.43	46.78	46.82	45.88	46.39	45.51

Hole#	6
An#	15
	gm
SiO_2	47.64
TiO_2	2.87
Al_2O_3	4.73
Fe_2O_3	0.00
Cr_2O_3	0.00
FeO^*	7.64
MnO	0.25
MgO	12.54
NiO	0.00
CoO	0.00
CaO	22.07
Na_2O	0.56
K_2O	0.01
P_2O_5	0.08
SrO	0.00
BaO	0.00
TOTAL	98.39
En	38.37
Fs	13.10
Wo	48.53
En+	40.34
Fs+	13.64
Wo+	46.02

FeO^* = total iron
c = core analysis, i/c = intermediate/core analysis
i/r = intermediate/rim analysis, r = rim analysis, gm = groundmass
En = enstatite, Fs = ferrosilite, Wo = wollastonite
En+, Fs+, Wo+ = Ca Tschermak ($CaAl_2SiO_6$) corrected

Table 12: Plagioclase compositions from the 83415 Nehawaiite

Hole#	1	1	1	1	1	1
An#	9	12	13	15	16	18
SiO_2	57.75	57.19	56.84	56.56	54.97	55.00
TiO_2	0.34	0.22	0.13	0.13	0.13	0.07
Al_2O_3	27.23	27.54	27.97	27.57	26.99	28.62
Fe_2O_3	0.00	0.00	0.00	0.00	0.00	0.00
Cr_2O_3	0.00	0.00	0.00	0.00	0.00	0.00
FeO*	0.43	0.25	0.24	0.35	0.18	0.25
MnO	0.03	0.01	0.00	0.07	0.00	0.00
MgO	0.11	0.05	0.05	0.04	0.06	0.07
NiO	0.03	0.02	0.04	0.00	0.07	0.00
CoO	0.00	0.00	0.00	0.00	0.00	0.00
CaO	8.48	8.96	9.32	8.99	8.75	10.27
Na_2O	6.34	5.99	5.61	5.88	5.49	5.09
K_2O	0.53	0.53	0.77	0.85	0.82	0.66
P_2O_5	0.10	0.04	0.00	0.01	0.00	0.01
SrO	0.00	0.00	0.00	0.00	0.00	0.00
BaO	0.00	0.00	0.00	0.00	0.00	0.00
TOTAL	101.36	100.80	100.96	100.45	97.44	100.05
An	41.17	43.87	45.72	43.55	44.50	50.65
Ab	55.75	53.04	49.82	51.58	50.53	45.46
Or	3.08	3.09	4.47	4.88	4.97	3.90

Hole#	1	1	1	1	1	2
An#	16	19	21	22	23	5
SiO_2	56.53	55.38	55.36	55.63	58.33	56.23
TiO_2	0.21	0.18	0.09	0.22	0.43	0.10
Al_2O_3	27.76	28.48	28.29	28.11	26.42	28.57
Fe_2O_3	0.00	0.00	0.00	0.00	0.00	0.00
Cr_2O_3	0.00	0.00	0.00	0.00	0.00	0.00
FeO*	0.25	0.19	0.26	0.40	0.68	0.35
MnO	0.00	0.00	0.03	0.00	0.00	0.02
MgO	0.05	0.03	0.04	0.05	0.10	0.05
NiO	0.00	0.02	0.03	0.03	0.04	0.03
CoO	0.00	0.00	0.00	0.00	0.00	0.00
CaO	9.21	10.04	10.10	9.90	7.78	9.96
Na_2O	5.54	5.25	5.22	5.36	6.53	5.54
K_2O	0.82	0.69	0.74	0.57	0.69	0.62
P_2O_5	0.06	0.06	0.01	0.02	0.04	0.00
SrO	0.00	0.00	0.00	0.00	0.00	0.00
BaO	0.00	0.00	0.00	0.00	0.00	0.00
TOTAL	100.41	100.31	100.15	100.28	101.05	101.47
An	45.60	49.30	49.42	48.83	38.09	48.02
Ab	49.59	46.69	46.24	47.81	57.86	48.39
Or	4.81	4.01	4.34	3.37	4.04	3.58

Hole#	2	2	2	3	3	3
An#	19	20	22	4	5	6
SiO_2	57.12	54.97	54.79	56.37	56.68	54.60
TiO_2	0.25	0.19	0.10	0.14	0.04	0.20
Al_2O_3	27.55	28.50	28.64	28.03	27.56	28.81
Fe_2O_3	0.00	0.00	0.00	0.00	0.00	0.00
FeO*	0.00	0.00	0.00	0.00	0.00	0.00
FeO	0.29	0.38	0.42	0.41	0.25	0.24
MnO	0.05	0.00	0.00	0.00	0.07	0.01
MgO	0.04	0.08	0.06	0.04	0.04	0.06
NiO	0.02	0.05	0.02	0.03	0.00	0.00
CoO	0.00	0.00	0.00	0.00	0.00	0.00
CaO	8.69	10.26	10.39	6.14	5.70	5.19
Na_2O	6.20	5.36	5.37	9.36	9.07	10.29
K_2O	0.51	0.50	0.47	0.48	0.86	0.66
P_2O_5	0.11	0.04	0.04	0.09	0.00	0.00
SrO	0.00	0.00	0.00	0.00	0.00	0.00
BaO	0.00	0.00	0.00	0.00	0.00	0.00
TOTAL	100.83	100.31	100.31	101.09	100.27	100.06
An	42.26	49.92	50.26	44.47	44.45	50.29
Ab	54.67	47.19	47.03	52.80	50.52	45.90
Or	2.97	2.90	2.72	2.73	5.03	3.81

Hole#	3	3	4	4	4	4
An#	7	8	3	5	6	13
SiO_2	54.73	54.70	55.64	57.26	55.50	56.47
TiO_2	0.15	0.17	0.13	0.24	0.29	0.27
Al_2O_3	28.73	28.63	27.50	27.50	28.20	27.66
Fe_2O_3	0.00	0.00	0.00	0.00	0.00	0.00
Cr_2O_3	0.00	0.00	0.00	0.00	0.00	0.00
FeO*	0.26	0.21	0.25	0.31	0.40	0.43
MnO	0.00	0.03	0.00	0.00	0.01	0.01
MgO	0.05	0.04	0.05	0.03	0.07	0.05
NiO	0.00	0.00	0.02	0.04	0.09	0.04
CoO	0.00	0.00	0.00	0.00	0.00	0.00
CaO	5.28	5.30	9.18	6.15	5.65	5.99
Na_2O	10.45	10.25	5.83	8.95	9.73	9.08
K_2O	0.62	0.68	0.76	0.59	0.38	0.55
P_2O_5	0.02	0.00	0.03	0.16	0.06	0.07
SrO	0.00	0.00	0.00	0.00	0.00	0.00
BaO	0.00	0.00	0.00	0.00	0.00	0.00
TOTAL	100.28	100.01	99.39	101.22	100.38	100.62
An	50.37	49.61	44.5	43.06	47.71	44.16
Ab	46.08	46.46	51.13	53.56	50.08	52.66
Or	3.55	3.93	4.37	3.39	2.22	3.18

Hole#	4	4	4	6	6	6
An#	17	18	20	1	2	3
SiO_2	54.65	56.61	60.19	54.47	55.94	55.94
TiO_2	0.21	0.23	0.30	0.22	0.11	0.14
Al_2O_3	28.46	27.70	26.00	28.37	27.88	27.88
Fe_2O_3	0.00	0.00	0.00	0.00	0.00	0.00
Cr_2O_3	0.00	0.00	0.00	0.00	0.00	0.00
FeO*	0.38	0.29	0.43	0.35	0.24	0.26
MnO	0.05	0.03	0.00	0.00	0.00	0.07
MgO	0.06	0.05	0.07	0.06	0.06	0.04
NiO	0.05	0.07	0.02	0.00	0.00	0.00
CoO	0.00	0.00	0.00	0.00	0.00	0.00
CaO	5.28	5.81	7.17	10.48	9.41	9.32
Na_2O	10.24	9.01	6.81	4.97	5.62	5.64
K_2O	0.60	0.70	0.90	0.60	0.78	0.79
P_2O_5	0.00	0.05	0.20	0.02	0.01	0.02
SrO	0.00	0.00	0.00	0.00	0.00	0.00
BaO	0.00	0.00	0.00	0.00	0.00	0.00
TOTAL	99.98	100.54	102.09	99.53	100.04	100.11
An	49.97	44.25	32.67	51.93	45.86	45.53
Ab	46.57	51.68	62.22	44.55	49.58	49.88
Or	3.46	4.07	5.11	3.52	4.55	4.59

Hole#	6	6	6	6	6	6
An#	4	5	6	7	9	10
SiO_2	56.02	58.22	54.69	54.85	55.04	55.59
TiO_2	0.11	0.14	0.12	0.18	0.23	0.12
Al_2O_3	28.00	26.89	28.63	28.61	28.35	28.23
Fe_2O_3	0.00	0.00	0.00	0.00	0.00	0.00
Cr_2O_3	0.00	0.00	0.00	0.00	0.00	0.00
FeO*	0.29	0.44	0.34	0.35	0.45	0.37
MnO	0.02	0.07	0.03	0.04	0.00	0.07
MgO	0.07	0.06	0.04	0.05	0.05	0.08
NiO	0.00	0.00	0.00	0.00	0.04	0.06
CoO	0.00	0.00	0.00	0.00	0.00	0.00
CaO	9.34	8.13	10.51	10.33	10.05	10.01
Na_2O	5.64	6.04	5.21	5.31	5.58	5.43
K_2O	0.74	1.04	0.62	0.55	0.51	0.69
P_2O_5	0.02	0.02	0.01	0.04	0.05	0.03
SrO	0.00	0.00	0.00	0.00	0.00	0.00
BaO	0.00	0.00	0.00	0.00	0.00	0.00
TOTAL	100.25	101.02	100.20	100.31	100.32	100.67
An	45.70	40.05	50.81	50.16	48.45	48.45
Ab	49.97	53.84	45.61	46.67	48.65	47.58
Or	4.33	6.11	3.59	3.17	2.90	3.98

Hole#	6	7	7	7	7	7
An#	11	1	2	3	4	5
SiO_2	56.51	55.59	54.92	55.46	57.18	56.50
TiO_2	0.20	0.08	0.10	0.22	0.13	0.10
Al_2O_3	28.77	28.54	28.69	28.36	27.81	27.70
Fe_2O_3	0.00	0.00	0.00	0.00	0.00	0.00
Cr_2O_3	0.00	0.00	0.00	0.00	0.00	0.00
FeO*	0.41	0.26	0.27	0.31	0.24	0.24
MnO	0.00	0.04	0.00	0.01	0.00	0.00
MgO	0.05	0.06	0.05	0.05	0.05	0.05
NiO	0.00	0.09	0.01	0.02	0.00	0.00
CoO	0.00	0.00	0.00	0.00	0.00	0.00
CaO	10.15	10.05	10.01	9.69	9.16	9.16
Na_2O	3.94	5.34	5.12	5.47	5.93	5.91
K_2O	0.65	0.73	0.73	0.79	0.87	0.87
P_2O_5	0.05	0.02	0.00	0.01	0.03	0.01
SrO	0.00	0.00	0.00	0.00	0.00	0.00
BaO	0.00	0.00	0.00	0.00	0.00	0.00
TOTAL	100.73	100.79	99.90	100.39	101.41	100.53
An	56.22	48.84	49.70	47.20	43.76	43.83
Ab	39.50	46.92	45.96	48.21	51.28	51.22
Or	4.28	4.24	4.34	4.60	4.95	4.96

Hole#	7	7	7	7	7	7
An#	6	7	8	9	10	11
SiO_2	56.00	57.79	56.26	57.72	57.58	55.03
TiO_2	0.11	0.14	0.18	0.12	0.17	0.04
Al_2O_3	27.51	27.19	27.93	27.30	27.36	28.51
Fe_2O_3	0.00	0.00	0.00	0.00	0.00	0.00
Cr_2O_3	0.00	0.00	0.00	0.00	0.00	0.00
FeO*	0.27	0.28	0.24	0.23	0.21	0.39
MnO	0.03	0.00	0.03	0.00	0.03	0.02
MgO	0.05	0.05	0.05	0.04	0.05	0.04
NiO	0.03	0.00	0.08	0.00	0.00	0.00
CoO	0.00	0.00	0.00	0.00	0.00	0.00
CaO	9.09	8.47	9.32	8.48	8.64	10.31
Na_2O	5.81	6.00	5.74	6.10	6.11	5.43
K_2O	0.85	0.98	0.78	1.03	1.00	0.47
P_2O_5	0.08	0.08	0.04	0.01	0.03	0.02
SrO	0.00	0.00	0.00	0.00	0.00	0.00
BaO	0.00	0.00	0.00	0.00	0.00	0.00
TOTAL	99.84	100.97	100.63	101.01	101.17	100.25
An	44.07	41.34	45.18	40.85	41.38	49.82
Ab	51.00	52.99	50.35	53.24	52.94	47.50
Or	4.93	5.67	4.45	5.91	5.68	2.68

Hole#	7	7	7	7	7	7
An#	12	13	15	16	17	18
SiO_2	54.82	55.20	55.77	55.92	54.09	55.18
TiO_2	0.01	0.17	0.20	0.07	0.23	0.14
Al_2O_3	28.52	29.11	28.91	28.65	29.49	28.83
Fe_2O_3	0.00	0.00	0.00	0.00	0.00	0.00
Cr_2O_3	0.00	0.00	0.00	0.00	0.00	0.00
FeO*	0.43	0.30	0.19	0.22	0.22	0.32
MnO	0.05	0.00	0.02	0.02	0.00	0.05
MgO	0.06	0.05	0.04	0.06	0.05	0.04
NiO	0.03	0.01	0.00	0.02	0.06	0.00
CoO	0.00	0.00	0.00	0.00	0.00	0.00
CaO	10.60	10.61	10.06	9.76	11.22	10.31
Na_2O	5.16	5.11	5.25	5.32	4.83	5.41
K_2O	0.53	0.60	0.70	0.73	0.58	0.73
P_2O_5	0.02	0.00	0.00	0.04	0.03	0.01
SrO	0.00	0.00	0.00	0.00	0.00	0.00
BaO	0.00	0.00	0.00	0.00	0.00	0.00
TOTAL	100.23	101.17	101.15	100.82	100.80	101.00
An	51.55	51.57	49.30	48.18	54.32	49.19
Ab	45.40	44.96	46.60	47.54	42.34	46.68
Or	3.05	3.46	4.11	4.28	3.35	4.14

Hole#	7	7	7	7	7	7
An#	19	20	21	22	23	24
SiO_2	55.33	55.74	54.85	54.87	55.68	56.89
TiO_2	0.22	0.20	0.07	0.23	0.18	0.22
Al_2O_3	28.86	28.64	28.87	28.72	28.61	29.10
Fe_2O_3	0.00	0.00	0.00	0.00	0.00	0.00
Cr_2O_3	0.00	0.00	0.00	0.00	0.00	0.00
FeO*	0.22	0.21	0.23	0.32	0.28	0.33
MnO	0.05	0.00	0.00	0.00	0.04	0.05
MgO	0.05	0.05	0.04	0.05	0.06	0.09
NiO	0.01	0.00	0.01	0.00	0.00	0.00
CoO	0.00	0.00	0.00	0.00	0.00	0.00
CaO	10.35	9.94	10.35	10.36	10.25	10.02
Na_2O	5.24	5.08	5.20	5.24	5.40	3.61
K_2O	0.66	0.74	0.71	0.67	0.46	0.39
P_2O_5	0.00	0.08	0.03	0.03	0.02	0.00
SrO	0.00	0.00	0.00	0.00	0.00	0.00
BaO	0.00	0.00	0.00	0.00	0.00	0.00
TOTAL	100.99	100.69	100.35	100.49	100.97	100.69
An	50.17	49.64	50.21	50.18	49.84	58.90
Ab	46.00	45.94	45.70	45.95	47.53	38.38
Or	3.83	4.41	4.09	3.88	2.64	2.72

Hole#	7	7
An#	26	27
SiO_2	57.27	57.68
TiO_2	0.21	0.06
$Al2O_3$	27.28	27.32
Fe_2O_3	0.00	0.00
Cr_2O_3	0.00	0.00
FeO^*	0.40	0.40
MnO	0.00	0.00
MgO	0.08	0.05
NiO	0.06	0.01
CoO	0.00	0.00
CaO	8.58	8.41
Na_2O	6.24	6.20
K_2O	0.68	0.65
P_2O_5	0.04	0.01
SrO	0.00	0.00
BaO	0.00	0.00
TOTAL	100.85	100.78
An	41.48	41.21
Ab	54.63	54.99
Or	3.90	3.80

FeO^* = total iron
An = anorthite, Ab = albite, Or = orthoclase

Table 13:Apatite from the 83415 Ne-hawaiite

Hole#	3	3	2
An#	2	12	5
SiO_2	0.25	0.25	0.24
TiO_2	0.00	0.00	0.10
Al_2O_3	0.04	0.03	0.08
Fe_2O_3	0.00	0.00	0.00
Cr_2O_3	0.00	0.00	0.00
FeO*	0.33	0.26	0.26
MnO	0.07	0.03	0.05
MgO	0.29	0.24	0.19
NiO	0.00	0.06	0.03
CoO	0.00	0.00	0.00
Na_2O	0.00	0.00	0.00
CaO	55.92	56.32	54.37
K_2O	0.02	0.00	0.02
P_2O_5	41.54	41.63	41.25
SrO	0.00	0.00	0.00
BaO	0.00	0.00	0.00
TOTAL	98.46	98.83	96.53

FeO* = total iron

Table 14: Olivine compositions
from the anorthoclase phonolite

Hole#	3	5	5	5	5	5
An#	8	6	28	29	30	31
	c	c	c	c	c	c
SiO_2	33.66	33.62	33.55	33.58	33.46	33.61
TiO_2	0.00	0.00	0.02	0.02	0.06	0.04
Al_2O_3	0.04	0.01	0.03	0.02	0.05	0.04
Fe_2O_3	0.00	0.00	0.00	0.00	0.00	0.00
Cr_2O_3	0.00	0.00	0.00	0.00	0.00	0.00
FeO*	41.69	41.05	41.47	40.70	41.15	41.03
MnO	2.50	2.68	2.66	2.86	2.52	2.60
MgO	20.85	20.64	20.30	20.71	20.60	20.80
NiO	0.00	0.04	0.03	0.01	0.00	0.05
CoO	0.00	0.00	0.00	0.00	0.00	0.00
CaO	0.54	0.52	0.54	0.52	0.52	0.51
Na_2O	0.04	0.04	0.04	0.03	0.04	0.03
K_2O	0.00	0.00	0.01	0.00	0.00	0.00
P_2O_5	0.06	0.02	0.04	0.02	0.06	0.04
SrO	0.00	0.00	0.00	0.00	0.00	0.00
BaO	0.00	0.00	0.00	0.00	0.00	0.00
TOTAL	99.38	98.63	98.68	98.46	98.46	98.74
Fo	47.14	47.26	46.60	47.564	47.16	47.47
Fa	52.86	52.74	53.40	52.436	52.84	52.53

Hole#	6	6	6	6	6	6
An#	3	19	20	21	22	23
	c	r	i/r	r	r	c
SiO_2	35.36	33.77	33.74	33.75	33.57	33.57
TiO_2	0.00	0.04	0.04	0.11	0.01	0.00
Al_2O_3	0.04	0.02	0.05	0.00	0.05	0.02
Fe_2O_3	0.00	0.00	0.00	0.00	0.00	0.00
Cr_2O_3	0.00	0.00	0.00	0.00	0.00	0.00
FeO*	34.95	41.50	41.53	41.92	41.44	40.93
MnO	2.06	2.68	2.71	2.62	2.55	2.56
MgO	26.69	20.48	20.65	20.53	20.52	20.50
NiO	0.00	0.01	0.10	0.01	0.02	0.00
CoO	0.00	0.00	0.00	0.00	0.00	0.00
CaO	0.48	0.48	0.49	0.52	0.51	0.69
Na_2O	0.02	0.04	0.00	0.02	0.06	0.05
K_2O	0.01	0.00	0.00	0.00	0.00	0.00
P_2O_5	0.06	0.02	0.06	0.08	0.09	0.08
SrO	0.00	0.00	0.00	0.00	0.00	0.00
BaO	0.00	0.00	0.00	0.00	0.00	0.00
TOTAL	99.65	99.04	99.36	99.56	98.83	98.39
Fo	57.65	46.80	46.98	46.62	46.89	47.165
Fa	42.35	53.20	53.02	53.38	53.11	52.835

FeO* = total iron
c = core analysis, i/r = intermediate/rim analysis, r = rim analysis
Fo = forsterite, Fa = fayalite

Table 15: Clinopyroxene compositions from the anorthoclase phonolite

Hole#	1	1	1	1	1	1
An#	1	5	6	7	8	12
	r	r	i/r	r	i/c	c
SiO_2	42.72	50.10	49.52	49.96	50.19	47.01
TiO_2	3.98	1.14	1.28	1.11	1.12	2.52
Al_2O_3	10.00	2.38	2.46	2.09	2.18	6.04
Fe_2O_3	0.00	0.00	0.00	0.00	0.00	0.00
Cr_2O_3	0.00	0.00	0.00	0.00	0.00	0.00
FeO*	9.02	10.66	10.67	10.58	10.31	8.45
MnO	0.22	0.86	0.71	0.72	0.74	0.35
MgO	11.15	11.46	11.36	11.51	11.66	12.75
NiO	0.00	0.04	0.04	0.00	0.06	0.01
CoO	0.00	0.00	0.00	0.00	0.00	0.00
CaO	20.59	20.98	21.13	21.58	21.55	20.92
Na_2O	0.76	1.04	1.27	0.86	0.84	0.77
K_2O	0.00	0.00	0.08	0.00	0.01	0.02
P_2O_5	0.08	0.00	0.04	0.06	0.00	0.04
SrO	0.00	0.00	0.00	0.00	0.00	0.00
BaO	0.00	0.00	0.00	0.00	0.00	0.00
TOTAL	98.51	98.65	98.55	98.46	98.66	98.86
En	35.96	35.24	34.92	34.93	35.41	39.19
Fs	16.32	18.39	18.41	18.01	17.56	14.58
Wo	47.72	46.38	46.68	47.07	47.03	46.23
En+	40.00	36.26	35.71	35.68	36.22	41.62
Fs+	18.13	18.68	18.68	18.38	17.84	15.61
Wo+	41.88	45.05	45.60	45.95	45.95	42.77

Hole#	1	1	2	2	2	2
An#	15	16	1	2	3	5
	c	c	r	i/r	c	r
SiO_2	47.95	46.51	50.32	50.39	50.62	50.59
TiO_2	2.24	2.90	1.17	1.08	1.14	1.07
Al_2O_3	5.04	6.41	2.40	2.46	2.48	2.45
Fe_2O_3	0.00	0.00	0.00	0.00	0.00	0.00
Cr_2O_3	0.00	0.00	0.00	0.00	0.00	0.00
FeO*	8.02	8.42	10.96	10.86	10.82	11.07
MnO	0.22	0.31	0.82	0.80	0.69	0.74
MgO	13.48	12.18	11.22	11.45	11.36	11.37
NiO	0.08	0.02	0.06	0.01	0.01	0.00
CoO	0.00	0.00	0.00	0.00	0.00	0.00
CaO	20.71	21.18	20.65	20.59	20.67	20.56
Na_2O	0.61	0.86	1.11	1.11	1.13	1.10
K_2O	0.03	0.02	0.00	0.00	0.01	0.00
P_2O_5	0.03	0.11	0.01	0.00	0.04	0.00
SrO	0.00	0.00	0.00	0.00	0.00	0.00
BaO	0.00	0.00	0.00	0.00	0.00	0.00
TOTAL	98.40	98.90	98.72	98.75	98.96	98.95
En	41.03	37.92	34.83	35.41	35.19	35.14
Fs	13.68	14.71	19.09	18.84	18.80	19.20
Wo	45.29	47.38	46.08	45.75	46.01	45.67
En+	43.18	40.35	35.36	35.91	35.91	35.91
Fs+	14.20	15.79	19.34	19.34	19.34	19.34
Wo+	42.61	43.86	45.30	44.75	44.75	44.75

Hole#	2	2	3	3	5	5
An#	6	7	5	6	4	6
	i/r	i/c	c	c	c	c
SiO_2	50.16	50.42	44.73	43.04	48.66	45.80
TiO_2	1.23	1.23	3.96	4.30	1.95	3.33
Al_2O_3	2.57	2.65	7.32	9.18	4.09	7.04
Fe_2O_3	0.00	0.00	0.00	0.00	0.00	0.00
Cr_2O_3	0.00	0.00	0.00	0.00	0.00	0.00
FeO*	10.97	10.75	8.96	8.70	8.79	9.00
MnO	0.73	0.80	0.38	0.20	0.41	0.41
MgO	11.69	11.61	11.19	11.12	12.88	11.44
NiO	0.04	0.02	0.08	0.04	0.00	0.05
CoO	0.00	0.00	0.00	0.00	0.00	0.00
CaO	20.36	20.34	20.90	20.82	21.17	20.48
Na_2O	1.08	1.07	1.00	0.80	0.71	0.99
K_2O	0.02	0.02	0.01	0.01	0.00	0.00
P_2O_5	0.06	0.00	0.08	0.04	0.12	0.00
SrO	0.00	0.00	0.00	0.00	0.00	0.00
BaO	0.00	0.00	0.00	0.00	0.00	0.00
TOTAL	98.90	98.90	98.59	98.24	98.78	98.54
En	35.99	35.98	35.82	35.92	39.00	36.66
Fs	18.95	18.70	16.10	15.76	14.94	16.19
Wo	45.06	45.32	48.09	48.33	46.07	47.16
En+	37.02	36.87	38.79	39.75	40.56	39.16
Fs+	19.34	18.99	17.58	17.39	15.56	17.47
Wo+	43.65	44.13	43.64	42.86	43.89	43.37

Hole#	5	6	6	6	6	6
An#	7	1	2	5	6	11
	c	c	c	i/r	i/c	c
SiO_2	48.92	49.06	42.86	49.54	50.55	50.53
TiO_2	1.85	1.77	4.54	1.57	0.89	1.10
Al_2O_3	3.98	3.67	9.36	3.40	2.45	2.25
Fe_2O_3	0.00	0.00	0.00	0.00	0.00	0.00
Cr_2O_3	0.00	0.00	0.00	0.00	0.00	0.00
FeO*	8.39	8.39	8.94	10.68	10.64	10.53
MnO	0.39	0.44	0.22	0.73	0.75	0.72
MgO	13.09	13.44	11.02	11.28	11.30	11.56
NiO	0.00	0.03	0.00	0.07	0.00	0.00
CoO	0.00	0.00	0.00	0.00	0.00	0.00
CaO	21.06	20.87	20.84	20.45	20.88	21.17
Na_2O	0.74	0.69	0.85	1.16	1.01	0.88
K_2O	0.01	0.03	0.02	0.01	0.00	0.00
P_2O_5	0.06	0.05	0.05	0.02	0.05	0.05
SrO	0.00	0.00	0.00	0.00	0.00	0.00
BaO	0.00	0.00	0.00	0.00	0.00	0.00
TOTAL	98.46	98.44	98.69	98.91	98.54	98.80
En	39.75	40.56	35.53	35.28	35.02	35.37
Fs	14.29	14.19	16.18	18.74	18.50	18.08
Wo	45.96	45.25	48.29	45.98	46.49	46.56
En+	41.11	41.99	39.38	36.16	35.71	35.87
Fs+	15.00	14.92	18.13	19.21	18.68	18.48
Wo+	43.89	43.09	42.50	44.63	45.60	45.65

Hole#	6	6	6
An#	13	26	28
	i/c	r	i/r
SiO_2	50.73	43.82	45.78
TiO_2	1.08	3.89	3.10
Al_2O_3	2.24	8.58	7.39
Fe_2O_3	0.00	0.00	0.00
Cr_2O_3	0.00	0.00	0.00
FeO*	10.83	9.14	8.94
MnO	0.80	0.22	0.30
MgO	11.54	11.01	11.63
NiO	0.00	0.00	0.03
CoO	0.00	0.00	0.00
CaO	20.84	20.85	20.32
Na_2O	1.06	0.90	1.01
K_2O	0.01	0.00	0.01
P_2O_5	0.01	0.05	0.04
SrO	0.00	0.00	0.00
BaO	0.00	0.00	0.00
TOTAL	99.12	98.44	98.55
En	35.40	35.38	37.21
Fs	18.64	16.47	16.05
Wo	45.96	48.15	46.74
En+	36.07	38.89	39.76
Fs+	19.13	17.90	17.47
Wo+	44.81	43.21	42.77

FeO* = total iron
c = core analysis, i/c = intermediate/core analysis
i/r = intermediate/rim analysis, r = rim analysis
En = enstatite, Fs = ferrosilite, Wo = wollastonite
En+, Fs+, Wo+ = Ca Tschermak ($CaAl_2SiO_6$) corrected

Table 16: Anorthoclase compositions
from the anorthoclase phonolite

Hole#	4	4	4	4	4	4
An#	1	2	3	4	5	6
	r	r	r	r	r	c
SiO_2	67.41	68.75	68.54	67.39	67.81	67.47
TiO_2	0.01	0.15	0.15	0.09	0.06	0.11
Al_2O_3	22.49	22.00	22.18	22.41	22.25	21.68
Fe_2O_3	0.00	0.00	0.00	0.00	0.00	0.00
Cr_2O_3	0.00	0.00	0.00	0.00	0.00	0.00
FeO*	0.14	0.25	0.20	0.20	0.19	0.16
MnO	0.01	0.00	0.00	0.00	0.00	0.00
MgO	0.02	0.00	0.01	0.01	0.03	0.02
NiO	0.00	0.00	0.00	0.00	0.00	0.00
CoO	0.00	0.00	0.00	0.00	0.00	0.00
CaO	2.10	1.57	1.89	2.16	2.00	1.70
Na_2O	7.13	6.70	6.99	6.94	7.20	6.80
K_2O	4.21	4.65	4.45	4.12	4.30	4.69
P_2O_5	0.03	0.01	0.04	0.03	0.01	0.04
SrO	0.00	0.00	0.00	0.00	0.00	0.00
BaO	0.00	0.00	0.00	0.00	0.00	0.00
TOTAL	103.55	104.07	104.46	103.34	103.84	102.67
An	10.49	8.17	9.55	10.99	9.92	8.69
Ab	64.48	63.05	63.74	63.99	64.65	62.80
Or	25.03	28.78	26.72	25.03	25.43	28.51

Hole#	4	4	4	4	4	4
An#	7	8	9	10	11	12
	c	i/c	i/c	c	r	r
SiO_2	66.50	67.53	67.07	66.32	67.15	68.04
TiO_2	0.15	0.00	0.00	0.07	0.14	0.17
Al_2O_3	22.47	22.26	22.33	22.87	22.50	22.59
Fe_2O_3	0.00	0.00	0.00	0.00	0.00	0.00
Cr_2O_3	0.00	0.00	0.00	0.00	0.00	0.00
FeO*	0.21	0.13	0.16	0.24	0.26	0.16
MnO	0.00	0.00	0.00	0.01	0.00	0.01
MgO	0.00	0.01	0.02	0.04	0.01	0.02
NiO	0.00	0.00	0.02	0.00	0.00	0.00
CoO	0.00	0.00	0.00	0.00	0.00	0.00
CaO	2.54	2.14	2.19	2.67	2.30	2.04
Na_2O	6.35	6.81	7.12	7.30	7.14	6.99
K_2O	3.62	4.05	3.96	3.53	3.86	4.20
P_2O_5	0.00	0.03	0.01	0.00	0.00	0.01
SrO	0.00	0.00	0.00	0.00	0.00	0.00
BaO	0.00	0.00	0.00	0.00	0.00	0.00
TOTAL	101.84	102.94	102.88	103.04	103.35	104.21
An	13.84	11.09	11.06	13.29	11.60	10.36
Ab	62.65	63.91	65.12	65.77	65.20	64.26
Or	23.51	25.00	23.82	20.95	23.20	25.39

Hole#	4	5	5	5	5	5
An#	13	1	2	3	4	5
	r	r	i/r	c	i/c	i/r
SiO_2	65.44	66.32	66.97	66.78	67.56	65.63
TiO_2	0.04	0.12	0.00	0.07	0.13	0.08
Al_2O_3	23.22	22.27	22.37	22.66	22.40	22.90
Fe_2O_3	0.00	0.00	0.00	0.00	0.00	0.00
Cr_2O_3	0.00	0.00	0.00	0.00	0.00	0.00
FeO*	0.23	0.22	0.24	0.14	0.24	0.22
MnO	0.00	0.00	0.00	0.03	0.00	0.05
MgO	0.03	0.01	0.02	0.03	0.03	0.00
NiO	0.02	0.01	0.00	0.02	0.00	0.00
CoO	0.00	0.00	0.00	0.00	0.00	0.00
CaO	3.19	2.41	2.41	2.31	2.14	2.89
Na_2O	7.39	7.51	7.09	7.16	6.95	7.31
K_2O	3.10	3.79	3.93	4.02	4.20	3.41
P_2O_5	0.00	0.03	0.03	0.02	0.01	0.00
SrO	0.00	0.00	0.00	0.00	0.00	0.00
BaO	0.00	0.00	0.00	0.00	0.00	0.00
TOTAL	102.65	102.69	103.06	103.24	103.66	102.48
An	15.77	11.76	12.10	11.52	10.84	14.31
Ab	66.02	66.23	64.39	64.61	63.82	65.56
Or	18.21	22.00	23.51	23.87	25.34	20.13

Hole#	5	5	5	5	5	5
An#	8	9	10	11	12	18
	i/r	i/r	i/c	r	i/c	r
SiO_2	66.09	66.84	66.63	66.46	66.32	66.73
TiO_2	0.18	0.17	0.13	0.10	0.14	0.02
Al_2O_3	22.76	22.78	22.46	22.68	22.46	22.91
Fe_2O_3	0.00	0.00	0.00	0.00	0.00	0.00
Cr_2O_3	0.00	0.00	0.00	0.00	0.00	0.00
FeO*	0.22	0.21	0.19	0.22	0.30	0.26
MnO	0.01	0.02	0.00	0.00	0.00	0.00
MgO	0.01	0.02	0.02	0.02	0.02	0.01
NiO	0.05	0.02	0.00	0.02	0.01	0.02
CoO	0.00	0.00	0.00	0.00	0.00	0.00
CaO	2.88	2.57	2.64	2.70	2.42	2.83
Na_2O	7.23	7.21	7.23	6.80	6.87	7.33
K_2O	3.39	3.67	3.65	3.65	3.90	3.38
P_2O_5	0.00	0.00	0.00	0.03	0.01	0.04
SrO	0.00	0.00	0.00	0.00	0.00	0.00
BaO	0.00	0.00	0.00	0.00	0.00	0.00
TOTAL	102.81	103.52	102.96	102.66	102.45	103.53
An	14.39	12.84	13.16	13.93	12.43	14.06
Ab	65.42	65.30	65.17	63.59	63.75	65.96
Or	20.19	21.87	21.67	22.47	23.83	19.98

Hole#	5	5	5	5	5	5
An#	19	20	21	22	23	24
	i/c	i/r	c	c	i/c	i/r
SiO_2	65.12	64.65	66.06	67.45	67.47	65.80
TiO_2	0.10	0.08	0.10	0.09	0.09	0.12
Al_2O_3	23.43	23.55	23.12	22.49	22.59	23.10
Fe_2O_3	0.00	0.00	0.00	0.00	0.00	0.00
Cr_2O_3	0.00	0.00	0.00	0.00	0.00	0.00
FeO*	0.19	0.25	0.14	0.20	0.23	0.17
MnO	0.00	0.04	0.01	0.04	0.07	0.03
MgO	0.02	0.02	0.03	0.03	0.02	0.04
NiO	0.00	0.00	0.02	0.02	0.00	0.02
CoO	0.00	0.00	0.00	0.00	0.00	0.00
CaO	3.60	3.67	3.19	2.43	2.35	3.00
Na_2O	7.49	7.31	7.07	7.24	7.16	7.12
K_2O	2.84	2.84	3.07	3.81	3.83	3.18
P_2O_5	0.01	0.05	0.05	0.04	0.04	0.00
SrO	0.00	0.00	0.00	0.00	0.00	0.00
BaO	0.00	0.00	0.00	0.00	0.00	0.00
TOTAL	102.80	102.46	102.87	103.85	103.84	102.56
An	17.54	18.11	16.24	12.11	11.81	15.24
Ab	66.01	65.22	65.16	65.28	65.25	65.52
Or	16.46	16.67	18.61	22.61	22.94	19.24

Hole#	5	5	5	5	5	5
An#	25	32	33	34	35	37
	i/r	i/c	i/c	c	c	i/r
SiO_2	67.24	67.63	66.63	65.86	66.65	66.78
TiO_2	0.08	0.13	0.07	0.11	0.08	0.11
Al_2O_3	22.46	22.14	22.70	22.59	22.60	22.54
Fe_2O_3	0.00	0.00	0.00	0.00	0.00	0.00
Cr_2O_3	0.00	0.00	0.00	0.00	0.00	0.00
FeO*	0.25	0.20	0.23	0.22	0.23	0.26
MnO	0.01	0.00	0.01	0.00	0.00	0.01
MgO	0.01	0.02	0.02	0.00	0.03	0.02
NiO	0.04	0.00	0.00	0.05	0.01	0.05
CoO	0.00	0.00	0.00	0.00	0.00	0.00
CaO	2.43	1.80	2.64	2.83	2.53	2.50
Na_2O	7.46	6.94	7.19	7.34	7.43	7.21
K_2O	3.61	4.49	3.51	3.46	3.64	3.74
P_2O_5	0.00	0.05	0.03	0.03	0.00	0.01
SrO	0.00	0.00	0.00	0.00	0.00	0.00
BaO	0.00	0.00	0.00	0.00	0.00	0.00
TOTAL	103.58	103.40	103.02	102.48	103.19	103.23
An	12.01	9.13	13.31	13.98	12.45	12.49
Ab	66.76	63.72	65.63	65.64	66.21	65.23
Or	21.23	27.15	21.06	20.38	21.34	22.28

Hole#	6	6
An#	29	30
	r	c
SiO_2	65.30	67.89
TiO_2	0.12	0.13
Al_2O_3	22.50	23.22
Fe_2O_3	0.00	0.00
Cr_2O_3	0.00	0.00
FeO^*	0.27	0.28
MnO	0.00	0.00
MgO	0.01	0.03
NiO	0.02	0.00
CoO	0.00	0.00
CaO	2.65	2.68
Na_2O	7.12	2.90
K_2O	3.53	2.72
P_2O_5	0.08	0.04
SrO	0.00	0.00
BaO	0.00	0.00
TOTAL	101.60	99.89
An	13.44	23.97
Ab	65.28	47.04
Or	21.29	28.99

FeO^* = total iron
c = core analysis, i/c = intermediate/core analysis
i/r = intermediate/rim analysis, r = rim analysis
An = anorthite, Ab = albite, Or = orthoclase

Table 17: Apatite compositins
from the anorthoclase phonolite

Hole#	1	1	1	3	5	5
An#	4	11	14	9	5	13
SiO_2	0.50	0.48	0.46	0.53	0.48	0.32
TiO_2	0.03	0.07	0.02	0.13	0.04	0.00
Al_2O_3	0.04	0.02	0.02	0.04	0.03	0.01
Fe_2O_3	0.00	0.00	0.00	0.00	0.00	0.00
Cr_2O_3	0.00	0.00	0.00	0.00	0.00	0.00
FeO*	0.44	0.43	0.29	0.32	0.31	0.28
MnO	0.18	0.11	0.03	0.10	0.20	0.14
MgO	0.15	0.11	0.11	0.17	0.12	0.12
NiO	0.08	0.05	0.07	0.00	0.01	0.00
CoO	0.00	0.00	0.00	0.00	0.00	0.00
CaO	54.52	54.58	53.94	54.40	54.21	54.65
Na_2O	0.00	0.00	0.00	0.00	0.00	0.00
K_2O	0.02	0.02	0.00	0.01	0.02	0.01
P_2O_5	41.88	40.78	41.20	41.02	40.81	41.17
SrO	0.00	0.00	0.00	0.00	0.00	0.00
BaO	0.00	0.00	0.00	0.00	0.00	0.00
TOTAL	97.82	96.63	96.15	96.70	96.23	96.70

Hole#	5	5	5	5	5	5
An#	14	15	16	17	26	27
SiO_2	0.25	0.22	0.23	0.31	0.29	0.39
TiO_2	0.00	0.00	0.00	0.01	0.00	0.10
Al_2O_3	0.02	0.02	0.05	0.02	0.04	0.03
Fe_2O_3	0.00	0.00	0.00	0.00	0.00	0.00
Cr_2O_3	0.00	0.00	0.00	0.00	0.00	0.00
FeO*	0.26	0.25	0.25	0.27	0.27	0.21
MnO	0.08	0.06	0.14	0.12	0.10	0.13
MgO	0.12	0.14	0.13	0.13	0.11	0.11
NiO	0.00	0.03	0.02	0.08	0.00	0.00
CoO	0.00	0.00	0.00	0.00	0.00	0.00
CaO	55.31	55.90	55.02	54.88	54.99	54.94
Na_2O	0.00	0.00	0.00	0.00	0.00	0.00
K_2O	0.01	0.00	0.00	0.00	0.01	0.00
P_2O_5	41.88	41.63	41.87	41.80	41.89	41.45
SrO	0.00	0.00	0.00	0.00	0.00	0.00
BaO	0.00	0.00	0.00	0.00	0.00	0.00
TOTAL	97.92	98.25	97.71	97.61	97.71	97.37

Hole#	6	6	6	6	6	6
An#	32	7	8	9	10	14
SiO_2	0.51	0.49	0.43	0.46	0.47	0.48
TiO_2	0.04	0.00	0.05	0.00	0.02	0.03
Al_2O_3	0.02	0.03	0.01	0.00	0.03	0.02
Fe_2O_3	0.00	0.00	0.00	0.00	0.00	0.00
Cr_2O_3	0.00	0.00	0.00	0.00	0.00	0.00
FeO*	0.32	0.24	0.31	0.33	0.27	0.26
MnO	0.17	0.13	0.16	0.17	0.19	0.08
MgO	0.15	0.16	0.16	0.15	0.16	0.14
NiO	0.00	0.00	0.00	0.03	0.00	0.00
CoO	0.00	0.00	0.00	0.00	0.00	0.00
CaO	53.96	55.02	54.21	54.33	54.31	54.72
Na_2O	0.00	0.00	0.00	0.00	0.00	0.00
K_2O	0.04	0.02	0.01	0.01	0.00	0.00
P_2O_5	40.07	41.15	40.62	40.76	40.34	39.97
SrO	0.00	0.00	0.00	0.00	0.00	0.00
BaO	0.00	0.00	0.00	0.00	0.00	0.00
TOTAL	95.27	97.24	95.97	96.24	95.78	95.69

Hole#	6	6	6	6	6	6
An#	15	16	17	18	24	25
SiO_2	0.43	0.46	0.41	0.50	0.45	0.48
TiO_2	0.05	0.07	0.00	0.05	0.06	0.10
Al_2O_3	0.02	0.01	0.03	0.01	0.04	0.02
Fe_2O_3	0.00	0.00	0.00	0.00	0.00	0.00
Cr_2O_3	0.00	0.00	0.00	0.00	0.00	0.00
FeO*	0.42	0.42	0.39	0.41	0.50	0.75
MnO	0.21	0.13	0.14	0.15	0.21	0.17
MgO	0.19	0.13	0.16	0.15	0.20	0.14
NiO	0.01	0.09	0.00	0.05	0.00	0.00
CoO	0.00	0.00	0.00	0.00	0.00	0.00
CaO	54.00	54.13	53.75	54.02	54.50	54.03
Na_2O	0.00	0.00	0.00	0.00	0.00	0.00
K_2O	0.00	0.00	0.01	0.05	0.01	0.00
P_2O_5	40.67	40.43	40.93	40.74	41.41	41.33
SrO	0.00	0.00	0.00	0.00	0.00	0.00
BaO	0.00	0.00	0.00	0.00	0.00	0.00
TOTAL	96.00	95.85	95.82	96.12	97.37	97.02

FeO^* = total iron

APPENDIX D

Table 1: Melt compositions for basanite (one atmopshere)

Temp (°C)	1224	1224	1224
Run #	11	11	11
SiO_2	42.48	42.53	42.45
TiO_2	4.65	4.94	4.65
Al_2O_3*	13.97	13.89	13.96
Fe_2O_3*	1.56	1.60	1.64
Cr_2O_3	0.11	0.05	0.07
FeO*	8.68	8.89	8.95
MnO	0.22	0.19	0.14
MgO	9.10	9.07	8.90
NiO	0.08	0.05	0.01
CoO	0.00	0.00	0.00
CaO	12.27	12.20	12.30
Na_2O	2.41	2.44	2.54
K_2O	1.29	1.23	1.26
P_2O_5	0.74	0.69	0.79
SrO	0.00	0.00	0.00
BaO	0.00	0.00	0.00
TOTAL	97.56	97.77	97.66
Mg#	65.14	64.52	63.93
Fo	86.20	85.80	85.50

Temp (°C)	1197	1197	1197	1197
Run #	8	8	8	8
SiO_2	42.13	42.13	42.21	42.04
TiO_2	4.77	4.67	4.73	4.58
Al_2O_3*	14.04	14.08	14.06	14.15
Fe_2O_3*	1.67	1.69	1.69	1.62
Cr_2O_3	0.07	0.08	0.02	0.07
FeO*	8.70	8.85	8.82	8.51
MnO	0.14	0.10	0.15	0.13
MgO	8.41	8.33	8.34	8.35
NiO	0.05	0.06	0.01	0.01
CoO	0.00	0.00	0.00	0.00
CaO	12.57	12.51	12.71	12.50
Na_2O	2.63	2.60	2.54	2.57
K_2O	1.32	1.34	1.35	1.34
P_2O_5	0.81	0.74	0.82	0.85
SrO	0.00	0.00	0.00	0.00
BaO	0.00	0.00	0.00	0.00
TOTAL	97.31	97.18	97.45	96.72
Mg#	63.29	62.67	63.62	62.76
Fo	85.20	84.80	85.40	84.90

Temp (°C)	1177	1177	1177	1177
Run #	9	9	9	9
SiO_2	42.02	41.39	42.36	42.41
TiO_2	4.86	5.28	4.94	5.03
Al_2O_3*	14.85	14.62	14.76	14.94
Fe_2O_3*	1.65	1.66	1.61	1.67
Cr_2O_3	0.04	0.03	0.05	0.07
FeO*	8.32	8.28	8.47	8.59
MnO	0.14	0.15	0.16	0.19
MgO	7.19	7.00	7.14	7.03
NiO	0.00	0.03	0.07	0.02
CoO	0.00	0.00	0.00	0.00
CaO	12.90	12.92	12.93	12.76
Na_2O	3.09	3.08	3.09	3.01
K_2O	1.52	1.56	1.49	1.45
P_2O_5	0.95	0.87	0.96	0.86
SrO	0.00	0.00	0.00	0.00
BaO	0.00	0.00	0.00	0.00
TOTAL	97.54	96.86	98.04	98.05
Mg#	60.63	60.12	60.04	59.35
Fo	83.70	83.40	83.40	83.00

Temp (°C)	1160	1160	1160
Run #	10	10	10
SiO_2	42.21	42.07	42.06
TiO_2	5.18	5.05	4.97
Al_2O_3*	15.14	15.00	15.08
Fe_2O_3*	1.54	1.58	1.61
Cr_2O_3	0.04	0.04	0.05
FeO*	8.03	8.27	8.32
MnO	0.21	0.18	0.25
MgO	6.35	6.52	6.60
NiO	0.02	0.00	0.05
CoO	0.00	0.00	0.00
CaO	13.25	13.04	13.16
Na_2O	3.07	3.05	3.20
K_2O	1.55	1.51	1.48
P_2O_5	0.97	0.84	0.95
SrO	0.00	0.00	0.00
BaO	0.00	0.00	0.00
TOTAL	97.55	97.15	97.79
Mg#	58.50	58.42	58.59
Fo	82.50	82.40	82.50

Temp (°C)	1138	1138
Run #	12	12
SiO_2	42.35	42.89
TiO_2	5.11	5.24
Al_2O_3*	15.82	15.81
Fe_2O_3*	1.56	1.51
Cr_2O_3	0.03	0.01
FeO*	8.46	8.30
MnO	0.13	0.19
MgO	6.14	6.11
NiO	0.00	0.05
CoO	0.00	0.00
CaO	12.73	12.62
Na_2O	3.01	2.91
K_2O	1.50	1.55
P_2O_5	0.99	0.99
SrO	0.00	0.00
BaO	0.00	0.00
TOTAL	97.82	98.18
Mg#	56.41	56.74
Fo	81.20	81.40

Temp (°C)	1120	1120	1120
Run #	13	13	13
SiO_2	43.10	43.09	42.93
TiO_2	5.33	5.24	5.35
Al_2O_3*	16.21	16.43	16.56
Fe_2O_3*	1.47	1.43	1.48
Cr_2O_3	0.02	0.00	0.03
FeO*	8.82	8.67	8.75
MnO	0.14	0.18	0.23
MgO	5.79	5.71	5.51
NiO	0.08	0.00	0.00
CoO	0.00	0.00	0.00
CaO	11.64	11.69	11.67
Na_2O	2.71	2.65	2.92
K_2O	1.34	1.31	1.35
P_2O_5	0.49	0.60	0.67
SrO	0.00	0.00	0.00
BaO	0.00	0.00	0.00
TOTAL	97.16	97.00	97.44
Mg#	53.94	54.00	52.87
Fo	79.60	79.60	78.90

Temp (°C)	1104	1104	1104
Run #	15	15	15
SiO_2	42.39	42.89	42.56
TiO_2	5.53	5.24	5.60
Al_2O_3	15.92	15.91	15.94
Fe_2O_3*	1.65	1.69	1.60
Cr_2O_3	0.00	0.01	0.01
FeO*	8.42	8.21	8.35
MnO	0.18	0.20	0.11
MgO	4.29	4.16	4.24
NiO	0.06	0.01	0.00
CoO	0.00	0.00	0.00
CaO	9.59	9.36	9.51
Na_2O	4.51	5.12	4.41
K_2O	2.73	2.79	2.59
P_2O_5	1.75	1.98	1.68
SrO	0.00	0.00	0.00
BaO	0.00	0.00	0.00
TOTAL	97.02	97.57	96.60
Mg#	47.61	47.47	47.49
Fo	75.20	75.10	75.10

* = FeO and Fe_2O_3 determined using method given by Kilinc et al., 1983

Table 2: Melt compositions for
DVDP2 hawaiite (one atmosphere)

Temp (°C)	1224	1224	1224	1224
Run #	11	11	11	11
SiO_2	48.36	47.85	48.78	48.24
TiO_2	3.24	3.23	3.07	3.06
Al_2O_3*	17.99	18.04	18.02	18.09
Fe_2O_3*	1.41	1.43	1.47	1.47
Cr_2O_3	0.02	0.03	0.00	0.05
FeO*	7.10	7.22	7.26	7.32
MnO	0.23	0.23	0.19	0.21
MgO	3.71	3.85	3.85	3.90
NiO	0.00	0.05	0.00	0.00
CoO	0.00	0.00	0.00	0.00
CaO	7.89	7.87	7.95	7.98
Na_2O	4.84	4.74	4.96	4.91
K_2O	2.57	2.61	2.66	2.63
P_2O_5	0.36	0.36	0.32	0.35
SrO	0.00	0.00	0.00	0.00
BaO	0.00	0.00	0.00	0.00
TOTAL	97.72	97.51	98.53	98.21
Mg#	48.23	48.73	48.59	48.71
Fo	75.60	76.00	75.90	76.00

Temp (°C)	1197	1197
Run #	8	8
SiO_2	47.61	47.27
TiO_2	3.19	3.34
Al_2O_3*	17.86	17.74
Fe_2O_3*	1.60	1.59
Cr_2O_3	0.00	0.00
FeO*	7.36	7.25
MnO	0.17	0.18
MgO	3.81	3.71
NiO	0.00	0.00
CoO	0.00	0.00
CaO	7.86	7.78
Na_2O	5.36	5.46
K_2O	2.71	2.72
P_2O_5	0.50	0.59
SrO	0.00	0.00
BaO	0.00	0.00
TOTAL	98.02	97.64
Mg#	48.00	47.69
Fo	75.50	75.20

Temp (°C)	1177	1177
Run #	9	9
SiO_2	46.85	47.80
TiO_2	3.25	3.09
Al_2O_3*	17.46	18.00
Fe_2O_3*	1.58	1.55
Cr_2O_3	0.00	0.01
FeO*	7.19	7.28
MnO	0.20	0.20
MgO	3.80	3.83
NiO	0.00	0.05
CoO	0.00	0.00
CaO	7.71	7.82
Na_2O	5.59	5.44
K_2O	2.85	2.77
P_2O_5	0.67	0.68
SrO	0.00	0.00
BaO	0.00	0.00
TOTAL	97.16	98.52
Mg#	48.50	48.40
Fo	75.80	75.80

Temp (°C)	1160	1160	1160	1160
Run #	10	10	10	10
SiO_2	46.47	47.39	47.29	47.54
TiO_2	3.06	3.15	3.14	3.05
Al_2O_3*	17.42	17.98	17.73	17.85
Fe_2O_3*	1.42	1.48	1.49	1.45
Cr_2O_3	0.03	0.01	0.05	0.00
FeO*	6.88	7.25	7.21	7.06
MnO	0.20	0.19	0.20	0.19
MgO	3.73	3.76	3.82	3.76
NiO	0.07	0.13	0.07	0.00
CoO	0.00	0.00	0.00	0.00
CaO	7.50	7.68	7.77	7.56
Na_2O	5.32	5.33	5.34	5.55
K_2O	2.86	2.85	2.89	2.72
P_2O_5	0.63	0.72	0.60	0.63
SrO	0.00	0.00	0.00	0.00
BaO	0.00	0.00	0.00	0.00
TOTAL	95.60	97.92	97.59	97.35
Mg#	49.17	48.02	48.58	48.71
Fo	76.30	75.50	75.90	76.00

Temp (°C)	1138	1138	1138
Run #	12	12	12
SiO_2	47.78	47.65	48.00
TiO_2	3.43	3.17	3.42
Al_2O_3*	18.17	18.11	18.22
Fe_2O_3*	1.45	1.46	1.44
Cr_2O_3	0.01	0.01	0.00
FeO*	7.26	7.30	7.21
MnO	0.24	0.24	0.20
MgO	3.84	3.79	3.86
NiO	0.02	0.06	0.01
CoO	0.00	0.00	0.00
CaO	7.94	7.83	7.76
Na_2O	5.22	5.22	5.29
K_2O	2.87	2.84	2.86
P_2O_5	0.58	0.69	0.69
SrO	0.00	0.00	0.00
BaO	0.00	0.00	0.00
TOTAL	98.79	98.37	98.96
Mg#	48.52	48.04	48.85
Fo	75.90	75.50	76.10

Temp (°C)	1120	1120	1120
Run #			
SiO_2	47.95	48.43	48.62
TiO_2	2.98	3.27	3.05
Al_2O_3*	18.04	18.05	18.37
Fe_2O_3*	1.27	1.27	1.26
Cr_2O_3	0.01	0.00	0.00
FeO*	6.89	6.96	7.11
MnO	0.28	0.25	0.23
MgO	3.85	3.82	3.97
NiO	0.11	0.06	0.00
CoO	0.00	0.00	0.00
CaO	7.94	8.06	8.03
Na_2O	4.84	4.70	4.59
K_2O	2.59	2.61	2.43
P_2O_5	0.24	0.21	0.16
SrO	0.00	0.00	0.00
BaO	0.00	0.00	0.00
TOTAL	96.97	97.68	97.82
Mg#	49.89	49.44	49.90
Fo	76.80	76.50	76.90

Temp (°C)	1104	1104	1104	1104
Run #	15	15	15	15
SiO_2	46.50	46.80	46.76	47.12
TiO_2	3.59	3.41	3.31	3.11
Al_2O_3*	17.08	17.15	17.18	17.13
Fe_2O_3*	1.52	1.45	1.56	1.53
Cr_2O_3	0.01	0.02	0.00	0.00
FeO*	7.58	7.21	7.64	7.65
MnO	0.26	0.23	0.22	0.13
MgO	3.45	3.41	3.44	3.51
NiO	0.00	0.00	0.00	0.01
CoO	0.00	0.00	0.00	0.00
CaO	7.31	7.32	7.43	7.68
Na_2O	5.74	5.85	5.95	5.67
K_2O	3.11	3.04	3.08	3.06
P_2O_5	0.84	0.77	0.86	0.69
SrO	0.00	0.00	0.00	0.00
BaO	0.00	0.00	0.00	0.00
TOTAL	96.99	96.64	97.43	97.28
Mg#	44.79	45.71	44.52	44.98
Fo	73.00	73.70	72.80	73.20

Temp (°C)	1089	1089	1089
Run #	17	17	17
SiO_2	47.82	47.39	47.67
TiO_2	3.85	3.77	3.86
Al_2O_3*	16.69	16.65	16.67
Fe_2O_3*	1.71	1.68	1.71
Cr_2O_3	0.00	0.01	0.01
FeO*	8.12	7.93	8.17
MnO	0.12	0.21	0.24
MgO	3.36	3.25	3.26
NiO	0.04	0.00	0.00
CoO	0.00	0.00	0.00
CaO	7.27	7.20	7.10
Na_2O	5.63	5.65	5.58
K_2O	3.23	3.25	3.22
P_2O_5	0.69	0.68	0.63
SrO	0.00	0.00	0.00
BaO	0.00	0.00	0.00
TOTAL	98.54	97.67	98.13
Mg#	42.46	42.23	41.53
Fo	71.10	70.90	70.30

Temp (°C)	1049	1049	1049	1049
Run #	16	16	16	16
SiO_2	49.00	48.63	50.28	49.64
TiO_2	3.36	3.25	3.20	3.33
Al_2O_3	17.17	17.15	17.56	17.55
Fe_2O_3*	1.54	1.37	1.21	1.29
Cr_2O_3	0.02	0.03	0.00	0.00
FeO*	7.45	6.92	6.11	6.54
MnO	0.19	0.29	0.25	0.17
MgO	2.54	2.53	2.21	2.36
NiO	0.00	0.00	0.00	0.07
CoO	0.00	0.00	0.00	0.00
CaO	6.13	6.02	5.40	5.55
Na_2O	6.24	5.90	6.27	6.24
K_2O	4.01	3.83	4.01	3.77
P_2O_5	1.49	1.42	1.05	0.90
SrO	0.00	0.00	0.00	0.00
BaO	0.00	0.00	0.00	0.00
TOTAL	99.14	97.33	97.54	97.41
Mg#	37.82	39.48	39.17	39.18
Fo	67.00	68.50	68.20	68.20

* = FeO and Fe2O3 determined using method

Table 3: Melt compositions for 83415 Ne-hawaiite (one atmosphere)

Temp (°C)	1224
Run #	11
SiO_2	50.19
TiO_2	2.33
Al_2O_3*	20.78
Fe_2O_3*	1.12
Cr_2O_3	0.03
FeO*	5.58
MnO	0.11
MgO	2.93
NiO	0.03
CoO	0.00
CaO	7.16
Na_2O	5.59
K_2O	2.79
P_2O_5	0.55
SrO	0.00
BaO	0.00
TOTAL	99.19
Mg#	48.34
Fo	75.70

Temp (°C)	1197	1197	1197
Run #	8	8	8
SiO_2	49.83	49.81	49.63
TiO_2	2.42	2.30	2.38
Al_2O_3*	20.37	20.54	20.33
Fe_2O_3*	1.10	1.09	1.11
Cr_2O_3	0.01	0.00	0.00
FeO*	5.35	5.40	5.52
MnO	0.18	0.18	0.13
MgO	2.86	2.87	2.78
NiO	0.00	0.08	0.04
CoO	0.00	0.00	0.00
CaO	7.18	7.07	6.93
Na_2O	5.73	5.61	5.53
K_2O	2.70	2.68	2.70
P_2O_5	0.50	0.45	0.42
SrO	0.00	0.00	0.00
BaO	0.00	0.00	0.00
TOTAL	98.23	98.08	97.51
Mg#	48.80	48.65	47.34
Fo	76.10	76.00	75.00

Temp (°C)	1177	1177	1177
Run #	9	9	9
SiO_2	49.91	49.32	48.83
TiO_2	2.31	2.42	2.38
Al_2O_3*	20.43	20.11	20.09
Fe_2O_3*	1.16	1.18	1.23
Cr_2O_3	0.00	0.00	0.00
FeO*	5.81	5.77	5.95
MnO	0.19	0.13	0.21
MgO	2.91	2.84	2.89
NiO	0.00	0.09	0.00
CoO	0.00	0.00	0.00
CaO	7.01	6.87	6.98
Na_2O	5.70	5.89	5.86
K_2O	2.80	2.77	2.79
P_2O_5	0.63	0.63	0.65
SrO	0.00	0.00	0.00
BaO	0.00	0.00	0.00
TOTAL	98.86	98.02	97.87
Mg#	47.17	46.73	46.44
Fo	74.90	74.50	74.30

Temp (°C)	1160	1160	1160	1160
Run #	10	10	10	10
SiO_2	49.62	49.44	50.06	50.89
TiO_2	2.67	2.57	2.72	2.54
Al_2O_3*	19.91	19.75	20.17	20.73
Fe_2O_3*	1.22	1.27	1.19	1.01
Cr_2O_3	0.00	0.01	0.00	0.02
FeO*	6.12	6.30	6.15	6.10
MnO	0.20	0.21	0.20	0.11
MgO	3.22	3.27	3.17	2.98
NiO	0.00	0.00	0.00	0.00
CoO	0.00	0.00	0.00	0.00
CaO	6.62	6.64	6.65	7.29
Na_2O	5.89	5.99	5.78	4.07
K_2O	3.08	3.00	2.95	2.71
P_2O_5	0.69	0.78	0.89	0.79
SrO	0.00	0.00	0.00	0.00
BaO	0.00	0.00	0.00	0.00
TOTAL	99.23	99.22	99.92	99.25
Mg#	48.40	48.07	47.90	46.55
Fo	75.80	75.50	75.40	74.40

Temp (°C)	1138	1138	1138
Run #	12	12	12
SiO_2	49.81	49.64	49.73
TiO_2	2.91	2.75	2.85
Al_2O_3*	19.25	19.44	19.37
Fe_2O_3*	1.33	1.33	1.30
Cr_2O_3	0.02	0.00	0.02
FeO*	6.71	6.53	6.50
MnO	0.20	0.18	0.23
MgO	3.27	3.37	3.28
NiO	0.00	0.00	0.03
CoO	0.00	0.00	0.00
CaO	6.28	6.38	6.32
Na_2O	5.79	6.08	5.98
K_2O	3.20	3.21	3.14
P_2O_5	0.76	0.67	0.70
SrO	0.00	0.00	0.00
BaO	0.00	0.00	0.00
TOTAL	99.52	99.58	99.42
Mg#	46.45	47.94	47.32
Fo	74.30	75.40	75.00

Temp (°C)	1120	1120
Run #		
SiO_2	51.43	51.43
TiO_2	2.23	2.34
Al_2O_3*	21.02	21.01
Fe_2O_3*	1.01	0.98
Cr_2O_3	0.00	0.01
FeO*	5.90	5.87
MnO	0.13	0.17
MgO	3.02	3.04
NiO	0.00	0.01
CoO	0.00	0.00
CaO	6.99	6.92
Na_2O	5.15	4.84
K_2O	2.64	2.69
P_2O_5	0.27	0.29
SrO	0.00	0.00
BaO	0.00	0.00
TOTAL	99.78	99.59
Mg#	47.71	48.01
Fo	75.30	75.50

Temp (°C)	1104	1104	1104
Run #	15	15	15
SiO_2	49.53	49.49	49.82
TiO_2	3.19	2.75	2.70
Al_2O_3*	18.56	18.58	18.42
Fe_2O_3*	1.19	1.21	1.17
Cr_2O_3	0.02	0.00	0.04
FeO*	6.39	6.17	6.69
MnO	0.22	0.17	0.26
MgO	2.97	2.99	3.00
NiO	0.00	0.05	0.09
CoO	0.00	0.00	0.00
CaO	5.77	5.75	5.80
Na_2O	5.64	6.31	4.82
K_2O	3.65	3.56	3.64
P_2O_5	0.95	0.94	1.03
SrO	0.00	0.00	0.00
BaO	0.00	0.00	0.00
TOTAL	98.08	97.97	97.48
Mg#	45.30	46.37	44.44
Fo	73.40	74.20	72.70

Temp (°C)	1089	1089	1089	1089
Run #	17	17	17	17
SiO_2	48.26	48.49	48.88	49.23
TiO_2	3.02	3.07	3.12	3.18
Al_2O_3*	17.35	17.58	17.73	17.60
Fe_2O_3*	1.68	1.59	1.63	1.52
Cr_2O_3	0.00	0.00	0.02	0.00
FeO*	8.08	7.69	7.85	8.20
MnO	0.20	0.20	0.23	0.21
MgO	2.94	2.97	2.97	2.98
NiO	0.00	0.05	0.01	0.00
CoO	0.00	0.00	0.00	0.00
CaO	5.65	5.74	5.72	5.72
Na_2O	5.76	5.84	5.96	4.57
K_2O	3.67	3.54	3.62	3.56
P_2O_5	1.36	1.09	1.10	1.24
SrO	0.00	0.00	0.00	0.00
BaO	0.00	0.00	0.00	0.00
TOTAL	97.97	97.85	98.84	98.01
Mg#	39.36	40.76	40.25	39.29
Fo	68.40	69.60	69.20	68.30

Temp (°C)	1049	1049
Run #	16	16
SiO_2	48.18	49.21
TiO_2	3.41	3.09
Al_2O_3*	16.96	16.98
Fe_2O_3*	1.43	1.30
Cr_2O_3	0.01	0.03
FeO*	7.08	6.72
MnO	0.32	0.26
MgO	2.65	2.53
NiO	0.00	0.00
CoO	0.00	0.00
CaO	5.64	5.69
Na_2O	6.14	5.93
K_2O	3.86	3.56
P_2O_5	1.44	1.59
SrO	0.00	0.00
BaO	0.00	0.00
TOTAL	97.12	96.89
Mg#	40.03	40.15
Fo	69.00	69.10

* = FeO and Fe2O3 determined using method given by Kilinc et al., 1983

Table 4: Melt compositions from anorthoclase phonolite (one atmosphere)

Temp (°C)	1177	1177	1177
Run #	9	9	9
SiO_2	55.71	55.78	56.38
TiO_2	1.52	1.54	1.53
Al_2O_3	19.45	19.53	19.69
Fe_2O_3*	1.04	1.02	1.01
Cr_2O_3	0.00	0.00	0.00
FeO*	4.69	4.60	4.70
MnO	0.32	0.26	0.30
MgO	1.44	1.41	1.41
NiO	0.03	0.02	0.00
CoO	0.00	0.00	0.00
CaO	3.35	3.29	3.37
Na_2O	7.25	7.22	6.99
K_2O	4.11	4.22	4.18
P_2O_5	0.32	0.21	0.28
SrO	0.00	0.00	0.00
BaO	0.00	0.00	0.00
TOTAL	99.23	99.12	99.85
$Mg_{\#}$	35.36	35.35	34.91
Fo	64.60	64.60	64.10

Temp (°C)	1160	1160	1160	1160	1160
Run #	10	10	10	10	10
SiO_2	55.98	55.86	55.95	55.61	55.70
TiO_2	1.53	1.41	1.51	1.61	1.51
Al_2O_3	19.66	19.34	19.26	19.50	19.60
Fe_2O_3*	0.99	1.03	1.02	1.01	0.98
Cr_2O_3	0.00	0.01	0.01	0.00	0.00
FeO*	4.73	4.88	4.77	4.70	4.70
MnO	0.24	0.22	0.31	0.24	0.32
MgO	1.35	1.44	1.39	1.41	1.48
NiO	0.00	0.00	0.00	0.00	0.06
CoO	0.00	0.00	0.00	0.00	0.00
CaO	3.43	3.37	3.37	3.42	3.40
Na_2O	6.96	7.09	7.25	7.30	6.94
K_2O	4.22	4.12	4.14	4.15	4.22
P_2O_5	0.34	0.37	0.32	0.32	0.36
SrO	0.00	0.00	0.00	0.00	0.00
BaO	0.00	0.00	0.00	0.00	0.00
TOTAL	99.44	99.14	99.30	99.25	99.30
$Mg_{\#}$	30.02	34.43	34.23	34.81	36.02
Fo	58.80	63.60	63.40	64.00	65.20

Temp (°C)	1160	1160	1160
Run #	10	10	10
SiO_2	56.00	56.23	56.70
TiO_2	1.46	1.40	1.48
Al_2O_3*	19.67	19.55	19.52
Fe_2O_3*	1.03	0.98	1.04
Cr_2O_3	0.00	0.00	0.00
FeO*	4.87	4.66	4.89
MnO	0.28	0.34	0.27
MgO	1.47	1.41	1.35
NiO	0.00	0.06	0.02
CoO	0.00	0.00	0.00
CaO	3.36	3.42	3.33
Na_2O	7.14	7.09	7.21
K_2O	4.23	4.18	4.22
P_2O_5	0.42	0.29	0.35
SrO	0.00	0.00	0.00
BaO	0.00	0.00	0.00
TOTAL	99.94	99.61	100.39
Mg#	34.97	35.06	33.03
Fo	64.20	64.30	62.20

Temp (°C)	1138	1138	1138	1138	1138	1138
Run #	12	12	12	12	12	12
SiO_2	56.40	56.64	56.35	56.48	57.00	56.44
TiO_2	1.59	1.44	1.57	1.55	1.50	1.68
Al_2O_3	19.79	19.67	19.40	19.70	19.87	19.45
Fe_2O_3*	0.97	0.91	0.99	0.96	0.94	0.95
Cr_2O_3	0.00	0.00	0.00	0.00	0.02	0.00
FeO*	4.75	4.55	4.80	4.76	4.65	4.71
MnO	0.24	0.31	0.31	0.30	0.22	0.22
MgO	1.42	1.44	1.42	1.46	1.38	1.39
NiO	0.00	0.01	0.03	0.04	0.00	0.00
CoO	0.00	0.00	0.00	0.00	0.00	0.00
CaO	3.36	3.25	3.45	3.40	3.23	3.30
Na_2O	6.90	6.66	6.85	6.86	6.88	6.74
K_2O	4.12	4.22	4.15	4.09	4.15	4.15
P_2O_5	0.29	0.25	0.28	0.25	0.16	0.22
SrO	0.00	0.00	0.00	0.00	0.00	0.00
BaO	0.00	0.00	0.00	0.00	0.00	0.00
TOTAL	99.83	99.34	99.60	99.84	100.00	99.25
Mg#	34.68	36.03	34.60	35.39	34.64	34.41
Fo	63.90	65.20	63.80	64.60	63.90	63.60

Temp (°C)	1120	1120
Run #	13	13
SiO_2	55.92	56.25
TiO_2	1.47	1.40
Al_2O_3*	19.74	19.55
Fe_2O_3*	0.97	0.94
Cr_2O_3	0.02	0.01
FeO*	5.01	4.86
MnO	0.20	0.32
MgO	1.48	1.42
NiO	0.02	0.00
CoO	0.00	0.00
CaO	3.52	3.34
Na_2O	6.66	6.77
K_2O	3.98	3.94
P_2O_5	0.30	0.18
SrO	0.00	0.00
BaO	0.00	0.00
TOTAL	99.31	98.97
Mg#	34.51	34.32
Fo	63.70	63.50

Temp (°C)	1104	1104	1104	1104
Run #	15	15	15	15
SiO_2	55.06	55.16	56.07	55.45
TiO_2	1.34	1.42	1.52	1.63
Al_2O_3*	19.30	19.38	19.57	19.35
Fe_2O_3*	0.94	0.94	0.93	0.91
Cr_2O_3	0.00	0.01	0.00	0.01
FeO*	4.70	4.63	4.76	4.64
MnO	0.27	0.26	0.28	0.28
MgO	1.41	1.41	1.55	1.44
NiO	0.04	0.01	0.05	0.00
CoO	0.00	0.00	0.00	0.00
CaO	3.29	3.23	3.22	3.26
Na_2O	7.35	7.48	7.22	7.16
K_2O	4.19	4.25	4.31	4.22
P_2O_5	0.48	0.42	0.48	0.58
SrO	0.00	0.00	0.00	0.00
BaO	0.00	0.00	0.00	0.00
TOTAL	98.38	98.60	99.95	98.93
Mg#	34.81	35.20	36.71	35.63
Fo	64.00	64.40	65.90	64.90

Temp (°C)	1089	1089	1089	1089	1089
Run #	17	17	17	17	17
SiO_2	55.29	55.16	55.93	55.77	55.75
TiO_2	1.43	1.50	1.35	1.43	1.38
Al_2O_3*	19.13	19.08	19.28	19.34	19.35
Fe_2O_3*	0.99	0.99	1.01	0.98	0.99
Cr_2O_3	0.00	0.00	0.01	0.00	0.00
FeO*	4.84	4.83	5.01	4.83	5.04
MnO	0.23	0.38	0.26	0.28	0.26
MgO	1.41	1.39	1.41	1.43	1.42
NiO	0.00	0.02	0.00	0.00	0.02
CoO	0.00	0.00	0.00	0.00	0.00
CaO	3.29	3.34	3.22	3.30	3.28
Na_2O	7.01	7.11	6.92	7.07	6.68
K_2O	4.13	4.10	4.12	4.13	4.08
P_2O_5	0.26	0.37	0.36	0.25	0.35
SrO	0.00	0.00	0.00	0.00	0.00
BaO	0.00	0.00	0.00	0.00	0.00
TOTAL	98.01	98.27	98.88	98.81	98.60
Mg#	34.20	33.85	33.48	34.59	33.50
Fo	63.40	63.00	62.70	63.80	62.70

Temp (°C)	1049	1049	1049
Run #	16	16	16
SiO_2	55.46	55.43	55.80
TiO_2	1.70	1.39	1.75
Al_2O_3*	18.22	18.30	18.06
Fe_2O_3*	1.01	1.07	1.06
Cr_2O_3	0.00	0.02	0.00
FeO*	5.59	5.60	5.54
MnO	0.35	0.36	0.38
MgO	1.59	1.64	1.70
NiO	0.00	0.00	0.00
CoO	0.00	0.00	0.00
CaO	2.90	2.90	2.81
Na_2O	7.13	6.85	6.94
K_2O	4.55	4.34	4.30
P_2O_5	0.39	0.52	0.43
SrO	0.00	0.00	0.00
BaO	0.00	0.00	0.00
TOTAL	98.89	98.41	98.78
Mg#	33.67	34.35	35.38
Fo	62.90	63.60	64.60

* = FeO and Fe2O3 determined using method given by Kilinc et al., 1983

Appendix E

Table 1: Olivine compositions of basanite (one atmosphere)

Temp (°C)	1224	1224	1224	1224	1224	1224
Run #	11	11	11	11	11	11
SiO_2	39.95	39.58	39.16	39.63	38.59	39.73
TiO_2	0.03	0.10	0.02	0.05	0.08	0.08
Al_2O_3	0.09	0.12	0.11	0.11	0.11	0.14
Fe_2O_3	0.00	0.00	0.00	0.00	0.00	0.00
Cr_2O_3	0.00	0.00	0.00	0.00	0.00	0.00
FeO*	12.59	12.55	12.35	12.56	12.44	12.72
MnO	0.17	0.15	0.16	0.18	0.22	0.20
MgO	45.87	45.84	45.65	46.08	46.06	45.64
NiO	0.11	0.11	0.24	0.16	0.20	0.16
CoO	0.00	0.00	0.00	0.00	0.00	0.00
CaO	0.53	0.47	0.47	0.48	0.48	0.52
Na_2O	0.03	0.00	0.00	0.02	0.02	0.03
K_2O	0.02	0.00	0.00	0.01	0.01	0.03
P_2O_5	0.04	0.02	0.08	0.02	0.08	0.07
SrO	0.00	0.00	0.00	0.00	0.00	0.00
BaO	0.00	0.00	0.00	0.00	0.00	0.00
TOTAL	99.43	98.95	98.25	99.29	98.29	99.30
Fo	86.80	86.87	86.93	86.87	87.06	86.36
Fa	13.20	13.13	13.07	13.13	12.94	13.64

Temp (°C)	1197	1197	1197	1197
Run #	8	8	8	8
SiO_2	39.77	40.29	39.75	39.78
TiO_2	0.04	0.05	0.05	0.07
Al_2O_3	0.07	0.11	0.07	0.08
Fe_2O_3	0.00	0.00	0.00	0.00
Cr_2O_3	0.00	0.00	0.00	0.00
FeO*	13.51	13.37	13.45	13.47
MnO	0.20	0.23	0.17	0.21
MgO	45.41	46.19	44.84	45.19
NiO	0.00	0.00	0.00	0.00
CoO	0.00	0.00	0.00	0.00
CaO	0.55	0.50	0.52	0.54
Na_2O	0.00	0.02	0.04	0.00
K_2O	0.03	0.01	0.01	0.00
P_2O_5	0.03	0.06	0.01	0.03
SrO	0.00	0.00	0.00	0.00
BaO	0.00	0.00	0.00	0.00
TOTAL	99.67	100.92	99.01	99.45
Fo	85.86	85.86	85.79	85.79
Fa	14.14	14.14	14.21	14.21

Temp (°C)	1177	1177	1177	1177	1177
Run #	9	9	9	9	9
SiO_2	39.76	39.77	40.00	40.17	39.26
TiO_2	0.17	0.02	0.06	0.04	0.06
Al_2O_3	0.08	0.08	0.05	0.09	0.09
Fe_2O_3	0.00	0.00	0.00	0.00	0.00
Cr_2O_3	0.00	0.00	0.00	0.00	0.03
FeO*	13.93	14.16	14.39	14.29	14.59
MnO	0.24	0.23	0.19	0.21	0.21
MgO	44.48	44.47	44.26	44.97	43.72
NiO	0.09	0.14	0.12	0.21	0.11
CoO	0.00	0.00	0.00	0.00	0.00
CaO	0.57	0.59	0.63	0.56	0.49
Na_2O	0.00	0.02	0.03	0.05	0.00
K_2O	0.00	0.00	0.03	0.00	0.00
P_2O_5	0.03	0.00	0.06	0.03	0.05
SrO	0.00	0.00	0.00	0.00	0.00
BaO	0.00	0.00	0.00	0.00	0.00
TOTAL	99.34	99.47	99.82	100.63	98.60
Fo	85.20	84.77	84.69	84.77	84.23
Fa	14.80	15.23	15.31	15.23	15.77

Temp (°C)	1160	1160	1160	1160
Run #	10	10	10	10
SiO_2	39.24	39.30	39.08	39.15
TiO_2	0.01	0.05	0.08	0.03
Al_2O_3	0.09	0.09	0.08	0.07
Fe_2O_3	0.00	0.00	0.00	0.00
Cr_2O_3	0.00	0.00	0.00	0.03
FeO*	15.30	15.37	15.12	15.16
MnO	0.20	0.19	0.24	0.20
MgO	43.53	43.01	43.60	43.54
NiO	0.06	0.12	0.15	0.07
CoO	0.00	0.00	0.00	0.00
CaO	0.55	0.56	0.48	0.57
Na_2O	0.02	0.02	0.01	0.04
K_2O	0.01	0.01	0.00	0.01
P_2O_5	0.02	0.01	0.05	0.05
SrO	0.00	0.00	0.00	0.00
BaO	0.00	0.00	0.00	0.00
TOTAL	99.03	98.72	98.89	98.92
Fo	83.33	83.25	83.84	83.66
Fa	16.67	16.75	16.16	16.34

Temp (°C)	1138	1138	1138	1138	1138	1138
Run #	12	12	12	12	12	12
SiO_2	39.22	39.10	39.00	39.22	39.15	39.13
TiO_2	0.17	0.13	0.07	0.04	0.00	0.03
Al_2O_3	0.04	0.07	0.07	0.10	0.09	0.06
Fe_2O_3	0.00	0.00	0.00	0.00	0.00	0.00
Cr_2O_3	0.00	0.00	0.00	0.00	0.00	0.00
FeO*	16.13	15.80	15.99	16.04	16.18	15.84
MnO	0.27	0.26	0.25	0.27	0.26	0.27
MgO	43.04	43.37	43.30	43.48	43.41	43.33
NiO	0.06	0.10	0.10	0.17	0.13	0.09
CoO	0.00	0.00	0.00	0.00	0.00	0.00
CaO	0.58	0.60	0.56	0.54	0.58	0.59
Na_2O	0.02	0.02	0.00	0.02	0.02	0.01
K_2O	0.01	0.00	0.00	0.00	0.00	0.00
P_2O_5	0.03	0.04	0.00	0.02	0.00	0.07
SrO	0.00	0.00	0.00	0.00	0.00	0.00
BaO	0.00	0.00	0.00	0.00	0.00	0.00
TOTAL	99.58	99.51	99.33	99.91	99.81	99.45
Fo	83.25	82.83	82.83	82.83	82.83	82.83
Fa	17.26	17.17	17.17	17.17	17.17	17.17

Temp (°C)	1120	1120	1120	1120	1120
Run #	13	13	13	13	13
SiO_2	38.31	38.37	38.14	38.00	37.98
TiO_2	0.10	0.17	0.14	0.14	0.03
Al_2O_3	0.09	0.07	0.08	0.08	0.07
Fe_2O_3	0.00	0.00	0.00	0.00	0.00
Cr_2O_3	0.05	0.05	0.05	0.00	0.00
FeO*	18.05	18.15	18.00	18.08	18.27
MnO	0.30	0.18	0.27	0.31	0.28
MgO	41.35	41.54	41.39	41.54	40.98
NiO	0.15	0.13	0.13	0.16	0.15
CoO	0.00	0.00	0.00	0.00	0.00
CaO	0.47	0.48	0.45	0.46	0.45
Na_2O	0.02	0.00	0.00	0.03	0.00
K_2O	0.00	0.00	0.00	0.00	0.00
P_2O_5	0.04	0.02	0.09	0.05	0.04
SrO	0.00	0.00	0.00	0.00	0.00
BaO	0.00	0.00	0.00	0.00	0.00
TOTAL	98.94	99.17	98.74	98.85	98.26
Fo	80.33	80.31	80.39	80.38	79.99
Fa	19.67	19.31	19.61	19.62	20.01

Temp (^{o}C)	1104	1104
Run #	15	15
SiO_2	38.01	37.89
TiO_2	0.05	0.12
Al_2O_3	0.08	0.05
Fe_2O_3	0.00	0.00
Cr_2O_3	0.00	0.00
FeO*	21.62	21.06
MnO	0.30	0.36
MgO	37.86	38.52
NiO	0.13	0.16
CoO	0.00	0.00
CaO	0.50	0.61
Na_2O	0.00	0.01
K_2O	0.01	0.01
P_2O_5	0.00	0.04
SrO	0.00	0.00
BaO	0.00	0.00
TOTAL	98.55	98.84
Fo	75.74	76.53
Fa	24.26	23.47

FeO* = total iron
Fo = forsterite, Fa = fayalite

Table 2: Olivine compositions for DVDP2 hawaiite (one atmosphere)

Temp (°C)	1104	1104
Run #	15	15
SiO_2	36.81	37.12
TiO_2	0.07	0.12
Al_2O_3	0.08	0.05
Fe_2O_3	0.00	0.00
Cr_2O_3	0.00	0.01
FeO*	23.23	23.17
MnO	0.53	0.60
MgO	36.55	36.74
NiO	0.00	0.00
CoO	0.00	0.00
CaO	0.55	0.49
Na_2O	0.00	0.07
K_2O	0.01	0.03
P_2O_5	0.27	0.11
SrO	0.00	0.00
BaO	0.00	0.00
TOTAL	98.10	98.51
Fo	73.72	73.87
Fa	26.28	26.13

Temp (°C)	1089
Run #	17
SiO_2	38.23
TiO_2	0.16
Al_2O_3	1.17
Fe_2O_3	0.00
Cr_2O_3	0.00
FeO*	24.18
MnO	0.57
MgO	33.09
NiO	0.00
CoO	0.00
CaO	0.85
Na_2O	0.23
K_2O	0.05
P_2O_5	0.06
SrO	0.00
BaO	0.00
TOTAL	98.58
Fo	70.93
Fa	29.07

Temp (°C)	1049	1049	1049
Run #	16	16	16
SiO_2	39.29	36.51	36.60
TiO_2	0.74	0.24	0.26
$Al2O_3$	3.93	0.06	0.05
Fe_2O_3	0.00	0.00	0.00
Cr_2O_3	0.02	0.00	0.02
FeO*	24.49	27.73	28.61
MnO	0.69	0.79	0.90
MgO	26.28	32.02	31.46
NiO	0.01	0.00	0.04
CoO	0.00	0.00	0.00
CaO	1.69	0.55	0.55
Na_2O	1.20	0.04	0.04
K_2O	0.78	0.03	0.03
P_2O_5	0.25	0.08	0.09
SrO	0.00	0.00	0.00
BaO	0.00	0.00	0.00
TOTAL	99.36	98.04	98.65
Fo	65.67	67.30	66.22
Fa	34.33	32.70	33.79

FeO* = total iron
Fo = forsterite, Fa = fayalite

Table 3: Olivine compositions of
83415 Ne-hawaiite (one atmosphere)

Temp (°C)	1104	1104
Run #	15	15
SiO_2	38.62	37.61
TiO_2	0.09	0.12
Al_2O_3	0.06	0.21
Fe_2O_3	0.00	0.00
Cr_2O_3	0.06	0.00
FeO*	15.40	23.42
MnO	0.27	0.53
MgO	42.84	36.16
NiO	0.10	0.08
CoO	0.00	0.00
CaO	0.33	0.49
Na_2O	0.00	0.06
K_2O	0.00	0.00
P_2O_5	0.04	0.11
SrO	0.00	0.00
BaO	0.00	0.00
TOTAL	97.81	98.81
Fo	83.22	73.35
Fa	16.78	26.65

Temp (°C)	1089	1089	1089	1089	1089
Run #	17	17	17	17	17
SiO_2	36.10	36.71	36.51	36.55	34.95
TiO_2	0.00	0.00	0.04	0.05	0.08
Al_2O_3	0.08	0.07	0.07	0.05	0.11
Fe_2O_3	0.00	0.00	0.00	0.00	0.00
Cr_2O_3	0.00	0.00	0.00	0.00	0.01
FeO*	26.67	27.10	26.90	27.15	26.71
MnO	0.65	0.59	0.62	0.62	0.57
MgO	32.79	33.29	33.32	32.79	33.59
NiO	0.06	0.02	0.01	0.05	0.06
CoO	0.00	0.00	0.00	0.00	0.00
CaO	0.39	0.40	0.40	0.39	0.38
Na_2O	0.05	0.07	0.04	0.03	0.04
K_2O	0.00	0.00	0.01	0.00	0.00
P_2O_5	0.03	0.07	0.06	0.04	0.08
SrO	0.00	0.00	0.00	0.00	0.00
BaO	0.00	0.00	0.00	0.00	0.00
TOTAL	96.82	98.31	97.97	97.72	96.57
Fo	68.67	68.65	68.83	68.29	69.15
Fa	31.33	31.35	31.17	31.71	30.85

Temp (°C)	1049	1049	1049	1049	1049
Run #	16	16	16	16	16
SiO_2	36.41	36.18	36.64	36.60	36.22
TiO_2	0.07	0.06	0.06	0.01	0.14
Al_2O_3	0.07	0.05	0.07	0.07	0.06
Fe_2O_3	0.00	0.00	0.00	0.00	0.00
Cr_2O_3	0.00	0.00	0.02	0.01	0.00
FeO*	27.36	27.00	27.65	27.87	27.94
MnO	0.72	0.78	0.80	0.73	0.83
MgO	32.24	32.13	31.92	32.61	32.18
NiO	0.04	0.01	0.00	0.00	0.06
CoO	0.00	0.00	0.00	0.00	0.00
CaO	0.49	0.46	0.47	0.39	0.46
Na_2O	0.02	0.08	0.00	0.00	0.08
K_2O	0.00	0.01	0.00	0.00	0.01
P_2O_5	0.06	0.06	0.05	0.04	0.03
SrO	0.00	0.00	0.00	0.00	0.00
BaO	0.00	0.00	0.00	0.00	0.00
TOTAL	97.49	96.81	97.68	98.34	98.00
Fo	67.74	67.96	67.30	67.60	67.25
Fa	32.26	32.04	32.70	32.40	32.75

FeO* = total iron
Fo = forsterite, Fa = fayalite

Table 4: Clinopyroxene compositions from basanite (one atmosphere)

Temp (°C)	1138	1138	1138	1138	1138
Run #	12	12	12	12	12
SiO_2	43.45	43.16	47.39	48.02	47.73
TiO_2	4.57	4.78	2.73	2.88	2.82
Al_2O_3	9.42	9.82	5.91	5.81	5.92
Fe_2O_3	0.00	0.00	0.00	0.00	0.00
Cr_2O_3	0.00	0.00	0.00	0.00	0.00
FeO*	4.92	4.88	4.74	4.75	4.53
MnO	0.06	0.01	0.06	0.08	0.11
MgO	12.29	12.13	14.17	14.39	14.42
NiO	0.10	0.03	0.01	0.02	0.06
CoO	0.00	0.00	0.00	0.00	0.00
CaO	22.94	22.74	22.77	22.93	22.80
Na_2O	0.34	0.35	0.31	0.30	0.29
K2O	0.00	0.00	0.02	0.00	0.00
P_2O_5	0.02	0.00	0.02	0.00	0.01
SrO	0.00	0.00	0.00	0.00	0.00
BaO	0.00	0.00	0.00	0.00	0.00
TOTAL	98.11	97.90	98.14	99.17	98.70
En	39.12	38.76	42.78	42.78	43.24
Fs	8.94	8.99	8.02	8.02	7.57
Wo	51.96	52.25	49.20	49.20	49.19
En+	43.21	43.13	45.20	45.20	45.71
Fs+	9.88	10.00	8.47	8.47	8.00
Wo+	46.91	46.88	46.33	46.33	46.29

Temp (°C)	1120	1120	1120	1120	1120
Run #	13	13	13 c	13 r	13 c
SiO_2	44.64	44.12	44.49	42.77	44.64
TiO_2	3.40	3.77	3.81	4.69	3.63
Al_2O_3	7.95	8.68	8.46	11.86	8.01
Fe_2O_3	0.00	0.00	0.00	0.00	0.00
Cr_2O_3	0.51	0.70	0.54	0.36	0.62
FeO*	5.32	5.31	5.55	6.87	5.78
MnO	0.01	0.13	0.08	0.09	0.09
MgO	13.41	12.80	13.18	10.13	13.20
NiO	0.00	0.09	0.05	0.00	0.01
CoO	0.00	0.00	0.00	0.00	0.00
CaO	21.60	22.04	21.76	18.72	21.55
Na_2O	0.27	0.29	0.31	0.99	0.24
K2O	0.00	0.01	0.01	0.41	0.00
P_2O_5	0.01	0.03	0.02	0.22	0.00
SrO	0.00	0.00	0.00	0.00	0.00
BaO	0.00	0.00	0.00	0.00	0.00
TOTAL	97.13	97.97	98.27	97.12	97.79
En	42.02	40.49	41.26	36.92	41.35
Fs	9.36	9.42	9.75	14.05	10.15
Wo	48.62	50.09	48.99	49.03	48.50
En+	45.51	44.51	44.85	41.73	45.18
Fs+	10.81	10.37	10.91	15.83	10.84
Wo+	44.31	45.12	44.24	42.45	43.98

Temp (°C)	1104	1104
Run #	15	15
SiO_2	45.10	42.87
TiO_2	4.02	5.34
Al_2O_3	7.36	8.94
Fe_2O_3	0.00	0.00
Cr_2O_3	0.02	0.02
FeO*	6.70	6.62
MnO	0.12	0.15
MgO	12.94	11.12
NiO	0.08	0.04
CoO	0.00	0.00
CaO	22.44	21.78
Na_2O	0.44	0.62
K2O	0.01	0.04
P_2O_5	0.04	0.15
SrO	0.00	0.00
BaO	0.00	0.00
TOTAL	99.27	97.69
En	39.43	36.47
Fs	11.44	12.19
Wo	49.13	51.35
En+	42.94	40.51
Fs+	12.35	13.29
Wo+	44.71	46.20

FeO* = total iron
En = enstatite, Fs = ferrosilite, Wo = wollastonite
En+, Fs+, Wo+ = Ca Tschermak ($CaAl_2SiO_6$) corrected

Table 5: Clinopyroxene compositions from DVDP2 hawaiite (one atmosphere)

Temp (^{o}C)	1104	1104
Run #	12	12
SiO_2	47.46	45.65
TiO_2	2.35	3.30
Al_2O_3	4.61	6.27
Fe_2O_3	0.00	0.00
Cr_2O_3	0.00	0.04
FeO*	6.98	7.92
MnO	0.21	0.19
MgO	13.08	12.17
NiO	0.06	0.06
CoO	0.00	0.00
CaO	21.86	21.61
Na_2O	0.55	0.68
K_2O	0.02	0.03
P_2O_5	0.08	0.10
SrO	0.00	0.00
BaO	0.00	0.00
TOTAL	97.25	98.01
En	39.99	37.87
Fs	11.97	13.83
Wo	48.04	48.31
En+	42.13	40.70
Fs+	12.36	14.53
Wo+	45.51	44.77

Temp (^{o}C)	1049	1049	1049
Run #	16	16	16
SiO_2	47.05	44.89	48.30
TiO_2	3.19	3.83	2.44
Al_2O_3	5.92	6.92	4.66
Fe_2O_3	0.00	0.00	0.00
Cr_2O_3	0.03	0.00	0.00
FeO*	7.65	7.59	7.31
MnO	0.21	0.24	0.20
MgO	11.98	11.62	13.00
NiO	0.02	0.00	0.00
CoO	0.00	0.00	0.00
CaO	21.50	21.38	22.18
Na_2O	0.72	0.60	0.52
K_2O	0.12	0.03	0.02
P_2O_5	0.05	0.04	0.12
SrO	0.00	0.00	0.00
BaO	0.00	0.00	0.00
TOTAL	98.42	97.14	98.72
En	37.77	37.19	39.35
Fs	13.52	13.62	12.41
Wo	48.71	49.18	48.25
En+	40	41.07	41.13
Fs+	14.12	14.88	12.96
Wo+	45.88	45.24	45.92

FeO* = total iron
En = enstatite, Fs = ferrosilite, Wo = wollastonite
En+, Fs+, Wo+ = Ca Tschermak ($CaAl_2SiO_6$) corrected

Table 6: Plagioclase compositions from the basanite (one atmosphere)

Temp (^{o}C)	1104	1104
Run #	15	15
SiO_2	48.25	49.25
TiO_2	1.00	0.47
Al_2O_3	29.08	30.31
Fe_2O_3	0.00	0.00
Cr_2O_3	0.03	0.00
FeO*	1.77	0.76
MnO	0.06	0.00
MgO	0.66	0.22
NiO	0.05	0.02
CoO	0.00	0.00
CaO	13.47	13.30
Na_2O	3.26	3.48
K_2O	0.69	0.46
P_2O_5	0.24	0.07
SrO	0.00	0.00
BaO	0.00	0.00
TOTAL	98.55	98.34
An	66.76	65.98
Ab	29.20	31.29
Or	4.05	2.73

FeO* = total iron
An = anorthite, Ab = albite, Or = or

Table 7: Plagioclase compositions from the DVDP2 hawaiite (one atmosphere)

Temp (°C)	1104	1104	1104	1104
Run #	15	15	15	15
SiO_2	51.74	51.38	52.05	51.63
TiO_2	0.20	0.22	0.23	0.15
Al_2O_3	29.04	29.04	29.24	29.51
Fe_2O_3	0.00	0.00	0.00	0.00
Cr_2O_3	0.00	0.02	0.01	0.00
FeO*	0.57	0.52	0.53	0.39
MnO	0.00	0.01	0.00	0.00
MgO	0.13	0.10	0.08	0.10
NiO	0.01	0.00	0.05	0.00
CoO	0.00	0.00	0.00	0.00
CaO	11.91	12.08	11.81	12.16
Na_2O	4.12	4.26	4.56	4.21
K_2O	0.50	0.45	0.46	0.42
P_2O_5	0.06	0.03	0.00	0.04
SrO	0.00	0.00	0.00	0.00
BaO	0.00	0.00	0.00	0.00
TOTAL	98.27	98.10	99.01	98.60
An	59.70	59.45	57.31	59.97
Ab	37.33	37.93	40.05	37.57
Or	2.97	2.63	2.64	2.46

Temp (°C)	1089	1089	1089
Run #	17	17	17
SiO_2	51.44	51.39	52.36
TiO_2	0.26	0.15	0.17
Al_2O_3	29.36	29.87	29.02
Fe_2O_3	0.00	0.00	0.00
Cr_2O_3	0.00	0.00	0.04
FeO*	0.58	0.59	0.82
MnO	0.02	0.03	0.00
MgO	0.10	0.10	0.21
NiO	0.00	0.00	0.00
CoO	0.00	0.00	0.00
CaO	12.33	12.46	11.90
Na2O	3.94	3.96	4.24
K_2O	0.46	0.45	0.57
P_2O_5	0.07	0.04	0.06
SrO	0.00	0.00	0.00
BaO	0.00	0.00	0.00
TOTAL	98.56	99.04	99.38
An	61.64	61.81	58.76
Ab	35.60	35.54	37.89
Or	2.76	2.65	3.35

Temp (°C)	1049	1049	1049
Run #	16	16	16
SiO_2	54.03	52.32	54.34
TiO_2	0.24	1.62	0.13
Al_2O_3	28.08	23.34	28.67
Fe_2O_3	0.00	0.00	0.00
Cr_2O_3	0.00	0.00	0.01
FeO*	0.62	4.34	0.49
MnO	0.00	0.10	0.04
MgO	0.08	1.20	0.09
NiO	0.01	0.00	0.00
CoO	0.00	0.00	0.00
CaO	10.37	8.38	10.61
Na_2O	4.90	5.27	4.90
K_2O	0.69	2.22	0.66
P_2O_5	0.06	0.58	0.00
SrO	0.00	0.00	0.00
BaO	0.00	0.00	0.00
TOTAL	99.08	99.37	99.92
An	51.68	40.75	52.38
Ab	44.24	46.37	43.77
Or	4.08	12.89	3.86

FeO* = total iron
An = anorthite, Ab = albite, Or = orthoclase

Table 8: Plagioclase compositions from the 83415 Ne-hawaiite (one atmosphere)

Temp (°C)	1160	1160	1160	1160	1160
Run #	10	10	10	10	10
SiO_2	52.16	52.03	51.56	52.07	51.00
TiO_2	0.25	0.39	0.20	0.15	0.14
Al_2O_3	29.90	29.95	31.03	31.12	29.75
Fe_2O_3	0.00	0.00	0.00	0.00	0.00
Cr_2O_3	0.00	0.00	0.00	0.00	0.03
FeO*	0.42	0.78	0.43	0.45	0.59
MnO	0.01	0.02	0.04	0.00	0.00
MgO	0.12	0.31	0.10	0.08	0.21
NiO	0.04	0.01	0.00	0.00	0.00
CoO	0.00	0.00	0.00	0.00	0.00
CaO	12.13	12.47	13.08	13.10	12.32
Na_2O	4.09	3.94	3.78	3.70	3.67
K_2O	0.43	0.57	0.36	0.34	0.45
P_2O_5	0.06	0.04	0.06	0.05	0.05
SrO	0.00	0.00	0.00	0.00	0.00
BaO	0.00	0.00	0.00	0.00	0.00
TOTAL	99.60	100.51	100.64	101.06	98.22
An	60.82	61.62	64.29	64.29	63.21
Ab	37.11	35.35	32.65	32.65	34.04
Or	2.06	3.03	2.04	2.04	2.75

Temp (°C)	1138	1138
Run #	12	12
SiO_2	51.51	51.68
TiO_2	0.20	0.29
Al_2O_3	30.30	29.99
Fe_2O_3	0.00	0.00
Cr_2O_3	0.00	0.00
FeO*	0.34	0.27
MnO	0.00	0.01
MgO	0.02	0.01
NiO	0.10	0.07
CoO	0.00	0.00
CaO	12.50	12.29
Na_2O	4.09	4.07
K_2O	0.37	0.40
P_2O_5	0.01	0.06
SrO	0.00	0.00
BaO	0.00	0.00
TOTAL	99.44	99.15
An	61.62	61.22
Ab	36.36	36.73
Or	2.02	2.04

Temp (°C)	1104	1104
Run #	15	15
SiO_2	53.99	53.35
TiO_2	0.20	0.13
Al_2O_3	27.95	28.67
Fe_2O_3	0.00	0.00
Cr_2O_3	0.02	0.01
FeO*	0.33	0.38
MnO	0.00	0.00
MgO	0.07	0.14
NiO	0.00	0.03
CoO	0.00	0.00
CaO	10.19	10.80
Na_2O	5.10	4.54
K_2O	0.60	0.58
P_2O_5	0.00	0.01
SrO	0.00	0.00
BaO	0.00	0.00
TOTAL	98.46	98.63
An	50.61	54.79
Ab	45.82	41.70
Or	3.57	3.51

Temp (°C)	1089	1089	1089
Run #	17	17	17
SiO_2	54.58	52.54	55.20
TiO_2	0.24	0.19	0.15
Al_2O_3	27.50	29.30	27.29
Fe_2O_3	0.00	0.00	0.00
Cr_2O_3	0.00	0.05	0.00
FeO*	0.26	0.45	0.29
MnO	0.01	0.00	0.00
MgO	0.09	0.08	0.07
NiO	0.00	0.03	0.00
CoO	0.00	0.00	0.00
CaO	9.76	11.32	9.54
Na_2O	5.34	4.32	5.56
K_2O	0.74	0.50	0.76
P_2O_5	0.01	0.00	0.08
SrO	0.00	0.00	0.00
BaO	0.00	0.00	0.00
TOTAL	98.54	98.78	98.93
An	48.09	57.32	46.53
Ab	47.55	39.64	49.04
Or	4.36	3.04	4.44

Temp (°C)	1049	1049
Run #	16	16
SiO_2	55.47	54.93
TiO_2	0.23	0.08
Al_2O_3	27.41	27.62
Fe_2O_3	0.00	0.00
Cr_2O_3	0.00	0.01
FeO*	0.57	0.46
MnO	0.00	0.00
MgO	0.05	0.07
NiO	0.00	0.00
CoO	0.00	0.00
CaO	9.50	9.52
Na_2O	5.31	5.20
K_2O	0.79	0.77
P_2O_5	0.03	0.04
SrO	0.00	0.00
BaO	0.00	0.00
TOTAL	99.37	98.70
An	47.40	47.96
Ab	47.90	47.44
Or	4.70	4.60

FeO* = total iron
An = anorthite, Ab = albite, Or = orthoclase

Table 9: Anorthoclase compositions from the anorthoclase phonolite (one atmosphere)

Temp (°C)	1049	1049	1049	1049	1049
Run#	16	16	16	16	16
SiO_2	58.86	59.56	57.95	58.83	58.44
TiO_2	0.10	0.15	0.27	0.17	0.11
Al_2O_3	24.87	25.37	24.73	25.58	25.45
Fe_2O_3	0.00	0.00	0.00	0.00	0.00
Cr_2O_3	0.00	0.01	0.00	0.00	0.00
FeO*	0.36	0.54	0.81	0.46	0.42
MnO	0.02	0.05	0.07	0.03	0.00
MgO	0.04	0.10	0.17	0.04	0.05
NiO	0.00	0.00	0.05	0.02	0.03
CoO	0.00	0.00	0.00	0.00	0.00
CaO	6.57	6.60	6.80	6.92	6.96
Na_2O	6.67	6.53	6.41	6.61	6.76
K_2O	1.30	1.27	1.32	1.13	1.11
P_2O_5	0.02	0.04	0.05	0.02	0.04
SrO	0.00	0.00	0.00	0.00	0.00
BaO	0.00	0.00	0.00	0.00	0.00
TOTAL	98.81	100.21	98.62	99.81	99.37
An	32.54	33.14	34.05	34.24	33.92
Ab	59.89	59.28	58.10	59.13	59.62
Or	7.65	7.58	7.85	6.63	6.46

FeO* = total iron
An = anorthite, Ab = albite, Or = orthoclase